Regulation of FGF Receptor signalling by Sprouty and Spred.

By
Faraz Khosravi Mardakheh

A thesis submitted to

The University of Birmingham

For the degree of Doctor of Philosophy.

College of Life and Environmental Sciences

School of Biosciences

University of Birmingham

May 2010

ABSTRACT

Signalling from Fibroblast Growth Factor Receptors (FGFRs) is under tight control by a wide variety of extrinsic and intrinsic regulatory mechanisms, many of which remain poorly defined. Sproutys and their related Spred proteins constitute two such families of signalling regulators with multiple developmental roles as well as potential tumour suppressive functions. However, the molecular mechanisms of these proteins have remained unclear and subject to many unresolved controversies. Using a mass spectrometry approach, several novel interacting partners of Sprouty with roles in endocytosis are identified here, suggestive of a potential endocytic-related function for Sproutys. In addition, comprehensive analysis of Sprouty phosphorylations and their dynamics by mass spectrometry reveal previously unknown but potentially crucial sites that might regulate Sproutys function. Next, a novel late-endosomal protein that directly binds to Spred is identified using a different approach. Neighbor of BRCA1-1 (NBR1) is shown to be necessary for attenuation of FGF signaling by Spred, and this is demonstrated to be via modulation of the trafficking itinerary of FGFRs. Finally, NBR1 is established as a novel regulator of RTK trafficking and signalling, and the interplay between its various regions for protein localisation and function is revealed.

ACKNOWLEDGEMENTS

I would like to thank John Heath for inspiring me through his lectures when I was an undergraduate student, and later for giving me the opportunity to work in his lab, and for his guidance and support as my supervisor throughout this project. I would also like to thank CRUK for funding this PhD studentship.

I am very grateful to Mona Yekezare, not only for her collaboration which was crucial to this project, but also her unwavering love and support as my soul mate, my partner, and my wife.

Special thanks go to Steve Sweet, Laura Machesky, Giulio Auciello, Josh Rappoport, and Tim Dafforn for their collaborations without which this project could have never reached where it stands now. I am also grateful to Susan Brewer for preparing many of the reagents and materials that were used in this project.

I would like to thank all the present and past members of the fifth floor, for their help, advice, support, and above all for the great time that we had together which I will never forget. In particular, I would like to thank Shiva Akbarzadeh, Anna Vecchione, and Lee Wheldon for helping me get on my feet when I had just started my project. I would also like to thank Kevin Ryan who worked very closely with me for a period of time, which I benefited from a lot. I am thankful to Debbie Cunningham for help with 2D gels and SILAC, and Nick Underhill-day for all the good times! Massive thanks also go to my fellow students Ania Dudka, Katie Ryan, and Kimberley Trim for their invaluable friendship and the great student experience we shared.

Last but not least, I would like to thank my parents Fariborz Mardakheh and Mahboobeh Jazebizadeh for their support, love, encouragement, and all the sacrifices they have made for me throughout my life.

TABLE OF CONTENTS

TABLE OF FIGURES

LIST OF ABBREVIATIONS

293T, Human embryonic kidney epithelial 293 cell-line with large T antigen;

2D, 2-Dimensional;

AB, Acid Box;

ACH, Achondroplasia;

AGM, Aorta-Gonad-Mesonephros;

AP2, Adaptor Protein complex-2;

APPL1, Adaptor protein containing PH domain, PTB domain, and Leucine zipper motif-1;

AVd, degradative Autophagosome;

AVi, immature Autophagosome;

BafA, Bafilomycin A1;

BN, Blue-Native;

Bnl, Branchless;

BSA, Bovine Serum Albumin;

CAV1, Caveolin1;

CBL, Casitas B-lineage Lymphoma;

CC, coiled-coiled;

CD, Circular-Dichroism;

CID, Collision Induced Dissociation;

CIN85: CBL-Interacting Protein of 85kDa;

CKI, Casein Kinase I;

CKII, Casein Kinase II;

CLH1, Clathrin heavy chain-1;

CNS, Central Nervous System;

COS7, African green monkey SV40-transfected kidney fibroblast cell-line 7;

CRKL, CRK-like adaptor protein;

DAG, Diacylglycerol;

DHB, 2,5-dihydroxybenzoic acid;

DMEM, Dulbecco's Modified Eagle Medium;

DNA, deoxyribonucleic acid;

dNTP, deoxynucleoside triphosphate;

DTT, Dithiothreitol;

DUSP, Dual Specificity Phosphatase;

ECD, Electron Capture Dissociation;

ECL, Enzyme Chemiluminescence;

EDTA, ethylenediaminetetraacetic acid;

EGF, Epidermal Growth Factor;

EGFR, Epidermal Growth Factor Receptor;

EPS15, Epidermal Growth Factor Receptor Substrate-15;

ERK, Extracellular Regulated Kinase;

ESCRT, Endosomal Sorting Complex Required for Transport;

Eve3, EVH1-only splice variant of Spred3;

EVH1, Enabled/VASP Homology-1;

FCS, Foetal Calf Serum;

FGF, Fibroblast Growth Factors;

FGFR, Fibroblast Growth Factors Receptor;

FLRT, Fibronectin-Leucine-Rich Transmembrane protein;

FPR, False-positive Rate;

FRS2, FGF Receptor Substrate-2;

FTICR, Fourier-transform ion cyclotron resonance;

FT-MS, Fourier-transform mass spectrometry;

GAB1, GRB2 Associated Binder-1;

GAP, GTPase Accelerating Protein;

GEF, Guanine Nucleotide Exchange Factor;

GFP, Green Fluorescent Protein;

GPCR, G Protein-Coupled Receptor;

GRB2, Growth factor Receptor Bound protein-2;

GSK-3β, Glycogen Synthase Kinase-3β;

GST, Glutathione S-Transferase

HBS, Heparin Binding Site;

HCH, Hypochondroplasia;

HEPES, 4-(2-hydroxyethyl)-1-piperazineethanesulfonic acid;

HMERF, Hereditary Myopathy with Early Respiratory Failure;

HRS, Hepatocyte growth factor-Regulated tyrosine kinase Substrate;

HSPG, Heparan Sulfate Proteoglycans;

HUVEC, Human Umbilical Vascular Endothelial Cell;

IB, Immunoblot;

ICM, Inner cell mass;

IF, Immunofluorescence;

Ig, Immunoglobulin;

IGH, Immunoglobulin heavy chain;

IL5, Interleukin-5;

ILV, Intra-Luminal Vesicle;

IM, Isolation Membrane;

IP, Immunoprecipitation;

IP3, Inositol(1,4,5)P_3;

JAK, Just Another Kinase;

JNK, Jun N-terminal Kinase;

JUBA, Juxta-UBA;

KAL1, Kallmann syndrome type 1;

KAL2, Kallmann syndrome type 2;

KBD, Kit Binding Domain;

KGFR, Keratinocyte Growth Factor Receptor;

LA, Ampicilin LB plates;

LAMP2, Lysosomal-associated membrane protein 2;

LB, Luria Bertani Broth;

LK, Kanamycin LB plates;

LC-MS/MS, Liquid Chromatography coupled with tandem mass spectrometry;

LC3, Microtubule Associated Protein Light Chain-3;

LIR, LC3 Interacting Region;

LIR2, secondary LC3 Interacting Region;

LTQ, Linear ion-trap;

MAPK, Mitogen Activated Protein Kinase;

MEK, MAPK/ERK Kinase;

MKP, Mitogen Activated Protein Kinase-Phosphatase;

Mnk1, Mitogen Activated Protein Kinase-Interacting Kinase 1;

MPR, Mannose 6-Phosphate Receptor;

MS/MS, Tandem mass spectrometry;

mTOR, mammalian Target of Rapamycin;

MuRF2, Muscle-specific RING-B-box ubiquitin ligase;

MVB, Multi-Vesicular Body;

MW, Molecular Weight;

NBR1, Neighbour of BRCA1-1;

NF1, Neurofibromin;

NGF, Nerve Growth Factor;

NO, Nitric Oxide;

NSC, Non-silencing control;

PA, Phosphatidic acid;

PAGE, Polyacrylamide Gel Electrophoresis;

PB1, phox/Bem1p;

PBS, Phosphate Buffered Saline;

PBST, PBS Tween;

PCR, Polymerase Chain Reaction;

PDGF, Platelet-Derived Growth Factor;

PDK1, Phosphoinositide-Dependant Kinase 1;

PC, Phosphatidylcholine;

PE, Phosphatidylethanolamine;

PH, Pleckstrin Homology;

PI3K, Phosphatidylinositol-3-OH Kinase;

PI3P, Phosphatidylinositol-3Phosphate;

$PI45P_2$, Phosphatidylinositol-4,5 phosphate;

PI51A, Phosphatidyl-4-phosphate 5-kinase;

PIP, Phosphatidylinositol-phosphate;

PIP_2, Phosphatidylinositol-4,5 phosphate;

$PI345P_3$, Phosphatidylinositol-3,4,5 phosphate;

PKB, Protein Kinase B;

PKC, Protein Kinase C;

PKD1, Protein Kinase D1;

PLC, Phospholipase-C;

PMSF, Phenylmethylsulfonyl fluoride;

PP1, Protein Phosphatase 1;

PP2A, Protein Phosphatase 2A;

PTB, Phospho-Tyrosine Binding;

PTP, Protein Tyrosine Phosphatase;

PVDF, Polyvinylidene fluoride;

RBM, RAF Binding Motif;

RNA, ribonucleic acid;

RT, room temperature;

RT-PCR, Reverse Transcriptase Polymerase Chain Reaction;

RTK, Receptor Tyrosine Kinase;

SADDAN, Severe Achondroplasia with Developmental Delay and Acanthosis Nigricans;

SDS, Sodium Dodecyl Sulphate;

SEF, Similar Expression to FGF;

SEFIR, SEF Interleukin17 Receptor-homology;

SFK, SRC family of kinases;

SH2, SRC Homology-2;

SH3, SRC Homology-3;

SHP2, SH2-containing Tyrosine-Phosphatase 2;

SIAH2, Seven in absentia homolog-2;

SILAC, Stable Isotope Labelling of Amino acids in Culture;

siRNA, small interference RNA;

SNT1, Suc1-Associated Neurotrophic factor Target 1;

SNP, Single Nucleotide Polymorphisms;

SNX9, Sorting Nexin-9;

SOS, Son of Sevenless;

SPRY, Sprouty;

SPRED, Sprouty Related with EVH1 Domain;

SQSTM1, Sequestosome-1;

SRF, Serum Response Factor;

STAM, Signal Transducing Adapter Molecule;

STAT, Signal Transducer and Activator of Transcription;

STRING, Search Tool for the Retrieval of Interacting Genes/Proteins;

TBE, Tris boric acid EDTA;

TBS, Tris Buffered Saline;

TD, Translocation Domain;

TDI, Thanatophoric dysplasia type I;

TDII, Thanatophoric dysplasia type II;

Tet, Tetracycline;

TESK1, dual specificity Testis-Specific Protein Kinase 1;

TFA, Trifluoroacetic acid;

TGFβR, Transforming Growth Factor-β Receptor;

Tmp21, Transmembrane emp24-like trafficking protein 10;

TrfR1, Transferrin Receptor-1;

Tris, Tris-(hydroxymethyl)-aminomethane;

TSC2, Tuberous Sclerosis Complex protein-2;

TSG101, Tumour Susceptibility Gene 101 Protein;

UBA, Ubiquitin Associated;

UBD, Ubiquitin Binding Domains;

UIM, Ubiquitin Interacting Motif;

USP8, Ubiquitin carboxyl-terminal hydrolase 8;

VEGF, Vascular Endothelial Growth Factor;

v/v, volume to volume ratio;

WCL, Whole Cell Lysate;

WT, Wild-type;

WT1, Wilms Tumour suppressor gene-1 transcription factor;

w/v weight to volume ratio;

w/w weight to weight ratio;

Y2H, Yeast two-Hybrid;

Z-VAD-FMK, carbobenzoxy-valyl-alanyl-aspartyl-[O-methyl]-fluoromethylketone;

ZZ, ZZ type zinc finger;

CHAPTER 1

Introduction

1.1 Receptor Tyrosine Kinases

In multi-cellular organisms, many key cellular functions such as growth, division, differentiation, migration, and survival are regulated non-autonomously by extracellular signalling molecules secreted in the organism. Such molecules are synthesised and released by signalling cells to act on specific target cells that have receptors for their detection. As most of these molecules cannot cross the cell-membrane, signal transduction often requires membrane spanning cell-surface receptors which can detect such molecules outside the cell and relay this signal inside. The signalling molecules act as biochemical ligands, binding to the extra-cellular part of a receptor. This causes a conformational change in the cytosolic part of the receptor, leading to the recruitment of signalling proteins and subsequent activation of downstream signal transduction pathways. These pathways ultimately convert the signal into changes of the cell behaviour by acting on critical cellular proteins in the nucleus, cytoskeleton, and other cellular compartments [Lodish et al., 2003].

Based on their structural features, trans-membrane signalling receptors can be classified into distinct groups. Receptor Tyrosine Kinases (RTKs) constitute one such group of membrane spanning cell-surface receptors which have intrinsic Tyrosine Kinase activity. These receptors contain an extra-cellular ligand binding domain which is connected to the intra-cellular part through a single trans-membrane α-helix. The intracellular part contains a Tyrosine kinase domain as well as additional regulatory sequences such as C-terminal tails which are involved in recruitment specific signalling proteins [Schlessinger, 2000; Dengjel et al., 2009] (Figure 1.1). Most RTKs are monomeric in the absence of their ligands. Under this state, the kinase domain is inactive. Ligand binding induces receptor dimerisation which leads to the activation of the kinase domains by trans-autophosphorylation (Figure 1.1). Subsequently, Tyrosine kinase activity leads to trans-autophosphorylation of other Tyrosine residues in the regulatory

sequences outside the kinase domain, which are the key to recruitment of downstream signalling proteins [Schlessinger, 2000; Dengjel et al., 2009]. The only exception to this model is the Insulin Receptor which exists as pre-formed disulphide linked dimers [Van Obberghen, 1994]. However, the quaternary structure of the dimers is such that little trans-autophosphorylation can occur in the absence of the ligand. Ligand binding induces a conformational change that results in trans-autophosphorylation and activation of the receptors in a similar manner to all other RTKs [Schlessinger, 2000].

Although the shared paradigm for RTK activation is ligand induced receptor dimerisation, the mechanism of dimerisation varies for different receptor-ligand complexes. Some ligands such as Platelet-Derived Growth Factors (PDGF) and Vascular Endothelial Growth Factors (VEGF) exist as homo-dimers, thereby utilising the simplest mechanism for induction of receptor dimerisation by binding to two receptors at the same time [Schlessinger, 2000]. As opposed to PDGF and VEGF, Epidermal Growth Factor (EGF) does not directly mediate receptor dimerisation. In contrast, EGF Receptor (EGFR) dimerisation is mediated by receptor-receptor interactions [Schlessinger, 2002]. A single monomeric EGF binds to a single EGFR molecule, and this induces a conformational change in the extra-cellular domain of the receptor, resulting in its increased affinity for another ligand-bound receptor [Schlessinger, 2002]. In case of Fibroblast Growth Factors (FGF), FGF Receptor (FGFR) dimerisation is mediated by both ligand-receptor and receptor-receptor interactions [Eswarakumar et al., 2005; Mohammadi et al., 2005]. Moreover, FGFR dimerisation requires further binding of Heparin or Heparan Sulfate Proteoglycans (HSPG) [Eswarakumar et al., 2005; Mohammadi et al., 2005]. HSPG makes molecular contacts with both FGFs and FGFRs and thereby stabilise the ligand-receptor complex [Eswarakumar et al., 2005; Mohammadi et al., 2005]. It is also believed that HSPGs may act to provide further specificity by spatially

restricting FGFR activation since their synthesis within tissues is often limited to specific areas of the extracellular matrix [Schlessinger, 2000]. The detailed molecular mechanism of FGFR activation is discussed later in this chapter.

Following trans-autophosphorylation, the majority of phosphorylated Tyrosine residues within the cytoplasmic regulatory segments function as specific binding sites for SRC Homology-2 (SH2) or Phospho-Tyrosine Binding (PTB) domains of distinct signalling proteins [Dengjel et al., 2009]. These proteins are either docking proteins/adaptors which recruit further signalling proteins, or enzymes - such as lipid kinases - the activity of which also results in further recruitment of signalling proteins and assembly of multi-protein signalling complexes [Dengjel et al., 2009]. This, consequently, leads to activation of different downstream signal transduction pathways including the RAS/Mitogen Activated Protein Kinase (MAPK) cascade - also known as the Extracellular Regulated Kinase 1 and 2 (ERK1/2) pathway - , the Phosphatidylinositol-3-OH Kinase (PI3K)/AKT pathway, and the Phospholipase-C (PLC)/Protein Kinase C (PKC) pathway [Dengjel et al., 2009]. Signalling by these and other downstream signal transduction cascades are discussed in detail later in this chapter.

A critical feature of RTK signalling is its tight regulation by a diverse group of signalling regulatory proteins. This is not surprising as in most multi-cellular organisms RTKs control several key processes such as pattern formation and organogenesis during development, or tissue regeneration and repair during adulthood. In fact, several developmental disorders as well as most cancers are linked to deregulated activity of RTKs [Vogelstein et al., 2004]. Regulation of RTK signalling is achieved at various levels. Many RTKs have auto-inhibitory mechanisms that insure receptor activity is fully prevented in the absence of ligand [Schlessinger, 2003]. Several extra-cellular proteins also act to attenuate receptor activation

by inhibiting ligand-receptor interaction [Schlessinger, 2000]. Another important level of regulation is dephosphorylation of the receptor and the associated downstream signalling molecules by Protein Tyrosine Phosphatases (PTPs) [Ostman and Böhmer, 2001; Ostman et al., 2006]. In addition, a number of downstream Serine/Threonine kinases such as PKC and ERK act in a feedback fashion to phosphorylate RTKs and their associated docking proteins/adaptors on specific residues which leads to their inhibition [Dengjel et al., 2009]. Furthermore, signal transduction pathways downstream of RTKs specifically activate gene expression of several attenuators of RTK signalling such as Sproutys, providing further means of feedback inhibition [Amit et al., 2007].

Parallel to the regulatory processes mentioned above, a key means of RTK signalling regulation is the endocytosis of activated RTKs from the plasma-membrane and their subsequent vesicular trafficking inside the cell. Different endocytic compartments can act as platforms for propagation of specific downstream signal transduction pathways, thereby providing pathway selectivity downstream of RTKs [Miaczynska et al., 2004b; Sorkin and von Zastrow, 2009; Scita and Di Fiore, 2010]. Eventually, the internalised receptors are either recycled back to the plasma-membrane for re-usage or trafficked to lysosomes for degradation and termination of signalling, and the balance between the two itineraries is a crucial determinant of the signalling outcome [Scita and Di Fiore, 2010]. Mechanisms of RTK signalling regulation including the endocytic trafficking of receptors are covered in great detail later in this chapter.

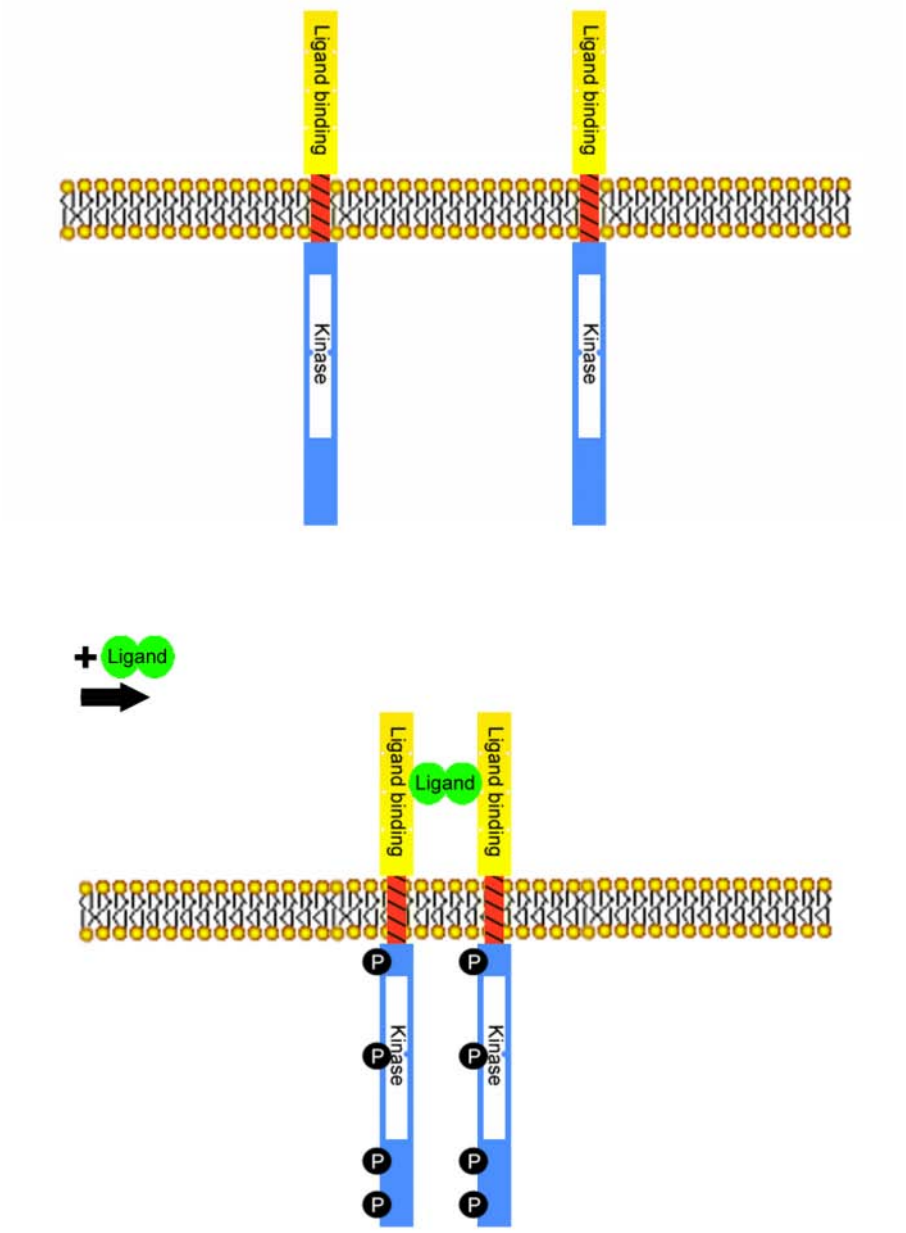

Figure 1.1. Schematic representation of RTK domains and ligand mediated receptor dimerisation and activation. RTKs are consisted of an N-terminal extracellular ligand binding domain, a single membrane spanning a-helix, and a C-terminal cytoplasmic part containing a Tyrosine kinase domain. TOP: in the absence of ligand, the receptor is monomeric with little Tyrosine kinase activity. BOTTOM: Ligand binding results in receptor dimerisation, which consequently leads to trans-autophosphorylation and activation of the catalytic kinase domains. In addition to the kinase domain (white), signal regulatory sequences within the C-terminal cytoplasmic portion (blue) are also trans-autophosphorylated, which act as recruitment sites for signalling proteins with phospho-Tyrosine binding domains.

1.2 Fibroblast Growth Factor Receptors

FGFRs constitute a key family of RTKs with a plethora of roles throughout the development as well as in adult life. Mammals contain four highly conserved homologues of FGFR, named FGFR1 to 4 respectively, which can bind to members of the FGF family of ligands and signal via activation of their catalytic kinase domains [Eswarakumar et al., 2005]. A related fifth receptor known as FGFR5 or FGFRL1 has also been described, but has no cytoplasmic kinase domain and is thought to negatively regulate signalling from other FGFRs by forming non-functional dimers [Wiedemann and Trueb, 2000].

Mammalian genomes encode for 22 FGF family members, 18 of which act as FGFR ligands (Table 1.1). The 4 FGF family members which do not bind to any FGFR (FGF11, FGF12, FGF13 and FGF14) are more correctly referred to as FGF homologous factors [Turner and Grose, 2010]. The majority of FGFR binding FGFs function as autocrine or paracrine ligands with HSPGs acting as their co-ligands. However, three FGF family members (FGF19, FGF21 and FGF23) function in an endocrine fashion as metabolic hormones. These family members do not associate with HSPGs and can diffuse from their secretion site into the circulation [Beenken and Mohammadi, 2009]. Instead, their interaction with FGFRs requires a transmembrane co-receptor known as Klotho [Kurosu and Kuro-o, 2008]. FGF mutations have been linked to a number of human diseases. These include loss of function germ-line mutations of FGF3 in deafness, FGF8 in Kallmann syndrome, and FGF10 in Lacrimo-auditory-dento-digital syndrome, as well as the gain of function mutations of the endocrine FGF23 in hypo-phosphataemic rickets [Beenken and Mohammadi, 2009].

All FGFs fold into a β-trefoil structure with 12 anti-parallel β strands split into three sheets (Figure 1.2) [Faham et al., 1996]. A positively charged Lysine/Arginine-rich region provides

the interaction surface with HSPGs, which are negatively charged (Figure 1.2). Interestingly, the amino acid sequence of the HSPG interacting region is significantly variable amongst different FGFs which probably accounts toward their differential affinity for HSPGs [Faham et al., 1996; Mohammadi et al., 2005].

1.2.1 Structure

Like all RTKs, FGFRs are composed of an N-terminal ligand binding extra-cellular portion, a single transmembrane helix, and a C-terminal cytoplasmic portion containing a Tyrosine kinase domain as well as additional regulatory segments [Eswarakumar et al., 2005]. The extracellular portion of FGFRs is consisted of three domains with immunoglobulin (Ig)-like folds named D1 to D3 [Plotnikov et al., 1999; Schlessinger et al., 2000] (Figure 1.3A). The linker connecting D1 and D2 domains has a stretch of eight negatively charged amino acids designated as the Acid Box (AB) [Plotnikov et al., 1999; Schlessinger et al., 2000]. A positively charged region involved in HSPG binding is present in D2, which is termed the Heparin Binding Site (HBS) [Plotnikov et al., 1999; Schlessinger et al., 2000] (Figure 1.3A). Ligand and HSPG binding is solely mediated by the D2, D3, and the linker region between them [Plotnikov et al., 1999; Schlessinger et al., 2000]. In fact, D1 and AB have been shown to have a negative impact on ligand binding and receptor activation by folding back and interacting with D2 and D3 ligand and HSPG binding surfaces [Wang et al., 1995; Olsen et al., 2004]. This provides an auto-inhibitory mechanism which ensures that the receptor remains in a self-sequestered inactive form until sufficient amounts of ligand is present to displace D1 and the acid box [Olsen et al., 2004; Mohammadi et al., 2005].

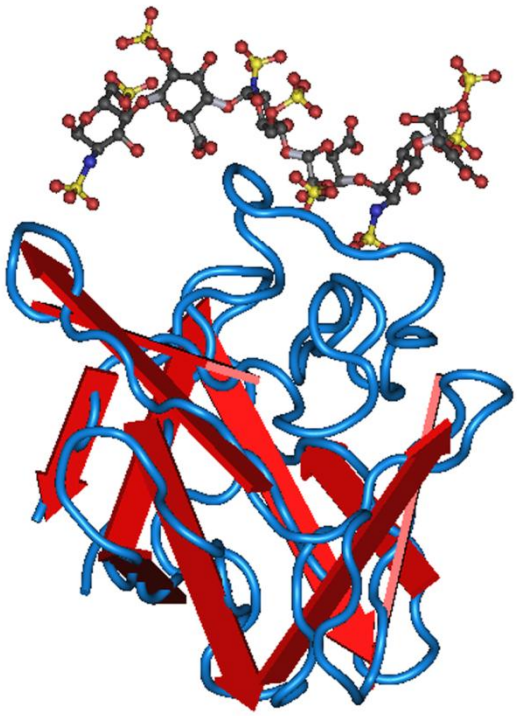

Figure 1.2. Crystal structure of FGF2 (beta sheets in red, back-bone in blue) with superposition of a hexasaccharide HSPG (balls on stick view). FGF2 exhibits a β-trefoil structure with 12 anti-parallel β strands split into three sheets. HSPGs make specific contacts with a Arginine/Lysine-rich loop. The X-ray structure was taken from Protein Data Bank (PDB ID: 1BFC).

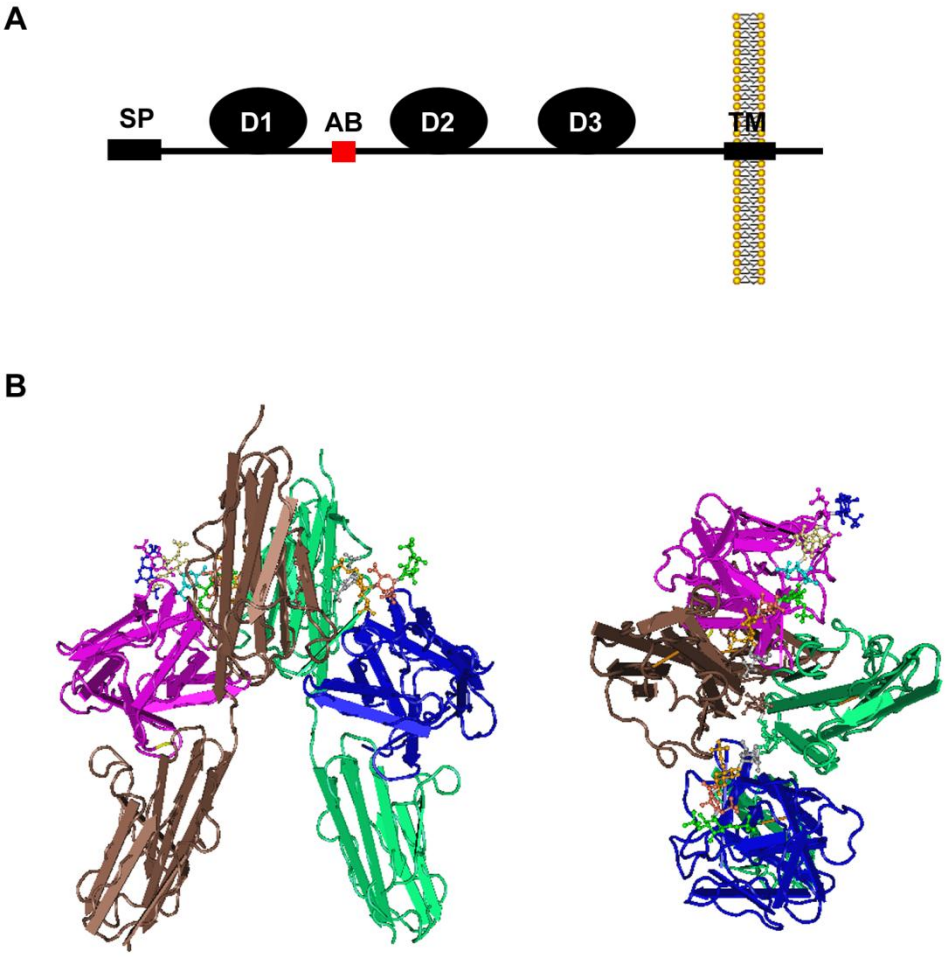

Figure 1.3. Structure of the extracellular portion of FGFR. Schematic representation of the extracellular portion of FGFRs with the membrane targeting signal peptide (SP), three Ig-like domains (D1 to D3), the acid box (AB), and the transmembrane (TM) region. D2, D3, and the linker region in between them provide FGF and HSPG binding while D1 and AB have an auto-inhibitory role **(A)**. The side view (Left) and top view (Right) of the X-ray crystal structure of FGFR1 D2 and D3 domains in complex with FGF and heparin. Each FGF molecule (shown in blue and purple) forms molecular contacts with both receptors (shown in brown and green), and each receptor also forms contacts with the other receptor via the end of their D2 domains. Two heparin molecules (shown in balls on a stick view) symmetrically bind to a positively charged canyon formed by HSPG interacting regions of the two FGF molecules and the D2 domains of two receptors **(B)**. The X-ray structure was taken from Protein Data Bank (PDB ID: 1FQ9).

The X-ray crystal structure of the extra-cellular portion of FGFR in ternary complex with FGF and Heparin has been solved, revealing a 2:2:2 stoichiometry with each ligand forming contacts with both receptors as well as the receptors forming contacts with each other through the end of their D2 domains (Figure 1.3B) [Schlessinger et al., 2000]. The HSPG interaction surface of the two FGFs as well as HBSs of the receptors form a positively charged groove which gets symmetrically occupied by two heparin molecules (Figure 1.3B) [Schlessinger et al., 2000]. Based on this structural data, heparin function must be to stabilise the binary interaction of an FGF with an FGFR molecule. This then indirectly facilitates receptor dimerisation as the secondary ligand-receptor and receptor–receptor interaction sites of the FGF-FGFR complex become stably available to attract another FGF-FGFR complex [Mohammadi et al., 2005]. It should be noted that, initially, some controversy surrounded this model as an independent structure showed a very different conformation, but it later became clear that this was due to an artefact created by a Proline *cis/trans* isomerisation event [Mohammadi et al., 2005].

The cytoplasmic part of FGFRs contains a juxta-membrane domain, a bi-lobed Tyrosine Kinase domain, and a C-terminal tail (Figure 1.4A) [Eswarakumar et al., 2005]. The juxta-membrane region of FGFRs is significantly longer than that of other RTKs, and serves as a binding site for the PTB domain of the docking protein FGF Receptor Substrate-2 (FRS2), also known as Suc1-Associated Neurotrophic factor Target 1 (SNT1) (Figure 1.4A) [Ong et al., 2000]. The PTB domain of FRS2 constitutively binds to the juxta-membrane region of FGFR1 in a phosphorylation independent manner [Ong et al., 2000]. In addition to FGFRs, FRS2 proteins also associate with a limited number of other RTKs such as TrkA, TrkB, RET, and ALK, but unlike their constitutive binding to FGFRs, binding of FRS2s to these receptors is dependent on phosphorylation of specific Tyrosine residues on the receptor which act as

PTB binding sites [Gotoh, 2008]. Two FRS2 family members named FRS2α and FRS2β exist in mammals with different expression profiles suggestive of distinct developmental roles [Gotoh, 2008]. Both proteins contain an array of Tyrosine residues which get phosphorylated by the receptor and act to recruit other phospho-Tyrosine interacting signalling proteins [Gotoh, 2008].

Similar to other RTKs such as PDGFR and c-Kit, the tyrosine kinase domain of FGFRs is bi-lobed, but the kinase insert region is considerably shorter in FGFRs compared to PDGFR or c-Kit [Eswarakumar et al., 2005]. The X-ray crystal structure of FGFR1 kinase domain has been determined, revealing the molecular details of how the kinase activity is regulated [Mohammadi et al., 1996b] (Figure 1.4B). Similar to other RTKs, the C-terminal lobe of the catalytic domain forms an activation loop which blocks the substrate binding site and keeps the kinase inactive in the absence of ligand [Mohammadi et al., 1996b] (Figure 1.4B). After ligand binding and receptor dimerisation, the activation loop is displaced and two conserved Tyrosine residues within the loop (Y653/Y654) are trans-autophosphorylated. These phosphorylations are necessary to keep the activation loop away from the substrate binding site, thus maintaining the kinase activity (Figure 1.4A and B) [Mohammadi et al., 1996b].

The C-terminal tail of FGFR contains a conserved Tyrosine residue (Y766) which is also a substrate for trans-autophosphorylation. Once phosphorylated, this residue acts as a specific binding site for the SH2 domain of Phospholipase-Cγ (PLCγ), leading to recruitment and activation of PLCγ at the plasma-membrane [Mohammadi et al., 1991; Mohammadi et al., 1992]. PLCγ then catalyses the hydrolysis of Phosphatidylinositol-4,5 phosphate (PI45P2), generating two signalling second messengers, Diacylglycerol (DAG) and Inositol(1,4,5)P3 (IP3), which in turn activate a number of downstream signalling cascades such as the PKC pathway [Mohammadi et al., 1991; Mohammadi et al., 1992].

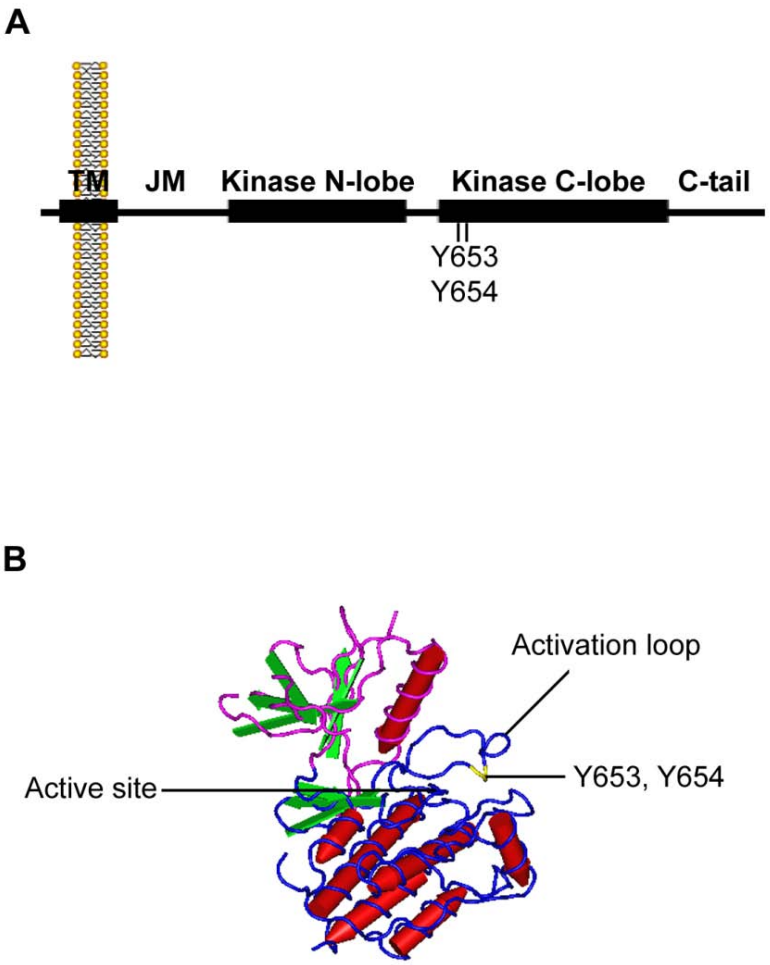

Figure 1.4. Structure of the intracellular portion of FGFR. Schematic representation of the cytoplasmic portion of FGFRs with the juxtamembrane domain (JM), the N-terminal and C-terminal lobes of the Tyrosine kinase domain (Kinase N- and C- lobes), and the C-terminal tail (C-tail) region. Phosphorylation of the pivotal Tyrosine residues (Y653 and Y654) of the activation loop is essential for maintainance of kinase activity **(A)**. The X-ray crystal structure of FGFR1 kinase domain showing the N-terminal lobe (purple), the C-terminal lobe (blue), and the pivotal Tyrosines of the activation loop (yellow). In the non-stimulated state, activation loop blocks the active site of the enzyme, restricting substrate access. Beta sheets are represented in green and alpha helices in red **(B)**. The X-ray structure was taken from Protein Data Bank (PDB ID: 1FGK).

Recently, a crystal structure showing two kinase domains of FGFR2 caught in the act of trans-autophosphorylation of Y769, the equivalent of Y766 in FGFR1, was reported, revealing details of the molecular interactions the enzyme and substrate-acting kinases engage it in order to trans-autophosphorylate the C-terminal tail [Chen et al., 2008]. These interactions are surprisingly strong, widespread, and not limited to the catalytic active site of the phosphorylating kinase and the target phosphorylation motif of the other [Chen et al., 2008].

1.2.2 Alternative splicing

An important feature of the FGFR family is its diversification by alternative splicing of its RNA transcripts. Alternative splicing can result in production of truncated secreted FGFRs as well as receptors that lack the auto-inhibitory D1 domain [Eswarakumar et al., 2005]. Another functionally significant alternative splicing event results in presence or absence of two consecutive residues (Valine-Threonine or VT) in the juxta-membrane region of FGFRs that are crucial for FRS2 binding [Burgar et al., 2002]. As FRS2 is pivotal for full activation of signalling cascades such as ERK1/2 downstream of FGFRs, the signalling potential of the receptor is significantly affected by this splicing event [Burgar et al., 2002]. But perhaps the most profound alternative splicing event is that of the D3 domain of FGFR1, 2 and 3. The N-terminal half of D3 is coded by exon 7 of FGFR1-3 whereas the C-terminal half can be coded by either exon 8 or 9 depending on the alternative splicing. The product D3 domain is designated IIIb if transcribed from exon 8, and IIIc if transcribed from exon 9 [Eswarakumar et al., 2005]. The IIIb and IIIc isoforms exhibit different ligand specificities (Table 1.1). Moreover, the two isoforms also display distinct developmental expression patterns [Eswarakumar et al., 2005]. For instance, FGFR2-IIIb, also known as Keratinocyte Growth

Factor Receptor (KGFR), is exclusively expressed in epithelial cells while FGFR2-IIIc is exclusively mesenchymal, allowing for differential interpretation of FGF signals by epithelial and mesenchymal cells during development [Orr-Urtreger et al., 1993].

1.2.3 FGFRs in development and disease

Mouse knockouts of most FGFs, and all FGFRs including individual isoforms have been generated, revealing a multitude of developmental processes that depend on FGF signalling (Table 1.2). At the very early stages of embryogenesis, signalling by FGF4 is crucial for regulation of Inner cell mass (ICM) proliferation and differentiation potential [Feldman et al., 1995; Kunath et al., 2007]. Targeted disruption of FGFR2 shows comparable ICM defects, suggesting that FGF4 signalling during early embryogenesis is probably mediated via this receptor [Arman et al., 1998]. FGF4 is also important for maintenance of the trophoblast, which gives rise to placenta in mammals [Tanaka et al, 1998]. In addition, FGF signalling plays a crucial role during gastrulation and mesoderm induction. Early studies in *Xenopus* embryos showed that interference with FGFR signalling disrupted mesoderm formation [Amaya et al., 1991]. Knockout studies in mice similarly revealed FGF signalling involvement in mammalian gastrulation with defects in cell migration through primitive streak due to loss of FGFR1 IIIc [Deng et al., 1994; Yamaguchi et al., 1994; Partanen et al., 1998]. A similar defect in gastrulation was observed with loss of FGF8 [Meyers et al., 1998; Sun et al., 1999], though several other problems in brain, heart, and craniofacial development were also detected (Table 1.2) [Meyers et al., 1998].

FGFR isoform	FGF specificity
FGFR1-IIIb	FGF1, 2, 3, and 10
FGFR1-IIIc	FGF1, 2, 4, 5 and 6
FGFR2-IIIb	FGF1, 3, 7, 10, and 22
FGFR2-IIIc	FGF1, 2, 4, 6, 9, 17 and 18
FGFR3-IIIb	FGF1, and 9
FGFR3-IIIc	FGF1, 2, 4, 8, 9, 17, 18 and 23
FGFR4	FGF1, 2, 4, 6, 8, 9, 16, 17, 18 and 19

Table 1.1. Ligand specificities for IIIb and IIIc isoforms of FGFRs. FGFR4 has a single D3 isoform. The table was adapted from [Eswarakumar et al., 2005].

In addition to its roles during early embryogenesis, FGF signalling is fundamental to a variety of later developmental processes such as neuronal and skin development [Meyers et al., 1998; Dono et al., 1998; Xu et al., 2000], limb formation [Cohn et al., 1995; Xu et al., 1998], lung development [Min et al., 1998; De Moerlooze et al, 2000; Colvin et al., 2001], hair and kidney development [Guo et al., 1996], muscle regeneration [Floss et al., 1997], heart development [Meyers et al., 1998; Lu et al., 2008], and skeletal system development [Colvin et al., 1996; Meyers et al., 1998; Liu et al., 2002; Ohbayashi et al., 2002; Eswarakumar et al., 2002] (Table 1.2). While loss of some FGFs such as FGF8 and 10 shows a wide range of defects suggestive of a broad functionality spectrum, others result in very specific phenotypes indicative of highly specialised roles (Table 1.2). Examples of the latter include a specific long hair "angora" phenotype due to loss of FGF5 [Hebert et al., 1994], or a midline cerebral development defect due to loss of FGF17 [Xu et al., 2000]. In addition, knockout of some FGFs and FGFRs does not result in any obvious phenotype (Table 1.2), suggesting that their function is possibly compensated by other family members.

Knockout	Lethality	Phenotype		Knockout	Lethality	Phenotype
FGF1	Viable	No phenotype		**FGF16**	E11.5	Heart defects
FGF2	Viable	Neuronal, skeletal and skin defects		**FGF17**	Viable	Midline cerebral development defects
FGF3	Viable	Inner ear, tail outgrowth		**FGF18**	Postnatal	Delayed ossification and increased chondrocyte proliferation; decreased alveolar spaces in the lung
FGF4	E5.5	ICM proliferation and differentiation, and Trophoblast maintenance defects		**FGF23**	Viable	Hyperphosphatemia, hypoglycemia, reduced bone density and infertility
FGF5	Viable	Long hair, "Angora" phenotype		**FGFR1**	E9.5	Gastrulation defects
FGF6	Viable	Muscle regeneration		**FGFR1 IIIb**	Viable	No obvious phenotype
FGF7	Viable	Hair follicle and kidney deficiency		**FGFR1 IIIc**	E9.5	Gastrulation defects
FGF8	E8.5	gastrulation, brain, heart and craniofacial defects		**FGFR2**	E10.5	ICM, placenta, and limb bud defects
FGF9	Postnatal	Lung defects, xy sex reversal		**FGFR2 IIIb**	Postnatal	Agenesis of lungs, anterior pituitary, thyroid, teeth and limb defects
FGF10	Postnatal	limbs, lungs, kidneys and other organ defects		**FGFR2 IIIc**	Viable	Delayed ossification, proportional dwarfism, synostosis of skull base
FGF14	Viable	Neurological phenotype-ataxia and a paroxysmal hyperkinetic movement disorder		**FGFR3**	Viable	Bone over growth; inner ear defect
FGF15	Viable	poor survival rate		**FGFR4**	Viable	No phenotype

Table 1.2. Mice knockout phenotypes of FGFs and FGFRs. The table was adapted from [Eswarakumar et al., 2005]. FGF16 phenotype was added from [Lu et al., 2008].

Germ-line mutations of FGFRs have been found as the underlying cause of several human diseases. The vast majority of these diseases are skeletal disorders, in line with the findings from mice which put FGF signalling at centre of the skeletal system development (Table 1.2). Most of these mutations are gain of function point mutations which result in enhanced kinase activity of the receptor [Wilkie, 1997; Webster and Donoghue, 1997]. Based on the mechanism by which they enhance kinase activity, such mutations can be divided into three

main categories. The first category is mutations which occur in the transmembrane and extracellular regions and cause receptor dimerisation in the absence of any ligand. Many of these mutations either substitute an existing Cysteine residue with a non-Cysteine amino acid, or substitute a non-Cysteine residue with a Cysteine. This causes an imbalance in the number of Cysteines which normally form intra-molecular disulphide bridges, leading to the formation of inter-molecular bridges between two neighbouring receptors instead [Wilkie, 1997; Webster and Donoghue, 1997]. Other mutations of this category, although not being directly involved in disulphide bond formation, affect the protein structure in such a way that destabilises intra-molecular disulphide bonds, thereby favouring inter-molecular bond formation [Wilkie, 1997; Webster and Donoghue, 1997]. The second category of mutations belongs to those which simply increase the affinity of the receptor for a given ligand, thus resulting in enhanced kinase activity [Wilkie, 1997; Webster and Donoghue, 1997]. These mutations are restricted to the extracellular ligand binding domains, and usually affect the ligand specificity of the mutated receptors as well [Anderson et al., 1998; Yu et al., 2000; Ibrahimi et al., 2001]. The third category of mutations is those which occur in the kinase domain and result in enhanced kinase activity in the absence of receptor dimerisation. Such mutations are mainly restricted to the activation loop of the kinase domain, leading to its displacement and consequent availability of the active site in a similar manner to Y653/Y654 phosphorylation [Wilkie, 1997; Webster and Donoghue, 1997; Eswarakumar et al., 2005].

FGFR related skeletal disorders display varying degrees of cranial, limb, digital, and stature abnormalities, depending on the exact receptor type as well as the exact point mutation involved. For example, Pfeiffer syndrome, characterised by craniosynostosis (skull abnormality and protruding eyes due to premature fusion of cranial sutures) as well as broadened thumbs and toes, is caused by gain of function mutations in the extracellular part of

FGFR1 [Wilkie, 1997; Eswarakumar et al., 2005]. Amongst many others, one of the identified mutations is a Proline to Arginine substitution (P252R) [Zhou, et al., 2000] which belongs to the second category of mutation mentioned above and changes ligand specificity as well as increasing the receptor affinity for its ligands [Anderson et al., 1998; Yu et al., 2000; Ibrahimi et al., 2001]. The equivalent mutation in FGFR2 (P253R) causes a different disorder called Apert syndrome, which is characterised by a severe symmetric fusion of hands and feet as well as craniosynostosis [Wilkie, 1997]. On the other hand, FGFR2 gain of function mutations which lead to receptor dimerisation by inter-molecular disulphide bond formation cause Crouzon or Jackson–Weiss syndromes [Wilkie, 1997]. Crouzon syndrome features include synostosis of coronal sutures, midface hypoplacia, and ocular proptosis, but no digital disorders [Wilkie, 1997]. Jackson-Weiss syndrome, in constrast, is characterised by craniosynostosis with foot abnormalities but no defects in hands [Eswarakumar et al., 2005].

Finally, gain of function mutations in FGFR3 cause slightly different disorders with mild or no detectable craniosynostosis but various limb and stature defects. Such FGFR3 mutations are the underlying cause of many skeletal dysplasia such as Hypochondroplasia (HCH), Achondroplasia (ACH), Thanatophoric dysplasia type I and II (TDI and TDII), and SADDAN (Severe Achondroplasia with Developmental Delay and Acanthosis Nigricans) [Eswarakumar et al., 2005]. ACH is the most common form of dwarfism characterised by short stature and midface deficiency [Webster and Donoghue, 1997]. HCH is a similar but slightly less severe disorder with short limbs and a large head circumference [Webster and Donoghue, 1997]. TDI is characterised by short curved femurs while TDII is characterised by Stright femurs with cloverleaf skull [Webster and Donoghue, 1997]. Both TDI and TDII are lethal [Eswarakumar et al., 2005]. FGFR3 mutations that cause SADDAN, HCH, and TDII are located in the

kinase domain [Eswarakumar et al., 2005]. For TDI and ACH, the mutations are within the transmembrane or extracellular domains [Eswarakumar et al., 2005].

In contrast to the above mentioned diseases which are caused by gain of function mutations of FGFRs, the autosomal dominant form of Kallmann syndrome (KAL2) is caused by somatic mutations of FGFR1 which impair its activity [Dode and Hardelin, 2004]. Kallmann syndrome is characterised by the absence of spontaneous puberty (hypogonadotropic hypogonadism) and lack of smelling sense due to underdevelopment of the olfactory bulb (anosmia) [Dode and Hardelin, 2004]. In the original type of Kallmann syndrome (KAL1), the disease is caused by an X-linked gene which encodes for a protein called Anosmin1, a modular heparin interacting glycoprotein present in the extracellular matrix [Franco et al., 1991; Legouis et al., 1991]. For KAL2, 15 different mutations of FGFR1 have been reported so far, all of which negatively affect FGFR1 activity [Dode and Hardelin, 2004]. Interestingly, wild-type but not KAL1 mutated Anosmin1 has been shown to enhance FGFR1 IIIc activity by forming a complex with the ligand and heparin bound receptors [González-Martínez et al., 2004; Hu et al., 2009]. Thus, both types of the Kallmann syndrome are either directly or indirectly linked to the impairment of FGFR1 activity.

1.2.4 FGFRs in cancer

At the cellular level, FGFR signalling controls crucial processes such as proliferation, differentiation, migration, and survival. It is, therefore, not surprising that aberrant FGFR acivity has been shown to be involved in pathogenesis of several cancer types [Turner and Grose, 2010]. Recently, the significance of FGFR signalling in tumourigenesis was further highlighted in a genomic screen of all kinases from 210 different human cancers [Greenman

et al., 2007]. The kinases of the FGF signalling pathway such as FGFRs and downstream MAPKs displayed the highest level of enrichment for non-synonymous mutations in these cancers [Greenman et al., 2007].

It has been proposed that deregulated FGFR signalling can contribute towards tumourigenesis in four major ways. First, it can enhance tumour cell proliferation. Second, it can promote tumour cell survival. Third, it can induce invasion and migration of the tumour cells, and last but not least, it can promote tumour angiogenesis [Turner and Grose, 2010]. Aberrant FGFR activity in tumour cells can be caused by a variety of means. These include activating point mutations, which lead to ligand independent dimerisation or constitutive kinase activation, similar to those found in FGFR related skeletal disorders [Turner and Grose, 2010]. Chromosomal translocations can also result in constitutive FGFR activity, usually by generating fusion proteins which contain the C-terminal kinase domain of FGFRs fused to the N-terminal of another protein with self-dimerisation tendency [Turner and Grose, 2010]. Gene amplification is another way by which cancer cells acquire ligand independent FGFR activation [Turner and Grose, 2010]. Gene amplification results in receptor overexpression above physiological levels [Turner and Grose, 2010], which can be auto-activating due to receptor-receptor inter-molecular interactions (Figure 1.3B) [Ong et al., 2000]. Over-expression of FGFRs due to epigenetic changes can similarly result in ligand independent receptor activation [Turner and Grose, 2010]. Finally, aberrant FGFR activity can be caused by an autocrine loop whereby the tumour cells produce and secrete the FGFs that they detect themselves [Turner and Grose, 2010].

Bladder cancer is the most well established type of cancer linked to activating FGFR mutations. Overall, around 50% of all bladder cancers bear somatic point mutations in the transmembrane or extracellular portion of FGFR3 [Cappellen et al., 1999]. The majority of

these somatic mutations are also found as germ-line mutations in TDI, and lead to ligand independent receptor dimerisation via intermolecular disulphide bond formation [Van Rhijn et al., 2002]. Some less common mutations are found within the kinase activation loop, resulting in constitutive activation independent of receptor dimerisarion [Munro and Knowles, 2003]. FGFR3 activating point mutations have also been found in other cancer types such as spermatocytic seminomas [Goriely et al., 2009], prostate cancer, multiple myeloma [Hernández et al., 2009], and cervical cancer [Rosty et al., 2005]. In addition to FGFR3, point mutations within the extracellular portion of FGFR2 have been identified in around 10% of endometrial carcinomas [Dutt et al., 2008]. Many of these FGFR2 mutations were identical to germ-line mutations found in Apert and Crouzon syndromes [Dutt et al., 2008].

Examples of FGFR gene amplifications are found in gastric and breast cancers. Approximately 10% of all gastric cancers harbour amplification of FGFR2 gene locus, and this correlates with poor prognosis [Takeda et al., 2007; Kunii et al., 2008]. On the other hand, amplification of a genomic region which contains FGFR1 locus occurs in around 10% of breast cancers [Courjal et al., 1997]. FGFR1 gene amplifications have also been identified in oral squamous carcinoma [Freier et al., 2007], ovarian cancer [Gorringe et al., 2007], bladder cancer [Simon et al., 2001], and rhabodomyosarcoma [Missiaglia et al., 2009].

With regards to FGFR related chromosomal translocations in cancer, several intragenic translocations which fuse the N terminal dimerisation part of a transcription factor to the C-terminal kinase domain of FGFRs have been reported in a number of different leukaemias and lymphomas [Xiao et al., 1998; Yagasaki et al., 2001; Roumiantsev et al., 2004]. In multiple myelomas which harbour a t(4;14) translocation (~10% of all multiple myelomas), the oncogenic mechanism is different as the chromosomal breakpoint is ~70 kb upstream of the FGFR3 gene [Chesi et al., 1997; Avet-Loiseau et al., 1998]. Instead of creating a dimer-

forming fusion protein, this translocation brings the FGFR3 gene under the control of the Immunoglobulin heavy chain (IGH) locus which is highly active in lymphoid cells, thus resulting in over-expression and consequent activation of FGFR3 [Chesi et al., 1997; Avet-Loiseau et al., 1998].

Examples of autocrine mediated FGFR activation in cancer include a number of melanomas that express high levels of FGFR1 and FGF2, resulting in creation of an FGF2–FGFR1 autocrine loop [Wang et al., 1997]. Interference with the expression of either FGFR1 or FGF2 results in inhibition of intra-tumoural angiogenesis and tumour regression in xenograft models of these melanomas [Wang et al., 1997]. An autocrine FGF2–FGFR1 loop has also been identified in non-small-cell lung cancer cells which exhibit resistance to anti-EGFR drugs [Marek et al., 2009]. Finally, FGF1 over-expression due to genetic amplification has been reported in a number of ovarian cancers, and it is possible that an autocrine FGF loop also exists in these cancers [Birrer et al., 2007].

Recently, a further link between FGFR signalling and cancer has been established through genome wide association studies. A number of Single Nucleotide Polymorphisms (SNPs) in FGFR2 were found to be significantly associated with a higher risk of breast cancer in European women [Easton et al., 2007; Hunter et al., 2007]. Surprisingly, rather than being located in a coding sequence, these SNPs were clustered in the second intron of FGFR2 [Easton et al., 2007; Hunter et al., 2007]. It remains to be determined how such minor intronic variations in the FGFR2 gene can result in increased breast cancer risk. In addition to the mentioned FGFR2 SNPs, an SNP in the FGFR4 gene, which results in substitution of a Glycine residue with an Arginine (G388R) in the extracellular portion of the receptor, has also been linked to cancer [Bange et al., 2002; Spinola et al., 2005]. This SNP does not increase the risk of developing cancer per se, but is instead associated with enhanced cancer

progression and poor prognosis in several cancer types [Bange et al., 2002; Spinola et al., 2005]. The means by which this allelic substitution (G388R) results in enhanced cancer progression is not fully clear, but increased cell motility and invasion as well as increased cancer resistance to chemotherapy are proposed as potential mechanisms [Bange et al., 2002; Thusbass et al., 2006].

1.3 Signalling from FGFRs

Ligand induced dimerisation of FGFRs results in kinase activation and trans-autophosphorylation of the cytoplasmic portion of the receptor. In addition to the receptor, the receptor associated docking protein FRS2 also gets phosphorylated on its several conserved Tyrosines as a result of receptor kinase activity. Phospho-Tyrosine residues on both FRS2 and the receptor then act as binding sites for SH2 and PTB domains of different signalling proteins which assemble into multi-protein signalling complexes, and function to activate various downstream signal transduction pathways, the collective action of which determines the cellular outcome to a given signal [Eswarakumar et al., 2005; Gotoh, 2008].

1.3.1 Autophosphorylation and assembly of signalling complexes

The cytoplasmic part of FGFR1 contains fifteen Tyrosine residues which could potentially undergo phosphorylation. Of these, seven residues (Y463, Y583, Y585, Y653, Y654, Y730, and Y766) were found as sites of autophosphorylation (Figure 1.5A) [Mohammadi et al., 1996a]. As mentioned earlier, Y653 and Y654 are situated within the activation loop of the kinase domain, and their phosphorylation is necessary for kinase activity (Figure 1.5A)

[Mohammadi et al., 1996b]. Y766, on the other hand, is situated in the C-terminal tail and mediates binding and activation of PLCγ (Figure 1.5A) [Mohammadi et al., 1991; Mohammadi et al., 1992]. Y463 resides in the juxtamembrane region and has been shown to bind to the SH2 domain of the adaptor protein CRK which mediates Jun N-terminal Kinase (JNK) and ERK1/2 signalling in endothelial cells (Figure 1.5A) [Larsson et al., 1999]. Y583 and Y585 are located within the insert region of the kinase domain while Y730 is located in the C-lobe of the kinase domain. The functional significance of these autophosphorylation residues is not clear.

Finally, a recent study by our group has also revealed that Y677, another tyrosine residue in the C-lobe of the kinase domain, could be phosphorylated to recruit and activate STAT-3, an SH2 domain containing transcription factor traditionally known to function downstream of the cytokine family of receptors (Figure 1.5A) [Dudka et al., 2010]. Y677 is not amongst the seven Tyrosine residues originally reported as FGFR autophosphorylation sites [Mohammadi et al., 1996a], so it remains to be determined whether it gets phosphorylated by the receptor itself or by another recruited kinase such as SRC. Interestingly, Y677 mediated STAT activation was specifically found in tumour cells that over-express FGFR due to gene amplification, suggesting it might be an important contributor to FGFR tumourigenesis [Dudka et al., 2010].

Studies of the dynamics of FGFR1 Tyrosine phosphorylation have revealed that autophosphorylation of the receptor occurs in a sequential and precisely ordered fashion [Furdui et al., 2006; Lew et al., 2009]. The first residue to undergo autophosphorylation is Y653 in the activation loop, resulting in 50 to 100 fold increase in the catalytic activity of the receptor [Furdui et al., 2006; Lew et al., 2009]. This leads to autophosphorylation of Y583, followed by Y463, Y766, and Y585 [Furdui et al., 2006; Lew et al., 2009]. Finally, the second

activation loop Tyrosine residue (Y654) is phosphorylated, resulting in an additional 10 fold increase in the kinase activity [Furdui et al., 2006; Lew et al., 2009]. Rather than being significant for receptor autophosphorylation, this additional enhancement of the kinase activity is thought to be important for efficient phosphorylation of other substrate proteins such as FRS2 and PLCγ [Furdui et al., 2006; Lew et al., 2009]. Interestingly, the precise order of autophosphorylation was found to be disrupted by a somatic point mutation in the kinase domain of FGFR1 that was present in some Glioblastomas, suggesting that a disruption of ordered autophosphorylation might be leading to aberrant oncogenic FGFR signalling in these Glioblastomas [Lew et al., 2009].

As mentioned earlier, members of the FRS2 family of docking proteins (FRS2α and FRS2β) are constitutively associated with the juxta-membrane region of FGFRs [Gotoh, 2008]. This interaction is mediated via the N-terminal PTB domain of FRS2s, despite being independent of receptor phosphorylation [Gotoh, 2008]. In addition to the PTB domain which mediates receptor binding, FRS2 family members contain a conserved myristoylation sequence in their N-termini which results in constitutive anchorage of the proteins to the plasma membrane (Figure 1.5B) [Kouhara et al., 1997; Gotoh et al., 2004]. The C-terminal of FRS2α has six Tyrosine phosphorylation sites, four of which are SH2 domain binding sites for the adaptor protein GRB-2 [Kouhara et al., 1997; Gotoh et al., 2004], and two are SH2 domain binding sites for the adaptor and Tyrosine phosphatase SHP-2 [Hadari et al, 1998; Gotoh et al., 2004] (Figure 1.5B). At the molecular level, FRS2α and FRS2β are highly similar. In fact, in Frs2α-null fibroblast cells, ectopic expression of Frs2β can compensate for the absence of Frs2α and restore the otherwise compromised FGFR signalling [Gotoh et al, 2004].

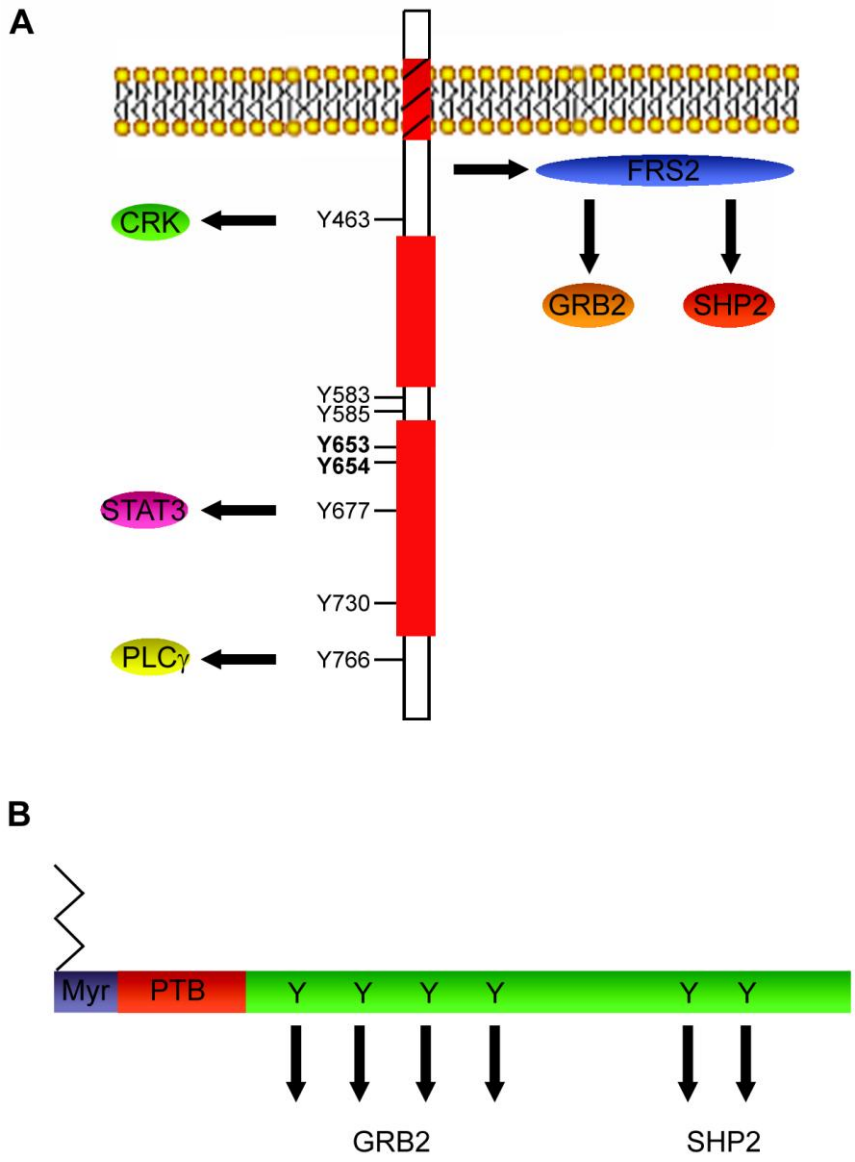

Figure 1.5. Schematic representation of FGFR1 signalling protein complex and FRS2. FGFR1 constitutively associates with the docking protein FRS2 while it recruits CRK, STAT3, and PLCγ via phosphorylation of Y463, Y677, and Y766 residues on the receptor, respectively. FRS2 in turn recruits GRB2 and SHP2 through its phosphorylation by the receptor. A total of eight phosphorylation sites on the receptor are known to exist. Y653/Y654 residues (indicated in bold) are activation loop phosphorylation sites needed for kinase activity **(A)**. FRS2 proteins contain an N-terminus myristoylation sequence which anchors the protein to the plasma membrane, a PTB domain which provides binding to FGFRs, and a C-terminal domain with several Tyrosine phosphorylation sites which act to recruit GRB2 and SHP2 **(B)**. FRS2α (depicted here) contains four GRB2 and two SHP2 SH2 binding sites.

Despite the structural and functional similarities of the two FRS2α and FRS2β, the embryonic expression patterns of the two proteins are drastically different [Gotoh et al, 2004]. While Frs2α is ubiquitously expressed throughout the development, Frs2β expression is strictly localised to certain tissues such as the neuroepithelium [Gotoh et al, 2004]. As no Frs2β mouse knockouts have been reported yet, the exact role of FRS2β in development is not clear. However, Frs2α mouse knockouts have been generated, with the embryos showing several defects in many FGF dependent early developmental processes which ultimately results in their lethality by E8 [Gotoh et al, 2005]. Such developmental processes include Inner Cell Mass (ICM) proliferation, trophoblast maintenance, and cell migration through the primitive streak, all of which depend on FGFs, further supporting the critical role of FRS2 in FGFR signalling [Gotoh et al, 2005].

1.3.2 Downstream signal transduction pathways

Through the variety of signalling proteins which FGFRs interact with, a number of downstream signal transduction pathways are ultimately activated. These include the RAS/ MAPK pathway [Kouhara et al., 1997], the PI3K/AKT pathway [Ong et al., 2001], PLC/PKC pathway [Mohammadi et al., 1991; Mohammadi et al., 1992], as well as the JAK/STAT pathway [Dudka et al., 2010]. The coordinated action of these and other signalling pathways result in the induction of a particular cellular outcome.

The RAS/MAPK cascade, also known the ERK1/2 pathway, is one of the most prominent signal transduction pathways activated downstream of FGFRs as well as other RTKs. Signalling through this cascade seems to be essential for most of the processes that are controlled by FGFRs during the development [Corson et al., 2003]. At the cellular level,

ERK1/2 signalling downstream of FGFRs is thought to be particularly important for induction of cell proliferation or differentiation [Turner and Grose, 2010]. FGFR dependent activation of the ERK1/2 pathway is mainly believed to be achieved through FRS2 dependent recruitment of GRB2 and SHP2 (Figure 1.6) [Eswarakumar et al., 2005; Gotoh, 2008]. GRB2 is a small adaptor protein with a central SH2 domain flanked by two Src Homology-3 (SH3) domains [Lowenstein et al., 1992]. The SH2 domain provides binding to specific phosphorylated Tyrosine residues such as those available on FRS2 while the SH3 domains provide constitutive binding to specific Proline-rich sequences on interacting proteins [Lowenstein et al., 1992]. The N-terminal SH3 domain of GRB2 is constitutively associated with a Guanine Nucleotide Exchange Factor (GEF) known as the Son of Sevenless (SOS) [Lowenstein et al., 1992]. As a result, recruitment of GRB2 also lead to concomitant recruitment of SOS to the membrane where it can activate RAS [Lowenstein et al., 1992], which is the first component of the RAS/MAPK - ERK1/2 – cascade (Figure 1.6) [Marshall, 1996].

RAS family of proteins are membrane anchored small GTPases which act as molecular switches downstream of many RTKs, and have been heavily implicated in a wide variety of cancers [Dhillon et al., 2007]. Three RAS family members, named K-RAS, H-RAS, and N-RAS, exist in mammals with distinct sub-cellular trafficking as well as varying oncogenic potentials [Dhillon et al., 2007]. When bound to GDP, RAS proteins are considered inactive, since they are incapable of interacting with their downstream effector proteins. However, when loaded with GTP, they undergo a conformational change which allows them to associate with their specific effector proteins [Marshall, 1996]. The GDP to GTP switch is facilitated by GEFs such as SOS while the hydrolysis of GTP to GDP is enhanced by GTPase Accelerating Proteins (GAPs) [Marshall, 1996].

The most well known effector proteins of RAS family members are RAF serine/threonine kinases, which are essential for ERK1/2 signalling (Figure 1.6) [Marshall, 1996]. Mammals contain three RAF homologues, named A-RAF, B-RAF, and C-RAF, which share significant similarity at the structural level but differ considerably in their tissue expression patterns and in vivo roles during development [Wellbrock et al., 2004; Galabova-Kovacs et al., 2006]. Furthermore, RAF family members significantly differ with regards to their RAS dependent activation as well as their signalling contribution to the ERK1/2 pathway [Wellbrock et al., 2004].

The mechanism of RAF activation is thought to be complex, involving RAS triggered membrane localization followed by rounds of phosphorylation and dephosphorylation, and changes in protein-protein interaction [Wellbrock et al., 2004]. For B-RAF, recruitment to the membrane by binding to GTP loaded activated RAS seems to be sufficient for triggering the full kinase activation *in vivo*. However, activation of C-RAF and A-RAF seem to be more strictly regulated and require additional factors [Wellbrock et al., 2004]. In line with these findings, oncogenic mutations of B-RAF but not C-RAF or A-RAF are highly common in malignant melanomas as well as with lower frequencies in many other cancer types [Dhillon et al., 2007].

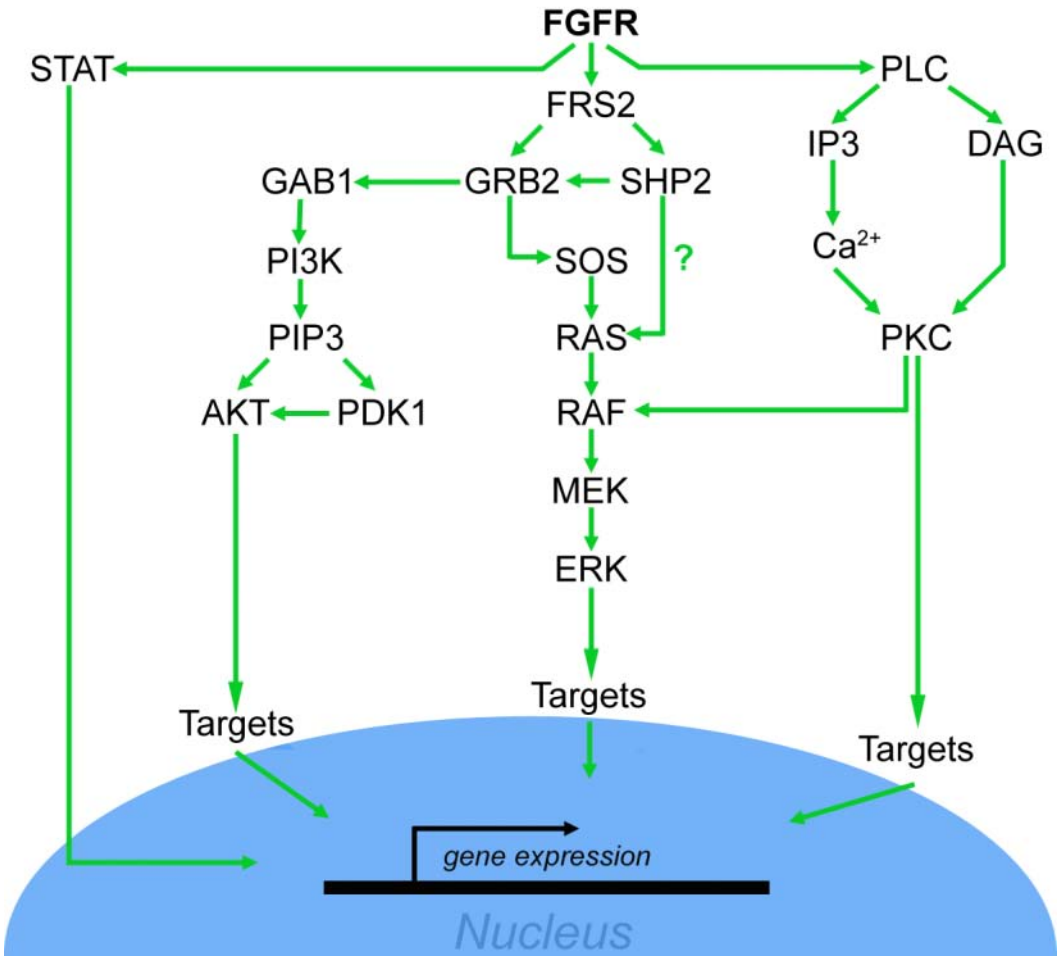

Figure 1.6. Wire diagram of FGFR downstream signal transduction pathways. The mechanism of SHP2 mediated RAS activation (indicated by a question mark) is currently unclear and subject to controversies. Once activated, AKT, ERK, and PKC phosphorylate an array of cellular targets including transcription factors as well as chromatin modifying and remodelling enzymes which results in changes of gene expression in the nucleus. STAT activation by FGFRs results in its translocation to the nucleus where it regulates gene expression. The diagram was adopted from [Eswarakumar et al., 2005] with modifications.

The only known kinase targets of RAF proteins are MAPK/ERK Kinases 1 and 2 (MEK1/2), the immediate upstream kinases of ERK1/2. Activated RAF phosphorylated MEK1/2 at two Serine residues within their activation loop which results in their activation. B-RAF is the strongest of all RAF homologues with regards to MEK activation [Marais et al., 1997]. Once activated, MEK1/2 phosphorylate ERK1 and ERK2 on both Tyrosine and Serine residues within their activation loop, thereby resulting in their activation and completion of the RAS/MAPK –ERK1/2 – cascade (Figure 1.6). Active ERK1/2 can in turn phosphorylate numerous cytoplasmic proteins, such as other kinases, phosphatases, and many cytoskeletal proteins. ERK1/2 can also translocate into nucleus and phosphorylate several transcription factors as well as chromatin modifying and remodelling enzymes, thus resulting in changes of gene expression, ultimately triggering processes such as cell-cycle progression or differentiation [Yoon and Seger, 2006].

As mentioned earlier, in addition to FRS2 dependent GRB2 recruitment, ERK1/2 pathway activation downstream of FGFRs in also mediated by SHP2 (Figure 1.6) [Eswarakumar et al., 2005; Gotoh, 2008]. In fact, knock-in mice in which SHP2 binding sites of FRS2α were mutated had much more severe phenotype than those which GRB2 binding sites were mutated, suggesting that signalling via SHP2 plays a more crucial role in FRS2 mediated developmental processes [Gotoh, 2008]. SHP2 is a Tyrosine phosphatase which contains two tandem SH2 domains through which it interacts with a number of RTKs as well as FRS2, a central Protein Tyrosine Phosphatase (PTP) domain, and a C-terminal tail which contains a number of Tyrosine phosphorylation sites [Matozaki et al., 2009]. Despite being a phosphatase which is recruited to activated receptor complexes, SHP2 is unusual as it acts as a positive regulator of signalling, promoting ERK1/2 activation downstream of multiple receptors [Matozaki et al., 2009]. The mechanism by which SHP2 promotes ERK1/2

signalling is subject to controversies. It was initially proposed that SHP2 could act as an adaptor protein independent of its enzymatic activity, binding to and recruiting more GRB2 proteins via its C-terminal tail Tyrosine phosphorylation sites [Kouhara et al., 1997; Hadari et al., 1998]. However, other studies have demonstrated that the phosphatase activity of SHP2 is essential for its enhancement of ERK1/2 signalling [Matozaki et al., 2009]. Three mechanisms have been proposed for how the phosphatase activity of SHP2 results in positive ERK1/2 regulation. First, SHP-2 was shown to promote RAS activation by dephosphorylating specific Tyrosine residues on RTKs as well as docking proteins which bind to and recruit a a RAS-GAP known as p120 [Matozaki et al., 2009]. Second, it was shown that SHP2 can dephosphorylate a crucial Tyrosine site on Sprouty family of ERK1/2 attenuators, resulting in their inactivation [Matozaki et al., 2009]. Finally, SHP2 was found to dephosphorylate a negative regulatory site on SRC family of kinases (SFKs), a group of cytoplasmic Tyrosine kinases which are crucial mediators of RTK signalling [Matozaki et al., 2009]. It is possible that a combination of all these mechanisms could be involved to varying degrees in SHP2 mediated ERK1/2 activation.

It should be noted that RAS family members are not the only small GTPases which can mediate RAF activation. Another Ras-like small GTPase known as RAP1 has also been shown to activate ERK1/2 via binding to and activating B-RAF but not C-RAF in certain cell-lined [Stork and Dillon, 2005]. RAP1 can be activated downstream of a wide variety of receptors, including RTKs and cytokine receptors, to regulate multiple cellular processes from adhesion and migration to cell proliferation and differentiation [Stork and Dillon, 2005]. A proteomics survey by our group identified RAP1 as an FGFR1 interacting partner, suggesting the potential involvement of this small GTPase in FGFR signalling [Vecchione et al., 2007].

In line with this, depletion of RAP1 in endothelial cells was recently shown to reduce FGF mediated ERK1/2 activation and inhibit FGF induced angiogenesis [Yan et al., 2008].

The PI3K/AKT signal transduction pathway is mainly known to counter apoptosis and enhance survival, but also affects motility, metabolism, cell size, and cell proliferation [Altomare and Testa, 2005]. Similar to the ERK1/2 pathway, activation of the PI3K/AKT pathway downstream of FGFRs requires FRS2 and GRB2 (Figure 1.6) [Ong et al., 2001; Hadari et al., 2001]. While the N-terminal SH3 domain of GRB2 binds SOS, its C-terminal SH3 domain constitutively binds to the GRB2 Associated Binder-1 (GAB1), a multi-domain docking protein with numerous Tyrosine phosphorylation sites in its C-terminal which are phosphorylated following its co-recruitment to FRS2 via GRB2 (Figure 1.6) [Ong et al., 2001; Hadari et al., 2001]. One of these Tyrosine phosphorylated residues on GAB1 then acts as a specific binding site for the SH2 domain of the 85 kDa subunit of PI3K (Figure 1.6) [Ong et al., 2001]. PI3K is a heterodimer consisted of an 85 kDa regulatory subunit and a 110 kDa catalytic subunit which phosphorylates the membrane lipid Phosphatidylinositol 4,5-phosphate (PIP2) on the 3-OH position to generate Phosphatidylinositol 3,4,5-phosphate (PIP3) [Woodgett, 2005]. PIP3 is specifically recognised by the Pleckstrin Homology (PH) domain of the Serine/Threonine kinase AKT, also known as Protein Kinase B (PKB), resulting in its recruitment to the plasma-membrane (Figure 1.6) [Woodgett, 2005]. Similarly, another Serine/Threonine kinase known as Phosphoinositide-Dependant Kinase 1 (PDK1), which is constitutively active, is recruited to the plasma-membrane via its PH domain [Woodgett, 2005]. This brings AKT and PDK1 into proximity, resulting in phosphorylation of a conserved Threonine residue (T308) in the activation loop of AKT by PDK1 (Figure 1.6) [Woodgett, 2005]. Phosphorylation of this Threonine as well as another residue located in the C-terminal of AKT (S473) triggers its kinase activation, although it is a matter of controversy

which kinase or kinases are responsible for S473 phosphorylation [Woodgett, 2005]. It should be noted that apart from the mentioned route via GAB1, PI3K has also been shown to be activated via RAS through its direct interaction with RAS-GTP [Rodriguez-Viciana et al., 1994]. However, the relevant contribution of this pathway towards FGFR mediated PI3K/AKT signalling has not been investigated.

Similar to ERK1/2, once activated, AKT can phosphorylate and regulate a wide variety of cellular proteins in the cytoplasm as well as nucleus, many of which are critical regulators of apoptosis (such as BAD, pro-CASPASE-9, and FOXO transcription factors) or key regulators of cell-cycle (such as, Glycogen Synthase Kinase-3 (GSK-3), p21, and p27). AKT activity also results in activation of the mammalian Target of Rapamycin (mTOR) which is a key regulator of protein synthesis and cell growth [Altomare and Testa, 2005].

In contrast to ERK1/2 and PI3K/AKT pathways, activation of PLC/PKC cascade does not rely on FRS2 and GRB2 (Figure 1.6). As mentioned before, the conserved Y766 autophosphorylation site in the C-terminal tail of FGFRs functions as a specific binding site for the SH2 domain of PLCγ, leading to its recruitment and subsequent phosphorylation and activation at the plasma-membrane [Mohammadi et al., 1991; Mohammadi et al., 1992]. Recruitment of PLCγ is further aided by PI3K mediated generation of PIP3, as PLCγ also contains a PH domain which can interact with PIP3 [Falasca et al., 1998]. Once localised to the plasma-membrane, PLCγ catalyses the hydrolysis of the membrane lipid PIP2 to generate Diacylglycerol (DAG) and Inositol(1,4,5)P3 (IP3), which ultimately result in activation of PKC family of Serine/Threonine kinases (Figure 1.6) [Mohammadi et al., 1991; Mohammadi et al., 1992]. There are nine PKC isoforms which can be categorised into three groups. The first group are the classical PKCs (PKCα, PKCβ, and PKCγ) which require binding to DAG as well as calcium for their activation. The second group are novel PKCs (PKCδ, PKCε,

PKCθ, and PKCη) which only require binding to DAG for activation. The final group are atypical PKCs (PKCζ and PKCι) which are not responsive to either DAG or calcium and therefore are not activated downstream of PLC [Griner and Kazanietz, 2007]. IP3 triggers release of calcium from ER into the cytoplasm which is required for activation of classical PKCs, while DAG binds to the regulatory region of both classical and novel PKCs and induces a conformational change that exposes their active site, thus resulting in kinase activation (Figure 1.6) [Griner and Kazanietz, 2007]. Similar to ERK1/2 and AKT, once activated, PKCs can phosphorylate diverse targets involved in various cellular processes such as cell-cycle progression, motility, and differentiation [Griner and Kazanietz, 2007]. Interestingly, PKC also feeds into the ERK1/2 pathway by phosphorylating and activating RAF independent of RAS (Figure 1.6) [Kolch et al., 1993; Ueda et al., 1996], as well as enhancing RAS dependent RAF activation [Marias et al., 1998]. At the cellular level, however, PLC/PKC pathway seems to be dispensable for FGFR induced cell proliferation [Mohammadi et al., 1992]. Nevertheless, analysis of knock-in mice which have Y766 mutated FGFR1 has revealed that this site specifically involved in anteroposterior patterning, though this was not shown to be PLC dependent and could, therefore, be through recruitment of another Y766 intracting partner [Partanen et al., 1998].

Finally, amongst the signalling pathways activated downstream of FGFRs is the JAK/STAT pathway. Signal Transducers and Activators of Transcription proteins (STATs) are transcription factors which are traditionally known to be recruited to cytokine receptors via their SH2 domains. Once recruited to the activated receptors, STATs get phosphorylated by the cytokine receptor associated Tyrosine kinase JAK, which induces their dimerisation and subsequent translocation to the nucleus where they regulate gene expression [Lim and Cao, 2006]. Activation of STATs downstream of the FGFRs had been observed for some time but

the molecular mechanism was not clear [Hart et al., 2000]. Recently, work in our group revealed that STAT3 could be recruited to FGFR1 via a conserved Tyrosine residue (Y677) within the C-lobe of the Tyrosine kinase domain, and this results in STAT3 Tyrosine phosphorylation and activation in an FGFR, SRC, and JAK kinase dependent manner (Figure 1.6) [Dudka et al., 2010]. As mentioned earlier, STAT activation was specifically found in tumour cells that over-express FGFRs due to gene amplification, suggesting it might be an important oncogenic contributor to FGFR dependent tumourigenesis [Dudka et al., 2010].

1.4 Signalling regulation

Like all other RTKs, FGFR signalling is under tight control by diverse groups of signalling modulators which function at multiple levels to regulate the signalling output. However, the molecular mechanisms involved in regulation of FGFR signalling are only beginning to be understood. At the receptor activation level, several internal features of FGFRs such as their extracellular auto-inhibitory regions as well as the kinase activation loops regulate signalling initiation. Various proteins also exist which modulate receptor activation by affecting receptor-ligand interactions. Another key group of FGFR signalling regulators are Tyrosine phosphatases which attenuate signalling by counteracting the kinase activity of the receptors. Furthermore, a multitude of positive and negative feedback mechanisms, which act to shape the temporal profile of signalling, have been identified downstream of FGFRs. These include negative feedback regulation by Sprouty family of signalling attenuators which is the main focus of this thesis. Finally, by means of spatial compartmentalisation, endocytic trafficking of the receptors provides a crucial platform for selective signal regulation the extent of which has become evident only very recently.

1.4.1 Auto-inhibition, ligand binding, and dephosphorylation

As mentioned earlier, two auto-inhibitory mechanisms ensure that FGFR activity is kept low in the absence of significant ligand concentrations. First mechanism is mediated via the extracellular D1 domain and the Acid box (AB) in the D1-D2 linker. In the absence of FGF, D1 folds back and interacts with the ligand binding site in the D2 and D3 domains while AB interacts with the basic heparin binding site (HBS) in the D2 region [Wang et al., 1995; Olsen et al., 2004]. Sufficient ligand concentrations disrupt these auto-inhibitory interactions, thus mediating receptor activation [Schlessinger, 2003]. The second and the more crucial auto-inhibitory region is the activation loop within the kinase domain which occupies the active site, thus blocking substrate access and Tyrosine phosphorylation [Mohammadi et al., 1996b]. Receptor dimerisation induces a conformational change which causes displacement of the activation loops followed by its trans-autophosphoryaltion on the two conserved Tyrosine residues (Y653 and Y654). Phosphorylation of these residues stabilises the activation loop conformation away from the substrate binding site which is key to maintain the kinase activity [Mohammadi et al., 1996b]. As discussed earlier, the importance of FGFR auto-inhibition via the kinase activation loop is demonstrated by the fact that mutations within this region which lead to displacement of the loop from the active site are found in a number of skeletal dysplasia as well as certain cancer types [Wilkie, 1997; Webster and Donoghue, 1997; Munro and Knowles, 2003].

A number of proteins act at the level of ligand-receptor interaction to modulate the activity of RTKs. A very well known example is Argos, an EGF-like secreted protein in *Drosophila* which competes with EGF for binding to EGFR, thus inhibiting EGFR activity [Jin et al.,

2000]. In the context of FGFR signalling, an example of regulation at the ligand-receptor interaction level is that of Anosmin1. As mentioned earlier, Anosmin1 is an extracellular modular glycoprotein that binds to FGFR1-FGF-Heparin ternary complex, and enhances signalling by stabilising this complex [González-Martínez et al., 2004; Hu et al., 2009]. The ability of Anosmin1 to diffuse through the extracellular matrix makes it a potential patterning factor which can further define the distribution of FGFR1 activity in specific tissues and organs [Hu et al., 2009].

Finally, Protein Tyrosine Phosphatases (PTPs) with the exception of SHP2 are thought to play a crucial role in negative regulation of FGFRs activity. Even in the absence any ligand, nearly all RTKs can be artificially activated by treating the cells with PTP inhibitors, which clearly demonstrates the key role of these proteins in counteracting the basal activity of RTKs [Schlessinger, 2000]. Mammals contain round 100 PTP genes, which is round same number of genes which encode for protein tyrosine kinases, suggesting a comparable level of complexity and regulation between the two antagonising families [Ostman et al., 2006]. Similar to Tyrosine kinases, PTPs can be divided into two groups of receptor-like and non-receptor-like phosphatases, with the former containing a single transmembrane region as well as variable extracellular domains [Ostman et al., 2006]. Specific family members from both receptor-like and non-receptor-like PTPs have been implicated in negative regulation of RTKs. For some RTKs, more than one PTP has been shown to be required for receptor dephosphorytion. For example, PDGFR dephosphorylation and inactivation has been shown to be mediated by DEP1 and PTPN2, the former is a receptor-like PTP and the later a non-receptor-like PTP [Ostman et al., 2006]. On the other hand, a single PTP might be involved in dephosphorylation of more than one RTK. For instance, PTP1B has been shown to dephosphorylate and inactivate both IR and EGFR [Ostman et al., 2006]. In addition,

individual PTPs can exhibit site-selectivity on their target RTKs, thus resulting in pathway specific signalling inhibition [Ostman et al., 2006]. The identity of FGFR phosphatases is currently unknown. It remains to be determined which PTPs dephosphorylate different FGFRs, and whether their activity is subject to deregulation in any FGFR related diseases and malignancies. However, LAR, a widely expressed receptor-like PTP, has been shown to specifically dephosphorylate FRS2, thus resulting in abrogation of ERK1/2 activation downstream of FGFRs [Wang et al., 2000]. Accordingly, LAR does not have any effect on EGF mediated ERK1/2 signalling [Wang et al., 2000].

1.4.2 Feedback regulation

A large number of regulatory mechanisms that act upon RTK signalling are triggered by the activation of RTKs themselves, thereby acting as feedback loops (Figure 1.7). Such feedback modes of regulation are crucial for defining the amplitude and duration of signalling and therefore a fundamental feature of RTK signalling. In the context of FGFR signalling, several feedback regulatory mechanisms with varying temporal profiles and pathway specificities have been identified. At the most immediate level, ERK1 and 2 kinases have been shown to phosphorylate FRS2 on a number of Serine/Threonine residues. This inhibits Tyrosine phosphorylation of FRS2, thus abrogating GRB2 and SHP2 recruitment and continuous ERK1/2 activation (Figure 1.7) [Gotoh, 2008]. Another layer of feedback inhibition is provided by Casitas B-lineage Lymphoma (CBL), a well known ubiquitin ligase involved in down-regulation of many RTKs by catalysing their ubiquitination which triggers receptor endocytosis and degradation in the lysosomes [Thien and Langdon, 2001]. The best studied case is EGFR down-regulation, where CBL is directly recruited via binding of its modified

SH2 domain to a conserved Tyrosine phosphorylation site (Y1045) on the receptor [Thien and Langdon, 2001]. In the case of FGFRs, CBL is indirectly recruited via FRS2 and GRB2 (Figure 1.7) [Wong et al., 2002b]. The N-terminal SH3 domain of GRB2 can bind to a conserved Proline-rich region within CBL, thus co-recruiting CBL which then ubiquitinates both the receptor and FRS2, triggering their endocytosis and subsequent degradation (Figure 1.7) [Wong et al., 2002b]. However, it should be noted that ligand induced FGFR endocytosis and degradation is only a partially affected by loss of FRS2α [Wong et al., 2002b]. This suggests that other FRS2 independent mechanisms of endocytosis must also exist, the identity of which remains to be determined. Regulation of FGFR signalling via endocytic trafficking of the receptors will be discussed in more detail later in this chapter.

Finally, a significant number of genes are induced downstream of RTKs which function as regulators of signalling themselves, thereby creating another layer of feedback loops. In the context of FGFR signalling, examples include genes for Sprouty proteins (SPRYs), MAPK phosphatases (MKPs) also known as Dual Specificity Phosphatases (DUSPs), Similar Expression to FGF proteins (SEFs), as well as Fibronectin-Leucine-Rich Transmembrane proteins (FLRTs) (Figure 1.7). Sprouty proteins are discussed in great detail later within this chapter. MKPs are a family of ten phosphatases induced by MAPKs that act to dephosphorylate and inactivate them [Owens and Keyse, 2007]. In particular, MKP3 was shown to act as a negative feedback regulator of ERK1/2 downstream of FGFR signalling (Figure 1.7) [Owens and Keyse, 2007]. Consistent with a specific FGFR-related role, mice lacking MKP3 exhibit skeletal dwarfism, craniosynostosis, and hearing loss [Li et al., 2007]. Nevertheless, the relative mildness of these phenotypes suggests that there could be some functional redundancy between MKP3 and other ERK1/2 feedback regulators downstream of FGFRs, including potentially other MKP family members [Li et al., 2007].

As implied by its name, Sef was initially discovered in a zebrafish in situ hybridization screen as a gene whose expression pattern strongly resembled that of FGF family members [Furthauer et al., 2002; Tsang et al., 2002]. Sef expression domains during chick and mouse embryogenesis were also found to heavily overlap with those of FGFs [Lin et al., 2002; Harduf et al., 2005]. This was due to the fact that Sef expression was specifically induced by FGFR signalling [Furthauer et al., 2002; Tsang et al., 2002; Lin et al., 2002; Harduf et al., 2005]. In zebrafish, the ERK1/2 pathway was found to be particularly important for induction of Sef, but the identity of downstream signalling pathways responsible for mammalian Sef induction have not been revealed yet [Ron et al., 2008]. A single Sef gene exists in all vertebrates, which encodes for a transmembrane protein with an extracellular portion consisted of an Ig-like domain as well as a fibronectin repeat, a single transmembrane α-helix, and an intracellular portion consisted of a conserved juxta-membrane Tyrosine phosphorylation site as well as a SEF Interleukin17 Receptor-homology (SEFIR) domain [Ron et al., 2008]. In mammals, an array of different isoforms such as secreted as well as cytosolic ones are generated by alternative splicing with divergent functional properties [Ron et al., 2008]. All Sef isoforms seem to be capable of interacting with FGFRs. However, Sef point of interception with FGFR signalling and its mechanism of action seems to be variable depending on the species, the exact splice isoform involved, and the cellular context within which it functions (Figure 1.7) [Ron et al., 2008]. For instance, while zebrafish Sef specifically acts to inhibit the ERK1/2 pathway, different mammalian isoforms have varying capacities to modulate the activity of ERK1/2, PI3K/AKT, p38, and JNK cascades, in a cell-type dependent manner [Ron et al., 2008].

Unlike in zebrafish, loss of Sef in mouse by genetic knockout does not result in any severe developmental defects [Lin et al., 2005; Abraira et al., 2007]. This might be either due to

incomplete loss of Sef expression or some functional redundancy between Sef and other feedback regulators of FGFR signalling such as Sproutys [Lin et al., 2005; Abraira et al., 2007]. In contrast, Sef seems to be important with regards to tumour suppression in adulthood. SEF expression is either lost or considerably reduced in the majority of human breast, ovary, prostate, and thyroid tumours [Ron et al., 2008]. The mechanism of SEF down-regulation in these cancer types remains to be determined.

FLRTs are different from all the above mentioned feedback regulators of FGFR signalling as they potentiate signalling downstream of FGFRs rather than inhibiting it (Figure 1.7). Three FLRT family members, designated FLRT 1, 2 and 3, exist in vertebrates which contain an extracellular fibronectin and leucine-rich repeat region involved in homotypic cell-cell adhesion, a single transmembrane α-helix, and a short cytoplasmic region without any known conserved domains or motifs [Böttcher et al., 2004; Haines et al., 2006; Wheldon et al., 2010]. In *Xenopus* FLRT3 was shown to be specifically induced by FGF signalling, and enhanced ERK1/2 signalling but not PI3K/AKT signalling downstream of FGFRs [Böttcher et al., 2004]. All mammalian FLRT family members were also revealed to exhibit distinct, highly restricted embryonic expression patterns, which significantly overlapped with centres of FGF signalling [Haines et al., 2006]. Moreover, all mammalian FLRTs were induced in response to FGF in cultured cells [Haines et al., 2006], and FLRT1 was demonstrated to be capable of enhancing FGF mediated ERK1/2 signalling in these cells [Wheldon et al., 2010]. FLRTs can interact with FGFR1 [Böttcher et al., 2004; Haines et al., 2006; Wheldon et al., 2010], and this seems to result in their phosphorylation on specific Tyrosine residues mutations of which leads to ligand independent ERK1/2 activation [Wheldon et al., 2010]. The exact molecular mechanism of signal propagation by FLRT family members remains to be determined.

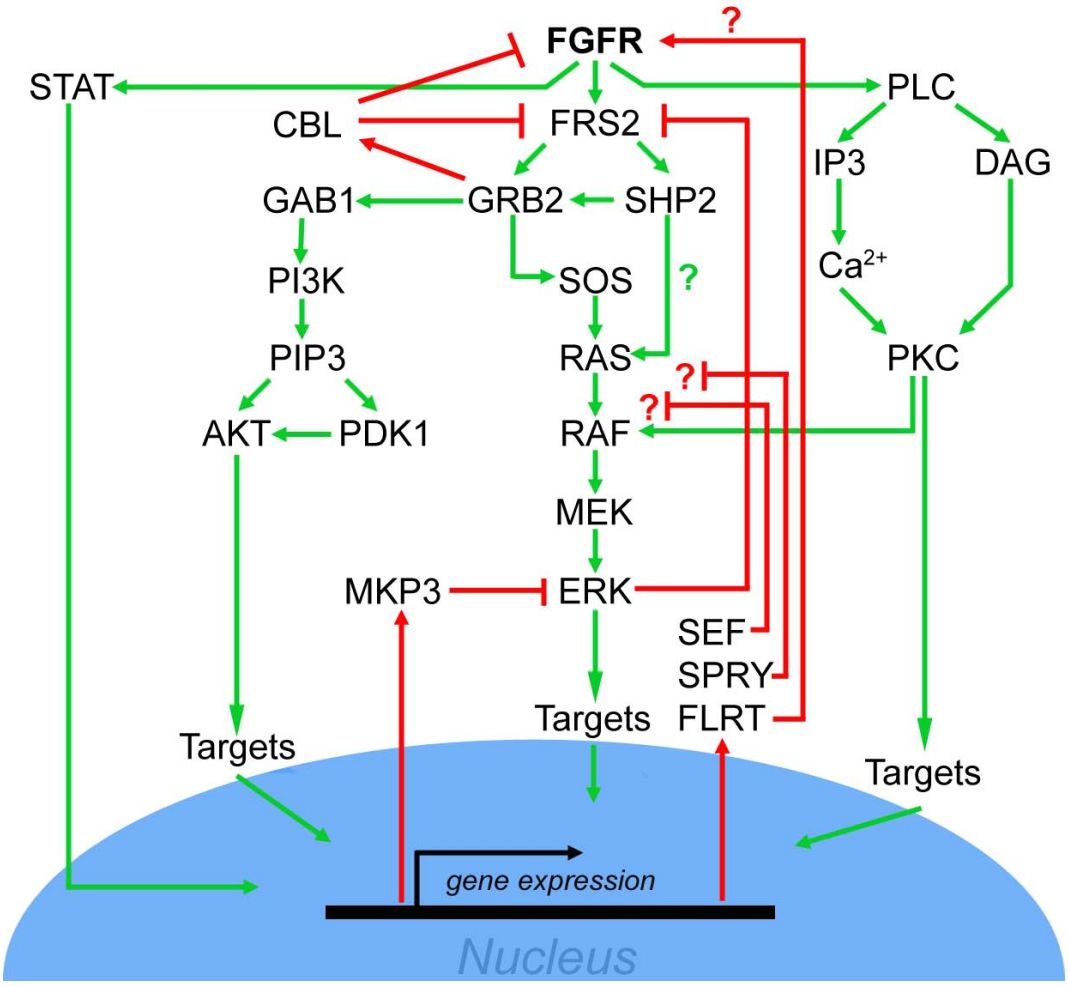

Figure 1.7. Wire diagram of feedback regulation of FGFR signal transduction pathways. CBL is recruited via GRB2 and ubiquitinates FGFRs and FRS2, targeting them for lysosomal degradation. ERK phosphorylates FRS2 on Serine/Threonine residues, blocking its Tyrosine phosphorylation. Expression of MKP3, SEF, SPRY, and FLRT are induced by FGFR dependent signal transduction pathways, which they then act upon to modulate. The exact mechanism of action/point of interception for SEF, SPRY, and FLRT are not clear and subject to controversies (hence indicated by question mark). The diagram was adopted from [Eswarakumar et al., 2005] with modifications.

1.4.3 Endocytic trafficking

Although signalling and endocytosis were once viewed as two independent cellular processes, it is now clear that they are intricately linked at the molecular level and intimately connected at the functional level. In fact, endocytic trafficking has emerged as a key regulator of signalling from many different receptors in recent years [Miaczynska et al, 2004b; Sorkin and von Zastrow, 2009]. These include, amongst others, G Protein-Coupled Receptors (GPCRs), Transforming Growth Factor-β Receptors (TGFβRs), Cytokine receptors, Wnt and Notch Receptors, as well as RTKs [Sorkin and von Zastrow, 2009].

Like most plasma-membrane proteins, nearly all signalling receptors can undergo internalisation at the cell surface. This is usually triggered by ligand binding and receptor activation, followed by association of the receptors with proteins of the endocytic machinery. Receptor internalisation can occur through Clathrin dependent or independent endocytosis mechanisms [Scita and Di Fiore, 2010]. The Clathrin dependent endocytosis is the best studied pathway, which is mediated by the multi-meric protein Clathrin, as apparent from its name. Clathrin forms coated pits on the cytosolic side of the plasma-membrane by assembling into a polyhedral lattice [Scita and Di Fiore, 2010]. Signalling receptors are usually recruited to these coated pits by interacting with Clathrin associated adaptor proteins such as the Adaptor Protein complex-2 (AP2), Epsins, Epidermal Growth Factor Receptor Substrate-15 (EPS15), and Dishevelled (Figure 1.8) [Sorkin and von Zastrow, 2009]. Once the receptors reside in these pits, the coated membrane invaginates into the cytoplasm, and is ultimately pinched off from the rest of the plasma-membrane in a process that is mediated by a GTPase known as Dynamin [Scita and Di Fiore, 2010]. Clathrin independent endocytosis is not characterised as well, and seems to be mediated by a number of distinct mechanisms. One of these mechanisms depends on a hairpin-like membrane protein known as Caveolin as well as

Dynamin, though both Caveolin and Dynamin independent mechanisms also exist [Doherty and McMahon, 2009].

Endocytic vesicles resulted from both Clathrin dependent and independent internalisation are trafficked to early/sorting endosomes, a distinct endocytic compartment marked by the presence of the small RAS-like GTPase RAB5 (Figure 1.8) [Sorkin and von Zastrow, 2009]. RAB proteins are at the centre of endosomal trafficking as they mark specific endosomal compartments and recruit crucial effector proteins which organise fission/fusion/maturation events on these endosomes [Grosshans et al., 2006]. Once inside early endosomes, signalling receptors can either be recycled back to the plasma-membrane, or trafficked to lysosomes for degradation. Recycling can occur rapidly via a RAB4 dependent process, or slowly via a RAB11 dependent recycling compartment (Figure 1.8) [Sorkin and von Zastrow, 2009]. For lysosomal trafficking, the early endosomes mature into late endosomes along with the process of Multi-Vesicular Body (MVB) formation (Figure 1.8) [Sorkin and von Zastrow, 2009]. Early to late endosomal maturation involves termination of recycling and conversion of RAB5 to RAB7, which specifically marks the late endocytic compartment [Sorkin and von Zastrow, 2009]. MVBs are generated by inward invagination of endosomal limiting membrane which results in formation of Intra-Luminal Vesicles (ILVs) [Piper and Katzmann, 2007]. MVB formation begins in early endosomes and continues in late endosomes before mature late-endocytic MVBs are finally fused with lysosomes for degradation [Piper and Katzmann, 2007]. Signalling receptors destined for degradation are transferred to the ILVs of MVBs (Figure 1.8). This renders them unable to interact with cytosolic signalling molecules, as well as increasing their susceptibility to degradation by lysosomal hydrolyses [Sorkin and von Zastrow, 2009; Piper and Katzmann, 2007].

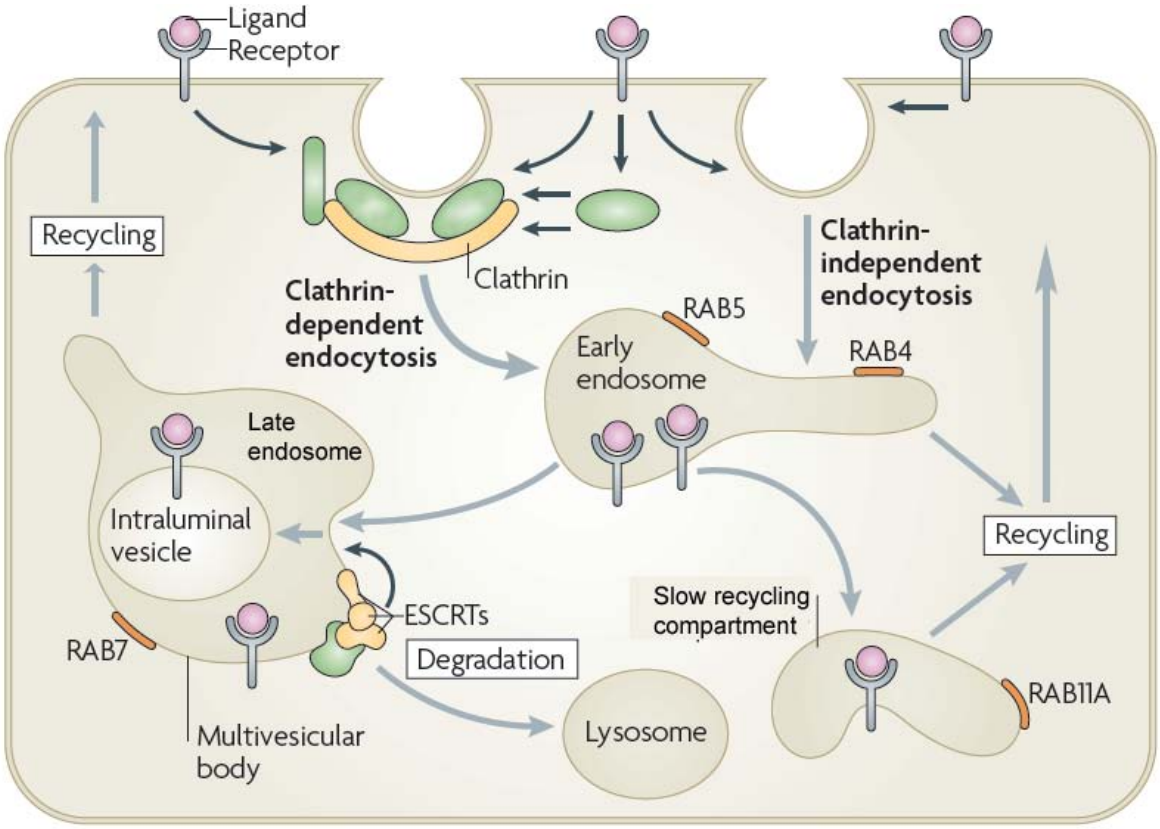

Figure 1.8. Schematic representation of receptor endocytosis. Adaptor proteins are shown in green and the endocytic machinery proteins in yellow. RAB proteins are marked as orange. Ligand binding and receptor activation triggers its internalisation via Clathrin dependent or independent mechanisms. For Clathrin dependent endocytosis, the receptor resides in Clathrin coated pits via interacting with Clathrin associated adaptor proteins. Internalised receptors via both Clathrin dependent and independent mechanisms are trafficked to early endosomes marked by RAB5, from which they are sorted for recycling back to the plasma-membrane or degradation in lysosomes. Recycling can occur rapidly via RAB4 or slowly via a RAB11 recycling compartment. For degradative route, receptors are trafficked to late endosomes marked by RAB7 along with a concomitant Multivesicular body (MVB) formation. Any remaining receptor not destined for degradation is recycled back. MVBs are created through the concerted action of ESCRT complexes, which generate Intraluminal Vesicles (ILV) and sort the receptors into them. Finally, mature MVBs fuse with lysosomes where their contents, including ILV trapped signalling receptors, are degraded by the action of lysosomal acid hydrolases. The diagram was adopted from [Sorkin and von Zastrow, 2009] with modifications.

The process of membrane inward invagination and fission inside MVBs as well as the sorting of the cargo into ILVs is orchestrated by proteins of Endosomal Sorting Complex Required for Transport (ESCRT) (Figure 1.8). Four distinct ECRT complexes, designated ESCRT-0, ECRT-I, ECRT-II, and ECRT-III, have been described which act in a sequential manner to generate cargo loaded ILVs [Piper and Katzmann, 2007]. ESCRT-0 is composed of two proteins named Hepatocyte growth factor-Regulated tyrosine kinase Substrate (HRS) and Signal Transducing Adapter Molecule (STAM), and is not part of core ESCRT machinery [Piper and Katzmann, 2007]. This is the first complex to be recruited, interacting with the cargos targeted for degradation on the limiting endosomal membrane and gathering them in Clathrin-rich sub-domains [Piper and Katzmann, 2007]. Following its recruitment, ESCRT-0 then recruits ESCRT-I and II complexes and transfers the cargos to them, which subsequently function to correctly assemble ESCRT-III. ESCRT-III subunits form of a polymeric coat that sequesters the cargos, followed by inward invagination and fission of ILVs into the lumen [Piper and Katzmann, 2007].

Ubiquitination is a key regulator of cargo sorting into the ILVs. Several cargos including RTKs are marked for ILV targeting and subsequent lysosomal degradation by being ubiquitinated [Sorkin and von Zastrow, 2009; Piper and Katzmann, 2007]. In fact, both HRS and STAM contain Ubiquitin Interacting Motifs (UIMs) through which they interact with cargos [Piper and Katzmann, 2007]. Moreover, several members of the ESCRT-I and II complexes such as Tumour Susceptibility Gene 101 Protein (TSG101) also contain Ubiquitin Binding Domains (UBDs) that allow cargo interaction [Piper and Katzmann, 2007]. The topology of ubiquitination for MVB sorting is distinct. Unlike Ubiquitin mediated proteosomal degradation which requires K48-linked poly-ubiquitination, MVB sorting is generally mediated by mono- or multi-ubiquitination, or in some cases by K63-linked oligo-

ubiquitination [Piper and Katzmann, 2007]. Finally, just before the cargo is entrapped in the ILVs, the majority of Ubiquitin molecules are removed by the action of de-Ubiquitinating enzymes, thus averting unnecessary Ubiquitin loss [Piper and Katzmann, 2007].

Ubiquitination also serves as an important regulator of the internalisation process, and targeting of many RTKs such as EGFR and TrkA to the Clathrin-coated pits depends on their ubiquitination [Sorkin and von Zastrow, 2009]. Epsins and ESP15, the two adaptor proteins thought to be involved in bringing these RTKs to Clathrin-coated pits, both do so by binding to ubiquitinated receptors via their UBDs [Sorkin and von Zastrow, 2009]. Ubiquitination is also thought to regulate the accessibility AP2 interacting motifs on some cargos [Sorkin and von Zastrow, 2009]. For RTKs, the E3 ubiquitin ligase CBL plays a crucial role in induction of endocytosis as well as the eventual lysosomal degradation of the receptors via MVB trafficking [Thien and Langdon, 2001]. As mentioned earlier, CBL recruitment to RTKs follows receptor activation at the plasma-membrane, and this recruitment can occur either directly via phospho-Tyrosine residues on the receptor that are recognised by the SH2 domain of CBL, or indirectly via GRB2 [Thien and Langdon, 2001; Wong et al., 2002b; Jiang et al., 2003].

It is now evident that endocytic trafficking can regulate RTK signalling at least at two levels. The first level is the well established down-regulation of signalling by lysosomal degradation which was mentioned above. En route to lysosomes, signalling receptors are removed from the limiting membrane of endosomes and enclosed within the ILVs of MVBs which effectively terminates their signalling prior to degradation by blocking access to cytosolic signalling proteins [Sorkin and von Zastrow, 2009]. The importance of RTK regulation by MVB sorting and lysosomal degradation is manifested by the fact that a variety of cancer associated genetic and epigenetic alterations specifically target this pathway [Mosesson et al.,

2008]. Once internalised, however, the lysosomal degradation route is not the only available itinerary for RTKs, as receptors can undergo recycling back to the plasma membrane, which would allow their re-usage and continuation of signalling [Scita and Di Fiore, 2010]. In fact, the balance between recycling and lysosomal degradation has been proposed to be a key determinant of RTK signalling outcome [Scita and Di Fiore, 2010]. The choice of internalisation pathway has been suggested as an important determinant of recycling versus degradation routes, as EGFR internalised via clathrin-dependent endocytosis was mainly found to be recycled whereas EGFR internalised by clathrin-independent endocytosis was targeted towards the lysosomal degradation pathway [Sigismund et al., 2008].

The second and more recently appreciated level of regulation is pathway specific propagation or down-regulation of signalling by compartmentalisation. Endocytic removal of activated RTKs from the plasma membrane results in specific down-regulation of those downstream signalling pathways which require plasma-membrane associated molecules. These include the PLC/PKC and the PI3K/AKT pathway, both of which require Phosphatidylinositol-4,5 phosphate (PI45P2) as substrate, which is absent in endosomes [Haugh and Meyer, 2002]. In contrast, ERK1/2 signalling is not limited to plasma membrane and many downstream components of the ERK1/2 pathway such as GRB2, SOS, and RAS seem to remain associated with RTKs long after internalisation [Di Guglielmo et al., 1994; Sorkin et al., 2000; Lu et al., 2009]. In fact, many studies have suggested that full ERK1/2 activation downstream of various RTKs depends on endocytosis [Vieira et al., 1996; Kranenburg et al., 1999; MacInnis and Campenot, 2002; Lampugnani et al., 2006]. This has been attributed to the endosomal ERK1/2 propagating scaffolding complex P14-MP1 [Wunderlich et al., 2001; Teis et al., 2002; Teis et al., 2006]. MP1 binds to both ERK and MEK and facilitates MEK phosphorylation of ERK [Schaeffer et al., 1998]. The P14-MP1 complex specifically localises

to late endosomes, thus resulting in specific ERK1/2 propagation from this compartment [Wunderlich et al., 2001; Teis et al., 2002; Teis et al., 2006]. The late endosomal localisation of P14-MP1 has been recently shown to be mediated by a lipid-raft anchor protein known as P18, the loss of which also abrogates ERK1/2 propagation from endosomes [Nada et al., 2009]. Another example of specific endosomal signal propagation has been shown for AKT. The Adaptor protein containing PH domain, PTB domain, and Leucine zipper motif-1 (APPL1) is a RAB5 effector protein which marks a distinct population of early endosomes [Miaczynska et al., 2004a; Zoncu et al., 2009]. APPL1 can specifically bind to AKT on early endosomes and enhance its activity [Schenck et al. 2008]. APPL1 also binds to Glycogen Synthase Kinase-3β (GSK-3β), a downstream AKT target, and increases its phosphorylation by AKT without affecting the phosphorylation of another AKT substrate Tuberous Sclerosis Complex protein-2 (TSC2), thereby providing pathway selectivity [Schenck et al., 2008].

Although the basic mechanisms of endocytic trafficking are presumed to be similar for most RTKs, receptor specific difference in the dynamics of trafficking, and the resultant differences in signalling regulation are believed to exist amongst different receptors. Unfortunately, with this in mind, the trafficking dynamics of FGFRs has been less well studied in comparison to other RTKs like EGFR and TrkA. Comparison of ligand induced internalisation and trafficking of different FGFRs revealed that while internalised FGFR1 mainly ended up in the late-endosomal/lysosomal compartment and was degraded, FGFR4 was mainly recycled [Haugsten et al., 2005]. FGFR2 and FGFR3 were also sorted to lysosomes for degradation albeit less efficiently than FGFR1 [Haugsten et al., 2005]. In contrast, a proteomics survey by our group revealed that a significant fraction of the early endocytic machinery proteins associate with a constitutively dimerised active FGFR1, revealing the potential importance of the early endosomal trafficking with regards to constitutively activated FGFR1 life-history

[Vecchione et al., 2007]. Several reports have also revealed changes in the trafficking itinerary of FGFRs as a result of disease related receptor mutations. For instance, activating mutations of FGFR3 found in Achondroplasia have been shown to inhibit lysosomal trafficking of the receptors by disrupting CBL mediated ubiquitination, resulting in their recycling and continuation of signalling instead [Cho et al., 2004]. Another interesting example is found in some gastric cancers where genetic amplification of FGFR2 is accompanied by a concomitant deletion of the last coding exon of the receptor [Ueda et al., 1999]. This results in over-expression of a C-terminally truncated FGFR2, which was recently shown to be deficient in internalisation, thus preventing the removal and subsequent lysosomal degradation of the receptor and leading to prolonged signalling at the plasma-membrane [Cha et al., 2009].

1.5 Sprouty

Sprouty was initially discovered in *Drosophila* as a negative regulator of Branchless (Bnl), a *Drosophila* homologue of FGF which functions during the development of the tracheal system [Hacohen et al., 1998]. It was subsequently shown that *Drosophila* Sprouty (dSpry) could also attenuate signalling from other RTKs such as Torso and EGFR, establishing it as a general antagonist of RTK signalling [Casci et al., 1999; Kramer et al., 1999; Reich et al., 1999]. While initial results were suggestive of an extra-cellular mode of action [Hacohen et al., 1998], later studies revealed that dSpry was in fact an intracellular protein, acting downstream of the receptor and upstream of ERK1/2 kinases [Casci et al., 1999].

dSpry is a 591 residues-long protein, with a characteristic 124 residues-long Cysteine-rich region in the C-terminal termed the Sprouty domain (SPRY domain) [Hacohen et al., 1998].

Based on sequence similarities, four mammalian, four chicken, two *Xenopus*, and two zebrafish homologues of Sprouty have been identified, all of which being considerably smaller than the *Drosophila* homologue but sharing the C-terminal SPRY domain (Figure 1.9A). In addition to the SPRY domain, which has the highest degree of homology between all Sproutys, a short stretch of amino acids within the N-terminal containing an invariant Tyrosine residue (Y201 in dSpry; Y55 in human SPRY2) is also found to be conserved in all Sproutys (Figure 1.9A and B). Among vertebrate Sproutys, Spry2 is the most conserved member, with 97% homology between human (SPRY2) and mouse (Spry2), and 85% between human and chicken. Spry2 also has the highest homology to dSpry, with 51% conservation between the C-terminal SPRY domains [Mason et al., 2005]. In all investigated organisms, the SPRY domain was found to be indispensable for Sprouty function [Casci et al., 1999; Lim et al., 2000; Yigzaw et al., 2001; Lim et al., 2002; Hanafusa et al., 2002].

1.5.1 Expression

All early *Drosophila* studies showed that expression of dSpry was induced by the signalling pathways it acted upon (e.g. EGF and FGF), thereby creating a negative feedback loop [Hacohen, et al., 1998; Casci et al., 1999; Kramer et al., 1999; Reich et al., 1999]. Expression of dSpry during development was shown to be tightly dependent on and following FGF and EGF expression patterns, such that blocking the signalling from these pathways totally abrogated dSpry expression. Moreover, expression of activated forms of EGF and FGF receptor resulted in an increase in the expression of dSpry, all supporting the presence of a negative feed-back mechanism [Hacohen et al., 1998; Casci et al., 1999; Kramer et al., 1999; Reich et al., 1999]. Similarly, expression of Sprouty genes during the vertebrate development

was shown to be in close association with FGF signalling centres, and induced by FGF signalling. However, unlike in *Drosophila*, little association was found between vertebrate Sproutys and known sites of EGF signalling, and expression of Sproutys was shown to be more restricted to known FGF centres [Minowada et al., 1999; de Maximy et al., 1999; Chambers et al., 2000a; Chambers et al., 2000b; Zhang et al., 2001]. This suggests that in vertebrates Sproutys might be acting more specifically on FGF signalling. Interestingly, different vertebrate Sprouty isoforms exhibit unique and complex expression patterns within the territories of FGF activity, indicative of the existence of additional cell/tissue specific factors that differentially effect the expression of specific Sprouty isoforms [Minowada et al., 1999; Zhang et al., 2001].

Compared to their embryonic expression profile, expression of Sproutys in adult tissues has been less well studied. In mature mouse microvascular endothelial cells where VEGF and FGF signalling pathways are known to operate, Spry1, 2 and 4 are expressed, and their over-expression is shown to suppress VEGF or FGF induced ERK activation [Impagnatiello et al., 2001]. Not much is known, however, about the detailed expression levels of different Sprouty isoforms in different adult tissues and organs, apart from an early study which employed northern blotting to show that Spry2 transcripts are present at high levels in adult brain, heart, lung, and to a lower extent in kidney and skeletal muscles [Tefft et al., 1999]. Postnatal expression of Spry2 is also reported in murine breast, with the expression levels following the changes of the breast tissue during adult life [Lo et al., 2004]. Briefly, in 2–6 week-old mice, Spry2 was shown to be expressed in developing mammary ducts. As mice reached puberty, the level of Spry2 decreased but this was reversed during pregnancy. Finally, Spry2 expression decreased during lactation and was totally absent during the involution phase [Lo et al., 2004].

The ERK1/2 pathway has been shown to induce the expression of Sprouty genes, thus forming a direct feedback loop downstream of RTKs [Ozaki et al., 2001]. Agents such as phorbol esters, or a constitutively active RAF kinase which activate ERK1/2 could also induce Sprouty expression, while a MEK inhibitor potently inhibited this, further supporting a direct role for ERK1/2 signalling in induction of Sprouty gene expression [Ozaki et al., 2001]. The PLC-PKC pathway has also been shown to be required for induction of mammalian Sproutys in some cells, and this might be contributing to the expression of Sproutys at embryonic sites such as limb bud mesenchyme where the ERK1/2 pathway is known to be inactive [Abe et al., 2004]. Other factors, such as tissue specific transcription factors, as well as certain non-RTK signalling pathways, have also been shown to affect the expression of Sproutys, which might explain some of the observed complexities in the expression patterns of individual Sprouty isoforms within the sites of FGF activity during vertebrate development [Minowada et al., 1999; Zhang et al., 2001]. One example of such tissue specific factors is Wilms Tumour suppressor gene-1 transcription factor (WT1), which has been shown to directly bind to and activate murine Spry1 promoter during kidney development [Gross et al., 2003]. Spry4, on the other hand, has been shown to be a specific target of Wnt-βCatenin signalling [Winn et al., 2005; Katoh et al., 2006; Taniguchi et al., 2007a], while Spry2 was found to be a major direct target for FOXO transcription factors in liver endothelial cells [Paik et al., 2007]. Finally, TGFβ-1 signalling was demonstrated to down-regulate Spry2 expression in 3T3 fibroblast cells, and this was shown to be ERK1/2 independent [Ding et al., 2007]. Interestingly, down-regulation of Spry2 by TGFβ signalling seems to be not only achieved at the transcription level, but also post-translationally through enhancing Spry2 degradation [Ding et al., 2007]. These findings reveal a fascinating cross-talk between TGFβ and RTK signalling pathways by means of regulating Spry2 expression [Ding et al., 2007].

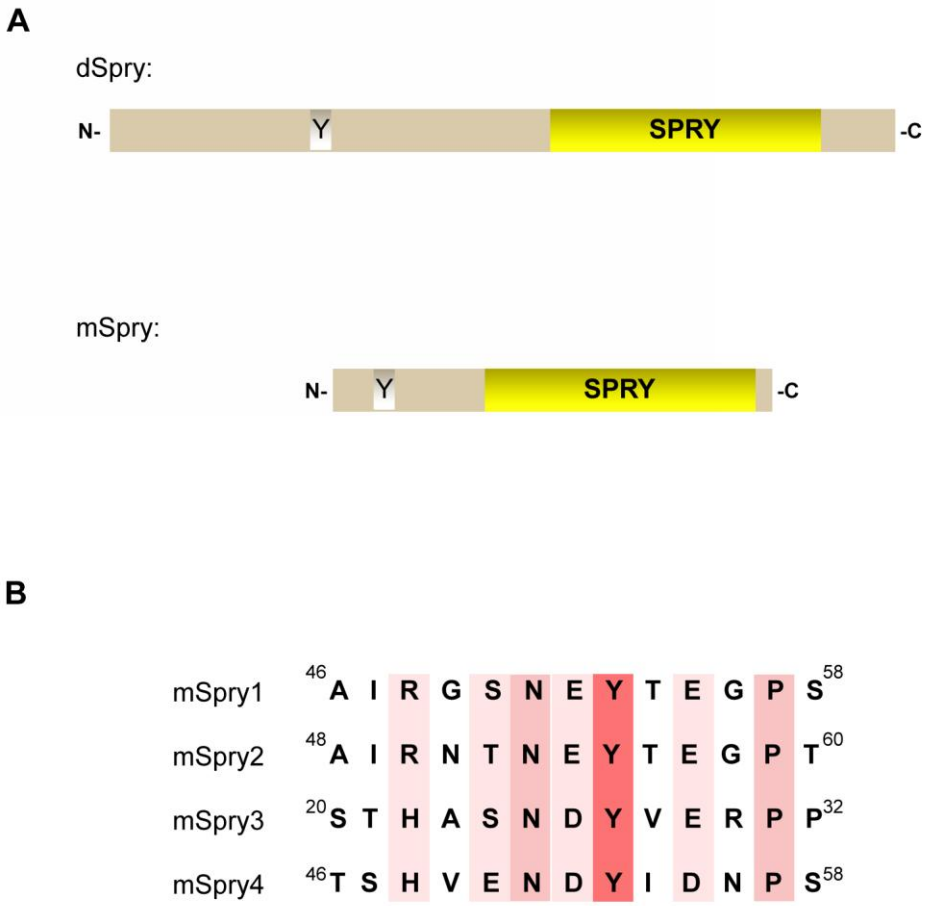

Figure 1.9. Schematic representation of Sprouty domains and motifs. *Drosophila* Sprouty (dSpry) contains a C-terminal Cysteine-rich SPRY domain as well as a conserved N-terminal Tyrosine residue (marked as Y). Mammalian Sproutys (mSpry) are considerably smaller, but still share the C-terminal SPRY domain and the conserved N-terminal Tyrosine residue with their fruitfly homologues **(A)**. Sequence comparison of the conserved N-terminal Tyrosine residue region of murine Sprouty isoforms (mSpry1-4) **(B)**.

1.5.2 Sprouty in development

Early studies in *Drosophila* revealed that several RTK dependent developmental processes were tightly regulated by dSpry [Hacohen, et al., 1998; Casci et al., 1999; Kramer et al., 1999; Reich et al., 1999]. For mammals, FGF dependent developmental processes such as mid-brain patterning and skeletal development were shown to be regulated by Sproutys [Minowada et al., 1999; Chambers et al., 2000b]. Subsequent generation of Spry knockout mice revealed a central role for Spry proteins in regulation of multiple developmental processes which does not confine to FGF. Particularly, all Sprouty proteins from *Drosophila* to human seem to be involved in regulation of developmental processes that include branching morphogenesis. Spry1 knockout mice exhibit defects due to improper branching morphogenesis in the ureteric bud and kidneys [Basson et al., 2005; Basson et al., 2006]. These defects arise due to the hyperactivity of RET, an RTK crucial for kidney development [Basson et al., 2005; Basson et al., 2006]. On the other hand, Spry2 knockout results in a shortened life span, accompanied by defects in inner ear development and deafness due to deregulated FGFR3 signalling [Shim et al., 2005]. In a separate study, loss of Spry2 was reported to cause enteric nerve dysplasia due to RET hyperactivity, thus resulting in severe gastrointestinal problems [Taketomi et al., 2005].

Spry4 knockout has also been generated, showing tooth development defects due to abnormal FGFR signalling [Klein et al., 2006]. An independent study, however, showed that Spry4 null mice exhibited growth retardation, and fusion of forelimb digits [Taniguchi et al., 2007a]. Interestingly, unlike Spry2 and 4 single knockouts which are not embryonic lethal, Spry2/4 double knockout mice die at E12.5 while exhibiting a plethora of developmental abnormalities in head, lung, and limbs [Taniguchi et al., 2007a]. This suggests that a significant degree of functional redundancy must exist between the two family members

during many developmental processes. No study regarding the role of Spry3 during development has yet been reported.

1.5.3 Tumour suppression

Being a negative regulator of RTK signalling, it is not surprising that Sprouty family members could act as tumour suppressors. In fact, a large body of evidence linking Spry to tumour suppression has been accumulating in recent years. One of the first lines of evidence in support of a tumour suppressive role for Sprouty was the observation in LM8 osteosarcoma cells that over-expression of Spry2 could inhibit tumour growth and metastasis *in vivo* [Miyoshi et al., 2004]. A large number of studies have since revealed that expression of various Sprouty isoforms is significantly down-regulated in many cancers. This will be discussed in detail below. Sprouty family members have also been found to be involved in oncogene induced senescence [Courtois-Cox et al., 2006], as well as regulation of tumour angiogenesis [Taniguchi et al., 2009].

A list of all known cancer types in which the expression of Sprouty genes is significantly altered is presented in (Table 1.3). The first evidence of Sprouty down-regulation in cancer came from a study using c-DNA array analysis which showed that SPRY2 and SPRY1 expression levels were down-regulated in a high proportion (96% for Spry2, 78% for Spry1) of breast cancer samples in comparison to their matched non-tumour tissues (Table 1.3). This was further confirmed by quantitative Real Time (RT)-PCR as well as *in situ* staining of breast tumour tissues [Lo et al., 2004]. The means by which SPRY1 and 2 were down-regulated was unclear, as it was neither due to chromosomal alterations nor hypermethylation of their associated promoters [Lo et al., 2004]. Interestingly, a dominant-negative SPRY2

mutant was shown to profoundly enhance the tumourogenic capabilities of MCF-7 breast carcinoma cells *in vitro* and *in vivo*, further supporting the notion that Sproutys are functioning as likely tumour suppressors, at least in the context of breast cancer [Lo et al., 2004].

A number of reports have also linked Sprouty down-regulation to prostate cancer (Table 1.3). An array analysis of 407 prostate cancer tissue samples and their matched normal peripheral tissue found SPRY1 to be down-regulated in around 40% of the cancerous samples, and this was confirmed by RT-PCR analysis, *in vivo*. Moreover, over-expression of SPRY1 in prostate cancer cell-lines was shown to decrease the proliferative as well as metastatic potential of these cells [Kwabi-Addo et al., 2004]. Surprisingly, a fraction of prostate cancer samples in the array showed an increase rather than a decrease in the expression of SPRY1 [Kwabi-Addo et al., 2004], but the cause of this up-regulation was not further investigated. SPRY2 expression was also reported to be significantly decreased in invasive prostate cancer cell-lines and high-grade clinical prostate cancers, in an independent study (Table 1.3) [McKie et al., 2005]. In 76-82% of high-these grade prostate cancers, SPRY2 promoter was shown to be extensively hypermethylated, and a correlation between methylation and down-regulation of SPRY2 expression in clinical samples was also observed [McKie et al., 2005]. Moreover, treatment of LNCaP and PC-3M prostate carcinoma cells with 5-aza-2'-deoxycytidine, an agent which abrogates DNA methylation, relieved the suppression of SPRY2 expression, further supporting the notion that hypermethylation is the likely cause of SPRY2 down-regulation in these carcinomas [McKie et al., 2005]. In addition to hypermethylation, a modest loss of heterozygosity was also found in the SPRY2 locus, although the epigenetic silencing was the main cause of down-regulation in these carcinomas [McKie et al., 2005]. In contrast, a subsequent study failed to detect any hypermethylation of SPRY2 promoter in

prostate cancer tissues and cell-lines where SPRY2 was down-regulated [Fritzsche et al, 2006]. In addition to SPRY2, expression of SPRY4 has also been shown to be down-regulated in around 50% of prostate cancers, and this down-regulation was similarly found to be due to DNA hypermethylation (Table 1.3) [Wang et al., 2006]. Interestingly, ectopic expression of SPRY4 in these prostate cancer cell-lines did not affect their proliferative capacity but inhibited cell migration, suggestive of a specific anti-metastatic role for SPRY4 [Wang et al., 2006].

Another cancer type in which SPRY proteins were found to be down-regulated is hepatocellular carcinoma (Table 1.3) [Fong et al., 2006; Lee et al., 2008]. In contrast to prostate cancer studies mentioned earlier, promoter hypermethylation or loss of heterozygosity were both ruled out as responsible mechanisms for SPRY2 down-regulation in hepatocellular carcinomas [Fong et al., 2006]. Exogenous expression of SPRY2 in hepatocellular carcinoma cell-lines inhibited both ERK activity as well as tumour cell proliferation [Fong et al., 2006]. Expression of a dominant negative SPRY2, on the other hand, enhanced neoplastic tumour formation by activated βCatenin, revealing cooperation between SPRY2 loss of function and the activity of other oncogenes such as βCatenin during tumourigenesis [Lee et al., 2008]. SPRY2 expression has also been shown to be down-regulated in a significant percentage of non-small-cell lung cancers (Table 1.3) [Sutterlüty et al., 2007]. Ectopic expression of SPRY2 in these cells inhibited cell proliferation *in vitro* and blocked tumour formation *in vivo* [Sutterlüty et al., 2007]. Although SPRY2 mediated ERK1/2 inhibition contributed to some aspects of tumourigenesis in these cells, inhibition of cell-proliferation by SPRY2 was not fully dependent on its activity on ERK1/2, suggestive of the existence of other downstream SPRY2 target pathways which are particularly crucial for tumourigenesis of non-small-cell lung cancer cells [Sutterlüty et al., 2007].

In contrast to the above mentioned cancers in which Sprouty family members were normally down-regulated, a reverse pattern is seen in most melanomas (Table 1.3). Oncogenic mutations of B-RAF have been shown to occur in up to 80% of nevi and metastatic melanomas. Of these, more than 90% has been shown to be a single missense mutation in the activation loop of the kinase domain (V600E), which renders B-RAF constitutively active [Wellbrock et al., 2004]. SPRY2 was found to be over-expressed in melanomas with a mutant B-RAF but not wild type B-RAF [Tsavachidou et al., 2004]. This is expected as hyperactivity of B-RAF results in ERK1/2 hyperactivity, thus up-regulating SPRY2 expression. Moreover, RNAi mediated knockdown of SPRY2 in wild-type B-RAF melanoma cells increased ERK1/2 activity and cell proliferation, while this was not the case in V600E mutant B-RAF cells, suggesting that SPRY2 must be acting at the level or upstream of RAF [Tsavachidou et al., 2004]. Interestingly, SPRY2 and 4 were both capable of binding to wild type but not V600E B-RAF, suggesting that the inability of Sprouty to suppress ERK1/2 downstream of V600E B-RAF might be due to its inability to bind to it [Tsavachidou et al., 2004]. Similar to SPRY2 expression in melanomas, SPRY1 expression was recently found to be up-regulated in embryonal Rhabdomyosarcomas that have activating RAS mutations (Table 1.3) [Schaaf et al., 2010]. Activating RAS mutations are found in more than 50% of all embryonal Rhabdomyosarcoma cases [Schaaf et al., 2010], and up-regulation of SPRY1 was due to ERK1/2 hyperactivity downstream of RAS [Schaaf et al., 2010]. Surprisingly, the function of SPRY1 in these tumours was changed from tumour suppressive to oncogenic. SPRY1 was shown to be essential for cell proliferation and survival of these cancer cells, and its depletion abolished tumourogenicity *in vivo* [Schaaf et al., 2010]. These results reveal that the effect of SPRY could vary from tumour suppressive to oncogenic depending on the oncogenic background, which could be very important therapeutically.

Cancer type	Up/down-regulation?	SPRY Isoform
Breast cancer	Down-regulated	1 and 2
Prostate cancer	Down-regulated	1, 2, and 4
Hepatocellular carcinoma	Down-regulated	2
Non-small-cell lung cancer	Down-regulated	2 and 4
Melanoma	Up-regulated (in a B-RAF mutant background)	2
Embryonic Rhabdomyosarcoma	Up-regulated (in a RAS mutant background)	1

Table 1.3. List of cancers in which the expression of SPRY isoforms has been found to be up/down-regulated. In melanomas, those cancers with oncogenic B-RAF mutations exhibit SPRY2 up-regulation while in Embryonic Rhabdomyosarcoma the ones with oncogenic RAS mutations show a similar up-regulation of SPRY1.

1.5.4 Sub-cellular localisation

In *Drosophila*, dSpry was found to be mainly localised to the plasma-membrane [Hacohen et al., 1998; Casci et al., 1999]. The SPRY domain of dSpry was shown to mediate this plasma-membrane localisation, resulting in its association to the inner surface of the plasma-membrane as well as to some endosomal structures where RTK signalling components are located [Casci et al., 1999]. Likewise, the SPRY domains of vertebrate Sproutys were shown to be required for their plasma-membrane localisation, though some variations with respect to different Sprouty isoforms and different cellular contexts were observed [Lim et al., 2000; Yigzaw et al., 2001; Lim et al., 2002; Hanafusa et al., 2002]. In COS1 and HEK 293T cells, over-expressed mammalian Sprouty proteins were primarily localised to the cytosol, with some human SPRY2 being associated to microtubules. After growth factor stimulation, however, Sproutys rapidly translocated to the leading edges of the plasma-membrane [Lim et al., 2000]. This membrane translocation was dependent on a region situated within the SPRY domain, termed the Translocation Domain (TD), which was shown to bind to and target

Sproutys to PIP2 containing membranes [Lim et al., 2002]. Microtubular localisation of SPRY2 in the resting state was also mapped to a region within the C-terminal [Lim et al., 2000]. Growth factor induced membrane recruitment has also been observed for endogenous SPRY1 in response to FGF stimulation in Human Umbilical Vascular Endothelial Cells (HUVECs). In HUVECs, the majority of SPRY1 is found in peri-nuclear regions and cytoplasmic endosomal compartments, but FGF stimulation results in translocation of a fraction of this to the plasma membrane, and in particular to the leading edges [Impagnatiello et al., 2001]. Peripheral anchorage of ectopically expressed SPRY1 and 2 to the plasma-membrane by palmitoylation of the SPRY domain has also been reported in HUVECs, which suggests that constitutive association of a fraction of SPRY to the plasma-membrane might be the result of this anchorage [Impagnatiello et al., 2001]. Similar to human SPRY2, over-expressed murine Spry2 in mouse epithelial lung cells has been shown to be mainly cytosolic in the resting state, but to translocate to the plasma membrane and to some endosomal structures following FGF stimulation [Tefft et al., 2002].

A more recent study has challenged the idea of a predominantly plasma-membrane associated SPRY after growth factor stimulation by showing that both endogenous and over-expressed Spry2 proteins exhibit a punctate cytoplasmic staining, which spatially overlap with RAB5 positive early endosomes after growth factor treatment [Kim et al., 2007]. This post-stimulation association of Spry2 with the early endosomal compartment was proposed to be involved in blocking the progression of internalised activated EGFR from early endosomes to late endosomes, thus spatially regulating the signalling output from endocytosed EGFR [Kim et al., 2007].

1.5.5 Mechanism of ERK1/2 inhibition

The conserved N-terminal Tyrosine residue of SPRY is thought to be crucial for its inhibitory effect on FGF but not EGF mediated ERK1/2 signalling. Mutation of this conserved tyrosine residue results in creation of a dominant negative phenotype that augments FGF but not EGF mediated ERK activity [Sasaki et al., 2001; Hanafusa et al., 2002; Mason et al., 2004]. For Spry1 and Spry2, it has been demonstrated that this tyrosine residue could undergo phosphorylation in response to both FGF and EGF stimulations [Hanafusa et al., 2002; Rubin et al., 2003; Mason et al., 2004; Li et al, 2004]. The kinase responsible for this phosphorylation has been identified as a SRC Family Kinase (SFK) [Mason et al., 2004; Li et al, 2004]. Since the sequences surrounding the Tyrosine are strongly conserved between all Sproutys (Figure 1.9B), it is likely that SRC mediated phosphorylation of this residue might be occurring in all Sprouty family members. Interestingly, Spry4 mutants lacking the conserved N-terminal Tyrosine residue are still capable of suppressing VEGF induced RAS-independent RAF activation, but not FGF induced RAS-dependent RAF activation, the former is mediated by direct interaction of Spry4 with RAF via its C-terminal SPRY domain (see below) [Sasaki et al., 2003].

Phosphorylation of the conserved N-terminal Tyrosine residue of Sproutys is proposed to create a potential binding site for SH2 domain containing proteins that are capable of recognising the specific set of amino acids flanking it, thus resulting in their recruitment to the sites of Sprouty activity. Due to the functional significance of this Tyrosine residue, it is believed that it must be recruiting a functionally critical partner of Sprouty, whose association is necessary for inhibition of FGF mediated ERK1/2 signalling. Up to now, only two SH2 domain containing proteins have been reported to bind to the conserved N-terminal Tyrosine residue of Sproutys. The adaptor protein GRB2 is the first protein that was claimed to bind to

the phosphorylated N-terminal tyrosine region of Sprouty via its SH2 domain, resulting in its disengagement from the signalling adaptors of the FGF signalling pathway such as FRS2 and SHP2, and consequent abrogation of signal transduction upstream of RAS [Hanafusa et al., 2002]. However, whether phosphorylated Sprouty can effectively compete with other SH2 binding targets of GRB2 under physiological conditions is a matter of controversy as the sequence surrounding the N-terminal conserved Tyrosine does not match the consensus recognition site for the SH2 domain of GRB2, which implies that the binding of GRB2 SH2 domain to Sprouty should be much weaker than its binding to FRS2 or SHP2 [Mason et al., 2006]. In addition, a number of subsequent reports have shown that Spry1 and Spry2 binding to GRB2 is constitutive rather than stimulation dependent, and that association of FRS2 with GRB2 remains unaffected in presence of these two Spry isoforms [Gross et al., 2001; Mason et al., 2004; Rubin et al., 2005].

Yet in one subsequent study, Spry2 interaction with GRB2 was proposed to be mediated via a Proline-rich sequence at the very C-terminal of Spry2, interacting with the first SH3 domain of GRB2 in an stimulation dependent manner [Lao et al., 2006]. The authors proposed that the Proline-rich sequence may be somehow cryptic in un-stimulated cells, but becomes available due to a conformational change after stimulation [Lao et al., 2006]. In contrast to a number of earlier studies which had shown that Sprys did not have any effect on SOS-GRB2 interaction [Gross et al., 2001; Hanafusa et al., 2002], this study claimed that binding of Spry2 to the SH3 domain of GRB2 could compete with SOS binding, thereby inhibiting GRB2 mediated SOS recruitment and activation of RAS [Lao et al., 2006]. Interestingly, the C-terminal Proline-rich motif of Spry2 is not conserved amongst other Spry family members, ruling out the possibility of a conserved function for all Sprouty homologues at the GRB2-SOS interface. However, in the context of FGF signalling, the effect of Spry2 on ERK1/2 pathway has been

shown to be considerably more potent than the other mammalian homologues [Mason et al., 2006]. This difference was proposed to be due to the unique Proline-rich SH3 recognition site present in the C-terminus of Spry2 [Lao et al., 2006].

The second protein that was reported to bind to the N-terminal Tyrosine residue of Sproutys is CBL [Hall et al., 2003; Rubin et al., 2003]. The sequence surrounding the N-terminal Tyrosine residue of Sproutys strongly matches the consensus recognition site for the SH2 domain of CBL [Ng et al., 2008], and several reports have demonstrated that CBL interacts with Sprouty through binding of its SH2 domain to the conserved N-terminal Tyrosine following stimulation [Hall et al., 2003; Rubin et al., 2003; Mason et al., 2004]. In case of Spry2, CBL has also been reported to additionally interact with another region in the N-terminal of the protein (residues 11 to 53) via its RING domain [Wong et al., 2000]. Surprisingly, CBL has been shown to be dispensable for Sprouty mediated inhibition of ERK1/2 downstream of FGF [Mason et al., 2004]. In fact, Sprouty binding to CBL has been shown to result in its ubiquitination, and subsequent proteosomal degradation [Hall et al., 2003; Mason et al., 2004], thus relieving signalling from Sprouty inhibition. These results suggest that the binding of another factor other than CBL must be mediating the inhibitory activities of Sproutys on FGF induced ERK1/2 signalling. Further studies are needed to clarify how phosphorylation of the conserved N-terminal Tyrosine can act as an activator and a down-regulator of Sprouty at the same time.

Since phosphorylation of the conserved N-terminal Tyrosine is vital for regulation of Sprouty stability and function, the phosphatase that dephosphorylates this residue should play a key role in regulation of Sprouty response. This phosphatase has been reported to be SHP2, whose interaction with Sprouty has been shown to have a negative impact on Sprouty function. SHP2 dephosphorylates the conserved N-terminal Tyrosine residue of Sprouty, thus resulting

in its inactivation in the context of FGF signalling [Hanafusa et al., 2004; Jarvis et al., 2005]. As mentioned earlier, it has been proposed that some of the stimulatory effects of SHP2 on FGF signalling may be accomplished by selective dephosphorylation and inactivation of Sprouty family members [Hanafusa et al., 2004; Jarvis et al., 2005].

The conserved N-terminal Tyrosine of Sprouty is not the only residue that has been shown to be subject to phosphorylation. FGF activity also results in phosphorylation of another conserved tyrosine residue (Y227) within the C-terminal of Spry2, and this seems to be essential for Spry2 inhibitory function on FGF mediated ERK1/2 signalling [Rubin et al., 2005]. The corresponding kinase and the molecular mechanism underlying the role of this phosphorylation with regard to Sproutys function remain unknown. Serine phosphorylation of a number of Sprouty residues has also been reported. An early study showed that murine Spry1 and 2 are Serine phosphorylated in HUVECs, and this phosphorylation results in a band-shift during SDS-PAGE analysis with the slower migrating band corresponding to phosphorylated Sprouty [Impagnatiello et al., 2001]. However, no differences in the level of serine phosphorylation of Spry1 and 2 were observed before and after FGF2 stimulation, suggesting that the underlying mechanism of phosphorylation must be constitutive [Impagnatiello et al., 2001]. A later report also confirmed serine phosphorylation of human SPRY2, but claimed that this phosphorylation occurred in an EGF dependent manner [DaSilva et al. 2006]. It went on further by identifying Mitogen Activated Protein Kinase-Interacting Kinase 1 (Mnk1) as the kinase responsible for phosphorylation of SPRY2 on two Serine residues (S112 and S121), located in a loosely conserved serine-rich stretch of amino acids within the N-terminal [DaSilva et al. 2006]. Mutation of these residues abrogated the SDS-PAGE band-shift in SPRY2 [DaSilva et al. 2006], suggesting that the two sites must be the main targets for serine phosphorylation. Phosphorylation of SPRY2 on these two residues

was found to abrogate Y55 phosphorylation, resulting in the reduction of CBL binding, and consequent stabilisation of SPRY2 [DaSilva et al. 2006]. To add a further twist, another study has argued that FGFR activity results in dephosphorylation of serine phosphorylated SPRY2 and a consequent disappearance of the band shift, suggesting that an FGFR dependent phosphatase activity must be involved [Lao et al., 2007]. Protein Phosphatase 2A (PP2A) was subsequently identified as the likely phosphatase which dephosphorylates SPRY2 in an FGF dependent manner [Lao et al., 2007]. This dephosphorylation was suggested to induce a conformational change [Lao et al., 2007], proposed to be needed for GRB2 binding to the C-terminal proline rich region of Spry2 in an earlier study by the same group [Lao et al., 2006]. Surprisingly, PP2A interaction with SPRY2 was shown to be dependent on the conserved N-terminal Tyrosine region and mutually exclusive with CBL binding, but not dependent on the phosphorylation of this Tyrosine, implying that while the presence of the conserved N-terminal region is vital for SPRY2 activity, its phosphorylation acts as an inhibitory mechanism by enhancing CBL binding rather than PP2A binding [Lao et al., 2007]. Point mutations of S110, S112, S115, S118, S121, T124, S125, S127, S128, S130, or S131 were all capable of abrogating the SPRY2 band-shift [Lao et al., 2007]. While phosphorylation of S112 and S115 were further confirmed by mass spectrometry analysis, further evidence would be needed to prove whether all of the above mentioned residues undergo phosphorylation [Lao et al., 2007]. In addition, mass spectrometry analysis also revealed a number of other phosphorylation sites of SPRY2 which were only present when FGFR was over-expressed (S138, S156, S167, Y176, T190, Y191, S197) [Lao et al., 2007]. The functional significance of these sites remains to be determined.

In contrast to the above mentioned FGF induced dephosphorylation model, a very recent study has reported that Spry2 undergoes phosphorylation on six Serine residues (S7, S42,

S112, S121, S140, S167 in human SPRY2) following ERK1/2 activation [Brady et al., 2009]. Mutations of these residues abrogate Spry2 band-shift and enhance ERK1/2 inhibition [Brady et al., 2009], which is in agreement with the earlier mentioned study on EGF induced Sprouty phosphorylation by Mnk1 [DaSilva et al. 2006]. The causes of these discrepancies are unknown.

1.5.6 Variations, and controversies

While all Sprouty family members share the common feature of acting on RTKs, the specific pathways affected, exact points of interception, and even the final outcome of the action for different Sprouty family members on different RTKs seem to be context dependent, variable, and subject to controversies. In *Drosophila*, dSpry activity was shown to result in abrogation of ERK1/2 kinase activity [Casci et al., 1999; Reich et al., 1999], placing it upstream of ERK1/2 and downstream of RTKs. However, the exact point at which dSpry acts on the ERK1/2 pathway remained controversial, with one study claiming it to be upstream of RAS [Casci et al., 1999], while another arguing for downstream or at the level of RAF [Reich et al., 1999]. A similar problem holds true for different vertebrate Sproutys. In NIH3T3 cells, murine Spry2 was shown to inhibit FGF induced ERK1/2 activation by acting upstream of RAS without affecting the PI3K/AKT pathway [Gross et al., 2001], which can also be a target for RAS [Rodriguez-Viciana et al., 1994]. An action upstream of RAS was also suggested in another study using *Xenopus* Spry1 (xSpry1) and mouse Spry2 [Hanafusa et al., 2002]. However, in another study in HEK 293T cells, murine Spry2 action was placed at the level of RAF, as RAF kinase activity but not RAS GTP binding was impaired by Spry2 over-expression [Yusoff et al., 2002]. The effect of Spry2 on PI3K signalling has also been

challenged with a report showing that human SPRY2 antagonises PI3K activity by both stabilising and activating the PIP3 phosphatase PTEN [Edwin et al., 2006]. This SPRY2 mediated PTEN activation was found to be crucial for anti-proliferative effects of SPRY2 [Edwin et al., 2006]. For Spry4, an early report suggested an action at the level or upstream of RAS in response to VEGF, and FGF stimulation [Lee et al., 2001]. However, a subsequent study showed that Spry4 functions on VEGF signalling by suppressing PKC-dependent, but not RAS-dependent, activation of C-RAF [Sasaki et al., 2003]. This was shown to be mediated by direct binding of C-RAF catalytic domain to a region within the SPRY domain of Spry4. This region, named RAF Binding Motif (RBM), is well conserved among all Sprouty family members [Sasaki, A. et al., 2003], indicating that PKC-dependent/RAS-independent inhibition of RAF activity might be a conserved feature of all Sproutys. As mentioned earlier, B-RAF can also directly interact with Spry2 and 4 in a similar manner to C-RAF [Tsavachidou et al., 2004]. Oncogenic mutations of B-RAF abrogate this interaction, suggesting that Spry-RAF interaction must be sensitive to the conformation of RAF kinase domain [Brady et al., 2009]. Interestingly, Spry2 association with B-RAF was also found to be negatively regulated by Serine phosphorylation of Spry2, which was triggered by ERK1/2 activity downstream of B-RAF, thereby creating an additional layer of feedback regulation [Brady et al., 2009].

A further example of variation in Sprouty response is seen in *Xenopus*. While xSpry1 seems to be able to suppress ERK1/2 activation in both *Xenopus* embryos and explants [Hanafusa et al., 2002], xSpry2 exerts its inhibitory effect on FGF induced PLC activity and Ca^{2+} release without affecting ERK1/2 signalling [Nutt et al., 2001]. dSpry does not inhibit Ca2+ signalling when ectopically expressed in *Xenopus* embryos, suggesting that this variation in Sprouty action is not due to differences in the cellular contexts, but rather results from an

evolutionary divergence in Sprouty function [Nutt et al., 2001]. Recently, attenuation of PLC mediated PIP2 hydrolysis, Ca^{2+} release, and PKC activation was also shown for mammalian Spry4 downstream of VEGF-A. This activity of Spry4 was attributed to its binding to PIP2, thereby limiting substrate availability to PLC [Ayada et al., 2009]. Another recent report has shown that SPRY2 could also inhibit PKCδ by directly binding to it [Chow et al., 2009]. SPRY2 binding did not affect the phosphorylation state of PKCδ itself, but blocked PKC mediated phosphorylation of its substrate Protein Kinase D1 (PKD1) [Chow et al., 2009]. Significantly, SPRY2 binding to PKCδ was shown to be important for attenuation of ERK1/2 signalling and inhibition of invasion in PC3 prostate cancer cells [Chow et al., 2009].

The most striking of all variations in Sprouty response is seen in the context of EGF signalling. While dSpry acts as an inhibitor of ERK1/2 signalling, downstream of both FGF and EGF [Casci et al., 1999; Kramer et al., 1999; Reich et al., 1999], several results have challenged a negative regulatory role for vertebrate Sproutys on EGF signalling. An early report showed that human SPRY1 and 2 are incapable of impeding EGF mediated ERK1/2 activation, despite inhibiting EGF induced cell proliferation [Impagnatiello et al., 2001]. Several following studies revealed that mammalian Sproutys even augment EGF mediated ERK1/2 signalling instead of suppressing it [Wong et al., 2002a; Sasaki et al., 2003; Hall et al., 2003; Rubin et al., 2003]. This positive effect was shown to be dependent on CBL, which binds to the conserved N-terminal Tyrosine residue of SPRY via its SH2 domain following growth factor induced phosphorylation by SRC [Wong et al., 2002a; Rubin et al., 2003; Fong et al., 2003; Mason et al., 2004]. Binding of SPRY to CBL can compete with binding of EGFR to CBL, thus resulting in inhibition of receptor ubiquitination, and lysosomal degradation, and a consequent augmentation of EGF mediated ERK1/2 activity (Figure 1.10) [Wong et al., 2002a; Sasaki et al., 2003; Hall et al., 2003; Rubin et al., 2003].

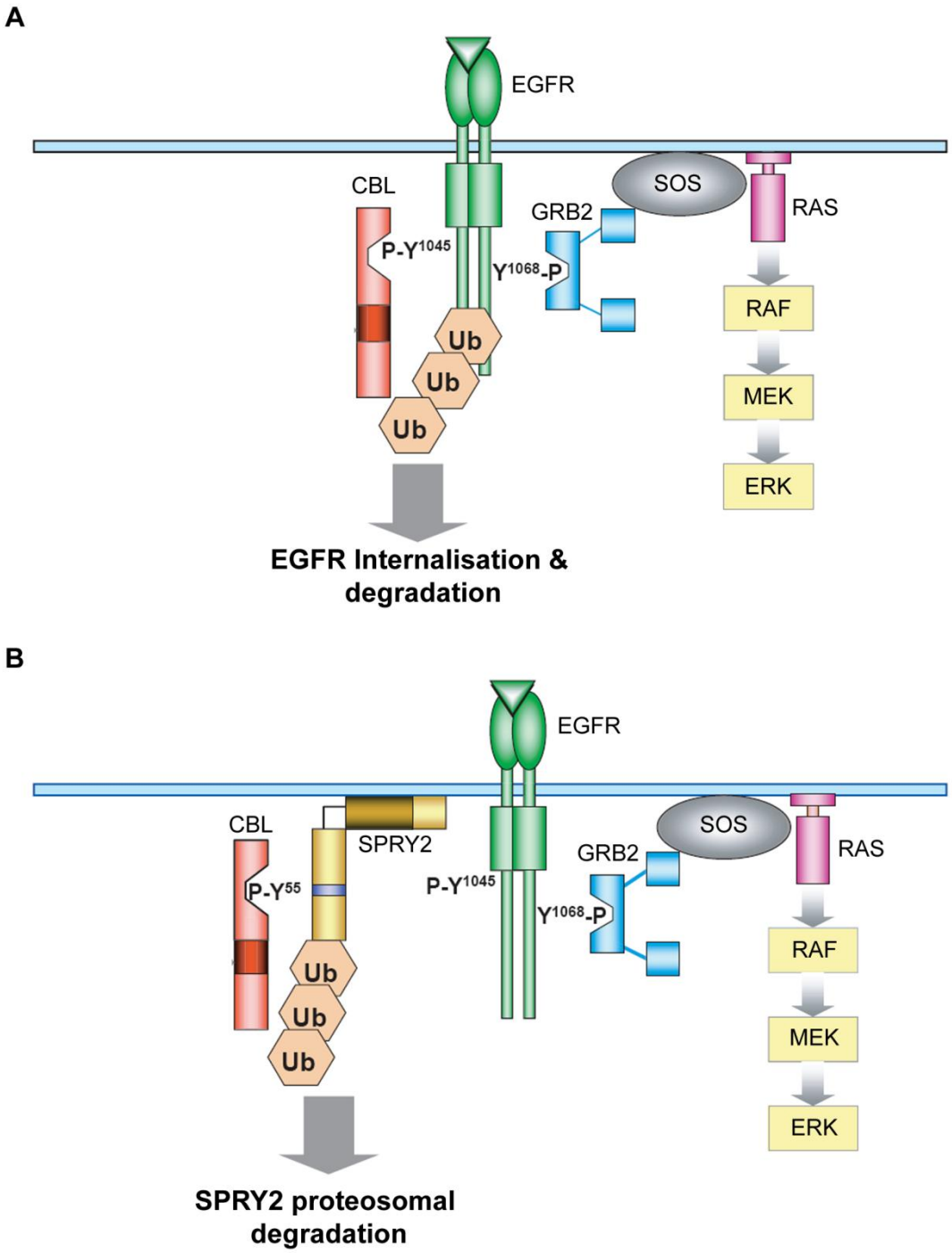

Figure 1.10. The proposed mechanism for SPRY2 mediated augmentation of ERK1/2 signalling downstream of EGFR. In the absence of SPRY2, CBL engages the EGF receptor via phosphorylated Y1045, and this results in ubiquitination of the receptor, triggering its internalisation and eventual lysosomal degradation **(A)**. In the presence of SPRY2, CBL is sequestered via its binding to phosphorylated Y55, thus resulting in abrogation of CBL mediated receptor down-regulation. At the same time, SPRY2 is ubiquitinated by CBL and targeted for destruction via the proteosomal degradation pathway **(B)**. Figure was taken with modifications from [Guy et al., 2003].

A possible explanation for the observed discrepancy between the effects of Sprouty on EGF and FGF could be the differential regulation of SPRY in each signalling context. In support of this view, apart from phosphorylation of the conserved N-terminal Tyrosine (Y55), FGF activity was also shown to result in phosphorylation of the C-terminal Tyrosine residue (Y227) in Spry2 which is essential for the inhibitory activity of the protein [Rubin et al., 2005]. However, EGF was shown to be less effective in inducing this modification, supporting the existence of pathway specific mechanisms that can differentially regulate SPRY function [Rubin et al., 2005]. In addition, the dynamics of N-terminal Tyrosine phosphorylation itself has also been shown to be considerably different between EGF and FGF signalling contexts. While EGF induces a transient phosphorylation of the N-terminal Tyrosine, FGF induces a much more prolonged phosphorylation [Mason et al., 2004]. However, it is not clear how this could contribute to the differences observed between SPRYs response to each growth factor. Whether other regulatory mechanisms exist that could explain some of the here listed variations and discrepancies remains to be determined. Nevertheless, it is possible that some of the controversial results were due to experimental artefacts, or non-physiological conditions such as over-expression, and were, therefore, irrelevant with regards to the physiological functions of Sproutys.

Yet, another possibility is that so far unknown differences between FGF and EGF signalling pathways exist, which can result in the two pathways being differentially affected by modulators of signalling like SPRYs. This view is in line with a report which showed that Spry2 affects the endocytic trafficking of activated EGFR [Kim et al., 2007]. Interestingly, this effect was not found to be dependent on CBL, but relied on binding of Spry2 to the endocytic regulatory protein HRS [Kim et al., 2007]. As mentioned, earlier, HRS is part of the ESCRT0 protein complex which plays a pivotal role in progression of the activated EGFR

from early endosomes to late endosomal MVBs [Sorkin and von Zastrow, 2009]. Binding of Spry2 to HRS competed with the binding of HRS to TSG101, an essential subunit of ESCRT-I, thus impeding the progression of EGFRs from early to MVB late endosomes [Kim et al., 2007]. As activated ERK1/2 progresses from early to late endosomes along with EGFR, expression of Spry2 blocked re-localisation of activated ERK1/2 from early to late endosomes too [Kim et al., 2007]. Thus, rather than affecting total levels of active ERK1/2 in response to EGF stimulation, Spry2 seems to specifically block ERK1/2 activity on late endosomes [Kim et al., 2007]. Discrepancy in the action of Sprouty on EGF versus FGF mediated ERK activation might, therefore, be due to differences between the endocytic pathways of FGF and EGF, or variations in the spatial distribution of ERK1/2 in each context. The validity of this hypothesis has yet to be tested. However, a splicing isoform of SEF has also been shown to act as a spatial regulator of ERK1/2 signalling by specifically inhibiting the translocation of activated ERK1/2 to the nucleus, while leaving the activated cytoplasmic ERK1/2 unaffected [Torii et al., 2004].

1.5.7 Interacting partners

Several interacting partners for Sprouty proteins have been identified, a number of which such as GRB2, CBL, RAF, SHP2, PP2A, and PKCδ have already been discussed in this chapter. Amongst others is Caveolin1 (CAV1), a critical lipid raft protein which has been shown to co-localise and physically interact with all mammalian Sproutys [Impagnatiello et al., 2001; Cabrita, et al., 2006]. This interaction is mediated via two regions in CAV1, a strongly binding C-terminus region (aa 135-178), and a weakly binding N-terminal region (aa 61-101). Notably, a single Spry2 point mutation (R252D) can totally abrogate CAV1 binding [Cabrita

et al., 2006], a mutation previously characterised for its inability to bind to PIP2 and translocate to the plasma-membrane after stimulation [Lim et al., 2002]. Though CAV1 on its own has been shown to act as an inhibitor of ERK1/2 signalling, the effect of SPRY2-CAV1 interaction on ERK1/2 inhibition seems to be complex, context dependent, and not fully understood [Cabrita et al., 2006].

Another notable Sprouty interacting partner is the dual specificity kinase TESK1, which has been shown to interact with SPRY2 and 4. TESK1 plays an important role in regulation of integrin mediated actin cytoskeleton, and cell spreading [Tsumura et al., 2005]. Through its C-terminal SPRY domain, SPRY4 binds to and inhibits the kinase activity of TESK1, which results in abrogation of cell spreading [Tsumura et al., 2005]. For SPRY2, binding to TESK1 has been shown to sequester SPRY2 to some vesicular compartment where it is unable to function through interacting with the SH3 domain of GRB2 [Chandramouli et al., 2008].

Two ubiquitin ligases in addition to CBL have been shown to interact with Sprouty proteins. One is Seven in absentia homolog-2 (SIAH2), which binds to a region within the N-terminal of Sproutys in a Tyrosine phosphorylation independent manner [Nadeau et al., 2007]. SIAH2 interaction with Spry1, 2, and 4 results in their ubiquitination and degradation independent of growth factor stimulation, thus controlling the state-state protein levels [Nadeau et al., 2007]. Accordingly, interference with SIAH2 mediated ubiquitination of SPRY2 in SW1 melanoma cells which have wild-type B-RAF resulted in increased SPRY2 protein levels and reduced tumourigenesis and metastasis potentials, *in vivo* [Qi et al., 2008].

Another more recently identified ubiquitin ligase that interacts with SPRY1 and 2 but not 3 and 4 is NEDD4 [Edwin et al., 2010]. NEDD4 interaction with SPRY1 and 2 requires its Serine phosphorylation at S112 and S121 sites [Edwin et al., 2010], which were previously

shown to destabilise SPRY2 [DaSilva et al. 2006]. However, this was previously suggested to be due to reduced CBL binding [DaSilva et al. 2006]. Depletion of NEDD4 increased SPRY2 levels and resulted in attenuation of FGF induced ERK1/2 activity, which could be prevented by co-knockdown of SPRY2 [Edwin et al., 2010], further supporting a negative regulatory role for NEDD4 with regards to SPRY2 function.

SPRY2 has also been shown to interact with the CBL-Interacting Protein of 85kDa (CIN85) [Haglund et al., 2005]. CIN85 is recruited to RTKs via CBL and acts to facilitate CBL mediated RTK endocytosis, so its sequestration along with CBL by SPRY2 further inhibits CBL mediated EGFR internalisation and contributes towards elevated EGFR activity by SPRY2 [Haglund et al., 2005]. CIN85 binding is specific to SPRY2, as it requires the C-terminal Proline-rich region that is only present in SPRY2. A secondary Proline-rich region within the N-terminal, which is also specific to SPRY2, may further enhance CIN85 binding [Haglund et al., 2005]. Both of these Proline-rich regions are recognised by CIN85 SH3 domain [Haglund et al., 2005].

One of the most recently reported interacting partners of Sprouty proteins is the CRK-like adaptor protein (CRKL), which contains an N-terminal SH2 domain followed by two tandem SH3 domains [Satoh et al., 2010]. Binding of CRKL to SPRY2 was shown to be stimulation dependent, and involved both the SH2 and SH3 domains of CRKL [Satoh et al., 2010]. Interaction of SPRY2 with CRKL inhibited CRKL mediated RAP1 activation, revealing the small GTPase RAP1 as a novel target of Sprouty [Satoh et al., 2010].

Finally, Sprouty proteins have been shown to also interact with each other via their SPRY domains [Hanafusa et al., 2002; Ozaki et al., 2005]. SPRY domain results in hetero/homo-oligomerisation of different Sprouty isoforms, which has been suggested to result in synergy

between them and enhancement of their inhibitory activities on signalling [Ozaki et al., 2005]. In another study, mammalian Sproutys were shown to form iron-sulphur clusters via their C-terminal SPRY domains, through which they assemble into huge monodisperse assemblies of 24 Sproutys [Wu et al., 2005]. The functional impact of these iron-sulphur clusters remains a mystery, though changes in the redox state of the iron-sulphur clusters by nitrosylation were shown to impair Sproutys function [Wu et al., 2005]. These results implicate a possible involvement of Nitric Oxide (NO) signalling in regulation of RTKs via Sprouty [Wu et al., 2005].

Despite identification of a considerable number of proteins which can interact with different Sprouty isoforms, behaviour of this family of signalling inhibitors is still not fully and convincingly explained. It is therefore possible that more, yet uncharacterised, functionally significant binding partners for Sprouty family members exist, whose identification could further elucidate some of the less well understood or controversial aspects of Sprouty function and regulation.

1.6 Sprouty Related with EVH1 Domain (SPRED)

Initially discovered in a screen for c-Kit interactors [Wakioka et al., 2001], the Spred family of proteins constitute a conserved group of signalling regulators which inhibit ERK1/2 signalling downstream of a variety of stimuli [Wakioka et al., 2001; Kato et al., 2003; Nonami et al., 2004; King et al., 2005; Bundschu et al., 2005; Sivak et al., 2005]. As it is apparent from their name, Spreds are related to the Sprouty family of RTK antagonists, sharing their characteristic Cysteine-rich C-terminal domain, but diverging by further containing a central Kit Binding Domain (KBD), and an N-terminal Enabled/VASP

Homology-1 (EVH1) domain (Figure 1.11) [Bundschu et al., 2006b]. Three mammalian, two *Xenopus*, and a single *Drosophila* Spred homologues have been described on the basis of sequence similarities [Bundschu et al., 2006b]. Whereas the ERK1/2 inhibitory activity of Sprouty family members seems to be restricted to certain RTKs, Spreds have been shown to act downstream of a wide range of RTK and non-RTK receptors such as Cytokine and Chemokine receptors [Wakioka et al., 2001; Kato et al., 2003; Nonami et al., 2004; King et al., 2005; Bundschu et al., 2005; Sivak et al., 2005]. The inhibitory effect of Spreds, however, is thought to be confined to the ERK1/2 pathway [Wakioka et al., 2001; Nonami et al., 2004; King et al., 2005]. Interestingly, a liver restricted alternative splice variant of Spred3 known as Eve3, which lacks all the conserved domains apart from EVH1, has also been reported (Figure 1.11) [King. et al., 2006]. Even this truncated isoform is capable of potently suppressing the ERK1/2 pathway in liver cells [King. et al., 2006].

1.6.1 Expression

To date, several studies have investigated the expression patterns of different murine Spred isoforms. Among different murine Spreds, Spred2 is the most widely expressed, with mRNAs being almost ubiquitously detected in RT-PCR and northern blot analyses of various adult as well as embryonic mouse tissues and organs, with brain exhibiting the highest levels [Kato et al., 2003; Engelhardt et al., 2004; Bundschu et al., 2005]. Spred1 mRNA is also highly expressed in brain, along with moderate and more restricted expression levels in a number of other tissues [Engelhardt et al., 2004]. Spred3 expression, on the other hand, is exclusively restricted to brain [Kato et al., 2003].

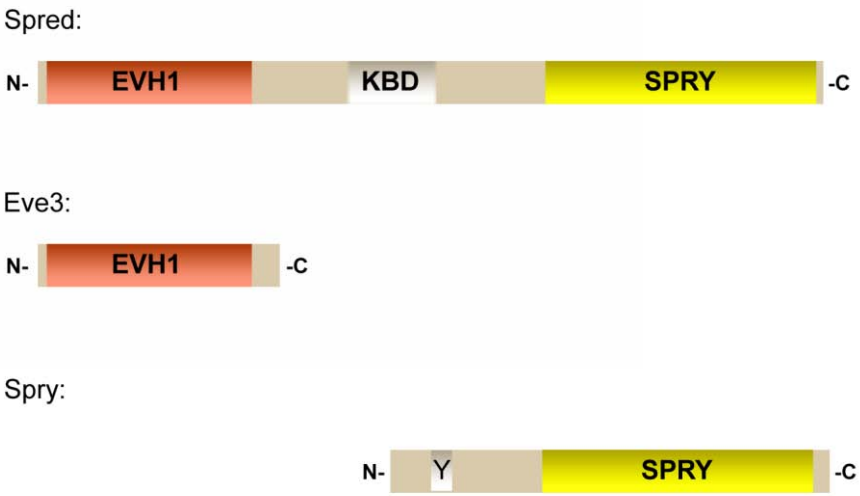

Figure 1.11. Schematic representation of Spred structure. TOP: Spred proteins are consisted of an N-terminal EVH1 domain, a central KBD, and a C-terminal Cysteine-rich SPRY domain. MIDDLE: Eve3 is a liver restricted splice variant of Spred3 which only contains the N-terminal EVH1 domain. BOTTOM: Sprouty proteins lack the N-terminal EVH1 domain and the central KBD, but share the SPRY domain with Spreds. Sprouty proteins also contain a conserved N-terminal Tyrosine residue (marked as Y) which is absent in Spreds.

A gene-trap study of Spred2 promoter activity in mice has further confirmed a widespread expression pattern in both new born and adult mice, with neuronal tissues exhibiting the highest expression levels [Bundschu et al., 2006a]. Immunohistochemical as well as western blot analysis of different mouse tissues and organs were also in line with a ubiquitous expression pattern for Spred2, although in some cases the protein expression levels differed significantly with those of mRNA levels or gene-trap activity [Engelhardt et al., 2004; Bundschu et al., 2006a]. As mentioned before, expression of Eve3, a truncated splice variant of Spred3, is exclusively restricted to liver [King et al., 2006].

1.6.2 Spred in development

In *Xenopus*, Spreds have been implicated along with Sproutys in regulation of gastrulation and mesoderm formation downstream of FGFs [Sivak et al., 2005]. However, both the timing and the target pathways of Spreds seemed to be distinct from those of Sproutys [Sivak et al., 2005], suggesting that the two proteins might be employing distinct molecular mechanisms. In mammals, a number of knockout studies have highlighted Spreds involvement in several developmental processes such as bone morphogenesis [Bundschu et al., 2005], haematopoiesis [Nobuhisa et al., 2004], allergen-induced airway eosinophilia [Inoue et al., 2005], neuronal plasticity and hippocampal learning [Denayer et al., 2008], and lymphatic vessel development [Taniguchi et al., 2007b].

Knockout of Spred2, the most widely expressed isoform of Spreds, results in a dwarf phenotype which mimics Achondroplasia, suggestive of a physiological link to FGFR3 signalling [Bundschu et al., 2005]. Spred2-null mice exhibit reduced body size, have a shorter tibia, and develop narrower bone growth plates compared to wild type mice, all suggestive of

FGFR3 hyperactivity [Bundschu et al., 2005]. In addition, an independent Spred2 knockout study reported defects in embryonic haematopoiesis due to hyperactive Cytokine signalling in the Aorta-Gonad-Mesonephros (AGM) region [Nobuhisa et al., 2004].

In contrast to Spred2, Spred1 knockout mice appear normal [Inoue et al., 2005]. However, lack of Spred1 enhances allergen-induced airway eosinophilia and hyper-responsiveness, and airway mucus production is increased [Inoue et al., 2005]. Both the production of eosinophils as well as their migration to the respiratory system seems to be increased in Spred1-null mice, and this is thought to be due to aberrant Interleukin-5 (IL5) signalling [Inoue et al., 2005]. Recently, it has been shown that Spred1-null mice also exhibit decreased learning and memory performance due defects in synaptic hippocampal plasticity [Denayer et al., 2008]. These defects were suggested to be due to elevated ERK1/2 signalling in hippocampus [Denayer et al., 2008]. A recent *in vivo* RNAi study has also suggested a role for Spred1 in neuronal development [Phoenix and Temple, 2010]. During development, Spred1 is highly expressed in the germinal zones of the Central Nervous System (CNS) [Phoenix and Temple, 2010]. Stable RNAi mediated depletion of Spred1 in the forebrain of mouse embryos causes defects in the apical-ventricular zone and loss of radial glia alignment, thus damaging the late neuronal migration and leading to formation of peri-ventricular heterotopias [Phoenix and Temple, 2010]. Interestingly, the phenotype of Spred1 depletion is very similar to that caused by mutations in a number of vesicular trafficking related proteins, implicating a potential role for Spred1 in endocytic trafficking [Phoenix and Temple, 2010]. In line with this hypothesis, Spred1 was found to localise to a specific vesicular compartment in cortical progenitor cells [Phoenix and Temple, 2010].

Double knockout of Spred1 and Spred2 have also been generated, which exhibit severe subcutaneous haemorrhage and embryonic lethality at E12.5 to E15.5 [Taniguchi et al.,

2007b]. This is due to defects in angiogenesis of lymphatic vessels, caused by aberrant VEGFR3 signalling [Taniguchi et al., 2007b]. These results clearly reveal a role for Spred1 and 2 in regulation of VEGFR signalling *in vivo*. Since no lymphatic defects were observed in single knockouts of Spred1 and 2, the function of these proteins must be compensatory to one another in the context of lymphatic VEGF signalling.

1.6.3 Tumour suppression and Neurofibromatosis

SPREDs have been proposed to have a specific role in suppressing tumour invasion and metastasis, as stable expression of Spred1 in LM8 osteosarcoma cells inhibited tumour metastasis in nude mice [Miyoshi et al., 2004]. *In vitro*, Spred1 could block chemokine induced cell migration in an EVH1 and SPRY domain dependent manner [Miyoshi et al., 2004]. This effect of Spred1 on cell motility was proposed to be the result of its direct interaction with RhoA, which inhibited RhoA activity and downstream actin stress fibre formation [Miyoshi et al., 2004].

Similar to SPRYs, the expression levels of both SPRED1 and 2 has been shown to be reduced in human Hepatocellular Carcinomas, with levels negatively correlating with malignancy [Yoshida et al., 2006]. Ectopic expression of Spred1 in hepatocellular carcinoma cells resulted in inhibition of cell proliferation, growth factor mediated cell motility, and secretion of matrix metalloproteinases 9 and 2, which are known to play an important role in invasion and metastasis of these cells [Yoshida et al., 2006]. It remains to be determined if SPREDs are also subject to down-regulation in cancers other than hepatocellular carcinomas.

Recently, germ-line loss-of-function mutations of SPRED1 have been reported in a Neurofibromatosis type1-like disorder termed Legius syndrome [Brems, et al., 2007].

Neurofibromatosis type1 is characterised by multiple café-au-lait spots on the skin, freckling of the groin or arm pit, Lisch nodules in the eye iris, and tumours of the nervous system. Loss of function mutations of a RAS GAP known as Neurofibromin (NF1) are the main known cause of the disease, although several similar disorders are caused by gain of function mutations of other components of the ERK1/2 pathway such as SHP2, SOS, K-RAS, H-RAS, B-RAF, MEK1 and MEK2 [Brems, et al., 2007]. A wide range of SPRED1 mutations were found to cause Legius syndrome, most of which generally resulting in truncation of SPRED1 and deletion of all or part of the SPRY domain [Brems, et al., 2007]. One mutation which resulted in a small deletion within the EVH1 domain was also detected [Brems, et al., 2007]. Collectively, these findings further support the notion that Spreds are physiological attenuators of the ERK1/2 pathway. Furthermore, a number of affected individuals exhibit learning difficulties [Brems, et al., 2007], which supports a role for SPRED in neuronal development and synaptic plasticity [Denayer et al., 2008].

1.6.4 Mechanism of ERK1/2 inhibition

As mentioned earlier, Spred proteins seem to be specific inhibitors of the ERK1/2 pathway downstream of a plethora of stimuli [Wakioka et al., 2001; Nonami et al., 2004; King et al., 2005]. A number of previous studies have shown that the N-terminal EVH1 domains of Spreds are essential for their inhibitory activity on ERK1/2 [Wakioka et al., 2001; King et al., 2005]. Deletion of the EVH1 domain of both Spred1 and 2 renders them incapable of down-regulating growth factor induced ERK1/2 signalling [Wakioka et al., 2001; King et al., 2005]. In contrast, KBD which provides binding to c-Kit is not essential for Spreds function, although its deletion seems to reduce their inhibitory activity [Kato et al., 2003; Nobuhisa et

al., 2004]. In line with this finding, Spred3 which has a non-functional KBD due to substitution of a key Arginine residue is still capable of inhibiting ERK1/2 signalling, albeit less efficiently than Spred1 and 2 [Kato et al., 2003]. The SPRY domain is also believed to be required for Spred function, as its deletion in Spred2 abrogated ERK1/2 inhibition [Wakioka et al., 2001; King et al., 2005]. In the original Spred discovery report, the same was also shown for Spred1, but a later report claimed this was not the case and Spred1 mediated ERK1/2 inhibition was SPRY domain independent [King et al., 2005]. As for Spred3, its EVH1-only splice variant (Eve3) is fully capable of attenuating ERK1/2, suggesting that the SPRY domain is needed for protein function [King et al., 2006]. Interestingly, addition of a plasma-membrane targeting C-terminal CAAX sequence to a SPRY deleted non-functional Spred2 mutant restores its capacity to inhibit ERK1/2, suggesting that the main role of the SPRY domain is to correctly localise Spred2 [King et al., 2005]. In fact, similar to Sprouty family members, the SPRY domain of Spred has been shown to be crucial for post-stimulation membrane targeting via interacting with PIP2 [Lim et al., 2002].

Similar to Sproutys, the point of action of Spred proteins is subject to debate and controversy. In the original Spred discovery report, Spred1 was shown to bind to both RAS and RAF and inhibit RAS mediated RAF activation [Wakioka et al., 2001]. However, a subsequent study showed that both Spred1 and 2 were acting upstream of RAS and downstream of the RTKs [King et al., 2005]. In addition to inhibiting RAS, Spred1 and 2 were also shown to inhibit RAP1, which can also feed into the ERK1/2 pathway [King et al., 2005].

The molecular mechanism of ERK1/2 inhibition by Spreds is currently unknown. In particular, it needs to be determined how the EVH1 domain is mediating the inhibitory activity of Spreds [Wakioka et al., 2001; King et al., 2005]. EVH1 domains are interaction modules found in various cytoskeletal and signalling proteins which bind to highly specific

Proline-rich stretches of amino acids on their target proteins [Ball et al., 2002]. Given the requirement of the EVH1 domain for ERK1/2 inhibition, it can be assumed that that some functionally significant binding partner of Spreds might be interacting with them through the EVH1 domain. No such EVH1 specific Spred interacting partner has been reported until now (see chapter four).

1.6.5 Interacting partners

The interactions of Spreds with RhoA, RAS and RAF were discussed earlier. Apart from these, CBL has also been reported to interact with Spred [Lock et al., 2006]. CBL was shown to bind to a double Tyrosine motif within the KBD of Spred2 which gets phosphorylated after growth factor stimulation or pervanadate treatment, and this binding results in ubiquitination and subsequent proteosomal degradation of Spred2 [Lock et al., 2006]. The identity of the kinase which phosphorylates Spred2 on the double Tyrosine motif is currently unknown.

Similar to Sprouty, Spred has also been shown to interact with TESK1, and this is believed to inhibit TESK1 kinase activity, thus resulting in modulation of the cytoskeleton [Chandramouli et al., 2008; Johne et al., 2008]. Caveolin1 (CAV1) has also been suggested to interact with Spreds [Nonami et al., 2005]. CAV1 and Spred1 were shown to interact in CAV1 positive lipid rafts (Caveola), and cooperate to inhibit ERK1/2 signalling [Nonami et al., 2005], although the mechanism of this cooperation was not clear.

As mentioned before, no EVH1 specific interacting partner for Spreds has been reported until now (see chapter four).

1.7 Neighbour of BRCA1-1 (NBR1)

In chapter four of this thesis, a novel interacting partner for Spred2 is described. Named Neighbour of *BRCA1*-1 (NBR1) due to the close proximity of its gene to the breast cancer susceptibility gene *BRCA1*, NBR1 is a relatively large (988 amino acids in mouse), highly conserved (~90% between mouse and human) multi-domain scaffold protein, which was initially thought to be the ovarian cancer antigen CA125 [Campbell et al., 1994]. Later it became clear that CA125 was coded by an entirely different gene called (MUC16) [Yin et al., 2001], and in fact no link between NBR1 and ovarian cancer exists. Similarly, no link between NBR1 and breast cancer has been demonstrated despite the close proximity of its gene to *BRCA1*.

NBR1 contains several protein-protein interaction domains including an N-terminal phox/Bem1p (PB1) domain, a ZZ type zinc finger (ZZ), a coiled-coiled (CC) region, and a C-terminal Ubiquitin Associated (UBA) domain (Figure 1.12) [Chambers and Solomon, 1996; Whitehouse et al., 2002; Kirkin et al., 2009; Waters et al., 2009]. At the domain architecture level, NBR1 is very similar to another multi-domain scaffold protein known as P62/Sequestosome-1(SQSTM1) (Figure 1.12). Nevertheless, no significant sequence homology exists between the NBR1 and P62. In comparison to NBR1, P62 is much better studied. A role for P62 has been demonstrated in many different cellular processes including RTK endocytic trafficking [Sanchez et al., 1998; Geetha et al., 2005], NF-κB signalling [Nakamura et al., 2010], extrinsic apoptosis pathway [Moscat and Diaz-Meco, 2009], and selective autophagy [Bjørkøy et al., 2005; Pankiv et al., 2007].

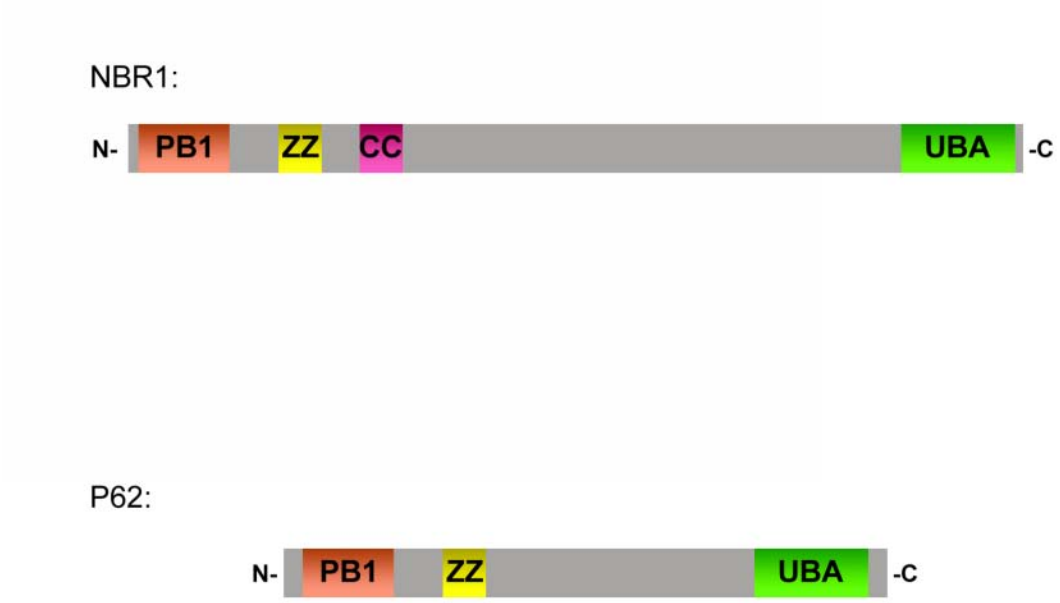

Figure 1.12. Schematic representation of NBR1 domains and motifs. TOP: NBR1 is consisted of an N-terminal PB1 domain, followed by a ZZ type zinc finger motif (ZZ), a Coiled-Coil (CC) region, and a C-terminal UBA domain. BOTTOM: P62 is shorter than NBR1, but similarly has an N-terminal PB1 domain, a ZZ motif, and a C-terminal UBA domain.

PB1 domains are homo/hetero-dimerisation modules found in a wide variety of proteins [Müller et al., 2006]. The PB1 domain of NBR1 has been shown to hetero-dimerise with the PB1 domain of P62 [Lange et al., 2005; Müller et al., 2006;]. On the other hand, the UBA domain of NBR1 has been shown to be capable of binding to both K48 and K63 type poly-ubiquitin chains [Kirkin et al., 2009; Waters et al., 2009]. The function of the ZZ domain is not clear at the moment, while the CC region is thought to mediate NBR1 self-association [Kirkin et al., 2009; Waters et al., 2009].

1.7.1 Expression

Northern blot analysis of several human adult tissues for NBR1 showed a ubiquitous expression [Chambers and Solomon, 1996; Whitehouse et al., 2002]. A smaller splice variant was also detected in testes, and some other tissues [Whitehouse et al., 2002]. *In situ* hybridization analysis of mouse embryos at E9 also suggested a ubiquitous Nbr1 expression in all embryonic tissues and organs. At E10.5 to E13, however, the expression seemed to be more restricted to neuronal cells, while the ubiquitous expression was restored in adult mice [Whitehouse et al., 2002].

1.7.2 Regulation of Titin signalling in muscle

In a Yeast 2-Hybrid screen, NBR1 was identified as an interacting partner for the giant muscle kinase Titin [Lange et al., 2005]. Spanning half the length of a sarcomere (from Z disk to M band), Titin is thought to be capable of sensing tension through mechanically induced changes in its kinase domain conformation [Lange et al., 2005]. NBR1 binds to the kinase

domain of Titin only in its mechanically open and active conformation [Lange et al., 2005]. This binding is mediated by the PB1 domain of NBR1, which is also required for interacting with P62 [Lange et al., 2005]. Via P62, NBR1-Titin interaction can regulate the nuclear localisation of a muscle-specific RING-B-box ubiquitin ligase (MuRF2), which is a specific P62 binding partner. If localised to the nucleus, MuRF2 can interact with Serum Response Factor (SRF) and inhibit its transcriptional activity [Lange et al., 2005]. Thus, changes of mechanical strain can result in changes of gene expression by Titin in a signalling pathway mediated by NBR1, P62, and MuRF2 [Lange et al., 2005]. Interestingly, a mutation in Titin which abrogates NBR1 binding leads to a hereditary muscle disease known as Hereditary Myopathy with Early Respiratory Failure (HMERF), indicating that Titin-NBR1-P62-MuRF2 signalling pathway must be important for normal muscle cell function [Lange et al., 2005].

1.7.3 Selective Autophagy

Autophagy is a degradative process through which certain cytoplasmic proteins and organelles become engulfed in a double lipid-membrane, removed from the cytosol, and digested via the lysosomal degradation pathway. In mammals, the process of autophagy is initiated by appearance of Isolation Membranes (IMs), which grow into double-membrane semi-spheres that engulf cytosolic contents, eventually closing and separating the engulfed material from the cytosol (Figure 1.13). The fully closed spherical double-membrane vesicles that are resulted are known as immature Autophagosomes (AVis) (Figure 1.13). AVis then fuse with lysosomes, or with endosomes en route to lysosomes, forming degradative Autophagosomes (AVds), the contents of which are eventually digested via lysosomal enzymes such as acid hydrolyses (Figure 1.13) [Longatti and Tooze, 2009].

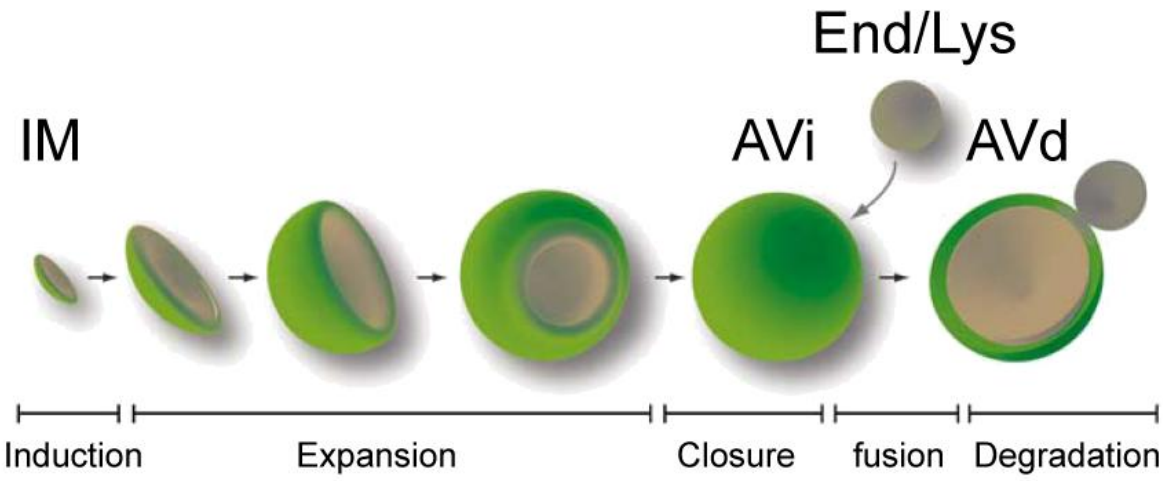

Figure 1.13. A schematic representation of the autophagy process in mammals. Autophagy is initiated by formation of an isolation membrane (IM) which expands into a hemi-sphere that engulfs cytosolic contents. Further growth followed by the eventual closure of the hemi-sphere creates a double-membrane vesicular entity known as immature autophagosome (AVi). AVis fuse with lysosomes (Lys) or endosomes en route to lysosomes (End), creating degradative autophagosomes (AVds). Ultimately, the contents of the AVd are digested by lysosomal enzymes. Figure adopted with modifications from [Longatti and Tooze, 2009].

Several proteins, many of which initially identified in yeast, regulate the various steps of autophagy. These are termed Atg proteins. At the centre of the autophagy machinery is Atg8, the yeast homologue of mammalian Microtubule Associated Protein Light Chain-3 (LC3), which associates with the autophagy machinery and the autophagosomal membranes throughout the process of autophagy [Longatti and Tooze, 2009]. LC3 is, therefore, commonly used as a marker for autophagy [Longatti and Tooze, 2009]. Full-length LC3 (LC3I) is a diffuse cytosolic and soluble protein. However, after induction of autophagy, LC3 is cleaved by a Cysteine protease (Atg4), and lapidated by a conserved ubiquitin-related conjugation system comprised of an E1 (Atg7), E2 (Atg3), and E3 (Atg16L complex), which conjugates Phosphatidylethanolamine (PE) to LC3. The cleaved and lapidated LC3 (LC3II) is then inserted into and remains attached to autophagosomal membranes throughout the autophagy, where it functions to expand, close, and possibly maturate autophagosomes [Longatti and Tooze, 2009].

By employing a Yeast 2-Hybrid approach, two very recent studies identified NBR1 as a direct binding partner of LC3 [Kirkin et al., 2009; Waters et al., 2009]. A main LC3 Interacting Region (LIR) and a secondary LC3 Interacting Region (LIR2) were shown to exist in the C-terminal of NBR1 [Kirkin et al., 2009]. It was also demonstrated that NBR1 could localise to autophagosomes, and get degraded in a LIR dependent manner by autophagy [Kirkin et al., 2009]. Since the UBA domain of NBR1 is believed to associate with poly-ubiquitinated proteins, and poly-ubiquitinated proteins accumulate in cells when autophagy is inhibited, it was proposed that NBR1 could be acting as an adaptor for targeting specific poly-ubiquitinated cargos to autophagosomes to be degraded along with NBR1 itself [Kirkin et al., 2009]. Interestingly, P62 can also associate with LC3, and a similar role as a selective autophagy adaptor has also been proposed for P62 [Bjørkøy et al., 2005; Pankiv et al., 2007].

The identity of any autophagosomal targeted ubiquitinated cargo for P62 or NBR1 is currently unknown.

1.8 Thesis aims

The aim of this is to understand the molecular mechanism of signal attenuation by Sprouty and Spred in the context of FGFR signalling. As described above, Sprouty and Spred constitute two key families of signalling regulators which control different aspects of normal development, and act as negative regulators of tumourigenesis during the adult life. In particular, members of both families have been shown to function as physiological regulators of FGFR signalling. However, their mechanism of action has remained unclear, incomplete, and subject to various controversies.

Specifically, this study set out to determine the following points:

What are the novel interacting partners of Sprouty, and what are the functional implications of these interaction? (Chapter 3)

What are the novel Sprouty phosphorylation sites, how do their dynamics change, and what are the functional implications? (Chapter 3)

What binds to the EVH1 domain of Spred, and what is the molecular mechanism of the EVH1 domain dependent Spred activity? (Chapter 4)

Finally, in answering the later point, this study was brought to investigate the involvement of NBR1 in regulation of RTK trafficking and signalling, and the potential cross-talk between this pathway and autophagy (Chapter 5).

CHAPTER 2

Materials and Methods

2.1 Materials

2.1.1 Buffers and solutions

General:

- Phosphate Buffered Saline (PBS): PBS pH 7.2 tablets (Oxoid) made up according to manufacturers' instructions.
- Tris Buffered Saline (TBS): 10 mM Tris-HCl pH 7.4, 75 mM NaCl.

Bacterial culturing:

- Luria Bertani Broth (LB): 10 μg/l tryptone, 5 g/l yeast extract, 10 g/l NaCl, pH 7.4
- Ampicilin plates (LA): LB + 15 g/l bactoagar, 100 μg/ml ampicilin
- Kanamycin plates (LK): LB + 15 g/l bactoagar, 50 μg/ml Kanamycin

DNA manipulation:

- DNA loading buffer (6x): 0.25 % bromophenol blue (w/v), 0.25 % xylene cyanol FF (w/v), 15 % Ficol (w/v)
- TBE buffer (5x): 54 g/l Tris, 27.5 g/l boric acid, 10 mM EDTA pH 8.0

Protein manipulation:

- Triton X-100 lysis buffer (1x): 150 mM NaCl, 50 mM Tris-HCl pH 7.4, 0.5% Triton X-100 (v/v), 1 mM EDTA, 50 mM NaF, 1 mM Na_3VO_4, 1 mM Phenylmethylsulfonyl fluoride (PMSF), and 1 tablet of protease inhibitor cocktail (Roche Diagnostics) per 10ml of buffer.

- BN/SDS Triton X-100 lysis buffer (1x): 50 mM NaCl, 50 mM Tris-HCl pH 7.4, 1% Triton X-100 (v/v), 1 mM EDTA, 50 mM NaF, 1 mM Na_3VO_4, 1 mM Phenylmethylsulfonyl fluoride (PMSF), and 1 tablet of protease inhibitor cocktail (Roche Diagnostics) per 10ml of buffer.
- SDS sample buffer (2x): 100 mM Tris-HCl pH 6.8, 10 % glycerol (v/v), 2 % SDS (w/v), 0.1 % bromophenol blue (w/v), 200 mM Dithiothreitol.
- Tris-Glycine running buffer: 25 mM Tris, 0.2 M glycine, 0.1 % SDS (w/v).
- MES running buffer (20x): Pre-made from (Invitrogen)
- MOPS running buffer (20x): Pre-made from (Invitrogen)
- Immunoblot transfer buffer: 25 mM Tris, 0.2 M glycine, 10 % methanol (v/v).
- PBS-Tween (PBST): PBS + 0.05% Tween 20 (v/v).
- Ponceau-S stain: 0.1 % Ponceau-S sodium salt (w/v), 5 % acetic acid (v/v).
- Coomassie stain: Pre-made Imperial Protein Stain from (Pierce).
- Immunoblot stripping buffer: 62.5 mM Tris pH 6.8, 2 % SDS (w/v) and 100 mM β-mercaptoethanol.
- Immunoblot blocking buffer: PBST + 5% Bovine Serum Albumin (BSA) or non-fat dried milk powder.

Immunofluorescence:

- Fixation solution: 4 % paraformaldehyde in PBS (v/v)
- Wash buffer: PBS
- Permeabilization solution: PBS + 0.2 % Triton X-100 (v/v)
- Blocking buffer: PBS + 4 % BSA

- Mowiol mounting solution: 10 % Mowiol 488 (w/v), 25 % glycerol (v/v), 0.1 M Tris/HCl pH 8.5, dissolved at 50°C, centrifugated at 5000g for 15 minutes, and 2 crystal grains of p-phenylendiamine added to each 5 ml, dissolved to completion, and stored at -80°C.

Trypsin digestion:

- Incubation/wash buffer: 25 mM ammonium bicarbonate.
- Dehydration/wash buffer: 50 % acetonitrile, 25 mM ammonium bicarbonate.
- Reduction buffer: 10 mM DTT, 25 mM ammonium bicarbonate.
- Alkylation Buffer: 55 mM iodoacetamid, 25 mM ammonium bicarbonate.
- Trypsin re-suspension buffer: Pre-made from (Promega).
- Digestion buffer: 10 µg/ml Trypsin, 25 mM ammonium bicarbonate.

Cell culture:

- Dulbecco's Modified Eagle Medium: Pre-made and supplemented with 4.5 g/L Glucose and Glutamine (Invitrogen).
- Foetal Calf Serum: purchased as frozen from (Labtech International)
- L-Glutamine (100x): Pre-made from (Invitrogen)
- Penicillin-Streptomycin Solution (100x): Pre-made from (Invitrogen)
- 0.05% Trypsin-EDTA Solution: Pre-made from (Invitrogen)

2.1.2 Reagents and Antibodies

All primary antibodies used in this study are listed in (Table 2.1). Non-specific rabbit IgG control was from Sigma. All fluorescently conjugated secondary antibodies (Cascade-blue, Alexa Fluor 488, Alexa Fluor 594, Alexa Fluor 645, and Texas Red) were from Invitrogen and used at 1:200 dilution. Horseradish peroxidase conjugated anti-mouse and anti-rabbit IgG secondary antibodies were from Amersham Biosciences Inc. and used at 1: 5000 dilution. IRDye infrared (700nm and 800nm) anti-mouse and anti-rabbit IgG secondary antibodies were from Li-COR Biosciences and used at 1:15000 dilution.

FGF2 was in-house prepared (work by Susan Brewer). EGF was purchased from Sigma. Z-VAD-FMK and Bafilomycin-A1 were also from Sigma. 4-12% NuPAGE Novex Bis-Tris Gels used for SDS-PAGE were purchased from Invitrogen.

Non-silencing control (NSC), P62, and NBR1 siRNAs were purchased from Santa Cruz Biotechnology Inc. An independent NBR1 targeting single siRNA was purchased from Dharmacon. All siRNAs were re-suspended in RNase-free water (Santa Cruz) to 10 µM and stored at -20°C prior to use.

LysoTracker-Red DND-99 was purchased from Invitrogen. Custom-made JUBA peptide was from Alta Bioscience. GST tagged PH domain of PLCδ1 (PIP_2 Grip) was purchased from Echelon-Inc. Membrane lipid strips, PIP arrays, and all phospholipids apart from Phosphatidylcholine were also purchased from Echelon-Inc. Phosphatidylcholine was purchased from Avanti Polar Lipids Inc.

Antibody	Species	Manufacturer	Working dilution
Spry2 (N-terminal)	RP	SIGMA	1:4000 (IB)
Spred2	RP	SIGMA	1:2000 (IB) – 1:100 (IF)
α-Tubulin (Clone DM 1A)	MM	SIGMA	1:5000 (IB)
P62 (clone 2C11)	MM	ABNOVA	1:1000 (IB)
NBR1 (clone 6B11)	MM	ABNOVA	1:500 (IB) – 1:50 (IF)
FGFR1 (flg)	RP	SANTA CRUZ	1:1000 (IB)
FGFR2 (bek)	RP	SANTA CRUZ	1:500 (IB)
Rab5	RP	SANTA CRUZ	1:50 (IF)
Rab7	RP	SANTA CRUZ	1:50 (IF)
ERK1	RP	SANTA CRUZ	1:2000 (IB)
pERK1/2(clone E-4)	MM	SANTA CRUZ	1:1000 (IB)
LAMP2 (clone H4B4)	MM	ABCAM	1:40 (IF)
LAMP2	RP	ABCAM	1:100 (IF)
MPR (clone 2G11)	MM	ABCAM	1:100 (IF)
NBR1	MM	ABCAM	1:500 (IB)
GRB2	RP	CELL SIGNAL	1:1000 (IB)
cRaf	RP	CELL SIGNAL	1:1000 (IB)
EGFR	RP	CELL SIGNAL	1:1000 (IB)
Cav1	RP	CELL SIGNAL	1:100(IF)
EEA1	RP	CELL SIGNAL	1:100(IF)
GM130	RP	CELL SIGNAL	1:100(IF)
myc (clone 71D10)	RM	CELL SIGNAL	1:200(IF)
GST	RP	CELL SIGNAL	1:1000 (IB)
cleaved PARP	RP	CELL SIGNAL	1:1000 (IB)
cleaved CASP-9	RP	CELL SIGNAL	1:1000 (IB)
RAB11	RP	INVITROGEN	1:25 (IF)
myc (clone 9E10)	MM	ROCHE	1:5000 (IB) – 1:500 (IF)
GFP (3E1)	MM	CRUK	1:2000 (IB)

Table 2.1. List of all primary antibodies and their dilutions used in this study. RP: Rabbit Polyclonal; MM: Mouse Monoclonal; RM: Rabbit Monoclonal; IB: Immunoblot; IF: Immunofluorecence.

2.1.3 Plasmids

Wild type (WT) human SPRY2 and Y55A mutant (Y55A) human SPRY2 constructs, cloned into pEFBOS-ires-Topaz vector, have been described before [Li, X. *et al.*, 2004]. For Gateway cloning, target sequences were first cloned into pDONR201 entry vector (Invitrogen), according to manufacturer's instructions. Myc tagged constructs were generated by recombining entry vectors into a Myc-pRK5 Gateway destination vector kindly provided by Laura Machesky, using LR clonase enzyme (Invitrogen). GFP tagged constructs were similarly generated using pcDNA DEST53 destination vector (Invitrogen). For bacterial 6XHis tagged protein expression pcDNA pDEST17 destination vector was used (Invitrogen), and for GST tagged bacterial protein expression pcDNA pDEST15 was employed.

Full-length SPRY2, Full-length Spred2, ΔEVH1 Spred2, ΔSPRY Spred2, SPRY-ONLY Spred2, and EVH1-ONLY Spred2, Full-length Nbr1, ΔUBA Nbr1, Δ856 Nbr1, ΔPB1 Nbr1, ΔPB1-ZZ Nbr1, and all the Nbr1 serial deletion constructs were generated by Gateway cloning as before, using gateway compatible primers targeted to the 5' and 3' ends of the desired sequences. The Y750A point mutation was generated by site-directed mutagenesis of the full-length Nbr1 pDONR201 entry clone using overlapping forward and reverse primers harboring the specific mutation in the middle. Nbr1 ΔJUBA mutation, and Spred ΔKBD mutation were generated from the full-length Nbr1 pDONR1 entry clone using primers with Age-I restriction digestion site 5'overhangs. These forward and reverse primers were targeted to just after and just before the JUBA or KBD coding sequences respectively, and were used in a PCR to amplify the whole construct minus the JUBA coding sequence. The linear product was then circularized by Age-I digestion (NEB) and self-ligation using T4 ligase (Invitrogen) according to manufacturer's instructions.

C-terminal GFP tagged NBR1 construct was a gift from Mathias Gautel. N-terminally FLAG tagged P62 construct was a gift from Robert Layfield. C-terminally GFP tagged TrfR1 was a gift from Joshua Rappoport, and C-terminally GFP tagged FGFR2 was a gift from John Ladbury.

2.1.4 Stable cell-lines

LC3-GFP 293A stable cell-line was a gift from Sharon Tooze (CRUK London Research Institute, London, UK). The cells were maintained in DMEM supplemented with 10 % Foetal Calf Serum (FCS) without any added antibiotics for no more than 20 passages.

2.2 Methods

2.2.1 Molecular cloning

Polymerase Chain Reaction (PCR):

PCR was performed using pfu polymerase (Promega) according to manufacturer's instructions. 2 units of enzyme, 1 μl of dNTP mix (Promega), ~50 ng of template, and 10 pmol of each primer was used per PCR reaction. The annealing temperature was chosen to be either 60°C or 5°C lower than the lowest primer melting temperature, which ever was the lowest. The extension time was varied depending on the length of the desired PCR product. Approximately 2 minutes was given for every kb.

Gateway cloning:

Gateway cloning was performed exactly according to Manufacturer's instructions (Invitrogen). Briefly, forward and reverse primers with in-frame gateway 5' overhangs corresponding to the beginning and end of a target sequence were used in a PCR to generate Gateway compatible coding fragments. These fragments were then recombined into pDONR201 entry vector (Invitrogen) using BP clonase enzyme (Invitrogen). Desired expression constructs were subsequently generated by recombination from the entry clones into destination vectors using LR clonase enzyme (Invitrogen).

Restriction digestion:

0.2-0.5 μg of DNA was digested by 5-10 units of total restriction enzyme (NEB) in a 20 μl reaction volume using the recommended buffer and temperature conditions according to the manufacturer. Digestion was carried for 1 hr to overnight.

DNA sequencing:

Sequencing was performed via Plasmid to Prolife service of the the Functional Genomics Laboratory (School of Biosciences, University of Birmingham). 200-500 ng of plasmid DNA along with 3.2 pmol of the desired sequencing primers in a 10 μl reaction were prepared for plasmid to profile. The results were analysed by Sequencher 4.9 software.

Transformation of competent cells**:**

0.1 μg of plasmid DNA, or any indicated amounts of product resulting from molecular cloning procedures was added to 100 μl of DH5α competent E.coli cells on ice for 20 minutes. The Cells were subsequently heat-shocked for 1 minute at 42°C, followed by incubation on ice for 2 more minutes. 1 ml of LB was added and the cells were incubated at

37°C for 1 hour with agitation. 50 to 250 µl of the mixture was then plated on LA or LK plates and incubated for overnight at 37°C.

Mini-prep and Maxi-prep:

For Mini-prep, single colonies of transformed E.coli were grown overnight in 2-5 ml of LB supplemented with 100 µg/ml ampicilin, or 40 µg/ml kanamycin at 37°C, 225 rpm, 100% humidity. For Maxi-prep the volume was increase to 500 ml. Cultures were pelleted by centrifugation at 6000g for 15 minutes at 4°C, the supernatant was discarded, and the extraction procedure was carried out using QIAGEN Mini- or Maxi-prep kits according to manufacturer's instructions. The concentration of the resulting DNA solutions were determined by measuring absorbance at 260 nm using a UV/light spectophotometer. The purity of the samples was always checked as well determining 260 nm/ 280 nm absorption ratio.

DNA electrophoresis:

DNA electrophoresis was done on 1 % agarose gels made in TBE, containing 0.2 µg/ml ethidium bromide. Gels were resolved as 100 V in TBE buffer, and the bands were visualised by UV illumination.

2.2.2 Cell culture, transfection, and stimulation

Cell culture:

Human Embryonic Kidney epithelial 293T (293T) cells were cultured at 37°C, 5 % CO_2 in DMEM supplemented with 10% foetal calf serum (FCS) (v/v) (Labtech International). As the

cells were weakly adherent, no trypsinisation was required prior to splitting and flasks could be knocked gently on a bench top to detach the cells. The cultures were generally split between 1/2 and 1/10 into new flasks with fresh medium. COS7 cells were cultured similarly but split using 0.05% Trypsin-EDTA (Invitrogen).

Transfection:

DNA transfections were performed using GeneJuice transfection reagent (Novagen), according to manufacturer's instructions. 1-3 μg of DNA was used per 35 mm dish. After transfection, cells were incubated for 24-48 hrs, or as indicated for the experiment, to allow sufficient expression of recombinant proteins. The efficiency of transfection was always estimated using a GFP-pEF-BOS transfected positive control. SiRNA transfections were performed using Lipofectamine2000 (Invitrogen), or Lipofectamine RNAiMAX (Invitrogen), according to manufacturer's instructions. 100 pmol of siRNA was used for a 35mm dish per transfection. For multiple siRNA transfections, cells were seeded at 20% and the first Transfection was carried out right after seeding (reverse transfection) followed by second and third Transfections at 24 hrs intervals. For DNA-siRNA co-transfections, Lipofectamine2000 was similarly used, according to manufacturer's instructions. 1μg DNA and 50 pmol of siRNA were used per co-transfection for a 35 mm dish.

Growth factor stimulation:

For growth factor stimulation, cells were washed with serum-free DMEM followed by incubation in the same for 6 hours in order to serum-starve the cells. FGF2, to the final concentration of 20 ng/ml, and heparin (Celsus labs), to the final concentration of 10 μg/ml, were added to the cells, with subsequent incubation for indicated amounts of time. For EGF stimulation, 50 ng/ml of EGF was added to the cells following starvation for indicated periods

of time. To terminate the stimulation, cells were washed with cold PBS and kept on ice before lysis/fixing. For stimulation with AlexaFuor-488 labelled EGF, serum starved cells were washed and incubated with 250 μg/ml of AlexaFuor-488 labelled EGF diluted on ice for 15 minutes. Serum-free DMEM supplemented with 20 mM HEPES, 0.1 % BSA (w/v) was used. The ligand was then washed off by ice-cold PBS and the cells were incubated at 37°C in DMEM to allow ligand internalisation for indicated periods of time.

2.2.3 Immunofluorescence and confocal microscopy

Immunofluorescence:

Cells grown on glass coverslips were washed with PBS before being fixed with 4% paraformaldehyde for 10 minutes at RT. Cells were subsequently washed three times with PBS and permeabilised with permeabilisation buffer for 3 minutes at RT. Following three more PBS washes, cells were blocked in blocking buffer for 15-60 minutes at RT. Diluted primary antibodies in blocking buffer were then applied to cover each coverslip and incubated for 45-60 minutes. Coverslips were washed three times with PBS before being subjected to fluorescently conjugated secondary antibodies in darkness for another 45-60 minutes. Finally, the coverslips were washed another three times with PBS followed by a final H_2O wash, before being mounted on microscope slides using Mowiol mounting solution. The slides were dried at RT, and stored -20°C until analysis by confocal microscopy.

LysoTracker staining:

For LysoTracker-Red staining, a 100nM solution of the dye in culture medium was applied to the cells prior to fixation for 2 hrs. All following steps were performed as before but in darkness.

Confocal Microscopy:

Sequential single section images were taken by LEICA TCS SP2 confocal microscope system using 63X objective lens under low speed (200Hz), minimum pinhole size (20μm), and optimal EXPAND settings to maximise image resolution. Final images were generated from averaging of 8 consecutive scans.

Image analysis:

All image analyses were carried out by Adobe photoshop 7.0 or ImageJ 1.37 software (Rasband, W.S., Image J, U.S. National Institute of Heath, Bethesda, Maryland, USA, 1997-2008). For quantification of co-localisations, ImageJ JACoP plugin (Bolte and Cordelières, 2006) was used to calculate percentage of co-localisation from Manders' overlapping coefficients (fraction of Green overlapping Red), using automatic noise threshold assignment.

2.2.4 Protein analysis

Cell lysis and protein concentration assay:

If just immunoblottings were to be carried out, cells were lysed by directly adding 2x SDS sample buffer (50 μl/cm^2 of cells). The lysate was vortexed vigorously and boiled for 2 x 5 minutes before being resolved on SDS PAGE. For immunoprecipitation or BN/SDS-PAGE analysis, relevant Triton X-100 lysis buffers were used (25 μl/cm^2 of cells). Lysates were

cleared by centrifugation at 14,000 g for 20 min at 4°C, and the pellets were discarded. All steps were performed at 4° C. Total protein concentrations of the cleared lysates were determined by Coomassie (Bradford) Protein Assay Kit (Pierce Biotechnology Inc.), according to manufacturer's instructions. A range of lysate dilutions were used and the concentrations were extrapolated from a standard curve of BSA samples. Concentrations in a single experiment were equalised by addition of lysis buffer, subsequently.

Immunoprecipitation, SDS PAGE, and immunoblotting:

Immunoprecipitation was carried out by addition of antibody and Sepharose-G (Sigma) beads at the same time to the lysate followed by 1 hr to overnight incubation at 4°C. Unless stated otherwise, 200-600µg of Whole Cell Lysate (WCL) along with 1-3 µg of antibody was used. 30 µl of 50% washed Protein G – Sepharose per 1 µg of antibody was added. For immunoprecipitation of endogenous SPRED2, ~4mg of cell-lysate was used per reaction along with 15µg of antibody. Beads were subsequently separated by short centrifugation, washed 5 times with 4° C 20x bed volume of the beads lysis buffer, re-suspended in 2 X SDS PAGE sample buffer, and boiled for 5 minutes at 100° C before analysis by SDS PAGE. For SDS PAGE analysis of the whole cell lysates, SDS PAGE sample buffer was added to the lysates, and mixes were boiled for 5 minutes at 100° C. Boiled samples were resolved on NuPAGE 4-12% pre-cast Bis-Tris gels (Invitrogen) using MOPS or MES buffers. For Immunoblotting (western blotting), proteins were transferred to Immobilon-FL PVDF membranes (Millipore) at 4° C using Immunoblot transfer buffer at 100V for 1:15 hours. The membranes were subsequently ponceau-S stained to check the transfer, before being dried. Dried membranes were incubated for 1 hour with primary antibody diluted in blocking buffer, washed five times with PBST, and incubated for another hour with the secondary antibody/antibodies of choice diluted in blocking buffer. This was followed by five further

washes with PBST, and a final wash with PBS. The membrane was then drained and incubated with Super-Signal enzyme chemiluminescence (ECL) reagent (Pierce) according to manufacturer's instructions. The proteins were finally visualised on Hyperfilm (Amersham Biosciences Inc.). In order to re-probe the blots, membranes were stripped for 30 minutes at 50° C in stripping buffer, washed three times with PBS, and dried prior to further use.

Protein staining of membranes/gels:

For ponceau-S staining, membranes were incubated in ponceau-S stain for 5 minutes, followed by washing by water until the desired contrast was achieved. For complete removal of the stain, the membranes were washed with PBS. For coomassie staining, gels were washed three times with 18MΩ water followed by incubation in Imperial Protein coomassie stain (Pierce) for 1 hr to overnight. Stained gels were then destained by washing in 18MΩ water until the desired contrast was reached.

Blue-Native (BN)/SDS-PAGE:

The method was based on [Camacho-Carvajal, et al., 2004] with modifications. First dimension 3-12% Native PAGE Bis-Tris gels were purchased from (Invitrogen). Samples were prepared and resolved according to Invitrogens manual, using dark and light blue cathode buffers and anode buffer (Invitrogen), at 4° C. To calibrate the gels, Native Mark Protein Standards (Invitrogen) were used. For the second dimension, resolved first dimension lanes were cut, and incubated in 2x SDS sample buffer for 1 hour with gentle shaking. Lanes were subsequently placed on 1.0 mm thick NuPAGE® Novex 4-12% Bis-Tris Gels (Invitrogen), and proteins were resolved using NuPAGE® MES SDS Running Buffer (Invitrogen) at 180 V for 2hrs. Subsequently, the gels were subjected to transfer and immunoblot as described.

2.2.5 Mass spectrometry

In gel trypsin digestion:

Cut gels were divided into multiple pieces and destained. Coomassie stained gels were destained by 15 minutes incubation with agitation in 30% acetonitrile followed by another 15 minutes in Dehydration/wash buffer (this was repeated until no staining remained). Gel pieces were dried by vacuum centrifugation for 5 minutes, and rehydrated in Reduction buffer, followed by incubation at 56°C for 45 minutes. Liquid was removed subsequently, and gels were re-suspended in Alkylation buffer for 45 minutes in the dark in order to alkylate the reduced Cysteine side-chains. Gels were then washed with Incubation/wash buffer, followed by two washes with Dehydration/wash buffer, before being dried by vacuum centrifugation as before. Trypsin digestion buffer was added to the dried gels and allowed to rehydrate for ~10 minutes on ice. Excess trypsin was taken and gels were covered with Incubation/wash buffer and incubated overnight at 37°C. The following morning, formic acid was added to the final concentration of 0.5%, and the solution was taken to a fresh tube. Further extraction was carried out using two 50% acetonitrile treatments, followed by a neat acetonitrile extraction. All supernatants were pulled together and the volume reduced to ~10 µl by vacuum centrifugation. Digests were kept at -80°C, until analysis by mass spectrometry.

TiO_2 enrichment:

Phosphopeptides enrichment was performed as in [Sweet et al., 2008]. Briefly, peptides were loaded onto TiO2 columns in 2% Trifluoroacetic acid (TFA). Columns were subsequently washed with 100 mg/mL 2,5-dihydroxybenzoic acid (DHB), 80% MeCN, 2% TFA, followed by an additional wash in the same buffer without DHB. Peptides were then eluted with 50

mM Na_2HPO_4 followed by dilute NH_4OH solution. Eluates were desalted using C18 ZipTips (Millipore) according to the manufacturer's instructions.

CID LC-MS/MS:

Mass spectrometry analysis was performed by Steve Sweet as in [Sweet et al., 2008]. Briefly, online liquid chromatography was performed using a Micro AS autosampler and Surveyor MS pump (Thermo Electron). Peptides were packed onto a 10 cm long 75 µm Integrafrit C8 resolving column (New Objective) and separated over a 40 minute gradient of 0 to 40 % acetonitrile. Peptides were eluted directly via a Triversa nanospray (Advion Biosciences) into a 7 Tesla LTQ FTICR mass spectrometer (Thermo Electron). For each FT-MS scan (m/z 395-1600) acquired, five CID MS/MS scans of the most abundant ions were performed in the LTQ cell. Survey scans were acquired in the ICR cell with a resolution of 100,000. A peptide isolation width of 3 Th was used. Only multiply-charged precursor ions were selected for MS/MS. CID was performed with helium gas at normalized collision energy of 35%. Ions activation was set at 30 ms. Data acquisition was controlled by Xcalibur software (Thermo Electron).

Targeted Electron Capture Dissociation (ECD):

ECD was performed by Steve Sweet as described in [Sweet et al., 2008]. Briefly, the mass spectrometer was setup to acquire FT-MS scans (m/z 395−1600) until an ion of interest listed in the inclusion list was detected. This triggered sequential CID and ECD MS/MS scans. Precursor ions were isolated in the ion trap and transferred to the ICR cell for ECD. Isolation width was 6 m/z. Automated gain control was used with a target value of 1000000 and a maximum fill time of 1 second. The electrons were produced by an indirectly heated barium tungsten cylindrical dispenser cathode, using a current of 1.1 A. Ions were irradiated with the

beam for 60 ms at 5% of total energy. 8 or 24 microscans acquired with a resolution of 25000 were added together to make one ECD MS/MS scan. A dynamic exclusion with a repeat count of two and an exclusion period of 30 seconds was used to save the instrument time. ECD data were manually assigned by Steve Sweet.

Data analysis:

Data were searched against the human SWISSPROT database using the SEQUEST software (University of Washington). For filtering search results, either the Xcorrelation (Xcor) vs. Charge score (1.5 for z=1, 2 for z=2, and 2.5 for z>=3) or the Protein probability P(pro) score was used. A reverse database search was also carried out in parallel to calculate the false-positive rate. For SILAC, data were searched by Mascot software (Matrix Sciences) and quantification was carried out by MaxQuant.

2.2.6 Fat blot, Liposomes, and Circular Dichroism

Fat blot:

Membrane lipid strips or PIP arrays (Echelon Inc) were blocked in Immunoblotting blocking buffer with milk for 1 hr at RT. GST or GST tagged protein of interest was then added at 1 μg/ml for 1 hr with gentle rocking. The membranes were washed with PBST for 5 times and immunoblotted with an anti-GST antibody as normal, followed by a peroxidase conjugated secondary antibody. The blots were visualised by ECL as normal.

Liposome preparation:

Liposomes were prepared as described in [Narayan and Lemmon, 2006]. Briefly, phosphatidylcholine and phosphatidylinositol-phosphate (PIP) of interest were mixed in a glass vial at 95:5 molar ratio. The lipid mixture was dried under an N2 gas stream, redissolved in 1:1 CHCl3:CH3OH, and dried again under N2 stream followed by vacuum centrifugation for 1 hour to remove any residual chloroform. The lipids were subsequently resuspended in ultrapure H_2O, and subjected to multiple rounds of freezing in -80°C and thawing in a 45°C sonicating water bath until the mixture became optically clear.

Circular-Dichroism:

Circular-Dichroism was performed as in [Conner et al., 2008]. Briefly, spectra were acquired on a Jasco J715 spectropolarimeter using 0.5mm cuvettes (Starna/Optiglass) with peptide concentrations of 1 mg/ml and Liposome concentrations of 2 mg/ml were applicable. Spectra were recorded from 300 nm to 180 nm with a bandwidth of 2 nm, a data pitch of 0.2 nm, a scan speed of 100 nm/min, and a response time of 0.5. Four consecutively recorded spectra were averaged for each sample and the relevant buffer baseline spectra were subtracted from each sample spectra.

CHAPTER 3

SPRY2: Analysis of Interacting Partners and Phosphorylation Sites

3.1 Introduction

Despite identification of a considerable number of proteins which can interact with Sprouty family members, their molecular mechanism is still subject of debate and controversy. Although it is possible that Sproutys can function through different mechanisms under different cellular conditions, an alternative hypothesis could be that there are other functionally significant but as yet unknown partners of Sprouty through which their seemingly complicated behaviour could be better explained. Another possible explanation for the observed variations in Sprouty response might be its differential regulation by post-translational modifications under different conditions. In support of this view, it has been shown that the dynamics of Sprouty N-terminal Tyrosine phosphorylation are different between EGF and FGF stimulatory contexts, with FGF inducing a much more prolonged phosphorylation [Mason, J. M. *et al*., 2004]. This could contribute towards the observed difference in Sprouty response to each signal. Furthermore, it has been shown that FGF activity also results in phosphorylation of another conserved tyrosine residue (Y227) within the C-terminal of Spry2 which is essential for the inhibitory activity of the protein, but EGF has been shown to be less effective in inducing this modification [Rubin, C. *et al*., 2005], further supporting the existence of pathway specific mechanisms that differentially regulate Sprouty function. Despite these, neither interacting partners nor post-translational modifications of Sprouty have been systematically analysed before.

It was therefore decided to search for novel interacting partners of Sprouty using a mass-spectrometry approach. SPRY2 was chosen for this purpose as it has been shown to be the most conserved as well as the most potent of all mammalian homologues with regards to ERK1/2 inhibition [Mason et al., 2006]. Here, a list of novel interacting partners of SPRY2 is reported. Interestingly, a significant number of these interacting partners have roles in

endocytic trafficking of receptors, suggestive of a potential endocytic regulatory function for SPRY2. In addition to identification of interacting partners, mass spectrometry was also used for a comprehensive identification and analysis of SPRY2 phosphorylations. A total of 16 phosphorylation sites were identified, 11 of which were novel. Of these novel sites one was T56 which is located right next to the critical N-terminal Tyrosine of SPRY2 (Y55). Interestingly, analysis of phosphorylation dynamics by quantitative mass-spectrometry revealed that while the majority of identified phosphorylations seem to be constitutive in response to stimulation, Y55 and T56 phosphorylations were reciprocally regulated. These results suggest a potentially critical role for T56 phosphorylation in regulation of Sprouty2 function.

3.2 Identification of SPRY2 binding partners by mass-spectrometry

First, the inhibition of ERK1/2 by SPRY2 in a time-course of FGF2 stimulation was assessed. This was done to reveal at which time-point the SPRY2 inhibition of ERK1/2 is maximal, since it might be likely that more of the functionally significant interacting partners of SPRY2 will be associated with it at such a time-point. 293T cells transfected with SPRY2 or GFP as control were serum starved and stimulated with FGF2 for a time-course of 3 hours. Subsequently, the cells were lysed and pERK1/2 and ERK1/2 levels were monitored by immunoblotting. Surprisingly, SPRY2 was found to inhibit ERK1/2 to a similar level at all investigated time-points (Figure 3.1A), suggesting there is no discrepancy in the ability of SPRY2 to inhibit ERK1/2 at different time-points post stimulation. As expected, a point mutation in the conserved N-terminal Tyrosine (Y55) abrogated SPRY2 ability to inhibit ERK1/2 (Figure 3.1B).

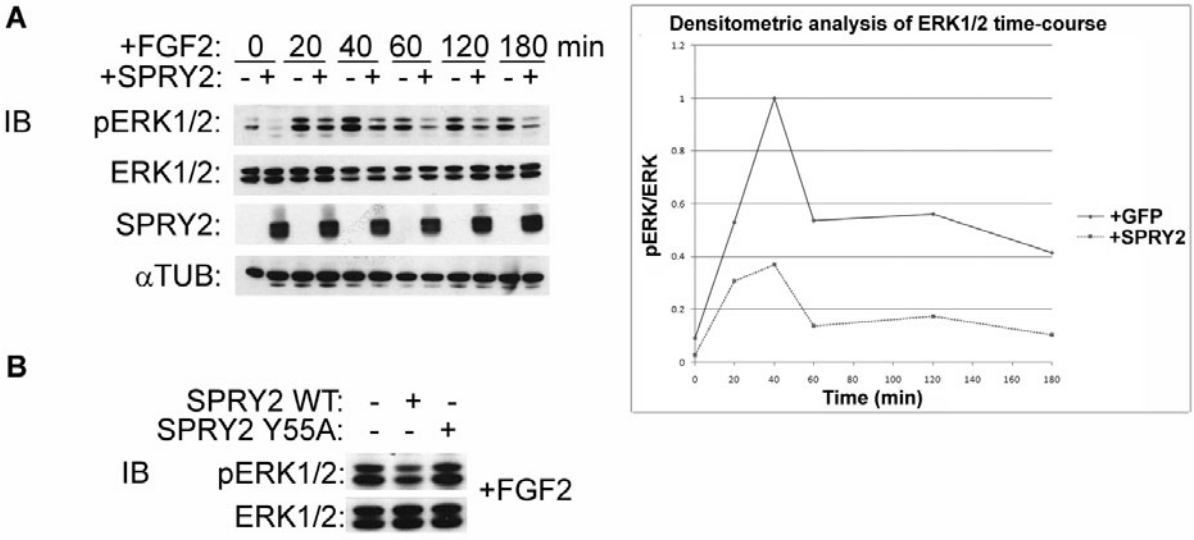

Figure 3.1. Sprouty inhibits ERK1/2 signalling at various time-points after FGF2 stimulation. 293T cells transfected with GFP or SPRY2 were serum starved and stimulated with 20 ng/ml FGF2 + 10 mg/ml Heparin. The cells were subsequently lysed and analysed by immunoblotting (IB) with indicated antibodies. SPRY2 similarly reduces pERK1/2 / ERK1/2 levels downstream of FGF2 at all time-points **(A)**. 293T cells transfected with WT, Y55A SPRY2 mutant, or GFP as control were serum starved and stimulated with 20 ng/ml FGF2 + 10 mg/ml Heparin for 40 minutes. Cells were subsequently lysed and analysed by immunoblotting with indicated antibodies. Unlike WT, Y55A SPRY2 mutant is incapable of reducing pERK1/2 levels **(B)**.

To identify novel interacting partners of SPRY2, a specific antibody against the protein was used to immunoprecipitate it from over-expressing 293T cells. GFP transfected cells were used as negative control. The cells were stimulated for 40 minutes as this was the time ERK1/2 activity was maximum (Figure 3.1A). After stimulation, the cells were lysed and subjected to immunoprecipitation overnight. Immunoprecipitates were subsequently washed and resolved by SDS PAGE, in-gel digested by trypsin, and the resulting peptides were extracted and analysed by online liquid-chromatography coupled with tandem mass-spectrometry (LC-MS/MS) using an FTICR-TRAP mass-spectrometer as described in materials and methods. The results were searched using the Sequest algorithm (Bioworks software) against the human SWISSPROT database, as well as a reversed human SWISSPROT database. The reverse search was performed to estimate the false-positive rate (FPR = the number of reverse to the number of forward identified hits) which was 3%. A total of 260 proteins were identified, 88 of which were only found in SPRY2 but not control immunoprecipitates (Table 3.1). When a more stringent FPR of 0.5% was applied, the total number of identified proteins was reduced to 200, 47 of which were only found in SPRY2 but not control immunoprecipitates (Table 3.1-bold). Interestingly a significant proportion of the identified SPRY2 specific interacting proteins under both low and high stringency FPR were related to endocytic trafficking (Table 3.1-green highlighted). The Serine/Threonine kinases Casein Kinase I and II (CKI & CKII) as well as the Protein Phosphatase 1 (PP1) catalytic subunit were also amongst the identified proteins (Table 3.1-yellow highlighted). Finally, a significant number of the identified proteins were either ribosomal subunits or chaperones involved in protein folding (Table 3.1-grey highlighted), which probably highlights the association of over-expressed SPRY2 with the translation and folding machineries during its synthesis.

TIF1B_HUMAN Transcription intermediary factor 1-beta	PERI_HUMAN Peripherin - Homo sapiens
RANB9_HUMAN Ran-binding protein 9	**TRI27_HUMAN Zinc finger protein RFP**
PARP1_HUMAN Poly [ADP-ribose] polymerase 1	RO52_HUMAN 52 kDa Ro protein
ACTN1_HUMAN Alpha-actinin-1	STAU1_HUMAN dsRNA-binding protein Staufen homolog1
RFIP5_HUMAN Rab11 family-interacting protein 5	PRP19_HUMAN Pre-mRNA-processing factor 19
ITSN2_HUMAN Intersectin-2	ZNF24_HUMAN Zinc finger protein 24
AP2A1_HUMAN AP-2 complex sub alpha-1	P53_HUMAN Cellular tumor antigen p53
DJC10_HUMAN DnaJ homolog subfamily C member 10	**MAEA_HUMAN Macrophage erythroblast attacher**
WDR26_HUMAN WD repeat protein 26	**EFTU_HUMAN Elongation. factor Tu**
DDX20_HUMAN Probable ATP-dependent RNA helicase	**BRE_HUMAN Protein BRE**
ATX2L_HUMAN Ataxin-2-like protein	CS062_HUMAN Uncharacterized protein C19orf62
CLH1_HUMAN Clathrin heavy chain 1	**PHF6_HUMAN PHD finger protein 6**
AP2B1_HUMAN AP-2 complex sub beta-1	**PRS10_HUMAN 26S protease regulatory sub S10B**
PLEC1_HUMAN Plectin-1 (PLTN)	**RMD5A_HUMAN Protein RMD5 homolog A**
LIMA1_HUMAN LIM domain and actin-binding protein 1	TF2H2_HUMAN TFIIH basal transcription factor complex p44
AMPD2_HUMAN AMP deaminase 2	KC1E_HUMAN Casein kinase I isoform epsilon
ABCF1_HUMAN ATP-binding cassette sub-family F member 1	**BRCC3_HUMAN BRCA1/BRCA2-containing complex sub 3**
UBP7_HUMAN Ubiquitin carboxyl-terminal hydrolase 7	**SPY2_HUMAN Sprouty homolog 2 (Spry-2)**
PKCB1_HUMAN Protein kinase C-binding protein 1 (Rack7)	**PP1A_HUMAN protein phosphatase PP1-alpha catalytic sub**
DREB_HUMAN Drebrin	**CSK21_HUMAN Casein kinase II sub alpha**
AP2A2_HUMAN AP-2 complex sub alpha-2	**CSK22_HUMAN Casein kinase II sub alpha'**
AP1B1_HUMAN AP-1 complex sub beta-1	**PRPS1_HUMAN Ribose-phosphate pyrophosphokinase I**
PI4KA_HUMAN Phosphatidylinositol 4-kinase alpha	**RL6_HUMAN 60S ribosomal protein L6**
NFM_HUMAN Neurofilament medium polypeptide (NF-M)	THIL_HUMAN Acetyl-CoA acetyltransferase
WDR6_HUMAN WD repeat protein 6	**RS15A_HUMAN 40S ribosomal protein S15a**
ARMC8_HUMAN Armadillo repeat-containing protein 8	**RS3A_HUMAN 40S ribosomal protein S3a**
GCP60_HUMAN Golgi resident protein GCP60	**RS13_HUMAN 40S ribosomal protein S13**
SNX9_HUMAN Sorting nexin-9	**PSME3_HUMAN Proteasome activator complex sub 3**
SNX18_HUMAN Sorting nexin-18	**BAG2_HUMAN BAG family molecular chaperone regulator 2**
KEAP1_HUMAN Kelch-like ECH-associated protein 1	RL38_HUMAN 60S ribosomal protein L38
RIB2_HUMAN Dolichyl-diphosphooligosaccharide	GBLP_HUMAN Guanine nucleotide-binding protein sub beta 2-like 1
HNRPQ_HUMAN Heterogeneous nuclear ribonucleoprotein Q	RS16_HUMAN 40S ribosomal protein S16
G3BP2_HUMAN Ras GAP-binding protein 2	RL14_HUMAN 60S ribosomal protein L14
TF2H1_HUMAN TFIIH basal transcription factor complex p62	RL7A_HUMAN 60S ribosomal protein L7a
ATPB_HUMAN ATP synthase sub beta	ELAV1_HUMAN ELAV-like protein 1
FBX21_HUMAN F-box only protein 21	RS20_HUMAN 40S ribosomal protein S20
PI51A_HUMAN Phosphatidylinositol-4-phosphate 5-kinase-1α	RL22_HUMAN 60S ribosomal protein L22
KLH12_HUMAN Kelch-like protein 12	PGAM5_HUMAN Phosphoglycerate mutase family member 5
CRNL1_HUMAN Crooked neck-like protein 1	RL30_HUMAN 60S ribosomal protein L30
FMR1_HUMAN Fragile X mental retardation 1 protein	RL8_HUMAN 60S ribosomal protein L8
IMA1_HUMAN Importin alpha-1 sub	RL21_HUMAN 60S ribosomal protein L21
FXR1_HUMAN FMR-related 1	S10A8_HUMAN Protein S100-A8
K0157_HUMAN Uncharacterized protein KIAA0157	RL35_HUMAN 60S ribosomal protein L35
ARP3_HUMAN Actin-like protein 3 (Actin-related protein 3)	**UBIQ_HUMAN Ubiquitin**

Table 3.1. List of identified SPRY2 specific interacting proteins (FPR = 3%) from over-expressing 293T cells. Proteins in bold are also passed by an FPR of 0.5%. [Green: Endocytic trafficking related proteins; yellow: Ser/Thr kinases and phosphatases; grey: translation/protein folding related proteins.]

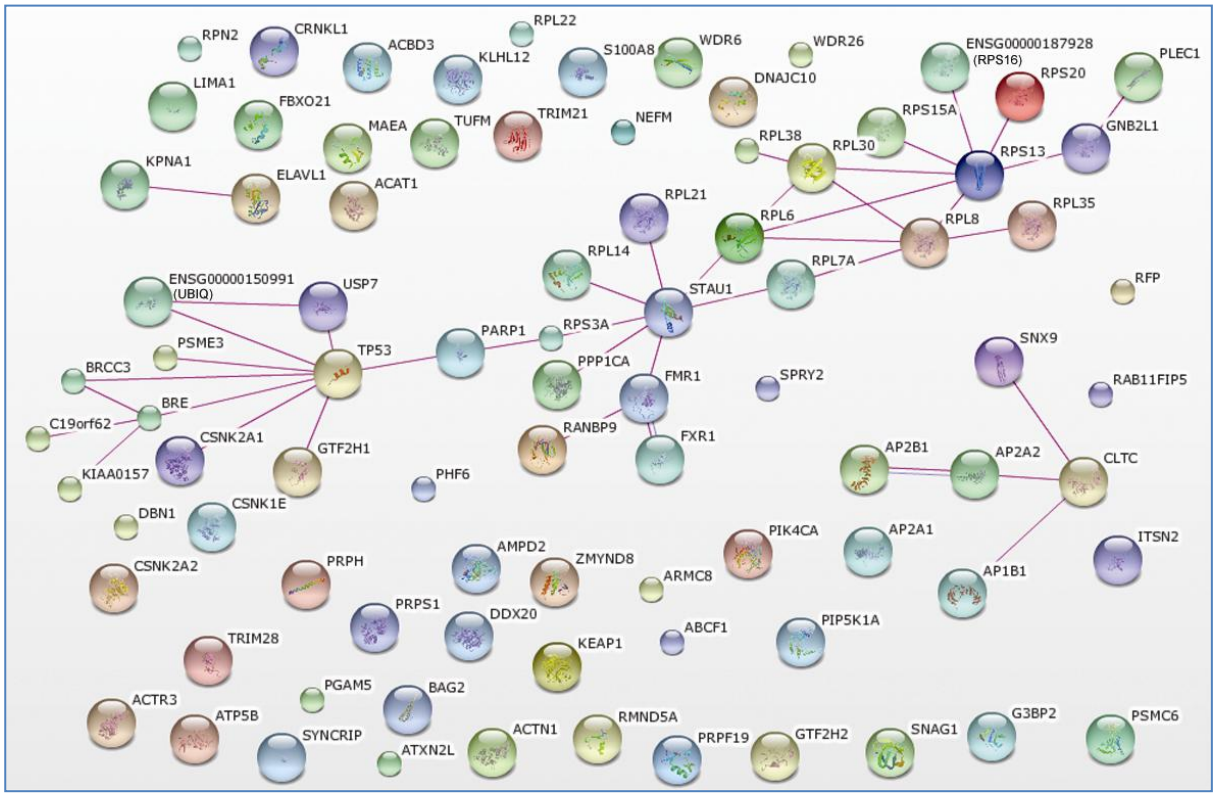

Figure 3.2. Analysis of mass-spectrometry identified SPRY2 novel interacting partners by STRING reveals two major distinct protein networks. Hits from Table 3.1 were used as inputs in STRING-8 [Jensen et al., 2009] protein-protein interaction web server (http://string-db.org/) to reveal known protein networks. The results were filtered to only include interactions for which experimental evidence was available (Purple lines). The default confidence score of 0.400 was used. Homologies are also shown were existed (Blue line). Two major networks were detected, one consisting of mainly ribosomal subunits as well as P53 (TP53) interacting proteins, and the other of a number of endocytosis related proteins centred on Clathrin (CLTC).

It should be noted that none of the known binding partners of SPRY2 including C-RAF, C-CBL, or GRB2 were amongst the identified hits (Table 3.1). As positive identification of a protein by mass-spectrometry is dependent on abundance, this could be the result of low cellular abundance of these proteins. Alternatively, it is possible that these proteins are not amongst the major interacting partners of SPRY2, and therefore, are not enriched significantly in SPRY2 immunoprecipitates in order to be detected by mass-spectrometry.

To get insight into protein networks that SPRY2 associates with, the identified interacting partners (Table 3.1) were analysed by STRING (Search Tool for the Retrieval of Interacting Genes/Proteins) [Snel et al., 2000]. STRING is a database and web-tool of known and predicted protein-protein interactions. It imports and predicts protein interactions based on information available on a wide variety of existing interaction databases as well as deducing interactions from literature by automatic text-mining. It then weighs, scores, and finally represents the results as networks of protein-protein associations [Snel et al., 2000]. Here, the results were filtered to represent only data from existing protein-protein interaction databases for which experimental evidence was available (Figure 3.2). Two major protein networks were revealed, one of which consisted of mainly ribosomal subunits which probably associates with SPRY2 during its synthesis, and the other of endocytosis related proteins centred on Clathrin (Figure 3.2). This suggests that an endocytic related protein network probably associates with SPRY2, highlighting a possible endocytic regulatory role for the protein. Surprisingly, the ribosomal subunits network also contained the tumour suppressor P53 and its interacting partners (Figure 3.2). However, this result must be interpreted with care as P53 was only identified by a single medium score peptide. In fact, P53 would be filtered out under high stringency FPR of 0.5% (Table 3.1-bold). It remains to be determined whether a physiologically significant interaction exists between SPRY2 and P53 *in vivo*.

3.3 Identification of SPRY2 phosphorylation sites by mass-spectrometry

Using the same SPRY2 mass-spectrometry dataset, modified peptides of SPRY2 were searched for and identified. Apart from Cysteine (C) carbamidomethylation , Methionine (M) oxidation, and Asparagine (N) / Glutamine (Q) deamidations, which occur naturally during the digestion procedure, the only detected post-translational modifications were phosphorylations. Seven phosphorylated peptides were identified from the initial dataset, including one which contained the pivotal N-terminal Tyrosine (Y55) (Table 3.2). However, apart from one phosphopeptide, all had at least two or more S/T/Y residues that could have been potential sites of phosphorylation (Table 3.2). To deduce the exact site of phosphorylation in these peptides, an algorithm known as Ascore was used [Beausoleil et al., 2006]. The algorithm gives a probabilistic confidence score (Ascore) for any localised site. If Ascore is equal or more than 20 for a specific site, it indicates a confident localisation (P = 0.01) while a lower score would mean uncertainty in localisation. Using this algorithm, the site of phosphorylation in two phosphopeptides were confidently localised, leaving the phosphorylation site in four other phosphopeptides ambiguous (Table 3.2).

Difficulty in site localisation is a common problem in phospho-proteomics as phospho groups are often lost during collision-induced dissociation (CID) which is the standard peptide fragmentation procedure used in tandem mass-spectrometry. This affects both the confidence in phosphopeptide identification as well as the unambiguous localisation of the phosphorylation site [Witze et al., 2007]. A number of different strategies have been developed to tackle this problem [Olsen et al., 2006; Edelson-Averbukh et al., 2007; Sweet et al., 2008]. Here, an approach devised by Steve Sweet, a post-doc in our lab, was employed [Sweet et al., 2008]. Briefly, in this approach CID is used in a first round of LC-MS/MS analysis for phosphopeptide discovery. This is followed by targeted Electron Capture

Dissociation (ECD) for site localisation in a second round of LC-MS/MS [Sweet et al., 2008]. ECD is a radical-driven fragmentation technique which uses an electron source [Cooper et al., 2005]. In contrast to CID, labile modifications such as phosphorylations are not lost during ECD fragmentation, giving it a significant advantage over CID for site localisation [Sweet and Cooper, 2007]. The other advantage of ECD is its high resolution fragmentation spectra due to the fact that it is acquired in the FTICR cell rather than the Ion trap [Sweet and Cooper, 2007]. However, ECD is significantly less efficient compared to CID and requires accumulation of considerably greater amounts of precursor ions which means a significant increase in scan times. In Steve's novel strategy, the efficiency of CID is combined with the advantages of ECD for phosphopeptide analysis: by performing a CID run the phosphopeptides can be efficiently discovered and by performing a subsequent targeted ECD the exact sites of phosphorylation can be deduced for them [Sweet et al., 2008].

We therefore repeated the SPRY2 immunoprecipitation, this time using a myc tagged SPRY2 in conjunction with an anti-myc antibody. This was because the anti-myc antibody was considerably cheaper than the anti-SPRY2 antibody initially used. Myc-SPRY2 Immunoprecipitates were run on an SDS gel and the SPRY2 corresponding band was excised, subjected to in-gel trypsin digestion, and the peptides were extracted as before. To increase the efficiency of phosphopeptide identification, an additional phosphopeptide enrichment step was also performed using TiO_2 Titansphere beads. TiO_2 specifically binds to phosphorylated peptides which are then eluted off using a phosphate solution followed by ammonium hydroxide (see Materials and Methods). The enrichment step results in eliminating the more abundant non-phosphorylated peptides and therefore reduces the sample complexity. This is particularly important for ECD as a larger isolation window is used to enable sufficient ion transfer to the FTICR unit [Sweet et al., 2008].

Phosphopeptide	Potential sites	Confidently localised to by Ascore	Ascore
R.AQS*GNGSQPLLQTPR.D	3	S7	66.7
R.DALT*QQVHVLSLDQIR.A	2	S42	127.5
R.AIRNT*NEYTEGPTVVPRPGLKPAPR.P	4	-	0
R.S*ISTVSSGSR.S	6	-	7.93
R.S*ISTVSSGSRSSTR.T	9	-	0
R.LLGS*SFSSGPVADGIIR.V	4	-	16.2
K.VPT*VPPR.N	1	T305	-

Table 3.2. List of identified SPRY2 phosphopeptides from the initial mass-spectrometry screen. Ascore algorithm was used to assess site localization with a score of ≥20 indicative of a confident localization (p = 0.01). * indicates phosphorylation. The pivotal Y55 is highlighted in grey

When the enriched samples were analysed by LC-MS/MS using CID fragmentation, 12 phosphopeptides were identified, which included 6 of the previously identified phosphopeptides and 6 novel ones (Table 3.3). Of the novel phosphopeptides, one was a shorter version of the previously identified Y55 containing phosphopeptide (Table 3.3). Two others were doubly phosphorylated versions of two previously identified phosphopeptides while one was a triply phosphorylated version of one of them (Table 3.3). Finally, two phosphopeptides with novel sequences were also discovered (Table 3.3). Next, the samples were rerun and subjected to LC-MS/MS, this time using targeted ECD. The targeted approach was done using an inclusion list of the identified phosphopeptides in Table 3.3 to help restrict the ECD events to the precursors of interest. The resulting data were then manually analysed by Steve Sweet [Sweet et al., 2008]. A total of 16 phosphorylation sites were identified, 11 of which were novel (Table 3.3- highlighted). All phosphorylations in 11 out of 12 identified phosphopeptides were unambiguously localised from the acquired ECD spectra by manual inspection (Table 3.3) while the phosphorylation site on the remaining phosphopeptide which

could not be deduced from the ECD spectra was successfully localised from the CID data by Ascore (Table 3.3). Surprisingly, ECD analysis revealed that the sites of phosphorylation on most of the phosphopeptides were variable (Table 3.3). These included the singly phosphorylated peptides AQS*GNGSQPLLQTPR, S*ISTVSSGSR, LLGS*SFSSGPVADGIIR, and NT*NEYTEGPTVVPR, the latter was found to be phosphorylated on either the known Y55 site or the novel T56 site (Table 3.3). A closer inspection of the ion chromatogram for the this phosphopeptide by Steve Sweet revealed that it was eluting as two separate peaks, in line with the notion that two differentially phosphorylated versions of the peptide existed (Figure 3.3). Moreover, ECD fragmentation spectra for each of the two individual peaks had been acquired and could clearly show that the first eluting peak was phosphorylated on Y55 and the second on T56 (Figure 3.3).

Phosphopeptide	Potential sites	Localisations
R.AQS*GNGSQPLLQTPR.D	3	S7, S11, T17
R.DALT*QQVHVLSLDQIR.A	2	S42
R.NT*NEYTEGPTVVPR.P	4	Y55, T56
R.S*ISTVSSGSR.S	6	S115, S116, S118
R.S*IS*TVSSGSR.S	6	S115, S116, S118
R.S*IS*TVSSGSRSSTR.T	9	S115, S116, S118
R.LLGS*SFSSGPVADGIIR.V	4	S138, S139, S141, S142
R.LLGS*S*FSSGPVADGIIR.V	4	S138, S139, S141, S142
R.LLGS*S*FS*SGPVADGIIR.V	4	S138, S139, S141, S142
K.S*ELKPGELKPLSK.E	2	S167 †
R.PLPS*DWICDK.Q	1	S197
K.VPT*VPPR.N	1	T305

Table 3.3. List of identified SPRY2 phosphopeptides and their site localisations. * indicates phosphorylation. † indicated site of phosphorylation was deduced from CID by Ascore algorithm (Ascore = 89.8) while all other site localisations were deduced from ECD spectra. The novel sites of phosphorylation are highlighted in yellow

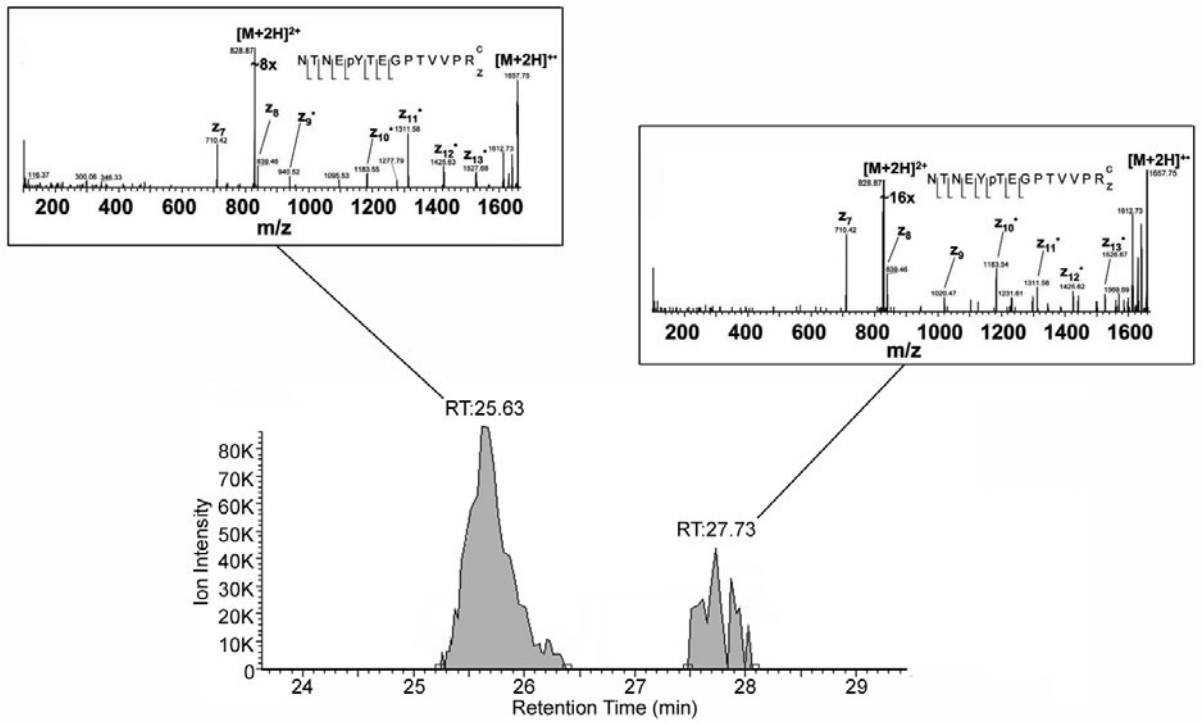

Figure 3.3. R.NT*NEYTEGPTVVPR.P phosphopeptide elutes off the chromatography column as two separate peaks which correspond to Y55 and T56 different phosphorylated forms. Ion chromatogram of R.NT*NEYTEGPTVVPR.P shows two individual peptide forms eluting at 25.63 and 27.73 minutes (BOTTOM). ECD fragmentation spectrum analysis of the eluting peaks reveals the phospho-group (p) is located on Y55 for the first peak (TOP LEFT) and on T56 for the second one (TOP RIGHT).

3.4 Analysis of SPRY2 phosphorylation dynamics by SILAC

Peptide analysis by mass-spectrometry is not an inherently quantitative assay. This is due to the fact that ion intensities can deviate significantly from run to run as a result of intrinsic variations in different steps of an LC-MS/MS run, including the liquid chromatography, the ionisation process, and even the transfer of ions within the mass-spectrometer. However, a number of strategies have been developed to allow for relative quantification of data acquired by mass-spectrometry. Most of these strategies employ some form of peptide labelling that allows different samples to be mixed and therefore analysed in a single run. As a result, corresponding ion intensities from different samples can be directly compared and relatively quantified [Iliuk et al., 2009]. One form of labelling used for quantitative mass-spectrometry which has recently gained considerable popularity is Stable Isotopic Labelling of Amino-acids in Culture (SILAC). In this method, heavy isotope labelled amino-acids are incorporated into the proteins during cells culture. This is usually performed by supplementing the growth medium with labelled amino-acids. As trypsin cuts after Arginines (R) and Lysines (K), these two are the most commonly used amino acids for labelling. Thus, nearly all tryptic peptides contain at least one labelled amino-acid (the terminal R or K), ensuring a high quantification coverage. In the standard SILAC method (Figure 3.4), proteins from heavy and light (no isotopes) labelled cell populations are mixed immediately after lysis, and all subsequent processing steps including trypsin digestion and LC-MS/MS analysis are performed on the mixture. As isotope labelling does not change the chemical properties of the peptides, the heavy and light labelled versions of a peptide behave identically in LC-MS/MS. As a result, the heavy to light ion intensity ratio for a given peptide can be an accurate measure of its relative abundance between the two samples. The protein ratios can be subsequently estimated using their corresponding peptide ratios [Ong et al., 2003].

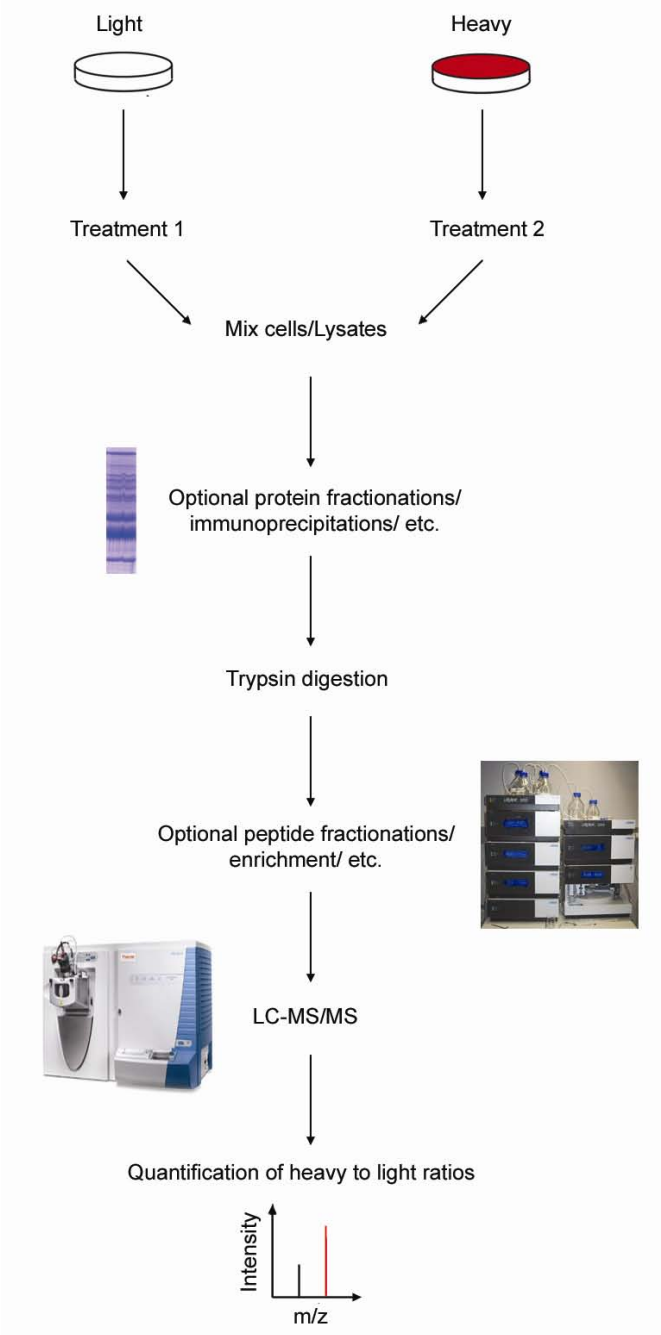

Figure 3.4. Schematic representation of SILAC methodology. Light and heavy labelled cells in culture are differentially treated as desired followed by mixing of the cells before or after cell lysis. The lysates can then be subjected to desired processing steps such as protein fractionation, immunoprecipitation, etc, before digestion by trypsin. The resulting peptides can then be subjected to desired peptide fractionation/enrichment steps before analysis by LC-MS/MS. The heavy to light peptide ratios are subsequently quantified, from which protein ratios can be calculated.

SILAC was therefore used to gain a quantitative insight into the dynamics of SPRY2 phosphorylations. In particular, it was asked which of the identified SPRY2 phosphorylations could change with FGF2 stimulation, and to what degree. Heavy and light labelled 293T cells were transfected with myc tagged SPRY2. The cells were then serum starved and the heavy labelled cells were stimulated with 20 ng/ml FGF2 + 10 mg/ml Heparin for 30 minutes while the light cells were left untreated. Cells were subsequently lysed and equal amounts of proteins from each lysates were mixed together and subjected to immunoprecipitation with anti-myc antibody for overnight. Immunoprecipitates were subsequently washed and resolved by SDS PAGE, in-gel digested by trypsin, and the resulting peptides were extracted, enriched, and analysed by LC-MS/MS as before. The results were searched using the Sequest algorithm (Bioworks software) against the human SWISSPROT database. 10 of the previous 12 identified phosphopeptides were detected this time (Table 3.4). These phosphopeptides were quantified by manual integration of their corresponding heavy and light peak intensities from the ion chromatogram. The calculated ratios were then normalised to the total average ratio from the lysate mix (Table 3.4). The quantification was performed manually due to the complications in automated data analysis caused by Arginine metabolic conversion to Proline. This is a cell specific issue which results in partial additional labelling of Prolines and thus splitting of the heavy peaks for peptides which contain a Proline. To quantify such peptides, the integrated intensities for any such split heavy peaks had to be added together manually. It should be noted that it was recently demonstrated that Arginine to Proline conversion could be completely inhibited by addition of excess Proline to the growth medium along with labelled Arginine [Bendall et al., 2008]. However, this was not known at the time these experiments were being carried out. Of the 10 phosphopeptides detected, 8 could be successfully quantified (Table 3.4). Interestingly, as Y55 and T56 phosphorylated versions of

the NT*NEYTEGPTVVPR phosphopeptide eluted separately, they could be quantified individually. While the Y55 phosphorylated form was found to be increased in FGF2 treated cells, the T56 phosphorylated version was significantly reduced compared to starved cells (Table 3.4). Such negative correlation between these two proximal sites suggests that some form of negative regulation of phosphorylation by one site on the other might exist. In contrast to Y55 and T56, the other identified phosphopeptides did not significantly change with FGF2 stimulation (Table 3.4), suggesting that they might be constitutively phosphorylated. Alternatively, these other phosphorylations might be responsive to stimulations other than FGF2.

Phosphopeptide	Site	Normalised H/L ratio (FGF2 vs Starved)
R.AQS*GNGSQPLLQTPR.D	S7, S11, T17	0.89
R.DALT*QQVHVLSLDQIR.A	S42	0.80
R.NT*NEYTEGPTVVPR.P	Y55	2.79
R.NT*NEYTEGPTVVPR.P	T56	0.67
R.S*ISTVSSGSR.S	S115, S116, S118	1.09
R.S*IS*TVSSGSRSSTR.T	S115, S116, S118	1.08
R.LLGS*SFSSGPVADGIIR.V	S138, S139, S141, S142	1.06
R.LLGS*S*FSSGPVADGIIR.V	S138, S139, S141, S142	1.14
K.S*ELKPGELKPLSK.E	S167	-
R.PLPS*DWICDK.Q	S197	-
K.VPT*VPPR.N	T305	0.99

Table 3.4. Normalised SILAC ratios for SPRY2 phosphopeptides between FGF2 treated (H) and starved (L) cells. Y55 and T56 phosphorylations could be individually analysed due to separate elutions. While Y55 phosphopeptide seems to be increased in response to FGF2 (highlighted in red), T56 is reduced (highlighted in blue). No ratios could be determined for K.S*ELKPGELKPLSK.E and R.PLPS*DWICDK.Q phosphopeptides due to insufficient peak intensities.

3.5 Conclusions

In this chapter, the results of mass-spectrometry analysis of SPRY2 interacting partners and phosphorylation sites were presented. It was found that SPRY2 could interact with a number of endocytic trafficking related proteins (Table 3.1 and Figure 3.2). These included proteins involved in Clathrin mediated endocytosis such as Clathrin heavy chain-1 (CLH1), subunits of Adaptor-related Protein complex-2 (AP-2), Sorting Nexin-9 (SNX9), as well as Phosphatidyl-4-phosphate 5-kinase (PI51A), suggesting that SPRY2 might have a role in regulation of receptor internalisation. An endocytosis related role for Sproutys could potentially address some of the controversies with regards to their function, as trafficking could affect signalling outcome but its dynamics would be dependent on the cellular context and the exact type of the receptor involved [Sorkin and von Zastrow, 2009]. A number of previous studies also argued for an endocytic role for SPRY2. For example, it was shown that SPRY2 could block receptor internalisation by competing with EGFR for c-CBL binding [Wong et al., 2002a; Rubin et al., 2003]. However, the negative effect of SPRY2 on FGF signalling was shown to be independent of c-CBL [Mason et al., 2004], so other interacting partners of the protein must be mediating its function downstream of FGF. In addition, SPRY2 was shown to directly interact with Phosphatidyinositol-4,5 phosphate (PIP2) [Lim et al., 2002], which is a crucial membrane lipid involved in Clathrin mediated endocytosis [Haucke, 2005]. Interestingly, PIP2 is the product lipid of the lipid kinase PI51 which was identified here as an SPRY2 interacting partner (Table 3.1).

The mass-spectrometry analysis of SPRY2 interacting partners also revealed the Serine/Threonine kinases Casein Kinase I and II (CKI & CKII) as well as the Protein Phosphatase 1 (PP1) (Table 3.1). It is therefore possible that SPRY2 might be regulated by these proteins through phosphorylation/dephosphorylation. On the other hand, it is also

possible that SPRY2 binding might be regulating the function of these proteins. A large number of ribosomal subunits and as well as molecular chaperones were also identified here (Table 3.1), which is probably an over-expression artefact reflective of the association of ectopic SPRY2 during its synthesis with the protein synthesis and folding machineries. The tumour suppressor protein P53 was also amongst the identified proteins, though as mentioned earlier, this result must be interpreted with care. Finally, analysis of protein interaction networks by STRING revealed two major networks existed for SPRY2 identified interacting partners. One was a network of protein synthesis related proteins and the other a network of endocytosis related proteins centred on Clathrin (Figure 3.2). These data suggest that such protein groups might be interacting with SPRY2 as pre-existing multi-protein complexes.

A key issue forward now would be to determine which of the here identified interacting partners of SPRY2 are important for its function downstream of FGF. Quantitative mass-spectrometry by SILAC could help determine if any of these interacting partners are Y55 dependent. As Y55 mutation abrogates SPRY2 inhibition of FGF dependent ERK1/2 signalling, those partners of SPRY2 which preferentially associate with wild-type compared to a Y55 mutant are likely to be crucial for the protein function.

The mass-spectrometry analysis of SPRY2 phosphorylation sites presented in this chapter revealed a total of 16 phosphorylation sites, 11 of which were novel (Table 3.3). In a subsequent mass-spectrometry analysis of SPRY2 phosphorylation sites by Mike Olson and colleagues, 3 out of these 11 sites were identified as well [Brady et al., 2009]. However, some of the previously reported phosphorylation sites of SPRY2 such as Y227, were not detected in our study. This could be either due to the low *in vivo* stoichiometry of these phosphorylations or cell-type specificity issues. Of all novel phosphorylation sites identified here, T56 phosphorylation is particularly attractive due to its close proximity to the pivotal Y55. It will

be interesting to know whether phosphorylation of T56 has any effect on the Y55 dependent SPRY2 function. In this regard, it should be noted that despite close manual inspections, a peptide mass corresponding to that of Y55-T56 doubly phosphorylated peptide could not be identified in our datasets. This could be indicative of a mutual exclusivity between the two phosphorylation events. In agreement with this hypothesis, quantitative analysis of SPRY2 phosphorylation dynamics by SILAC revealed a negative correlation between Y55 and T56 phosphorylations, suggestive of a potential negative regulation by one site on the other (Table 3.4). The functional significance of T56 phosphorylation on SPRY2 function remains to be determined. Generation of T56 non-phosphorylatable as well as phospho-mimicking point mutants should help shed light on the role of this phosphorylation site in SPRY2 function.

CHAPTER 4

SPRED: Mechanism of Signal Attenuation

4.1 Introduction

In this chapter, the mechanism of signal attenuation by Spred family of proteins is investigated. As mentioned earlier, Spreds constitute a conserved family of growth factor inhibitors that share a C-terminal Cysteine-rich SPRY domain with Sproutys, but diverge from them by further containing a central Kit Binding Domain (KBD), and an N-terminal EVH1 domain [Wakioka et al., 2001]. Mammals have three Spred homologues with roles in bone morphogenesis [Bundschu et al., 2005], hematopoiesis [Nobuhisa et al., 2004], allergen-induced airway eosinophilia and hyper-responsiveness [Inoue et al., 2005]. Spred2 was specifically chosen for this study as its knockout in mice results in a dwarf phenotype that mimics the phenotype of FGFR hyperactivity [Bundschu et al., 2005], indicative of a physiological relevance to FGF signalling.

Previous studies have shown that the N-terminal EVH1 domain of Spreds is essential for their inhibitory activity on ERK1/2 [Wakioka et al., 2001; King et al., 2005]. However, the molecular mechanism of this EVH1 dependent action was unknown. Since EVH1 domains are protein-protein interaction modules [Ball et al., 2002], one hypothesis was that an unidentified critical partner of Spreds might be interacting with the EVH1 domain to mediate their function. Interestingly, a Yeast two-Hybrid screen for binding partners of the EVH1 domain of Spred2 had been carried out by Mona Yekezare in Laura Machesky's lab, identifying NBR1 as a potential binding partner of Spred2 EVH1 domain. It was therefore decided to determine whether NBR1 truly interacts with Spred2 in an EVH1 domain dependent manner, and if this is the case, whether the interaction is significant with regards to Spred2 mediated inhibition of ERK1/2.

The results of this chapter confirm NBR1 as an EVH1 domain specific binding partner of Spred2. As discussed in chapter one, NBR1 is a multi-domain scaffold protein that contains a number of putative protein-protein interaction modules and has been previously implicated in signal transduction downstream of the giant muscle kinase Titin [Lange et al., 2005], as well as in selective autophagy [Kirkin et al., 2009; Waters et al., 2009]. Here it is demonstrated that NBR1 is a specific late endosomal protein, and that it interacts with Spred2 in an EVH1 domain dependent manner, *in vivo*. Inhibition of ERK1/2 signalling by Spred2 is dependent on its interaction with NBR1, and is achieved by targeting activated receptors to the lysosomal degradation pathway. These findings provide a mechanism for the EVH1 dependent actions of Spred2, and implicate NBR1 as a novel regulator of receptor trafficking and signalling for the first time.

4.2 Spred2 interacts with Nbr1 in an EVH1 domain dependent manner

The Yeast two-Hybrid screen performed in Laura Machesky's lab had identified NBR1 as a potential binding partner of Spred2 EVH1 domain. Of the total 22 positive hits in this screen, more than 70% corresponded to the C-terminal end of NBR1, with the the shortest cDNA only coding for the 131 C-terminal amino acids, suggesting that the binding site for Spred2 EVH1 domain must be located within these 131 amino acids (Figure 4.1A) [Mardakheh et al., 2009]. To confirm the existence of a direct interaction between the EVH1 domain of Spred2 and the C-terminal NBR1, an *in vitro* pull-down experiment was performed. Purified bacterially expressed GST tagged C-terminal 133 amino acids of Nbr1 (Corresponding to the C-terminal 131 amino acids of NBR1) or GST alone as negative control were mixed with purified bacterially expressed His tagged EVH1 domain of Spred2, incubated for 30 minutes

at 4°C, and the mixture was subjected to pull down by Gluthatione beads for another 30 min at 4°C. After extensive washes, the proteins were eluted with a 10 mM Glutathione solution, and the eluates were resolved and visualised on an SDS gel along with the input mixtures (Figure 4.1B). His-EVH1 domain of Spred2 could be pulled down with GST tagged C-terminal of Nbr1 but not GST on its own (Figure 4.1B), confirming the direct interaction of the two protein regions, *in vitro*. It should be noted that there are no canonical proline-rich EVH1 binding sequences within this region of NBR1. However, this is in agreement with the previously solved tertiary structure of the Spred EVH1 domain which indicates a distinct binding mechanism to other EVH1 domains, favouring a less proline-rich consensus binding site [Harmer et al., 2005].

To confirm NBR1-Spred2 interaction *in vivo,* it was first checked whether over-expressed NBR1 could be co-immunoprecipitated with over-expressed Spred2 in mammalian cells. 293T cells were transfected with GFP tagged NBR1 or GFP alone as control, along with myc tagged Spred2, and subjected to immunoprecipitation by an anti-myc antibody. In these cells, GFP-NBR1 could be co-immunoprecipitated with myc-Spred2 irrespective of stimulation (Figure 4.1C), suggesting that NBR1 and Spred2 can interact constitutively *in vivo*. To confirm the interaction of SPRED2 with NBR1 in a physiological context, a neuronal cell-line (SH-SY5Y neuroblastoma) was used since SPRED2 has been shown to be expressed at relatively high levels in neuronal tissues [Engelhardt et al., 2004; Bundschu et al., 2006]. SH-SY5Y cell lysates were subjected to immunoprecipitation using an antibody against endogenous SPRED2 or a non-specific IgG as negative control. Irrespective of stimulation, endogenous NBR1 could be co-immunoprecipitated with endogenous SPRED2 from these lysates (Figure 4.1D), supporting the existence of a constitutive interaction at physiological protein levels.

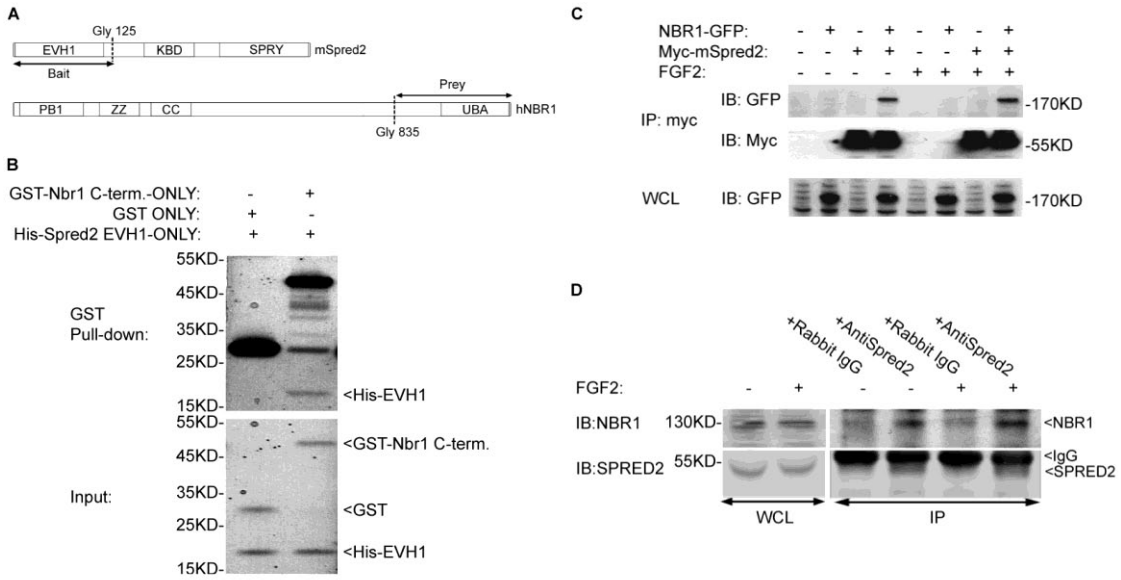

Figure 4.1. Spred2 EVH1 domain directly binds to the C-terminal of Nbr1 *in vitro*, and Spred2 and NBR1 interact *in vivo*. A schematic representation of Spred2 and NBR1 domain architecture with the bait and prey regions from the Yeast two-Hybrid screen marked respectively **(A)**. 20μg/ml GST-Nbr1C-term.-ONLY or GST-ONLY as control was mixed with 20μg/ml His-Spred2 EVH1-ONLY in a 500μl total volume and incubated for 30 min at 4°C. 20μl bed volume of Glutathione beads (Pierce) was then added to each mixture and incubated for another 30 min at 4°C. The beads were washed 5 times with 20 bed volume of beads and proteins were eluted off by 20μl of 10mM Glutathione. 5μl of input mixtures along with 10μl of eluates were subsequently resolved by SDS-PAGE and visualized by coomassie (for Input mixtures), or silver staining (for eluates). His-Spred2 EVH1-ONLY directly binds to GST-Nbr1C-term.-ONLY but not GST alone **(B)**. 293T cells were transfected with either GFP alone or NBR1-GFP with or without myc-Spred2. After 36 hours, the cells were serum starved for 6 hours, and either left unstimulated or stimulated with 20 ng/ml FGF2 (+10 μg/ml Heparin) for 30 minutes before lysis and immunoprecipitation by anti-myc antibody. The whole cell lysates (WCL) and immunoprecipitates (IP) were subsequently analysed by immunoblotting (IB) with indicated antibodies. NBR1-GFP co-immunprecipitates with myc-Spred2 irrespective of stimulation **(C)**. SH-SY5Y neuroblastoma cells were serum staved and either left unstimulated or stimulated with 20 ng/ml FGF2 (+10 μg/ml Heparin) for 30 minutes before being lysed and subjected to immunoprecipitation by an anti-Spred2 antibody, or a non-specific rabbit IgG as control. Around 4 mg of lysate and 15 μg of antibody was used per immunoprecipitation, overnight at 4°C. IP and WCL samples were analysed by immunoblotting (IB) with indicated antibodies. Endogenous NBR1 can also be immunoprecipitated with endogenous Spred2 **(D)**.

Finally, it was investigated whether Spred2 interaction with NBR1 was EVH1 domain dependent also *in vivo*. Similar to over-expressed NBR1, endogenous NBR1 could be co-immunoprecipitated with myc-Spred2 in 293T cells irrespective of the stimulation state (Figure 4.2A). Interestingly, endogenous P62, a known binding partner of NBR1 with a similar domain architecture [Lange et al., 2005], could also be co-immunoprecipitated along with endogenous NBR1 (Figure 4.2A). When myc tagged WT and various deletion mutants of Spred2 were compared for their ability to interact with NBR1 in this setup, WT and KBD deleted mutant could co-immunoprecipitate endogenous NBR1 while EVH1 or SPRY domain deleted mutants could not (Figure 4.2B). This reveals that unlike *in vitro*, Spred2 interaction with NBR1 requires both EVH1 and SPRY domains *in vivo*. It should be noted that while NBR1 is detected as a doublet in 293T lysates, only the top band seems to be immunoprecipitated with Spred2 (Figure 4.2).

4.3 Spred2 colocalises with NBR1 in an EVH1 domain dependent manner

After confirming the existence of an interaction, the sub-cellular localisation of Spred2 and NBR1 was investigated by immunostaining and confocal microscopy. In COS7 cells, the majority of transfected myc-Spred2 exhibits a cytoplasmic punctuate staining (Figure 4.3A). Similar staining was observed for endogenous SPRED2, in SH-SY5Y neuroblastoma cells (Figure 4.3B), ruling out the possibility of an artefact due to over-expression. To investigate the sub-cellular localisation of NBR1, a C-terminally GFP tagged NBR1 construct was transfected into COS7 cells. NBR1-GFP was found to localize to the limiting membranes of some peri-nuclear vesicular structures (Figure 4.3C). These vesicles were occasionally found attached to one another which gave them an aggregate-like appearance, but this was

dependent on the level of NBR1-GFP expression. The same vesicular localisation was observed for an N-terminally GFP tagged murine Nbr1 (see chapter 5), suggesting that it must be a conserved feature and that it is not affected by the position of the tag. Endogenous levels of NBR1 were below detection limits by immunostaining in COS7, SH-SY5Y, and HeLa cells. However, it has been shown that by treating the cells with the lysosomal inhibitor Bafilomycin A1 (BafA), endogenous NBR1 levels could be increased to immunostaining detectable levels since NBR1 is degraded via the lysosomal degradation pathway [Kirkin et al., 2009; Waters et al., 2009]. This was in fact the case, and in COS7 cells treated with 200 nM BafA for overnight endogenous NBR1 was found to exhibit a peri-nuclear vesicular localisation similar to GFP tagged NBR1 (Figure 4.3D).

Next, colocalisation of NBR1 and SPRED2 was investigated in SH-SY5Y cells. Again the cells were treated with 200 nM BafA for overnight to accumulate endogenous NBR1 before immunostaining and confocal microscopy. In these cells, endogenous NBR1 and SPRED2 co-localised with each other in cytoplasmic punctae (Figure 4.4). Similarly, myc-Spred2 and NBR1-GFP colocalised with each other in co-transfected COS7 cells (Figure 4.5A). To confirm that colocalisation of NBR1 and Spred2 is EVH1 domain dependent, various myc tagged deletion mutants of Spred2 were co-transfected along with NBR1-GFP into COS7 cells. In agreement with the co-immunoprecipitation results (Figure 4.2B), deletion of either EVH1 or SPRY domain abolished the co-localisation while deletion of KBD had no effect on it (Figure 4.5B, 4.5C, and 4.5D). Interestingly, deletion of the SPRY domain had a profound effect on Spred2 localization, causing it to entirely lose its punctate cytoplasmic localization and mainly mis-localise to the nucleus (Figure 4.5D). This finding can explain why both EVH1 and SPRY domains of Spred2 are required for an interaction *in vivo* (Figure 4.2B): EVH1 is required for protein interaction and SPRY is required for vesicular localisation.

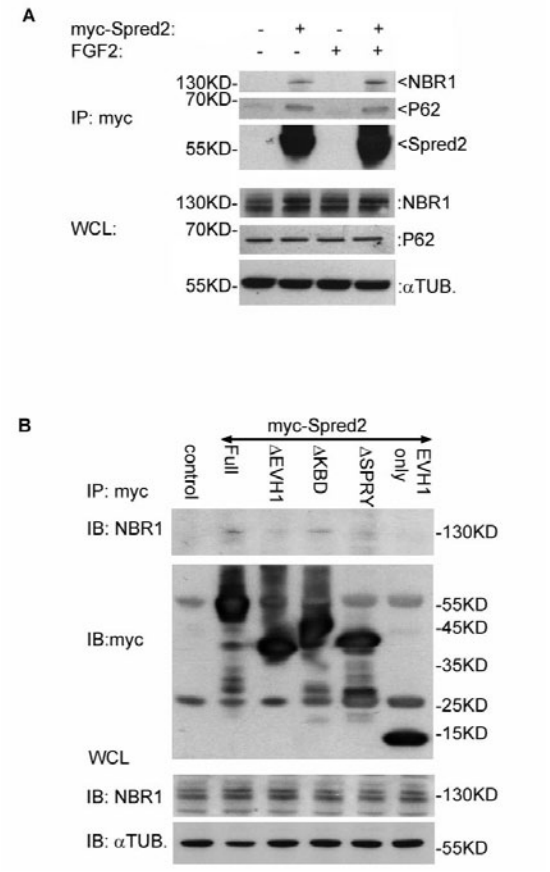

Figure 4.2. Spred2 and NBR1 interact in an EVH1 and SPRY domain dependent manner *in vivo*. 293T cells transfected with myc-Spred2 were serum starved and either left unstimulated or stimulated with 20 ng/ml FGF2 (+10 μg/ml Heparin) for 30 minutes before lysis and immunoprecipitation with anti-myc antibody. Immunoprecipitates (IP) and whole cell lysate (WCL) samples were analysed by immunoblotting (IB) with indicated antibodies. Endogenous NBR1 as well as its interacting protein P62 can be immunoprecipitated with myc-Spred2 irrespective of FGF2 stimulation **(A)**. 293T cells were transfected with myc tagged WT, ΔEVH1, ΔKBD, ΔSPRY, and EVH1-only Spred2 constructs, or a GFP construct as control. Cells were lysed and subjected to immunoprecipitation by anti-myc antibody. Immunoprecipitates (IP) and whole cell lysates (WCL) were analysed by immunoblotting (IB) with indicated antibodies. Endogenous NBR1 can only be immunoprecipitated with WT and ΔKBD mutant of Spred2 but not ΔEVH1 or ΔSPRY mutants **(B)**.

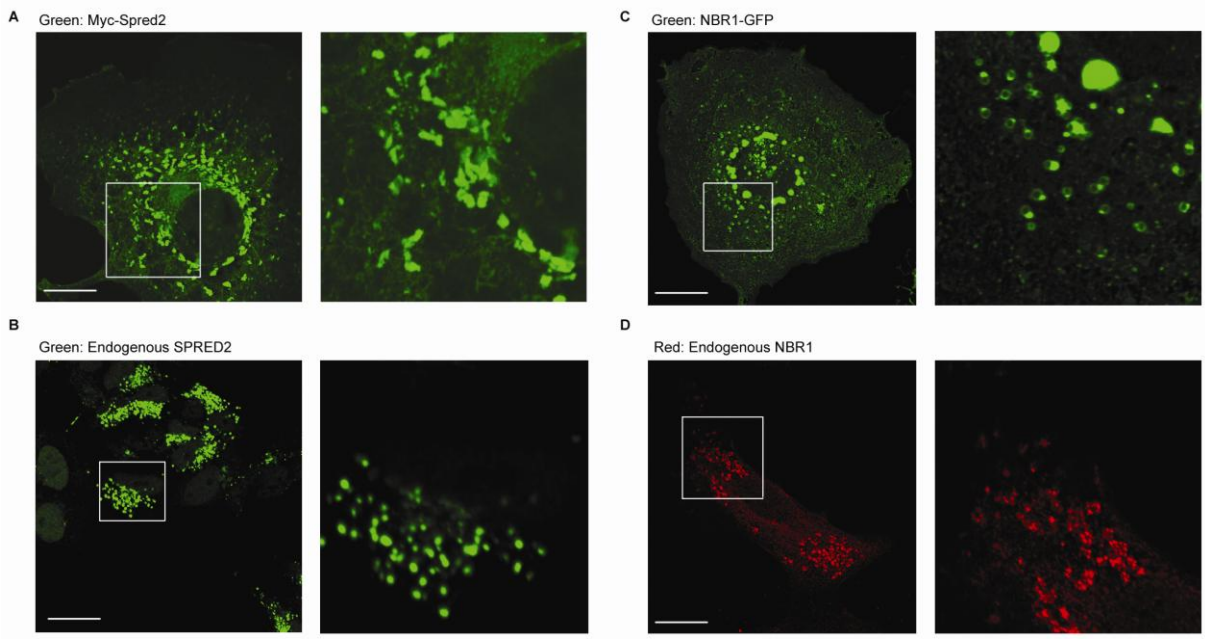

Figure 4.3. NBR1 and Spred2 exhibit intra-cellular vesicular localisations. Images on the right or insets are higher magnifications of the indicated areas on the left. All scale bars represent 10μm. COS7 cells transfected with myc-Spred2 were immunostained with anti-myc antibody and analysed by confocal microscopy. The majority of myc-Spred2 exhibits a punctate cytoplasmic localisation **(A)**. SH-SY5Y cells were immunostained with an anti-Spred2 antibody and analysed by confocal microscopy. Endogenous SPRED2 also localises to cytoplasmic punctae **(B)**. COS7 cells transfected with NBR1-GFP were analysed by confocal microscopy. NBR1-GFP is localized to the limiting membrane of some vesicular structure **(C)**. COS7 cells treated with 200 nM BafA for overnight were immunostained with an anti-NBR1 antibody and analysed by confocal microscopy. Endogenous NBR1 similarly localises to vesicular structures **(D)**.

Figure 4.4. Endogenous NBR1 and SPRED2 colocalise with each other in SH-SY5Y neuroblastoma cells. Scale bars represent 10µm. SH-SY5Y cells were treated with 200 nM BafA for overnight before being immunostained with anti-Spred2 and anti-NBR1 antibodies and analysed by confocal microscopy. Endogenous NBR1 co-localises with endogenous SPRED2 in cytoplasmic vesicular structures.

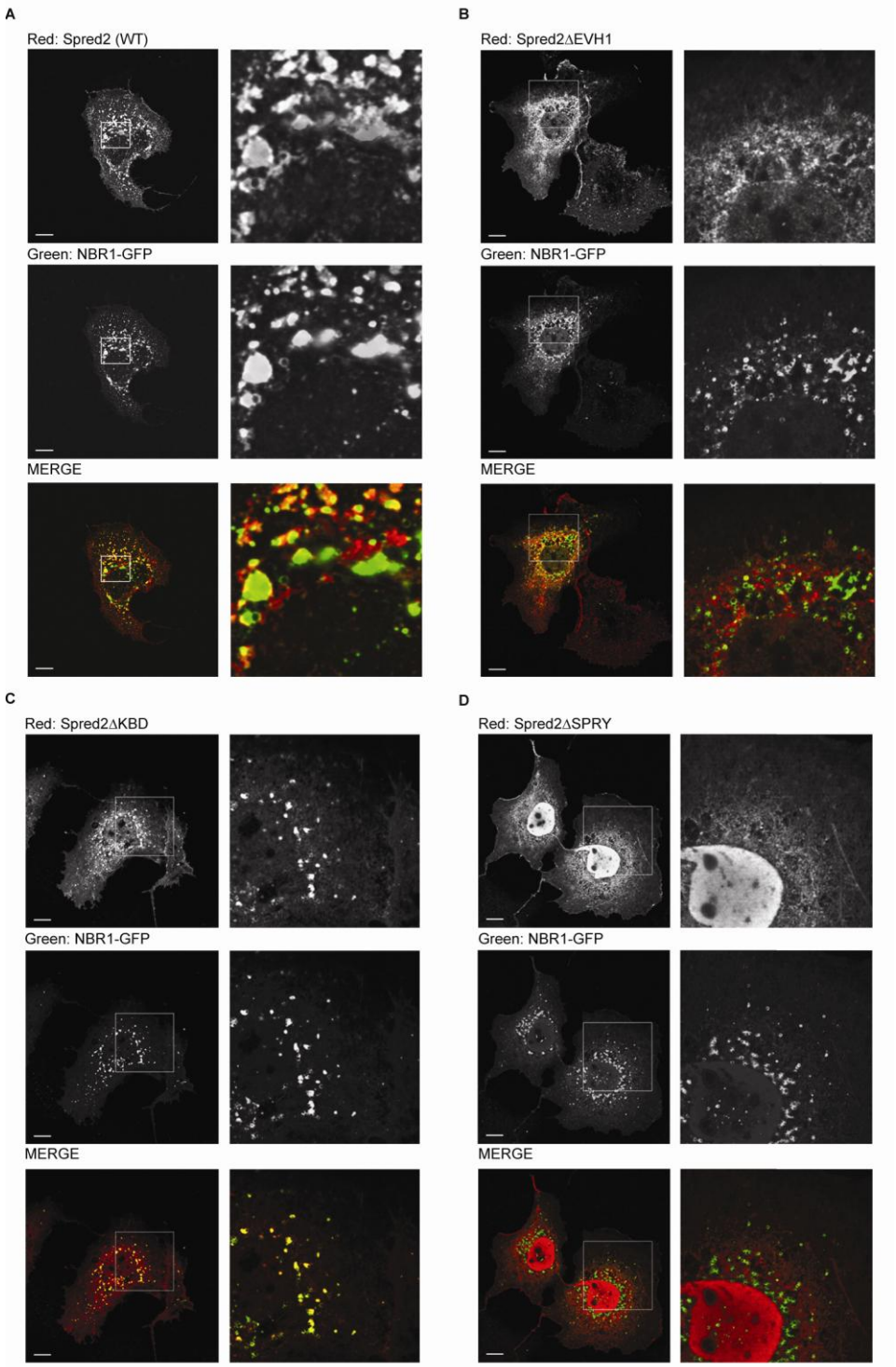

Figure 4.5. Spred2 colocalises with NBR1 in an EVH1 and SPRY domain dependent manner. Images on the right are higher magnifications of the indicated areas on the left. Scale bars represent 10μm. COS7 cells were transfected with myc tagged WT, ΔEVH1, ΔKBD, and ΔSPRY Spred2 along with GFP tagged NBR1 and subjected to immunostaining with anti-myc antibody and confocal microscopy analysis. NBR1-GFP co-localises with WT **(A)** but not ΔEVH1 myc-Spred2 **(B)**. NBR1-GFP also co-localises with ΔKBD but not ΔSPRY myc-Spred2, probably due to its mis-localisation to the nucleus **(D)**.

4.4 NBR1 is specifically late endosomal

Having shown that NBR1 was specifically localised to the limiting membrane of some vesicular structures, the identity of these structures was investigated next. COS7 cells were transfected with NBR1-GFP, immunostained by antibodies against various endocytic markers, and analysed by confocal microscopy to check for colocalisation with NBR1 positive vesicular structures. No co-localisation was observed between NBR1-GFP and the early endosomal marker EEA1, which is a RAB5 specific effector (Figure 4.6A), or the recycling endosomal marker RAB11 (Figure 4.6B). However, a strong co-localisation was detected between NBR1-GFP and the late endocytic marker LAMP2 (Figure 4.6C). LAMP2 specifically stains both late endosomes and lysosomes [Nakamura, et al., 2000], so to discriminate between the two, an antibody against Mannose 6-Phosphate Receptor (MPR), a late endosomal marker which is specifically absent in lysosomes [Ghosh et al., 2003], was used. A similarly strong co-localisation between NBR1-GFP and MPR was detected (Figure 4.6D). Conversely, when LysoTracker-Red was used, an acidotrophic dye that specifically stains lysosomes, no co-localisation with NBR1-GFP was observed (Figure 4.6E). Similarly, no co-localisation was observed between LysoTracker-Red and myc tagged Nbr1, ruling out the possibility of GFP fluorophore inactivation in low lysosomal pH (Figure 4.7A). No co-localisation was also observed between NBR1-GFP and the caveosome marker CAV1 (Figure 4.7B), or the Golgi marker GM130 (Figure 4.7C). Finally, late endocytic localisation of NBR1 could also be shown for endogenous NBR1 in COS7 cells treated with 200 nM BafA for overnight (Figure 4.6F). These results collectively show that NBR1 positive vesicles are specifically late endosomal in character. Since NBR1 is primarily degraded via the lysosomal degradation pathway [Kirkin et al., 2009] its exclusive late endosomal localisation could be a steady-state phenomenon resulting from its rapid degradation in lysosomes.

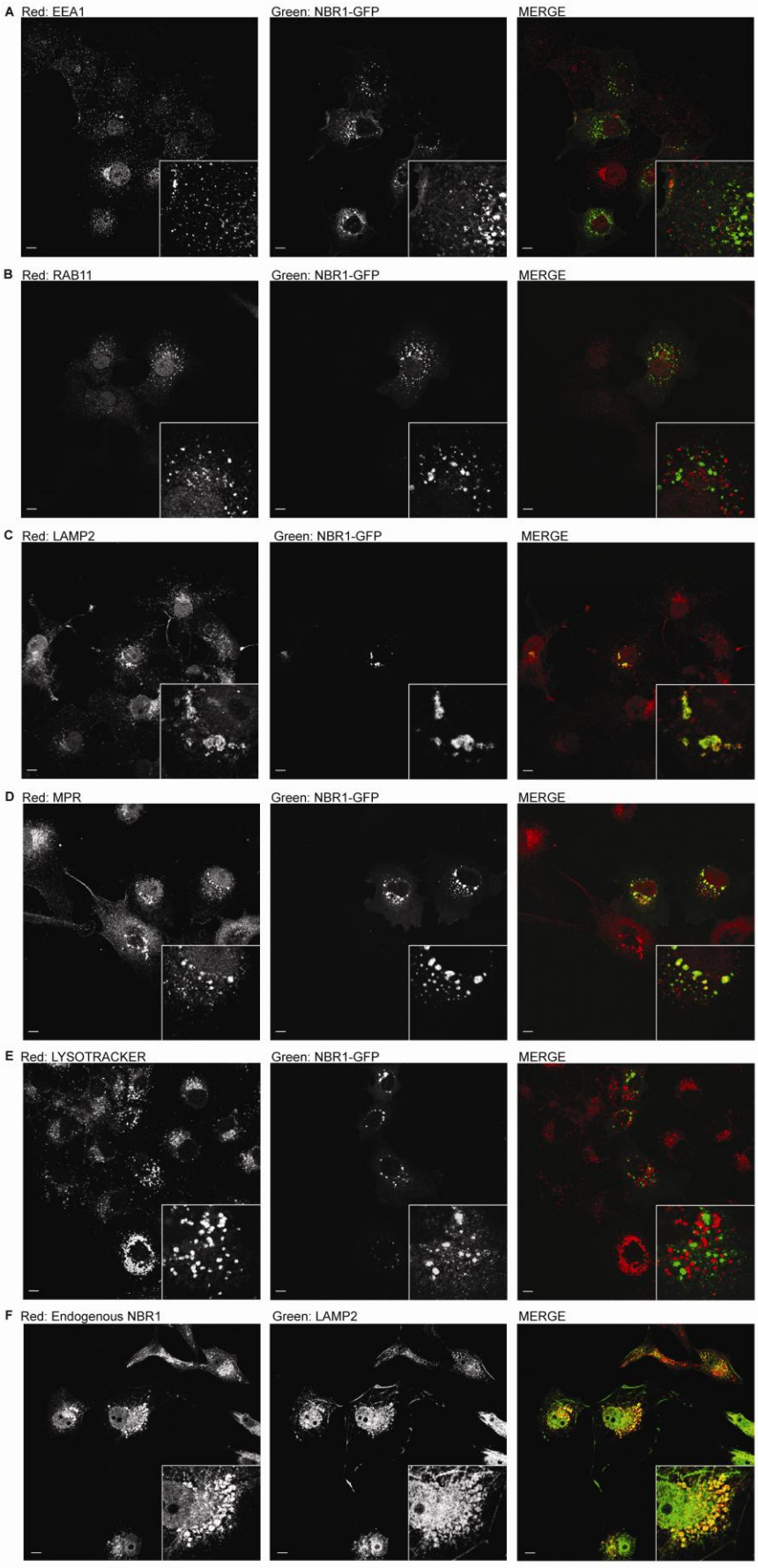

Figure 4.6. NBR1 specifically localises to late endosomes. Scale bars represent 10μm. COS7 cells were transfected with GFP tagged NBR1 and subjected to immunostaining with antibodies against various endocytic markers, or staining with LysoTracker-Red, before analysis by confocal microscopy. NBR1-GFP does not co-localise with the early endosomal marker EEA1 **(A)** or the recycling-endosomal marker RAB11 **(B)**. NBR1-GFP strongly colocalises with the late endosomal/lysosomal marker LAMP2 **(C)** and the late endosomal/*trans*-Golgi marker MPR **(D)**, while no colocalisation is detected with the lysosomal specific dye LysoTracker-Red **(E)**. COS7 cells were treated with 200 nM BafA for overnight to increase endogenous NBR1 levels. The cells were immunostained with anti-NBR1 and anti-LAMP2 antibodies and analysed by confocal microscopy. Endogenous NBR1 also colocalises with LAMP2 **(F)**.

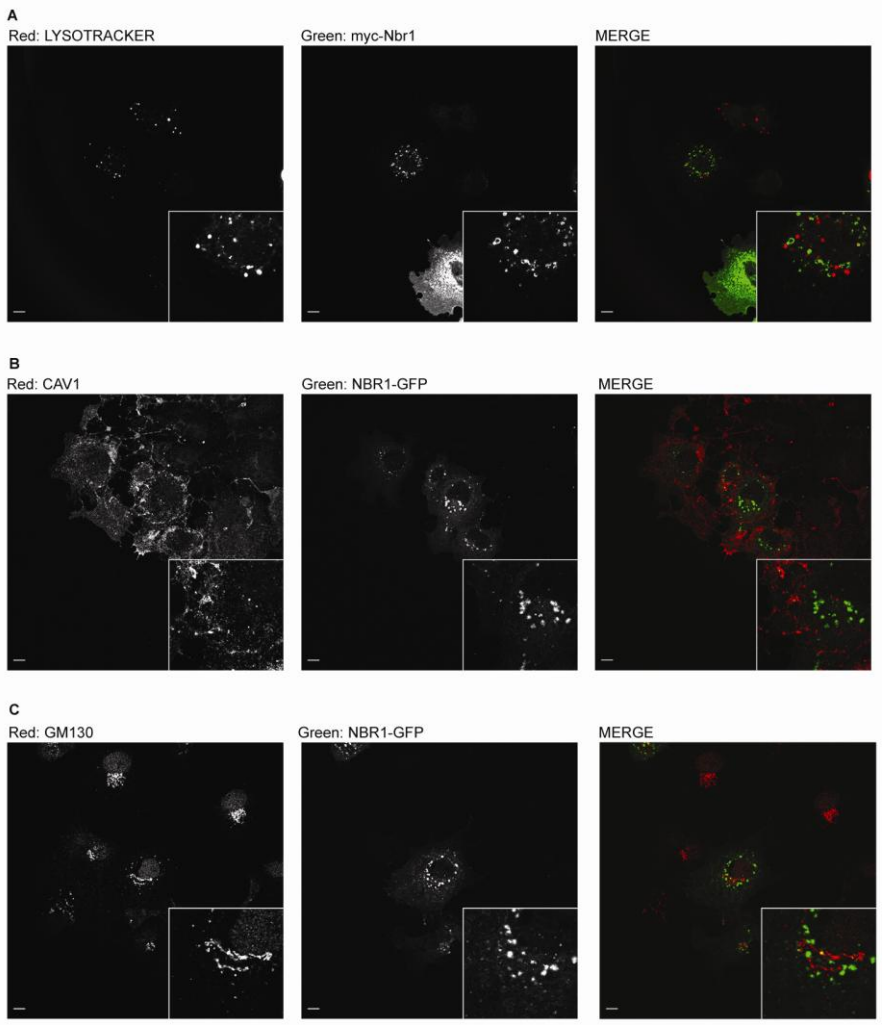

Figure 4.7. NBR1 colocalisation with lysosome, caveosome, and cis-Golgi markers. Scale bars represent 10μm. COS7 cells were transfected with myc tagged Nbr1, stained with LysoTracker-Red, and subjected to immunostaining with anti-myc antibody and confocal microscopy analysis. Myc-Nbr1 does not colocalise with the lysosomal specific dye LysoTracker-Red **(A)**. COS7 cells transfected with NBR1-GFP were immunostained with anti-CAV1 antibody and analysed by confocal microscopy. NBR1-GFP does not colocalise with caveosome marker CAV1 **(B)**. COS7 cells transfected with NBR1-GFP were immunostained with anti-GM130 antibody and analysed by confocal microscopy. NBR1-GFP does not colocalise with the *cis*-Golgi marker GM130 **(C)**.

Late endocytic localization of NBR1 is interesting in the view that NBR1 partner P62 has also been previously shown to localize to the late endosomal/lysosomal compartment [Sanchez et al., 1998]. In fact, when COS7 cells were co-transfected with FLAG tagged P62 and NBR1-GFP and subjected to immunostaining and confocal microscopy, a strong co-localisation was detected between P62 and NBR1 when both proteins were expressed in COS7 cells (Figure 4.8A). When myc-Spred2 was also expressed, it co-localised with NBR1-P62 positive endosomes (Figure 4.8B), in agreement with the earlier co-immunoprecipitation results (Figure 4.2A). Furthermore, when lysates of 293T cells transfected with NBR1-GFP, FLAG-P62, and myc-Spred2 were subjected to Blue-Native/SDS 2-dimensional gel electrophoresis, a fraction of these proteins co-migrated in the native dimension as a single high molecular weight multi-protein complex that could be disrupted with SDS pre-treatment of the lysate (Figure 4.8C). These results lead to the conclusion that a NBR1-P62-SPRED multi-protein complex might exist in the late endosomal compartment, *in vivo*.

4.5 Spred2 mediated attenuation of ERK1/2 signalling is dependent on the interaction with NBR1

The functional significance of the interaction with NBR1 for Spred2 mediated inhibition of ERK1/2 was investigated next. First, the effect of Spred2 over-expression on ERK1/2 signalling downstream of FGFR was examined. 293T cells transfected with myc tagged Spred2 or GFP as control were serum starved and stimulated with 20 ng/ml FGF2 (+ 10 μg/ml Heparin) for a time-course of 3 hours and pERK1/2 levels were checked by immunoblotting. Over-expression of myc-Spred2 could constitutively reduce FGF2 mediated ERK1/2 activity after stimulation (Figure 4.9). Next, the effect of deleting different Spred2

domains on its activity was examined. 293T cells transfected with WT, ΔEVH1, ΔKBD, and ΔSPRY myc-Spred2 were serum starved and stimulated with 20 ng/ml FGF2 (+ 10 μg/ml Heparin) before being lysed and analysed by immunoblotting for pERK1/2 levels. In agreement with previous studies [Wakioka et al., 2001; King et al., 2005], inhibition of ERK1/2 activity by Spred2 was found to be dependent on both EVH1 and SPRY domains (Figure 4.10A), the two domains which were also found to be essential for interaction and co-localization with NBR1 (Figure 4.2B, 4.5B, and 4.5D). In contrast, KBD which was shown to be dispensable for interaction and co-localization with NBR1 (Figure 4.2B and 4.5C) did not affect Spred2 mediated inhibition of ERK1/2 (Figure 4.10A). Therefore, inhibition of ERK1/2 signalling by Spred2 mutants correlates with the ability to interact with NBR1.

Next the effect of NBR1 co-expression with Spred2 on inhibition of ERK1/2 activity was investigated. 293T cells transfected with NBR1-GFP or GFP alone as control with or without myc-Spred2 were starved and stimulated with FGF2 as before. When over-expressed on its own, NBR1 did not reduce ERK1/2 activity and even slightly increased it (Figure 4.10B). However, when co-expressed along with Spred2, NBR1 further enhanced Spred2 mediated ERK1/2 inhibition (Figure 4.10B). This enhancement of Spred2 activity supports the notion that formation of a Spred2-NBR1 complex is important for Spred2 mediated inhibition of ERK1/2, as co-expression of NBR1 must in principle be forcing more of Spred2 into forming a complex with NBR1. Finally, the effect of depleting endogenous NBR1 by siRNA on Spred2 mediated ERK1/2 inhibition was investigated. 293T cells were transfected with 100 pmol of non-silencing control or NBR1 siRNAs. After 24 hours the cells were re-transfected with 50 pmol of siRNA along with Spred2. A Tetracycline (Tet) inducible Spred2 was used to ensure that the protein is expressed only after NBR1 is sufficiently depleted. After another 24 hours, Spred2 expression was induced and cells were simultaneously serum starved and

stimulated with FGF2 as before. While induction of Spred2 in control siRNA background inhibited ERK1/2 activity (Figure 4.10C), knock-down of NBR1 significantly reduced this inhibition (Figure 4.10C). To rule out the possibility of an off target effect, two independent siRNA oligos were used, both of which gave similar results (Figure 4.10C). These results reveal that inhibition of ERK1/2 activity by Spred2 is dependent on NBR1.

To further confirm that the interaction with NBR1 is necessary for Spred2 activity, it was examined whether the rescue of Spred2-NBR1 interaction would also rescue the function of an EVH1 deleted Spred2 mutant. Whilst investigating the interaction of NBR1 and Spred2 earlier, a surprising observation was made. Despite the fact that Spred2 interaction with endogenous NBR1 in 293T cells required both EVH1 and SPRY domains (Figure 4.2B), over-expression of NBR1 in these cells could rescue the interaction with a ΔEVH1 Spred2 mutant (Figure 4.11A). This was a cell-type specific phenomenon as it could not be seen in COS7 cells (Figure 4.11A). The ability to rescue Spred2-NBR1 interaction in a cell-type specific manner for an otherwise non-interacting/non-functional ΔEVH1 Spred2 mutant provided a way to test the functional significance of this interaction. It was hypothesised that if the role of EVH1 domain is to interact with NBR1, then ectopic expression of NBR1 in 293T cells should rescue the inability of ΔEVH1 Spred2 mutant to inhibit ERK1/2 signalling. To check this, 293T cells were transfected with myc tagged WT or ΔEVH1 Spred2, with or without NBR1-GFP, serum starved and stimulated with FGF2 as before prior to analysis by immunoblotting. While myc-Spred2ΔEVH1 mutant alone was not capable of inhibiting FGF2 mediated ERK1/2 activity, inhibition of ERK1/2 was restored with co-expression of NBR1 (Figure 4.11B). As before, NBR1 expression on its own did not affect ERK1/2 activity (Figure 4.11B). These results strongly suggest that Spred2 inhibition of ERK1/2 is dependent on the interaction with NBR1, and that the role of the EVH1 domain is to bind NBR1.

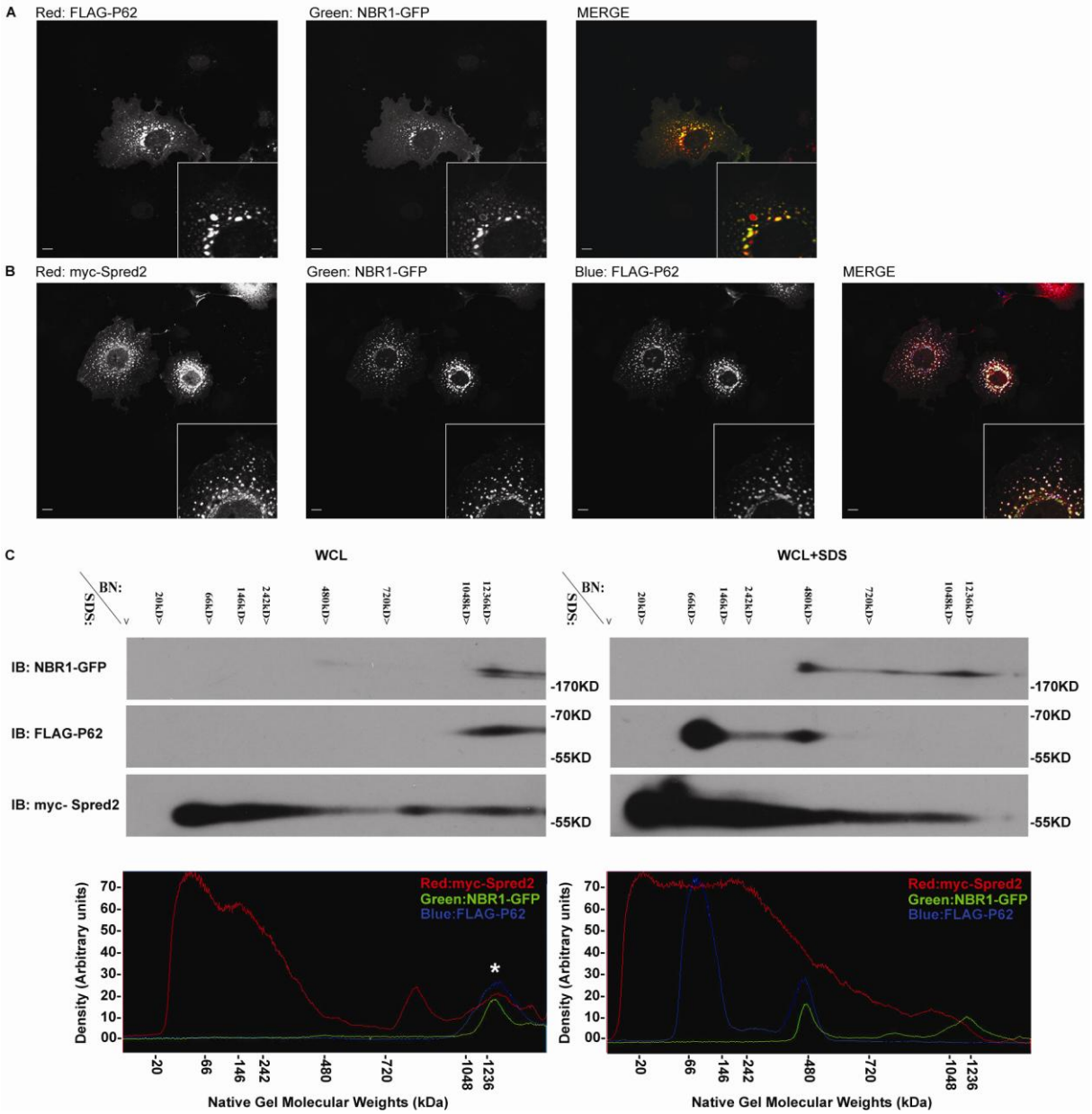

Figure 4.8. NBR1, P62, and a fraction of Spred2 colocalise and form a complex *in vivo*. scale bars represent 10µm. COS7 cells transfected with NBR1-GFP and FLAG-P62 were immunostained and analysed by confocal microscopy. NBR1-GFP and FLAG-P62 exhibit a strong co-localization **(A)**. COS7 cells transfected as above with the addition of myc-Spred2 were immunostained and analysed by confocal microscopy. NBR1-GFP, FLAG-P62, and myc-Spred2 co-localise with each other **(B)**. 293T cells transfected with myc-Spred2, FLAG-P62, and NBR1-GFP were lysed and protein complexes under native conditions were separated in the first dimension by Blue-Native gel electrophoresis, followed by a denaturing SDS-PAGE second dimension. TOP: A high MW (>1236kDa) complex of NBR1, P62, and Spred2 could be detected in the co-transfected 293T WCL under native conditions (left), but not in SDS pre-treated WCL (right). BOTTOM: Densitometric analysis of the above. The high MW complex is marked by * **(C)**.

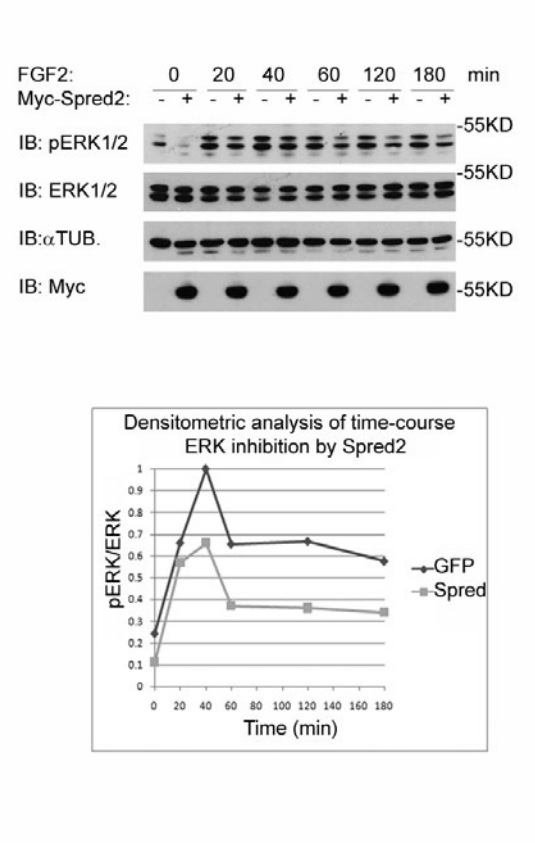

Figure 4.9. Spred2 inhibits ERK1/2 activation downstream of FGF. 293T cells transfected with myc-Spred2 or GFP as control were serum starved and stimulated for a time-course of 3 hours with 20 ng/ml FGF2 + 10 μg/ml Heparin. TOP: Cells were lysed and analysed by immunoblotting with indicated antibodies. BOTTOM: Densitometric analysis of the normalized pERK/ERK ratios from the top. Spred2 was capable of reducing ERK1/2 activity at all investigated time points after FGF2 stimulation.

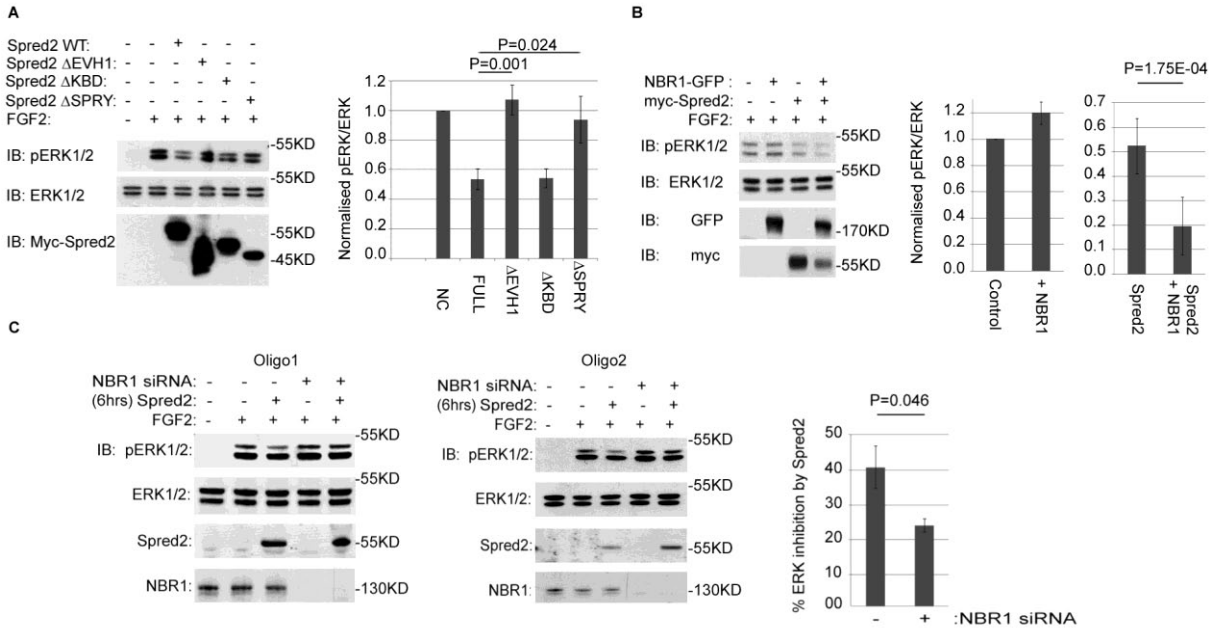

Figure 4.10. Inhibition of ERK1/2 activity by Spred2 is dependent on NBR1. Densitometric analysis of the blots on left are shown on right. All error bars represent Standard Error of Mean (SEM). 293T cells transfected with WT myc-Spred2, various deletion mutants of myc-Spred2, or GFP as control, were serum starved and stimulated with 20 ng/ml FGF2 + 10 μg/ml Heparin. Cells were subsequently lysed and analysed by immunoblotting with indicated antibodies. Inhibition of ERK1/2 by myc-Spred2 was significantly reduced by the loss of both EVH1 and SPRY domains but not KBD **(A)**. 293T cells transfected with NBR1-GFP or GFP as control, with or without mycSpred2 were serum starved, and stimulated with 20 ng/ml FGF2 + 10 μg/ml Heparin. Three fold more NBR1-GFP or GFP was transfected to ensure the majority of myc-Spred2 expressing cells also express NBR1-GFP. Cells were lysed and analysed by immunoblotting with indicated antibodies. NBR1-GFP on its own did slightly increased pERK/12 levels but when co-expressed with myc-Spred2, it significantly enhanced the ability of Spred2 to reduce pERK1/2 levels **(B)**. 293T cells were double transfected (100pmol and 50pmol per 35 mm dish respectively) with either non-silencing control siRNA oligos or NBR1 specific siRNA oligos. Tet-inducible Spred2 construct was co-transfected with Tet-Repressor (1:6 ratio to insure that every Spred transfected cell also expresses TR) along with the oligos on the second transfection. Cells were serum starved and simultaneously Spred2 expression was induced 6hrs prior to stimulation by 1μg/ml of Tetracycline. Cells were stimulated with 20 ng/ml FGF2 + 10 μg/ml Heparin before being lysed and analysed by immunoblotting with indicated antibodies. Two independent NBR1 siRNA oligos were used (Oligo1 and 2). Spred2 mediated inhibition of ERK1/2 activity was significantly reduced in NBR1 knockdown cells **(C)**.

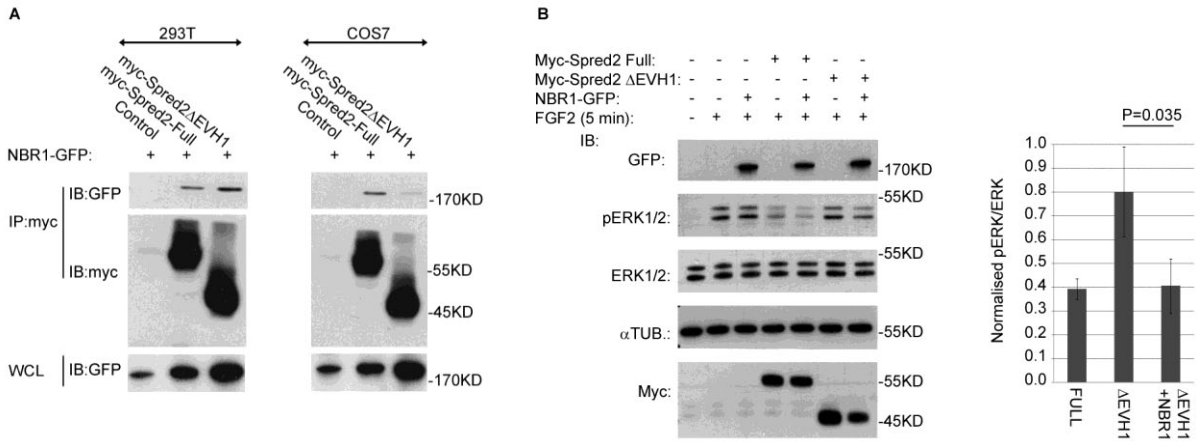

Figure 4.11. Rescuing NBR1-Spred2 interaction also rescues the function of a non-interacting, otherwise non-functional ΔEVH1 Spred2 mutant. Error bars represent Standard Error of Mean (SEM). 293T or COS7 cells were co-transfected with NBR1-GFP along with WT myc-Spred2, ΔEVH1 myc-Spred2, or empty vector as negative control. Cells were subsequently lysed and subjected to immunoprecipitation by myc antibody. While the interaction of over-expressed NBR1 with myc-Spred2 was EVH1 domain dependent in COS7 cells, over-expressed NBR1 could still interact with ΔEVH1-Spred2 in 293T cells **(A)**. 293T cells transfected with NBR1-GFP or GFP as control along with WT myc-Spred2, myc-Spred2ΔEVH1, or empty vector as negative control, were serum starved and stimulated with 20 ng/ml FGF2 + 10 μg/ml Heparin as shown. Three-fold more NBR1-GFP or GFP for controls was transfected to ensure the majority of Spred2 expressing cells also express NBR1-GFP. Cells were subsequently lysed and analysed by immunoblotting with indicated antibodies. Myc-Spred2ΔEVH1 could not reduce ERK1/2 activity alone, but pERK1/2 reduction by myc-Spred2ΔEVH1 mutant was rescued back to WT levels when ectopic NBR1-GFP was also expressed in order to rescue the interaction **(B)**.

4.6 Spred2 targets FGFRs to lysosomal degradation via the interaction with NBR1

Finally, the mechanism by which Spred2 results in attenuation of ERK1/2 signalling was investigated. Considering the localisation of NBR1 to the late endosomal compartment, it was reasoned that Spred2 might regulate the endocytic trafficking of activated receptors via the interaction with NBR1. It is widely recognised that receptor endocytosis can act to down-regulate signalling by targeted degradation of activated receptors via the lysosomal degradation pathway. Therefore, it was examined whether Spred2 acts to enhance degradation of activated receptors. 293T cells were transfected with either FGFR1 or a tagged Transferin receptor I (TrfR1) as control, with or without myc-Spred2, and subjected to analysis by immunoblotting. As over-expression of FGFR1 is auto-activating [Ong et al., 2000], no FGF stimulation was needed. A marked decrease in the level of ectopic FGFR1 was seen in presence of Spred2, whereas levels of TrfR1 did not change significantly (Figure 4.12A), ruling out the possibility of a non-specific effect on co-transfected protein levels by Spred2. No decrease in the levels of downstream signalling components GRB2, C-RAF, or ERK was detectable either (Figure 4.12A), indicating that the effect of Spred2 is restricted to the receptor itself. Moreover, Spred2 induced reduction in FGFR1 levels could be inhibited by treating cells with 200 nM BafA from 1 hour prior to transfection, providing evidence for mediation of the decrease via the lysosomal degradation pathway (Figure 4.12B).

Next, WT myc-Spred2 was compared with the ΔEVH1 myc-Spred2 mutant that lacks the ability to interact with NBR1 for their ability to target FGFR1 for degradation. Cells were transfected with FGFR1 along with WT or ΔEVH1 myc-Spred2. While WT Spred2 decreased the level of ectopic FGFR1 as before, Spred2ΔEVH1 was incapable of inducing such reduction (Figure 4.12C). Finally, it was investigated if Spred2 expression had a similar

effect on endogenous FGFR levels and whether this was NBR1 dependent. Instead of FGFR1, endogenous FGFR2 was monitored as it was readily detectable in 293T cells. 293T cells were transfected with 100 pmol of non-silencing control or NBR1 siRNAs. After 24 hours the cells were re-transfected with 50 pmol of siRNA along with a Tet-inducible Spred2. Again, Tet inducible Spred2 was used to ensure that the protein is expressed only after NBR1 is sufficiently depleted. After another 24 hours, Spred2 expression was induced and cells were simultaneously serum starved and stimulated with FGF2 for 1 hour as before. In FGF2 stimulated cells, induction of Spred2 expression resulted in a slight reduction of endogenous FGFR2 as expected (Figure 4.12D). However, knock-down of NBR1 by specific siRNA oligos significantly reduced this effect (Figure 4.12D). Two independent siRNA oligos were used, both of which gave similar results, ruling out the possibility of an off target effect (Figure 4.12D). We therefore conclude that Spred2 can reduce endogenous FGFR levels, and as with inhibition of ERK1/2 activity this reduction appears to be NBR1 dependent.

To monitor the induced change in sub-cellular localisation of FGFR by Spred2, a functional GFP tagged FGFR2 [Ahmed et al., 2008] was used. COS7 cells were transfected with FGFR2-GFP with or without WT myc-Spred2 or ΔEVH1 myc-Spred2. The cells were subsequently immunostained with anti-LAMP2 (Red channel) and anti-myc (Blue channel-not shown) antibodies, and analysed by confocal microscopy. Like FGFR1, over-expression of FGFR2-GFP was auto-activating so no additional FGF stimulation was necessary. A significant fraction of FGFR2-GFP exhibited an endosomal localisation (Figure 4.13). However, in the absence of myc-Spred2, only a fraction of this endosomal FGFR2-GFP colocalised with LAMP2 (Figure 4.13). In the presence of WT myc-Spred2, however, the majority of FGFR2-GFP endosomes were LAMP2 positive (Figure 4.13). This increase in co-localisation of the receptor with LAMP2 could be reversed by deletion of the EVH1 domain,

as seen in ΔEVH1 myc-Spred2 co-transfected cells (Figure 4.13). Collectively, these results suggest that the EVH1/NBR1 dependent down-regulation of signalling by Spred2 is achieved via directed endosomal trafficking of activated receptors into the late endosomal/lysosomal degradation pathway.

4.7 Conclusions

Collectively, the evidence presented in this chapter reveals that the EVH1 domain of Spred2 is required to engage with the late endosomal protein NBR1, and this is necessary for Spred2 mediated inhibition of FGF signalling. The results also suggest that Spred2 functions by targeting signalling receptors to the lysosomal degradation pathway via interacting with NBR1. This adds to the large body of evidence which implicates receptor trafficking as a key means for regulation of signalling dynamics [Vieira et al., 1996; Kranenburg et al., 1999; Sandilands et al., 2007; Sigismund et al., 2008]. As mentioned before, several reports have also suggested a trafficking role for Sprouty in the context of EGFR signalling [Wong et al., 2002a; Rubin et al., 2003; Kim et al., 2007]. However, there seems to be a functional divergence along with the structural divergence between Sproutys and Spreds: Sprouty interferes with lysosomal degradation of the receptors by inhibiting Cbl mediated receptor internalization [Wong et al., 2002a; Rubin et al., 2003] and/or Hrs dependent early to late endosomal transition [Kim et al., 2007], whereas Spred seems to promote lysosomal targeting of the receptors via engaging with NBR1.

An intriguing issue is the fact that the inhibitory activity of Spred2 is reported to be limited to the ERK1/2 pathway [Wakioka et al., 2001; Nonami et al., 2004; King et al., 2005]. As discussed in the chapter one, several studies have highlighted that endocytosis does not

simply act as a means for receptor removal and degradation, but that specific endosomal compartments themselves can act as selective platforms for downstream signal propagation [Miaczynska et al., 2004b]. ERK1/2 activation downstream of EGFR, for instance, has been shown to be dependent on receptor endocytosis [Vieira et al., 1996; Kranenburg et al., 1999], while PLC/PKC and PI3K/AKT pathways are activated on the plasma-membrane and are inhibited by receptor internalisation [Vieira et al., 1996]. ERK1/2 activation by Nerve Growth Factor (NGF) has also been shown to need internalisation of the receptor while PI3K/AKT activation does not [MacInnis and Campenot, 2002]. Localisation of certain signalling components and scaffolds to specific endosomal vesicular compartments is thought to be important for such selective signal propagation after endocytosis of the receptor. For example, The GTP bound active form of Rap1, a Ras-related small GTPase which can also activate ERK1/2, has been shown to be preferentially enriched on endosomes [Ohba et al., 2003]. Interestingly, Spred2 has also been shown to be capable of inhibiting Rap1 activation [King et al., 2005]. Moreover, the scaffolding protein complex MP1-P14, which acts to selectively activate ERK1/2 but not other MAPKs such as p38, has been shown to be enriched on late endosomes [Wunderlich et al., 2001; Teis et al., 2002;] via the anchor protein P19 [Nada et al., 2009]. Interestingly, p14 was reported as a potential NBR1 interacting protein identified in a Yeast 2 Hybrid screen [Waters et al., 2009]. It remains to be determined if this interaction occurs *in vivo*, and whether it plays a role in Spred2 mediated ERK1/2 inhibition via NBR1. Nevertheless, these considerations predict that in a short timescale of up to a few hours post-stimulation, diversion of endosomal receptor trafficking by Spred2 could be preferentially affecting a subset of downstream signalling pathways such as ERK1/2 which require specific endosomal compartments as platforms for signal propagation.

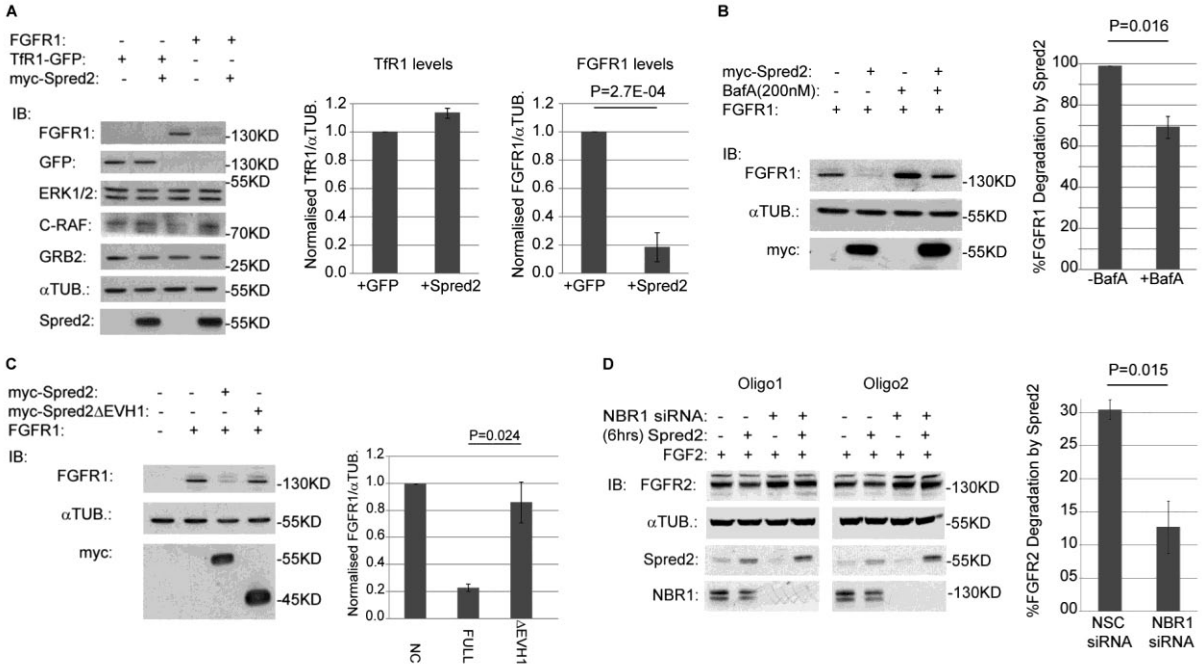

Figure 4.12. Spred2 targets activated receptors to the lysosomal degradation pathway via NBR1. Error bars represent Standard Error of Mean (SEM). 293T cells transfected with FGFR1 or TfRI-GFP as control with or without myc-Spred2 were lysed and analysed by immunoblotting with indicated antibodies. Five-fold more Spred2 (or GFP alone for controls) was transfected to ensure the majority of receptor expressing cells also co-express myc-Spred2.Levels of ectopic active FGFR1 are significantly decreased in presence of Spred2 while those of ectopic TrfR1-GFP or downstream signalling components such as ERK, C-RAF, or GRB2 do not change **(A)**. 293T cells were transfected with FGFR1 plus or minus myc-Spred2 as above, with or without 200 nM BafA pre-treatment 1 hour prior to transfection. Five-fold more myc-Spred2 (or GFP for controls) were transfected to ensure the majority of receptor expressing cells also co-express myc-Spred2. Cells were analysed by immunoblotting with indicated antibodies 12 hrs after transfection. BafA treatment hinders Spred2 induction of FGFR1 degradation **(B)**. 293T cells transfected with FGFR1 with or without WT myc-Spred2 or myc-Spred2ΔEVH1 were lysed and analysed by immunoblotting with indicated antibodies. Five-fold more myc-Spred2 or myc-Spred2ΔEVH1 (or GFP for controls) were transfected to ensure the majority of receptor expressing cells also co-express Spred2. Contrary to WT myc-Spred2, myc-Spred2ΔEVH1 does not induce FGFR1 degradation in co-transfected 293T cells **(C)**. 293T cells were double transfected (100pmol and 50pmol per 10cm well respectively) with either non-silencing control (NSC) or two independent NBR1 siRNAs (oligos 1 & 2). Tet-inducible Spred2 was co-transfected with Tet-Repressor (1:6 ratio to insure that every Spred transfected cell also expresses TR) along with the oligos on the second transfection. Spred2 expression was induced 6hrs prior to stimulation by 1μg/ml Tet. The cells were serum starved and stimulated with 20 ng/ml FGF2 + 10 μg/ml Heparin before lysis and analysis by immunoblotting with indicated antibodies. Spred2 reduces endogenous FGFR2 levels in NSC knockdown cells but this is significantly reduced in NBR1 knockdown cells **(D)**.

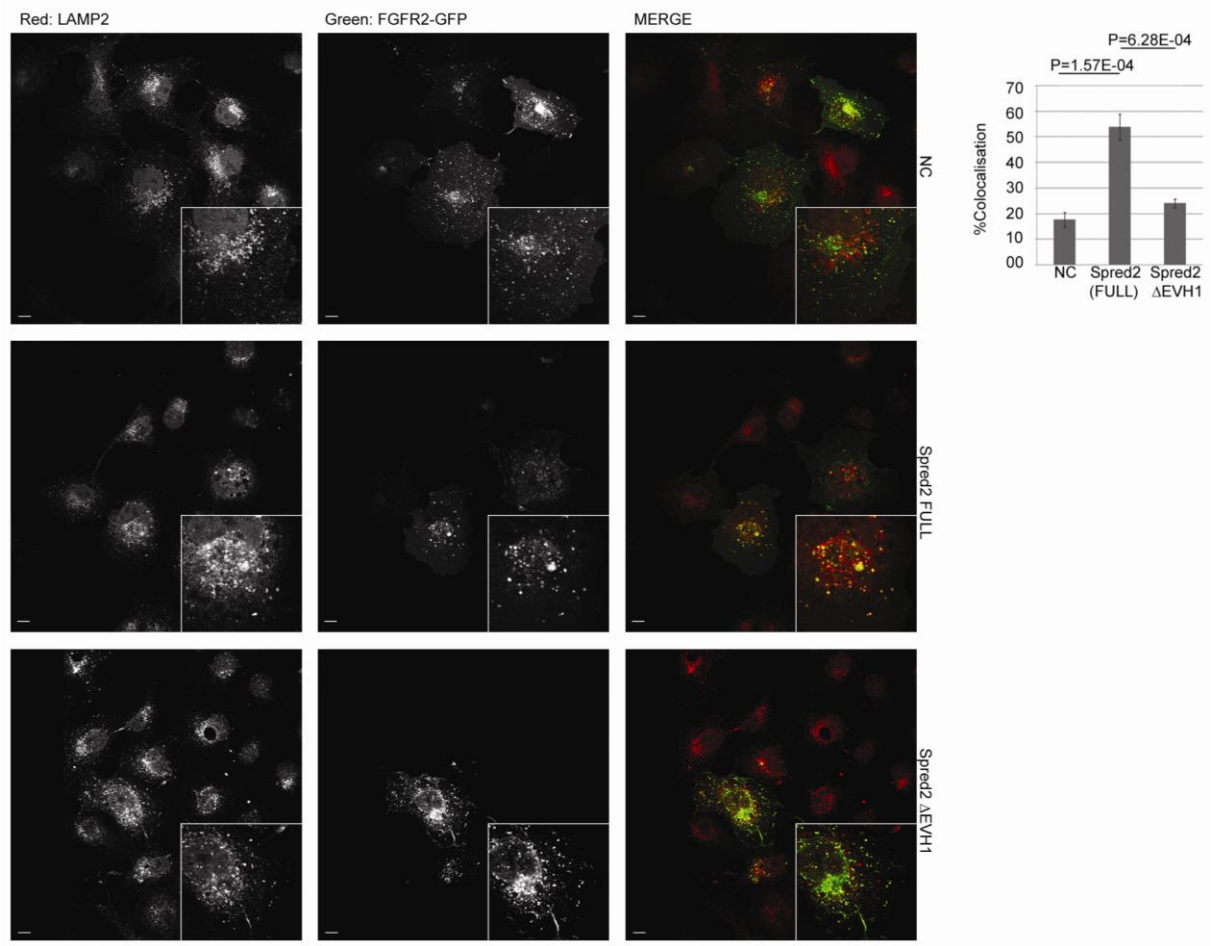

Figure 4.13. Spred2 diverts FGFR trafficking to the late endosomal/lysosomal compartment. Scale bars represent 10μm. Error bars represent Standard Error of Mean (SEM). LEFT: COS7 cells were transfected with FGFR2-GFP plus empty vector as control (NC), WT myc-Spred2 (FULL), or mycSpred2 ΔEVH1. Cells were subsequently immunostained for LAMP2 and analysed by confocal microscopy. [In order to identify Spred2 co-transfected cells, cells were also stained for Spred2 (Blue Channel-not shown) using an anti-Spred2 antibody]. The majority of endosomal receptor does not co-localise with LAMP2 in control cells (NC). However, most of endosomal receptor co-localises with LAMP2 in WT myc-Spred2 co-transfected cells (FULL). Deletion of the EVH1 domain, however, results in the loss of this Spred2 induced LAMP2 co-localisation as seen with myc-Spred2ΔEVH1 co-transfected cells. RIGHT: The percentage of FGFR2-GFP co-localisation with LAMP2 was quantified and averaged. Measurements were from 9 or more cells for each co-transfection, from 2 separate experiments.

Finally, the findings reported in this chapter implicate NBR1 as a novel regulator of RTK trafficking. Interestingly, the NBR1 binding partner P62 has also been shown to regulate RTK trafficking [Geetha et al., 2005], and here it was demonstrated that NBR1, P62, and a fraction of Spred2 co-localise and form a protein complex *in vivo* (Figure 4.8). It remains to be determined whether there are any functional links between the two proteins in the context of RTK trafficking regulation. The exact role of NBR1 in this context is examined in chapter five.

CHAPTER 5

NBR1: A Novel Regulator of Receptor Trafficking

5.1 Introduction

Having shown that Spred2 interaction with NBR1 results in diversion of FGFR trafficking and down-regulation of downstream ERK1/2 signalling, the next step was to investigate the role of NBR1 in the context of receptor trafficking in more detail. The fact that NBR1 was specifically late endosomal, as well as its necessity for Spred2 mediated regulation of trafficking and signalling, led to the hypothesis that it might have a key function in RTK trafficking. This is supported by the fact that NBR1 interacts with a number of proteins which have roles in vesicular trafficking. These include the scaffold protein P62 which associates with NBR1 through its PB1 domain [Lange et al., 2005]. As mentioned earlier, P62 also localises to the late endosomal compartment [Sanchez et al., 1998], and has been shown to regulate TrkA sorting via modulation of TRAF6-dependent K63 polyubiquitination of the receptor [Geetha et al., 2005]. Three other trafficking related proteins reported to bind to NBR1 are the late endosomal adaptor protein P14, Transmembrane emp24-like trafficking protein 10 (Tmp21), and Ubiquitin carboxyl-terminal hydrolase 8 (USP8/UBPY), all of which were found in a Y2H screen for NBR1 interacting partners [Waters et al., 2009]. As mentioned earlier, P14 in association with MP1 constitutes an adaptor complex which binds to both MEK and ERK1/2 and enhances the activation of the latter on the late endocytic compartment [Teis et al., 2002]. This activity of P14 in turn affects late endosomal trafficking [Teis et al., 2006]. On the other hand, Tmp21 is a member of p24 cargo protein family that mainly resides in ER but is also present on the plasma membrane [Blum et al., 1996], and has been implicated in ER/Golgi trafficking and protein anchorage to this compartment [Jenne et al., 2002; Wang et al., 2010], as well as modulating γ-secretase activity on the plasma membrane [Chen et al., 2006]. Finally, USP8 is a de-ubiquitinating enzyme the loss of which results in blockage of EGFR degradation [Row et al., 2006; Alwan and van Leeuwen, 2006].

It is thought that USP8 mediated de-ubiquitination of EGFR is essential for ESCRT dependent MVB sorting and subsequent receptor degradation [Row et al., 2006; Alwan and van Leeuwen, 2006]. In addition, USP8 has a role in regulation of ESCRT ubiquitin recognition machinery itself by de-ubiquitinating their components [Mizuno et al., 2006].

The results of this chapter establish Nbr1 as a negative regulator of ligand mediated RTK degradation, and reveal the relationship between its different regions for protein localisation and function. It is here shown that Nbr1 expression blocks ligand mediated lysosomal degradation of RTKs without affecting early to late endosomal transition. The C-terminal of Nbr1 is essential but not sufficient for this function. The C-terminal of Nbr1 is also essential but not sufficient for the late endocytic localisation of the protein, revealing correlation between protein localisation and function. Furthermore, the analysis of Nbr1 C-terminal reveals that in addition to the UBA domain it contains a novel membrane interacting amphipathic α-helix named JUBA. Both UBA and JUBA are necessary for the late endocytic localisation of the protein. Moreover, the late endocytic and autophagic localisations of Nbr1 are independent, suggesting that the function of Nbr1 in each context might be distinct. Loss or over-expression of Nbr1 does not affect autophagy, ruling out the involvement of the protein in autophagy machinery. Finally, it is here shown that similar to the loss of NBR1, expression of a C-terminal only Nbr1 mutant induces cell death by apoptosis, suggestive of a dominant negative activity for some vital NBR1 function, and this vital function is independent of Nbr1 autophagy-related roles. Quantitative mass spectrometry analysis of the binding partners for Nbr1 C-terminal reveals a number of potential interacting partners which might give clues into its mechanism of action on RTKs as well as any additional roles.

5.2 Nbr1 abrogates ligand mediated RTK degradation without affecting early to late endosomal transition

To monitor ligand mediated RTK degradation, 293T cells transfected with myc tagged Nbr1 or GFP as control were serum starved and stimulated with either EGF (50 ng/ml) or FGF2 (20 ng/ml + 10 μg/ml Heparin) for a time-course of 2 hours and endogenous receptor and pERK1/2 levels were checked by immunoblotting. Nbr1 expression blocked ligand mediated degradation of endogenous EGFR and enhanced downstream ERK1/2 signalling without affecting basal receptor levels (Figure 5.1A). Similarly, ligand mediated degradation of endogenous FGFR2 was blocked and downstream ERK1/2 signalling was enhanced (Figure 5.1B). To confirm that the observed effect of Nbr1 on EGFR or FGFR2 was due to blockage of lysosomal degradation, cells were pre-treated with the lysosomal inhibitor BafA (200 nM) and stimulated for 1 hour with EGF or 2 hours for FGF2 as before. In presence of BafA, the effect of Nbr1 expression on EGFR and FGFR2 levels post stimulation were minimal, supporting the notion that the observed difference in receptor levels is in fact due to the abrogation of lysosomal degradation (Figure 5.1C & 5.1D). These results suggest that Nbr1 acts to abrogate ligand mediated lysosomal degradation of RTKs and enhance downstream ERK1/2 signalling. Surprisingly, a 48 hour siRNA knockdown of endogenous NBR1 in 293T cells did not have any impact on ligand mediated degradation of FGFR2 (Figure 5.2). Cells were transfected with 100pmol of non-silencing control or NBR1 siRNA for 48 hours with transfection being renewed after 24 hours. A pool of three siRNA oligos (siRNA1) and an independent siRNA oligo (siRNA2) were used to rule out any off target effects. After serum starvation, cells were stimulated with 20 ng/ml FGF2 + 10 μg/ml Heparin as before. The lack of an effect on receptor levels might be due to insufficient depletion of NBR1 after 48 hours (See below). Alternatively, NBR1 function could be compensated by other proteins.

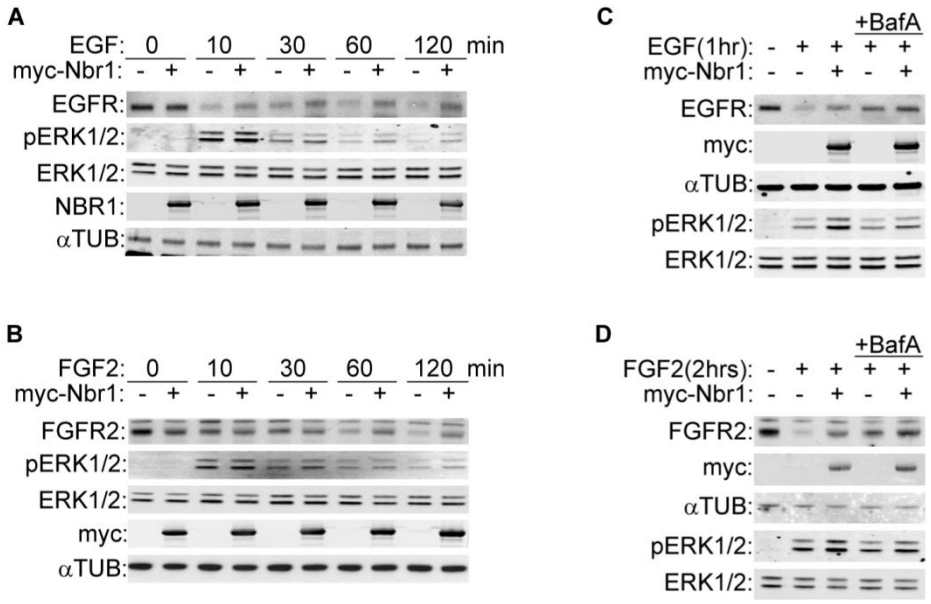

Figure 5.1. Over-expression of Nbr1 blocks ligand mediated RTK degradation and enhances downstream ERK1/2 signalling. 293T cells transfected with myc-Nbr1 or GFP as control were serum starved and stimulated for indicated time-points with 50 ng/ml EGF **(A)**, or 20 ng/ml FGF2 + 10 μg/ml Heparin **(B)**. Cells were lysed and analysed by immunoblotting with indicated antibodies. Nbr1 blockage of ligand mediated RTK degradation is BafA sensitive. 293T cells transfected with myc-Nbr1 or GFP as control were starved and stimulated for indicated times with 50 ng/ml EGF **(C)**, or 20 ng/ml FGF2 + 10 μg/ml Heparin **(D)**. 30 minutes prior to stimulation, the specified cells were pre-treated with 200nM BafA. Cells were lysed and analysed by immunoblotting for indicated antibodies

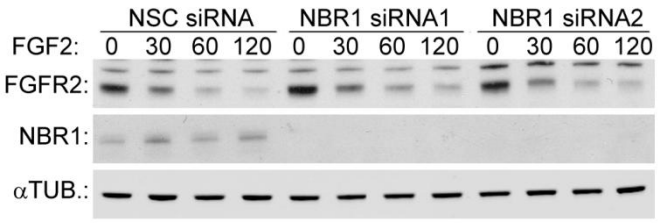

Figure 5.2. Knockdown of NBR1 does not affect ligand mediated FGFR2 degradation. 293T cells were transfected with non-silencing control (NSC) or NBR1 siRNAs (NBR1 siRNA1 and NBR1 siRNA2) for 48 hours with transfection being renewed after 24 hours. Cells were serum starved and stimulated with 20 ng/ml FGF2 + 10 μg/ml Heparin before being lysed and analysed by immunoblotting with indicated antibodies.

Theoretically, Nbr1 could act at various levels during the trafficking of RTKs in a way that could ultimately lead to the abrogation of receptor degradation. These could be inhibition of receptor internalisation or enhancement of receptor recycling back to the plasma membrane, blockage of early to late endosomal transition, inhibition of late endocytic MVB maturation, or blockage of mature MVB fusion with lysosomes. As mentioned in the introduction, mature MVBs have their receptors trapped within the Intra-luminal vesicles (ILVs), thus are incapable of signalling. As Nbr1 action seems to be enhancing downstream ERK1/2 activity, it suggests that it is probably not functioning at the MVB – lysosome fusion step. However, considering the late endosomal localisation of Nbr1, blockage of early to late endosomal transition could be a likely point of action. In fact, multiple proteins of the ESCRT machinery such as HRS, STAM, and TSG101 act at this stage and their loss of function has been shown to result in a similar abrogation of RTK degradation and blockage of early to late endosomal receptor transition [Lu et al., 2003; Kanazawa et al., 2003]. Therefore, the effect of Nbr1 expression on early to late endosomal transition was investigated. To do this, we employed fluorescently labelled EGF to track receptor trafficking inside the cell. Unlike other EGFR ligands such as TGFα, EGF stably associates with the receptor throughout the endosomal compartments and the majority of it also gets degraded in lysosomes [Ebner and Derynck, 1991], so following the ligand can be used as a suitable substitute for direct following of the receptor which would require good quality antibodies.

The results are represented in (Figure 5.3). COS7 cells were used and internalisation events were synchronised by stimulation on ice, where endocytosis is blocked. Serum starved cells were stimulated with 250 μg/ml of AlexaFuor-488 labelled EGF (Green channel) for 15 minutes by washing and incubating the cells at 37°C to allow internalisation. Cells were then fixed, stained for the early and late endosomal markers EEA1 and LAMP2 (Red channel), and

analysed by confocal microscopy. Cells were also stained for Nbr1 in order to identify Nbr1 transfected cells from non-transfected ones (Blue channel - not shown). In control cells, EGF appeared in early endosomes after 10 minutes (Figure 5.3A) but was absent from late endosomes (Figure 5.3C). However, EGF was mainly present in late endosomes (Figure 5.3D) and completely absent from early endosomes (Figure 5.3B) after 60 minutes. No difference was observed in Nbr1 transfected cells as EGF was first localised to early and not late endosomes (Figure 5.3E & 5.3G), but this was later reversed (Figure 5.3F and 5.3H). Up to 10 cells were investigated in each case, all of which gave similar results. These results suggest that the action of Nbr1 is not due to a blockage in early to late endosomal transition.

5.3 C-terminal of Nbr1 is essential but not sufficient for protein function

The functional significance of Spred2 binding implicated that the C-terminal of NBR1 might be important for its function. The effect of full-length Nbr1 to that of a C-terminal deleted mutant lacking the last 133 amino acids (P856-Y988) on ligand mediated RTK degradation was therefore compared. 293T cells were transfected with myc-Nbr1, myc-Nbr1ΔCterm., or GFP as control. After serum starvation, cells were stimulated with 50 ng/ml EGF for 1 hour, or 20 ng/ml FGF2 + 10 μg/ml Heparin for 2 hours before being lysed and analysed by immunoblotting. Unlike full-length, the C-terminal deleted mutant could not block EGFR degradation after EGF treatment (Figure 5.4.A). Similar results were obtained for FGFR2 as well (Figure 5.4.B), and the enhancement of downstream ERK1/2 signalling was also lost for both EGF and FGF2 (Figure 5.4A and 5.4B).

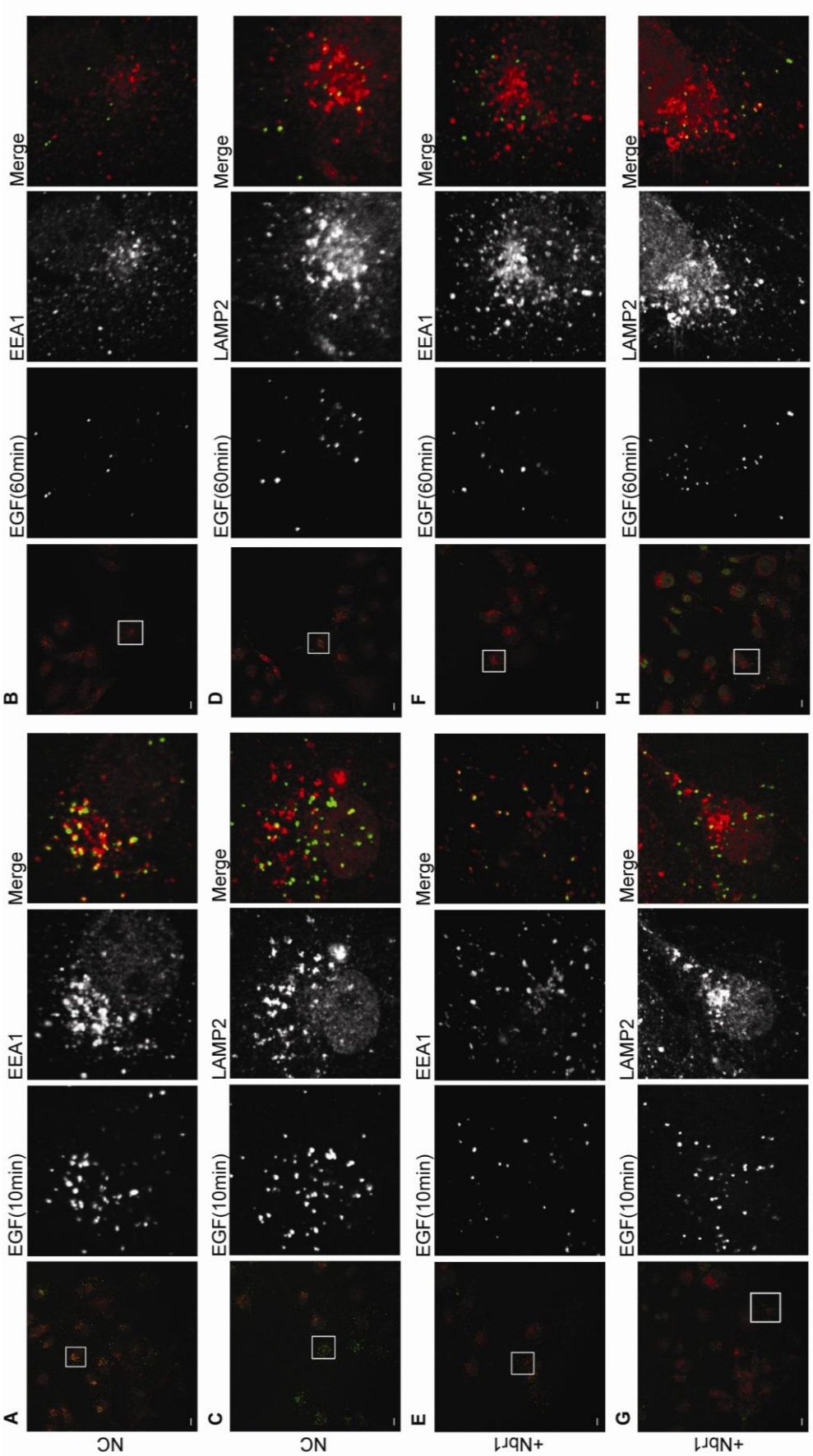

Figure 5.3. Nbr1 expression does not affect early to late endosomal transition. Scale bars = 10µm. Pictures on the right are higher magnifications of the indicated areas [white boxes] on the left: EGF colocalisation after 10 minutes with EEA1 **(A)** and LAMP2 **(C)** in non-transfected control cells. EGF colocalisation after 60 minutes with EEA1 **(B)** and LAMP2 **(D)** in non-transfected control cells. EGF colocalisation after 10 minutes with EEA1 **(E)** and LAMP2 **(G)** in Nbr1 expressing cells. EGF colocalisation after 60 minutes with EEA1 **(F)** and LAMP2 **(H)** in Nbr1 expressing cells.

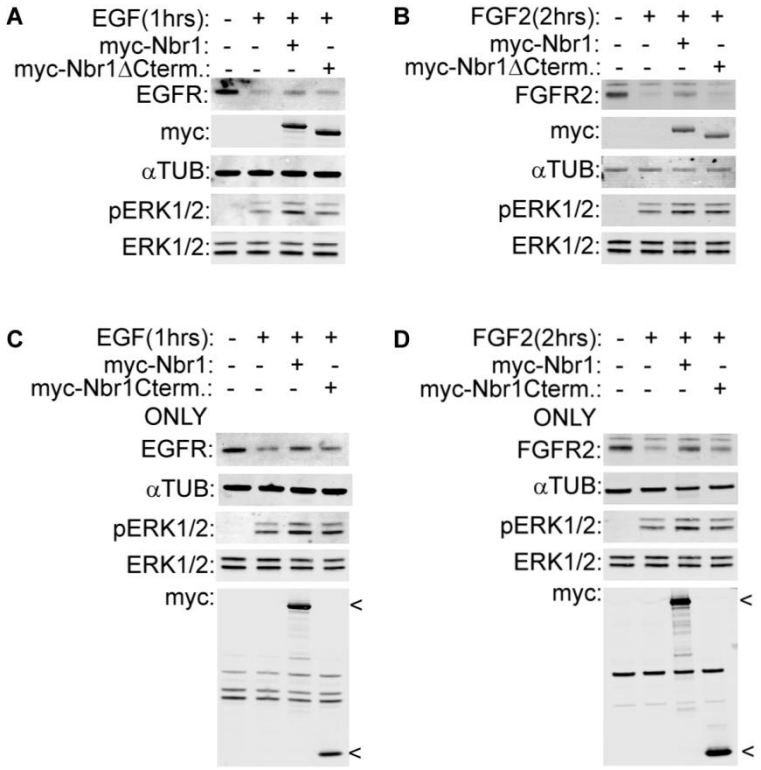

Figure 5.4. C-terminal 133 amino acids of Nbr1 are essential but not sufficient for protein function. 293T cells were transfected with myc-Nbr1, myc-Nbr1ΔCterm., or GFP as control. Cells were serum starved and stimulated for 1 hour with 50 ng/ml EGF **(A)**, or 2 hours with 20 ng/ml FGF2 + 10 μg/ml Heparin **(B)** before being lysed and analysed by immunoblotting with indicated antibodies. 293T cells were transfected with myc tagged full-length Nbr1 (myc-Nbr1), myc-Nbr1Cterm. (P856-Y988), or GFP as control. 50 μM Z-VAD-FMK was added to all cells in order to block cell death by apoptosis. Cells were serum starved and stimulated for 1 hour with 50 ng/ml EGF **(C)**, or 2 hours with 20 ng/ml FGF2 + 10 μg/ml Heparin **(D)** before being lysed and analysed by immunoblotting with indicated antibodies. Full-length and C-terminal-ONLY Nbr1 corresponding bands are indicated by <.

Next, we compared full-length Nbr1 with a C-terminal-ONLY mutant (P856-Y988) which just contains the last 133 amino acids. 293T cells were transfected with myc-Nbr1, myc-Nbr1Cterm.(P856-Y988), or GFP as control. Surprisingly, the C-terminal-ONLY mutant induced cell death by apoptosis (see below), so the cells had to be treated with a general Caspase inhibitor (z-VAD-FMK) in order to block death and allow sufficient time of analysis in these experiments. After serum starvation, cells were stimulated with 50 ng/ml EGF for 1 hour, or 20 ng/ml FGF2 + 10 μg/ml Heparin for 2 hours before being lysed and analysed by immunoblotting. Like the C-terminal deleted mutant, C-terminal-ONLY Nbr1 was not capable of blocking ligand mediated EGFR (Figure 5.4C) or FGFR2 (Figure 5.4D) degradation, and enhancement of downstream ERK1/2 signalling was also lost (Figure 5.4C and 5.4D). Together, these results suggest that while the C-terminal of Nbr1 is essential for blockage of RTK trafficking, it is not sufficient for this function.

5.4 C-terminal of Nbr1 is essential but not sufficient for protein localisation

As Nbr1 specifically localises to the limiting membrane of late endosomes, this localisation might be important for the observed effect on RTK trafficking. Therefore, confocal microscopy was used to determine whether there is a link between loss of Nbr1 function and its localisation. COS7 transfected with different GFP tagged mutants of Nbr1 were used. The cells were fixed, immunostained for the late endocytic marker LAMP2, and analysed by confocal microscopy for colocalisation of Nbr1 with LAMP2. As expected, full-length Nbr1 showed significant colocalisation with the late endocytic marker LAMP2 (Figure 5.5A). Deletion of the two N-terminal domains of Nbr1 (PB1 and ZZ domains) did not affect this colocalisation (Figure 5.5B), suggesting that these N-terminal domains are not critical for

protein localisation. However, loss of the C-terminal 133 amino acids (P856-Y988) which also results in loss of protein function (Figure 5.4A and 5.4B), had a dramatic impact on localisation (Figure 5.5C). This deletion not only resulted in loss of colocalisation with LAMP2, but the protein exhibited a diffuse cytosolic localisation instead of a vesicular localisation (Figure 5.5C). On the other hand, when a C-terminal-ONLY (P856-Y988) Nbr1 mutant was investigated, it showed no colocalisation with LAMP2, but the mutant was still localised to the limiting membrane of some intra-cellular vesicular structures (Figure 5.5D). These vesicular structures were relatively enlarged compared to full-length Nbr1 (Figure 5.5A), suggestive of a defect in vesicle maturation or fission. Interestingly, when colocalisation with the early endosomal marker EEA1 was investigated, unlike full-length Nbr1 which did not show a significant colocalisation (Figure 5.6A), the C-terminal-ONLY mutant strongly colocalised with EEA1 (Figure 5.6B). These results suggest that the C-terminal of Nbr1 is essential but not sufficient for its correct localisation. The effect of Nbr1 on RTK trafficking, therefore, correlates with its ability to correctly localise to the late endocytic compartment. Moreover, the C-terminal-ONLY mutant exhibits a defect in trafficking and seems to be mislocalised to the early endocytic compartment.

5.5 C-terminal of Nbr1 is constituted of UBA and JUBA both of which are essential for protein localisation

After the importance of Nbr1 C-terminal (P856-Y988) for protein localisation and function was established, this region was subjected to further in detail investigations. The C-terminal of Nbr1 contains a well conserved UBA domain. However, careful analysis the protein sequence also revealed another region of high conservation within the C-terminal that was

located 10 amino acids N-terminal to the UBA domain (Figure 5.7A). Due to its proximity to the UBA domain it was named Juxta-UBA (JUBA). JUBA is only 22 amino acids long and secondary structure prediction by JPRED-3 software [Cole et al., 2008] suggested that it might predominantly have an α-helical fold (Figure 5.7B). Interestingly, projection along the helical axis of the predicted α-helix of JUBA showed a highly amphipathic conformation, with charged or polar amino acids arranged on one side of the helix and the hydrophobic amino acids on the other (Figure 5.7C).

Amphipathic α-helices are found in many proteins that peripherally associate with membrane bilayers. Examples include Epsin, Amphiphysin, endophilin, Arf and Arl proteins [McMahon and Gallop, 2005]. These helices are unfolded until they come into contact with a target lipid membrane where the hydrophobic side is inserted into the bilayer while the polar/charged side remains outside, making ionic contacts with the negatively charged head-groups of membrane lipids such as Phosphatidylinositol-Phosphates (PIPs) [McMahon and Gallop, 2005]. To find out whether JUBA is in fact one of such α-helices, we used Circular-Dichroism (CD) spectroscopy. CD is the difference in absorption of left-handed and right-handed circular polarised light. It could be used as a powerful method to determine the secondary structure of peptides since each secondary structure exhibits unique CD spectra signatures [Conner et al., 2008]. Unfolded peptides give spectra with a single minimum around 200 nm whereas α-helical peptides give a maximum at around 192 nm and two minima at around 208 nm and 222 nm. On the other hand, a beta-sheet conformation results in a single minimum of around 217 nm.

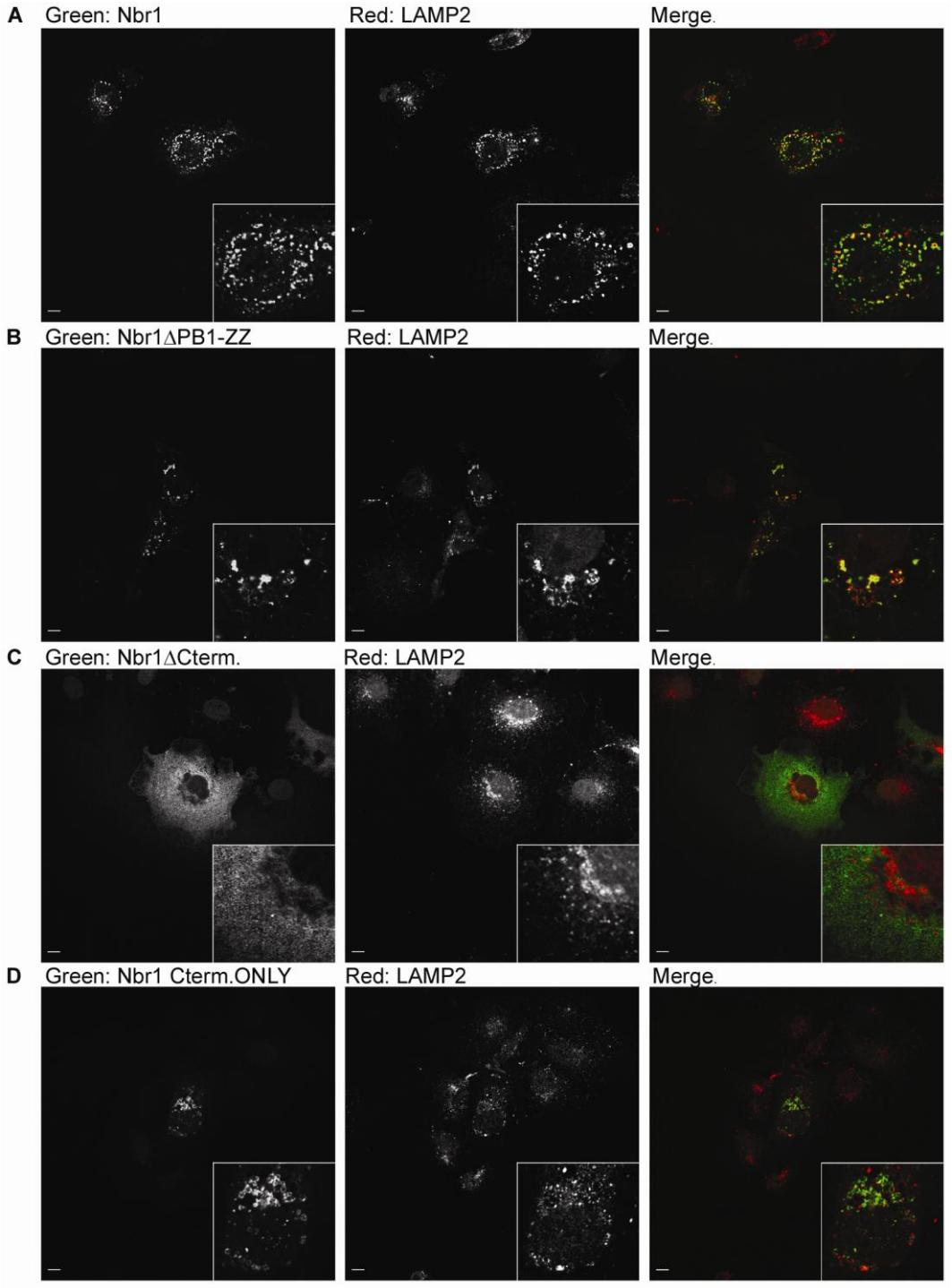

Figure 5.5. C-terminal of Nbr1 is essential but not sufficient for its correct localisation. Scale bars = 10μm. GFP tagged WT or various mutants of Nbr1 were transfected into COS7 cells, before being fixed, immunostained for the late endocytic marker LAMP2, and analysis by confocal microscopy. WT Nbr1 **(A)** as well as Nbr1ΔPB1-ZZ mutant **(B)** colocalise with LAMP2. However, Nbr1ΔCterm. which lacks the last 133 amino acids does not colocalise with LAMP2 and shows a diffuse cytoplasmic distribution **(C)**. Nbr1Cterm.ONLY also does not colocalise with LAMP2 but shows localisation to some enlarged vesicular structures **(D)**.

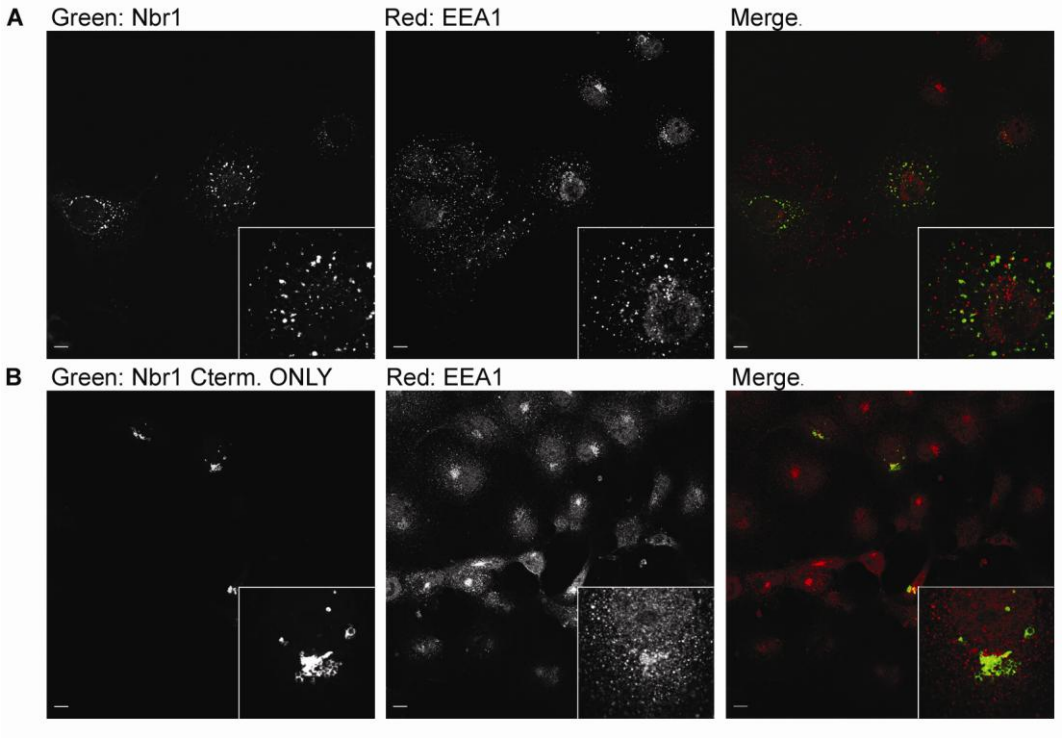

Figure 5.6. C-terminal-ONLY Nbr1 mutant expressing the last 133 amino acids (P856-Y988) is mislocalised to the early endosomes. Scale bars = 10μm. GFP tagged WT Nbr1 or a C-terminal-ONLY mutant (P856-Y988) were transfected into COS7 cells before being fixed, immunostained for the early endocytic marker EEA1, and analysed by confocal microscopy. While WT Nbr1 does not colocalise with EEA1 **(A)**, Nbr1Cterm.ONLY significantly colocalises with EEA1 **(B)**.

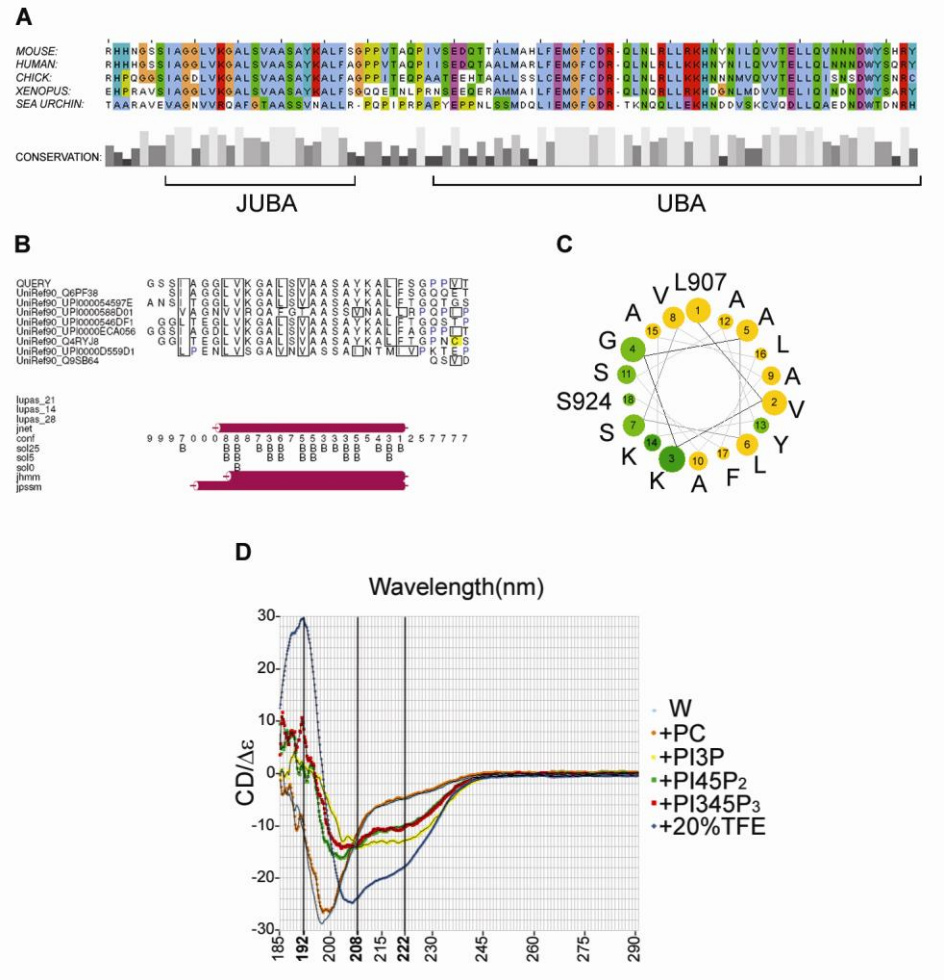

Figure 5.7. C-terminal of Nbr1 contains UBA and JUBA. Cross-species multiple alignment (www.ebi.ac.uk/clustalw) of the C-terminal 93 amino acids of Nbr1 by reveals JUBA, a novel conserved stretch of amino acids next to the UBA domain **(A)**. Output from JPRED-3 secondary structure prediction software (www.compbio.dundee.ac.uk/www-jpred/) [purple cylinder: α-helical; B: buried for solvent accessibility] for the JUBA region suggests it folds into an α-helix **(B)**. Projection along the helical axis of the predicted α-helix of JUBA (L907-S924) suggests it would be amphipathic, with polar (light green) and charged (dark green) amino acids on one side and hydrophobic amino acids (yellow) on the other **(C)**. A peptide corresponding to the predicted α-helix of JUBA was subjected to CD spectroscopy as in materials and methods. The marked 192, 208, and 222 nm peaks are characteristic to α-helices and the 200 nm peak is characteristic of unfolded sequences. The peptide exhibits unfolded CD spectra signatures in water or in presence of Phosphatidylcholine liposomes, and α-helical spectra signatures in presence of various Phosphatidylinositol-Phosphate containing liposomess or the α-helix inducing agent Trifluoroethanol (20%) **(D)**. [light-blue: Water (W); orange: Phosphatidylcholine (PC); yellow: Phosphatidylinositol-3Phosphate (PIP3); dark-blue: 20% Trifluoroethanol (TFE); green: Phosphatidylinositol-4,5Phosphate ($PI45P_2$); red: Phosphatidylinositol-3,4,5Phosphate ($PI345P_3$)].

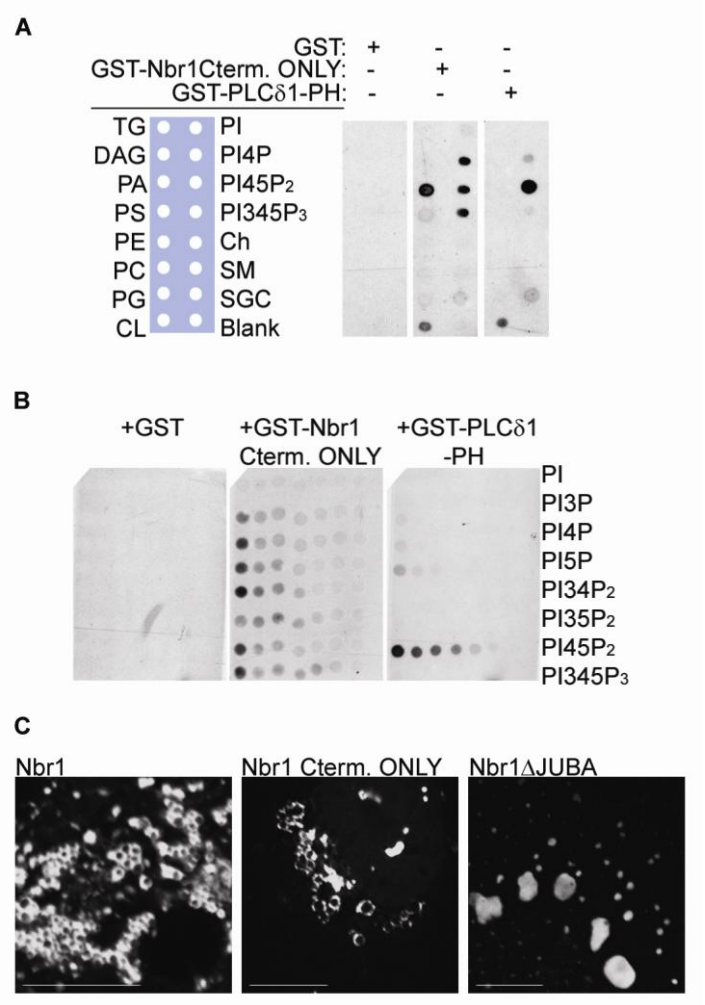

Figure 5.8. C-terminal of Nbr1 interacts with lipids *in vitro*, and binds to the limiting membrane of vesicular structures *in vivo* in a JUBA dependent manner. Membranes pre spotted with 15 different biologically relevant lipids [TG: Triglyceride, DAG: Diacylglycerol, PA: Phosphatidic acid, PS: Phosphatidylserine, PE: Phosphatidylethanolamine, PC: Phosphatidylcholine, PG: Phosphatidylglycerol, CL: Cardiolipin, PI: Phosphatidylinositol, PIxPn: Phosphatidylinositol-xPhosphate, Ch: Cholestrol, SM: Sphingomyelin, SGC: 3-Sulfogalactosylceramide] where incubated with GST alone, GST-Nbr1Cterm.ONLY, or GST-PLCδ1-PH which specifically binds PI-4,5P_2, and the bound proteins were detected by blotting with an anti-GST antibody. C-terminal of Nbr1 associated with all PIPs and PA *in vitro* **(A)**. Membranes pre spotted with increasing amounts of various PIPs [100, 50, 25, 12.5, 6.25, 3.13, and 1.58 pmol] were incubated with GST-Nbr1Cterm.ONLY, GST, or GST-PLCδ1-PH as above and blotted with an anti-GST antibody. C-terminal of Nbr1 did not show specificity to any PIP **(B)**. COS7 cells transfected with GFP-Nbr1, GFP-Nbr1Cterm.ONLY (P856-Y988), or GFP-Nbr1ΔJUBA, were fixed and analysed by confocal microscopy for Nbr1 localisation at high magnification. Scale bars = 10μm. While both WT and the C-terminal-ONLY mutant could associate with vesicular limiting membranes *in vivo*, deletion of JUBA abrogated this membrane association **(C)**.

When a peptide corresponding to the predicted α-helix of JUBA (L907-S924) was subjected to CD spectroscopy, it gave an unfolded signature spectrum in water (Figure 5.7D). Addition of liposomes containing just the background lipid Phosphatidylcholine (PC) did not affect the folding as the spectrum remained unchanged (Figure 5.7D). However, when liposomes containing various PIPs (5% in 95% PC molar percentage) were added to the peptide solution, they all induced an α-helical fold as judged by the disappearance of the ~200 nm minimum as well as the appearance of the ~192 nm maximum and ~208 and ~222 nm minima (Figure 5.7D). Finally, as a positive control the addition of 20% Trifluoroethanol, an α-helix inducing agent, also resulted in induction of an α-helical fold (Figure 5.7D). These results show that as expected for membrane interacting amphipathic α-helices, JUBA is unfolded in aqueous solutions but folds into an α-helix once in contact with PIP containing lipid bilayers. Since every tested PIP could induce an α-helical fold (Figure 5.7D), the results also suggest that JUBA on its own does not have specificity towards a particular PIP.

Having shown that JUBA folds into a membrane interacting α-helix, next it was tested whether the C-terminal of Nbr1 has therefore got lipid binding capacity, *in vitro*. Hydrophobic membrane strips dotted with 15 different physiologically relevant lipids were used in a technique commonly known as fat-blotting. In this method, the membrane is blocked as in immunoblotting, layered with a GST tagged protein of interest, and bound proteins are subsequently detected by immunoblotting with an anti-GST antibody. 1 μg/ml of GST alone or GST tagged proteins were used. While GST on its own did not associate with any of the lipids, GST tagged C-terminal of Nbr1 (P856-Y988) could bind to all present PIPs as well as Phosphatidic acid (PA) (Figure 5.8A). As a positive control we used the GST tagged Pleckstrin Homology domain of PLC-δ1 that specifically binds $PI45P_2$ [Lomasney et al.,

1996], which gave the expected result (Figure 5.8A). Similar to PIPs, PA has a bivalent phosphate in the head-group, suggesting that JUBA might be interacting with such bivalent phosphates. To further confirm that the C-terminal of Nbr1 does not have specificity towards a particular PIP, another fat-blot was performed this time using membranes dotted with increasing concentrations of 7 physiologically relevant PIPs. Again, GST alone was used as a negative control, which did not bind to any lipids while GST tagged C-terminal of Nbr1 (P856-Y988) could associated with all PIPs without a significant preference to any particular one (Figure 5.8B). As a positive control GST-PLC-δ1-PH was used again, which only bound $PI45P_2$ (Figure 5.8B). These results confirm that, *in vitro*, the C-terminal of Nbr1 can bind to PIPs without exhibiting any specificity towards a particular one.

Nbr1 specifically localises to vesicular limiting membranes, *in vivo*, and as shown earlier this localisation depends on the C-terminal of the protein (Figure 5.5C and 5.5D). To determine whether *in vivo* vesicular membrane association specifically depends on JUBA, we compared the localisations of full-length and C-terminal-ONLY Nbr1 (P856-Y988) mutant with that of a JUBA deleted mutant. COS7 cells transfected with GFP-Nbr1, GFP-Nbr1Cterm.ONLY, or GFP-Nbr1ΔJUBA, were fixed and analysed by confocal microscopy for Nbr1 localisation. As before, full-length Nbr1 was found to specifically localise to the limiting membrane of vesicular structures *in vivo* (Figure 5.8C). Similarly, the C-terminal-ONLY mutant (P856-Y988) exhibited localisation to the vesicular limiting membranes, although as mentioned earlier the vesicles were relatively enlarged compared to those of full-length (Figure 5.8C). However, the JUBA deleted Nbr1 showed no localisation to vesicular limiting membranes and instead exhibited an aggregate-like localisation (Figure 5.8C). These results reveal that JUBA is essential for Nbr1 *in vivo* association with vesicular limiting membranes.

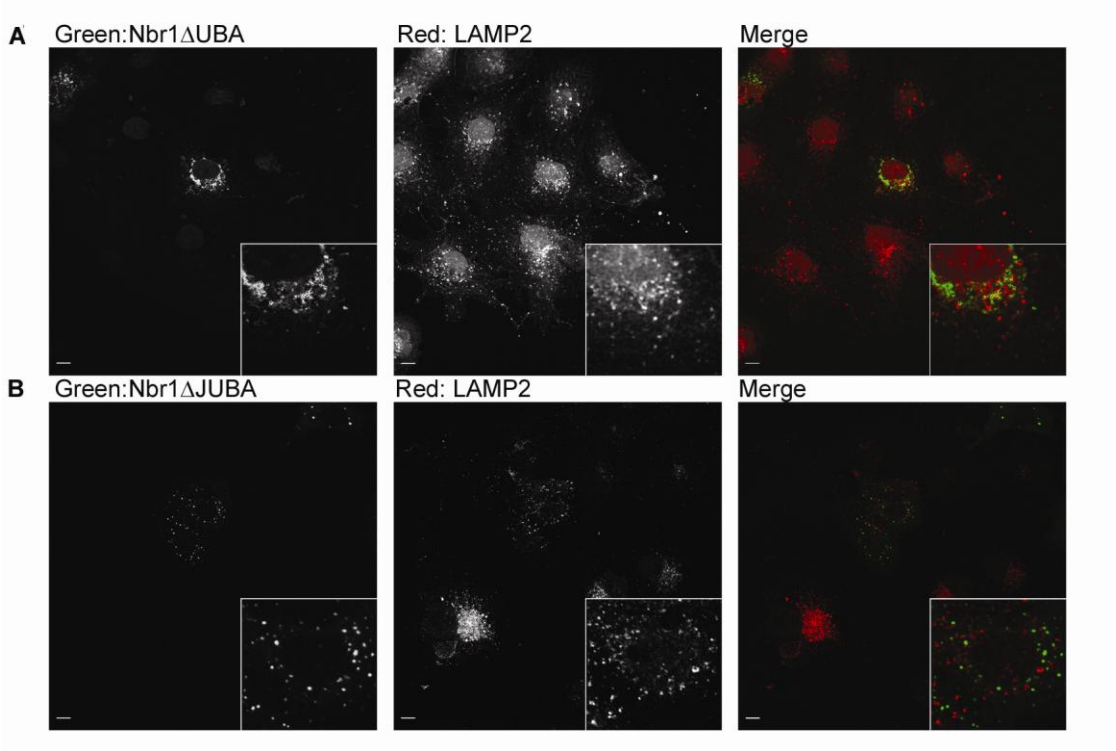

Figure 5.9. Both JUBA and UBA are necessary for late endocytic localisation of Nbr1. COS7 cells were transfected with GFP-Nbr1ΔUBA, fixed, immunostained for LAMP2, and analysed by confocal microscopy. Scale bars = 10μm. Deletion of UBA domain abrogated Nbr1 colocalisation with LAMP2 **(A)**. COS7 cells were transfected with GFP-Nbr1ΔJUBA, fixed, immunostained for LAMP2, and analysed by confocal microscopy. Deletion of JUBA also abrogated Nbr1 colocalisation with LAMP2 **(B)**.

Finally, having established that the C-terminal of Nbr1 consists of UBA and JUBA, and that JUBA is an amphipathic membrane interacting α-helix which targets Nbr1 to vesicular limiting membranes, the contribution of each of the two C-terminal regions to the late endosomal localisation of Nbr1 was determined using confocal microscopy. COS7 cells were used and GFP tagged UBA or JUBA deleted mutants of Nbr1 were transfected into the cells, followed by fixing and immunostaining the cells with the late endocytic marker LAMP2. Deletion of Nbr1 UBA domain resulted in loss of colocalisation with LAMP2 (Figure 5.9A). Similarly, deletion of JUBA resulted in loss the colocalisation (Figure 5.9B). Interestingly, the effect of loss of both regions together (Figure 5.5C) is more dramatic than that of each one individually, suggesting that the two regions cooperate to localise Nbr1.

5.6 Late endocytic localisation of Nbr1 is LIR independent

Nbr1 contains two LIRs which can bind to LC3 and target Nbr1 to autophagosomes [Kirkin et al., 2009]. As the C-terminal-ONLY (P856-Y988) Nbr1 mutant that lacks both LIRs cannot correctly localise to late endosomes (Figure 5.5D), it was asked whether association with autophagosomes via LIRs is another important factor for the late endocytic localisation of Nbr1. This is a possibility since autophagosomes commonly fuse with early or late endosomes on their route towards lysosomal degradation [Simonsen and Tooze, 2009]. The main LIR is located close to the C-terminal of the protein (V739-E779) and contains a pivotal Tyrosine (Y750), mutation of which abrogates its interaction with LC3 [Kirkin et al., 2009]. The second LIR (LIR2) is located further N-terminal (A543-P634) and can compensate for the loss of main LIR [Kirkin et al., 2009]. Two GFP tagged Nbr1 mutants were tested for their ability to colocalise with the late endocytic marker LAMP2 in COS7 cells. First one was an

N-terminal truncation mutant of Nbr1 expressing residues C-terminal to G694 (Nbr1 G694>), therefore lacking all the N-terminal domains as well as LIR2 while containing the main LIR. This mutant could still colocalise with LAMP2 (Figure 5.10A), suggesting that loss of LIR2 alone does not have an effect on Nbr1 localisation. Next, the pivotal Tyrosine in the main LIR (Y750) was also mutated. Surprisingly, despite loss of both LIRs this mutant (Nbr1 G694> Y750A) could still colocalise with LAMP2 (Figure 5.10B). To confirm that LC3 interaction and autophagosomal association was lost for this double LIR mutant, a 293A cell-line stably expressing GFP tagged LC3 was used [Chan et al., 2007]. In these cells GFP-LC3 has a diffuse distribution under normal conditions. However, after induction of autophagy, or blockage of autophagosomal clearance, it accumulates in cytoplasmic punctae representative of autophagosomes [Chan et al., 2007]. The cells were transfected with myc tagged full-length, Nbr1 G694>, and Nbr1 G694> Y750A mutants before being treated with 200 nM BafA for 4 hours to accumulate autophagosomes. While both full-length and the Nbr1 G694> mutant colocalised with LC3 punctae (Figure 5.11A and 5.11B), Nbr1 G694> Y750A mutant did not (Figure 5.11C), confirming that it had lost its ability to associate with autophagosomes.

These results reveal that the late endocytic localisation of Nbr1 is independent of its autophagosomal localisation. Interestingly, in the same experimental setup it was also observed that the C-terminal of Nbr1 (P856-Y988), which is crucial for the late endocytic localisation of the protein, is not needed for autophagosomal localisation (Figure 5.11D). This result suggests that the late endocytic and autophagic localisations of Nbr1 are independent of one another: Autophagic localisation of Nbr1 requires at least one LIR but not the C-terminal of the protein while the late endocytic localisation requires the C-terminal but not any of the LIRs.

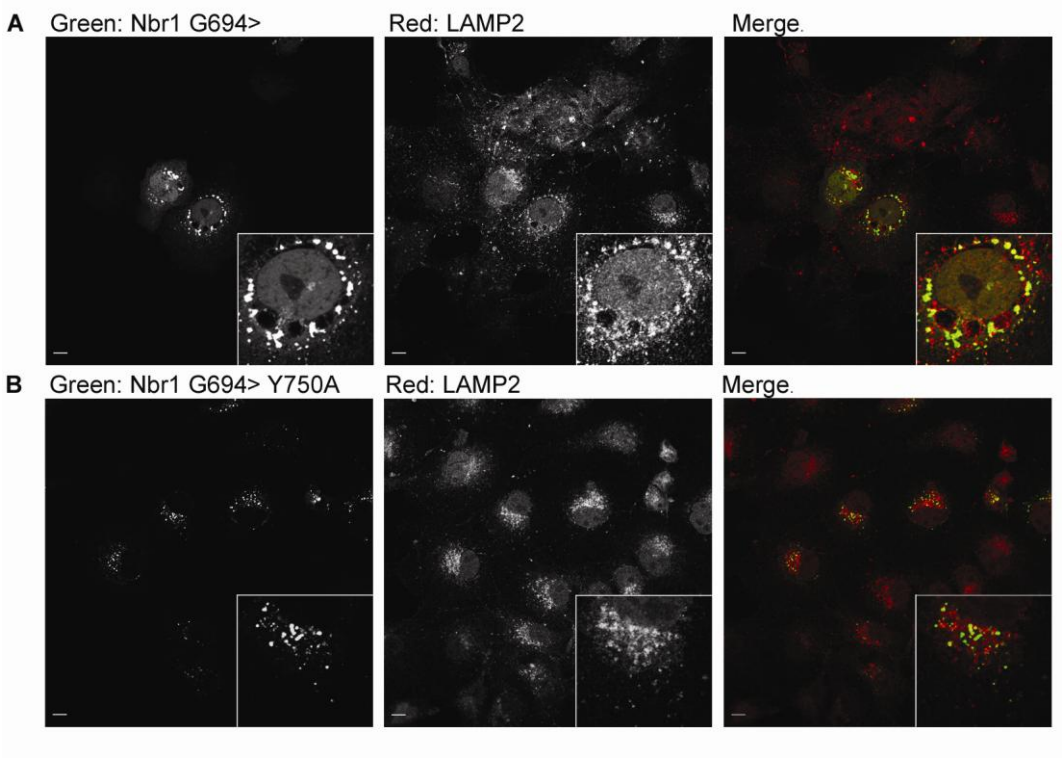

Figure 5.10. Late endocytic localisation of Nbr1 is independent of LIRs. Scale bars = 10μm. COS7 Cells were transfected with GFP-Nbr1G694> which lacks LIR2. The cells were fixed, immunostained for LAMP2, and analysed by confocal microscopy. GFP-Nbr1G694> could colocalise with LAMP2 **(A)**. COS7 Cells were transfected with GFP-Nbr1G694>Y750A which lacks both functional LIRs. The cells were fixed, immunostained for LAMP2, and analysed by confocal microscopy. Nbr1G694>Y750A could similarly colocalise with LAMP2 **(B)**.

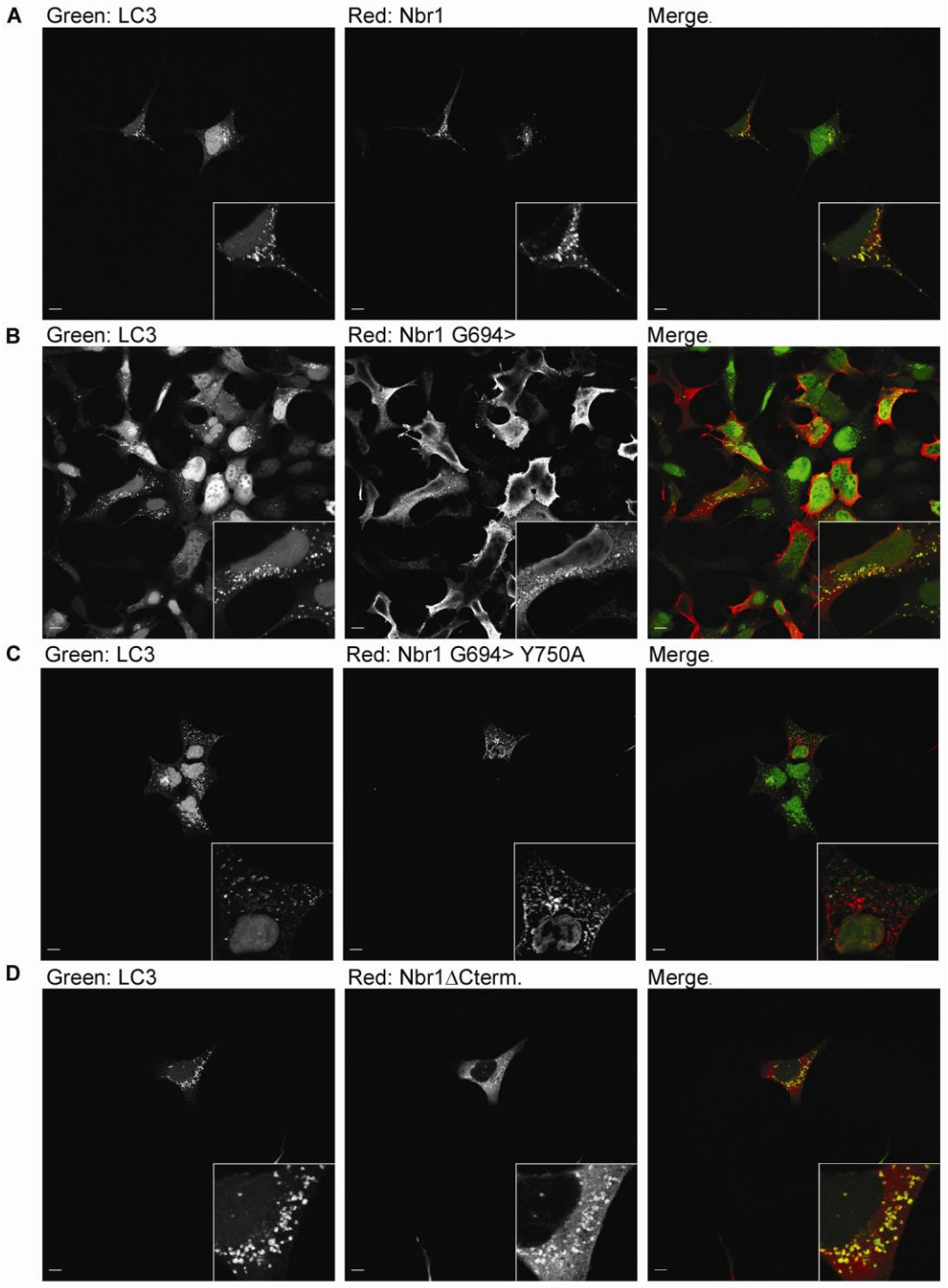

Figure 5.11. Colocalisation of Nbr1 with accumulated autophagosomes depends on LIR but not the C-terminal. Scale bars = 10μm. 293A cells stably expressing GFP-LC3 were transfected with WT or different Nbr1 mutants. The cells were treated with 200nM BafA for 4hrs to accumulate autophagosomes before being fixed, immunostained for myc, and analysed by confocal microscopy for colocalisation with LC3. WT Nbr1 **(A)** and Nbr1G694> mutant lacking LIR2 **(B)** both colocalise with LC3 while Nbr1G694>Y750A mutant lacking both functional LIRs does not **(C)**. Nbr1ΔCterm. mutant lacking the last 133 amino acids (P856-Y988) also colocalises with LC3 **(D)**.

5.7 Nbr1 neither induces nor inhibits the autophagy machinery

As mentioned earlier, 293 GFP-LC3 cells display a diffuse GFP distribution under normal conditions, but after induction of autophagy or blockage of autophagosomal clearance GFP-LC3 accumulates in cytoplasmic punctae representative of autophagosomes (Figure 5.12A and 5.12B) [Chan et al., 2007]. Surprisingly, whilst investigating myc tagged Nbr1 localisation in 293 GFP-LC3 cells, it was realised that over-expression of Nbr1 on its own was leading to induction of a punctate LC3 distribution pattern even before BafA treatment of the cells (Figure 5.12C). This suggested that Nbr1 over-expression could be inducing autophagosome accumulation. However, a key requirement of autophagy is cleavage and lipidation of LC3, so detection of a punctate cytoplasmic LC3 distribution is not sufficient to deduce true autophagosome accumulation [Klionsky, et al., 2008]. The cleavage of GFP-LC3 was therefore investigated by immunoblotting, using an anti-GFP antibody.

293 GFP-LC3 cells treated with a time-course of 200 nM BafA gradually accumulate cleaved GFP-LC3 (GFP-LC3II) protein, which is detected as a lower MW band under uncleaved GFP-LC3 (GFP-LC3I) (Figure 5.13A). This is indicative of autophagosome accumulation due to their blockage of lysosomal degradation. However, 293 GFP-LC3 cells treated with a time-course of 50 μg/ml Rapamycin, which induces autophagy without blocking lysosomal clearance, concomitantly accumulate GFP alone (Figure 5.13A). This is due to the fact that LC3II is highly acid labile while GFP is relatively resistant to low pH, so after autophagosomal acidification by lysosomal fusion the LC3II part of the GFP-LC3II is rapidly degraded while the GFP part remains stable for some time [Klionsky, et al., 2008]. Due to this difference one can also differentiate between induction of autophagy or blockage of its lysosomal clearance [Klionsky, et al., 2008]. When the effect of Nbr1 over-expression in 293 GFP-LC3 cells was investigated by immunoblotting with an anti-GFP antibody, neither GFP-

LC3II nor GFP alone was found to be accumulated after a time-course of 6 hours (Figure 5.13A). A constitutive 24 hour over-expression of Nbr1 also did not accumulate either corresponding bands (Figure 5.13B). These results suggest that the observed punctate GFP-LC3 staining in 293 GFP-LC3 stable cells after Nbr1 over-expression must be an artefact of LC3 mis-localisation to Nbr1 vesicles and not the result of true autophagosomal accumulation (Figure 5.12C). Nbr1 over-expression, therefore, neither induces autophagy nor blocks autophagosomal clearance.

Next, the possibility that Nbr1 might be blocking the autophagy machinery due to mis-localisation of LC3 was investigated. Normal 293T cells were used, as higher LC3 expression levels in 293 GFP-LC3 stable cells could override Nbr1 over-expression effects. An LC3 antibody which just detects LC3II was utilised. The cells were transfected with myc tagged Nbr1 or GFP as control and treated with a time-course of 200 nM BafA to accumulate autophagosomes. No difference was observed between control transfected and myc-Nbr1 transfected cells in the level of LC3II accumulation, suggesting that Nbr1 over-expression was not blocking autophagy induction (Figure 5.13C). A C-terminal-ONLY mutant was also investigated, which gave similar results (Figure 5.13C). Finally, the effect of Nbr1 depletion on accumulation of endogenous LC3II was also investigated. 293T cells were transfected with non-silencing control or two independent NBR1 siRNAs (100 pmol) for 48 hours with transfection being renewed after 24 hours. The cells were then treated with 200 nM BafA or for 4 hours or left untreated for the same period of time, before being analysed by immunoblotting with LC3II antibody. No significant difference in the levels of LC3II was observed between control or NBR1 knockdown cells before or after BafA treatment (Figure 5.13D). Collectively, these results suggest that Nbr1 neither induces nor inhibits autophagy.

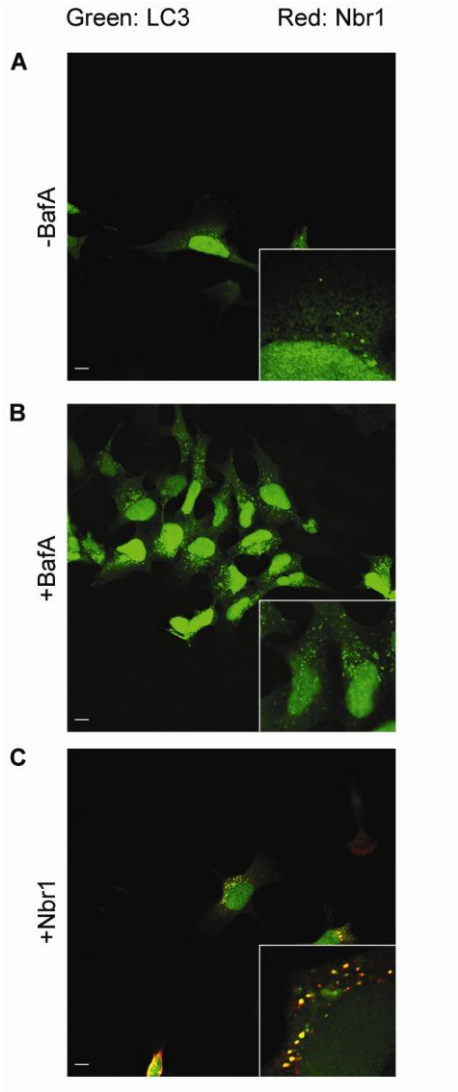

Figure 5.12. Over-expression of Nbr1 leads to punctate GFP-LC3 distribution. Scale bars = 10μm. 293A cells stably expressing GFP-LC3 were left untreated **(A)**, treated with 200nM BafA for 4hrs to accumulate autophagosomes **(B)**, or transfected with myc-Nbr1 for 24 hours **(C)**, before being fixed, immunostained for myc, and analysed by confocal microscopy.

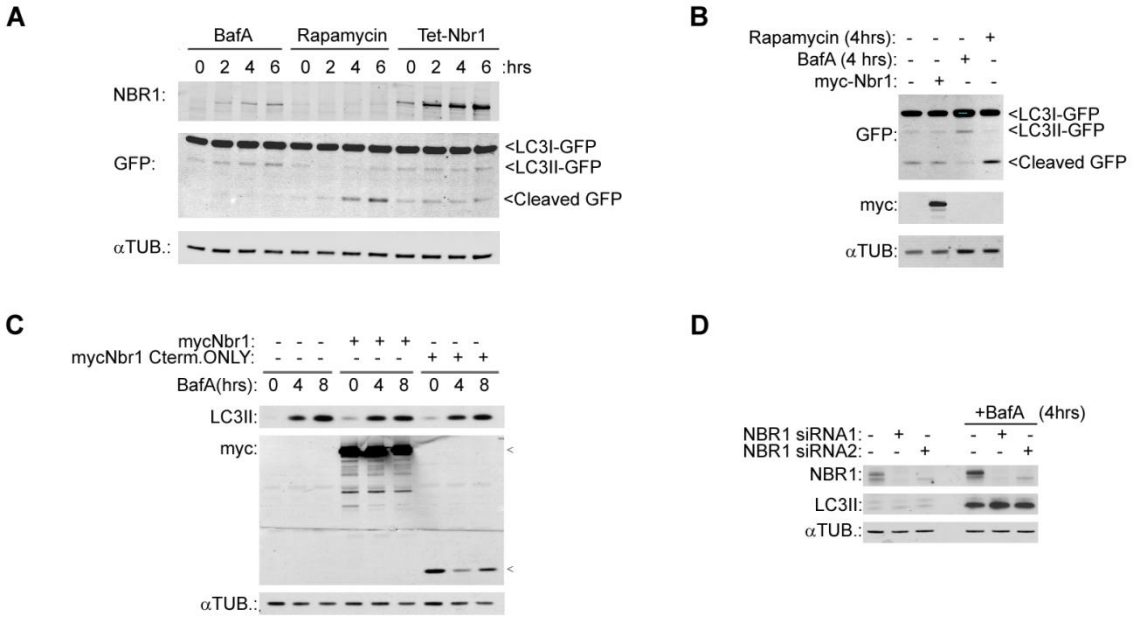

Figure 5.13. Nbr1 does neither induce nor block autophagy. 293A cells stably expressing GFP-LC3 were transfected with constructs for Tet inducible Nbr1 as well as Tet-Repressor (TR). The ratio of Nbr1 to TR was 1:6 to insure every Nbr1 expressing cell also expresses TR. The cells were treated for a time-course of 6 hours with BafA (200 nM) to block autophagosomal clearance, Rapamycin (50 μg/ml) to induce autophagy formation, or Tetracycline (1 μg/ml) to induce Nbr1 expression. Cells were analysed by immunoblotting using indicated antibodies. Nbr1 expression does not mimic either BafA or Rapamycin effects **(A).** 293A cells stably expressing GFP-LC3 were transfected with myc-Nbr1 or left untransfected as control. The control cells were left untreated, treated with BafA (200 nM), or with Rapamycin (50 μg/ml), before analysis by immunoblotting using indicated antibodies. Myc-Nbr1 expression does not mimic either BafA or Rapamycin effects **(B).** 293T cells were transfected with myc-Nbr1, myc-Nbr1DCterm.ONLY or GFP as control. Cells were treated with z-VAD-FMK (50 μM) to block death by apoptosis, before being subjected to a time-course of BafA (200 nM). Cells were subsequently analysed by immunoblotting with indicated antibodies. Nbr1 expression does not block BafA induced LC3II accumulation **(C)**. 293T cells were transfected with 100 pmol of Non-Silencing Control (NSC) or NBR1 siRNAs (siRNA1 and 2) for 48 hours with the transfection being renewed after 24 hours. Cells were left untreated or treated with BafA (200 nM) for 4 hours before analysis by immunoblotting with indicated antibodies. NBR1 knockdown does not affect LC3II levels before or after BafA treatment **(D)**.

5.8 Prolonged loss of NBR1 or expression of a C-terminal-Only Nbr1 mutant induces cell death by apoptosis

Finally, the issue of cell death by C-terminal-ONLY Nbr1 (P856-Y988) mutant was addressed. As mentioned earlier, it was observed that expression of this mutant induced cell death. To determine whether the underlying cause of cell death was apoptosis, 293T cells were transfected for various times with myc- Nbr1Cterm.ONLY or GFP as control and analysed by immunoblotting for specific apoptotic markers such as cleaved PARP and cleaved activated CASPASE-9 (Figure 5.14A). Furthermore, cell death after myc-Nbr1Cterm.ONLY transfection could be inhibited by treating the cells with increasing concentrations of the general Caspase inhibitor z-VAD-FMK (Figure 5.14B), confirming a caspase mediated apoptotic cell death as the underlying cause of lethality. Interestingly, while optimising siRNA mediated knockdown of NBR1 in 293T cells, it was also found that prolonged depletion of NBR1 could result in a similar induction of cell death by apoptosis (Figure 5.14C). Since expression of a deletion mutant seems to mimic the phenotype of loss of NBR1, the mutant is likely acting as a dominant-negative. Moreover, the lethality of NBR1 loss suggests that the protein must have some vital cellular functions which can also be disrupted by the C-terminal-ONLY mutant. It should be noted that while apoptosis by C-terminal-ONLY mutant was induced relatively quickly (Figure 5.14A), apoptosis due to depletion of NBR1 was only detected after 72 hours of siRNA treatment with the transfection being renewed every 24 hours (Figure 5.14C). As knockdown generally improves with the time and the number of transfections, the most likely explanation is that depletion of NBR1 by siRNA at earlier time-points is simply insufficient for complete removal of NBR1. In contrast, interference of a dominant negative mutant with endogenous NBR1 function can occur rapidly.

5.9 Apoptotic cell death by C-terminal-ONLY Nbr1 mutant is LIR independent

To map the region of Nbr1 the loss of which was causing a dominant negative phenotype in C-terminal-ONLY (P856-Y988) mutant, serial N-terminal deletions of Nbr1 were generated and tested for their ability to induce cell death (Figure 5.15A). 293T cells transfected with myc tagged full-length Nbr1, myc tagged serial deletion mutants, or GFP as control were analysed by immunoblotting for induction of apoptosis. Only P856-Y988 and S895-Y988 mutants could induce cell death by apoptosis, suggesting that deletion of G694-P856 must be crucial for induction of cell death (Figure 5.15A). Since the main LIR is located within the G694-P856 region of Nbr1, it was a possibility that loss of LC3 interaction might be the underlying cause of death by apoptosis. However, no cell death was noticed when mutants lacking one or both functional LIRs were being investigated earlier (Figure 5.11). To confirm this, myc tagged mutants of Nbr1 lacking one or both functional LIR, along with full-length Nbr1 and the C-terminal-ONLY (P856-Y988) mutant were transfected into 293T cells. Cells were analysed for induction of apoptosis by immunoblotting as before. Unlike for the C-terminal-ONLY mutant, no cell death could be detected for the single or double LIR mutants as well as full-length (Figure 5.15B). This confirms that the lethality of the C-terminal-ONLY mutant is not due to the loss of LIRs and therefore LC3 binding. Thus, loss of another region within G694-P856 must be the underlying cause dominant negativity and induction of cell death by apoptosis. The identity of this region remains to be determined. Having ruled out LIRs and therefore an autophagy related function, it also remains to be determined whether the vital function of Nbr1 is related to its role in regulation of RTK trafficking, or whether there are other crucial functions for NBR1 which are currently unknown.

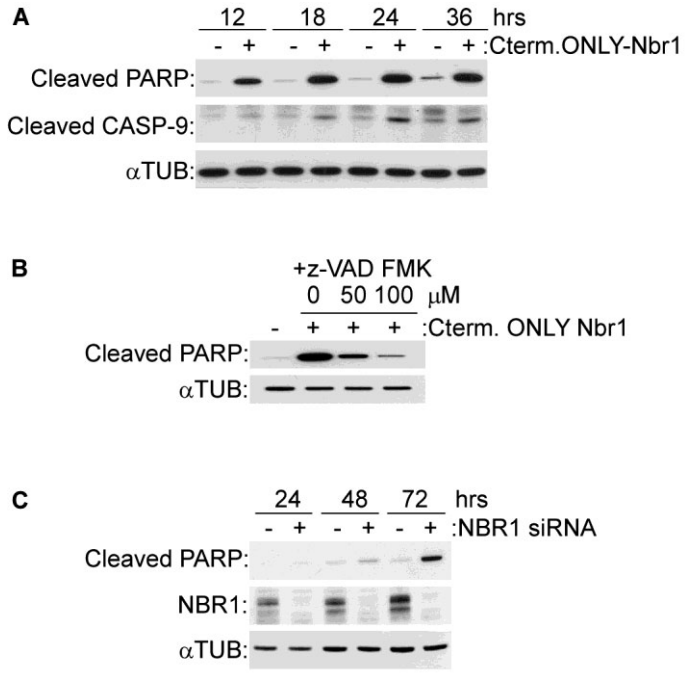

Figure 5.14. A C-terminal-ONLY (P856-Y988) Nbr1 mutant induces cell death by apoptosis which mimics loss of NBR1. 293T cells were transfected with myc-Nbr1Cterm.ONLY or GFP as control for indicated times. Cells were lysed and analysed by immunoblotting with indicated antibodies. Nbr1Cterm.ONLY induces cell death by apoptosis **(A)**. 293T cells transfected with myc-Nbr1Cterm.ONLY or GFP as control were treated with increasing concentrations of z-VAD-FMK. PARP cleavage induced by C-terminal-ONLY Nbr1 mutant is inhibited by z-VAD-FMK **(B)**. 293T cells were transfected by 100pmol NBR1 or non-silencing control (NSC) siRNAs for 24, 48, or 72 hours with transfection being renewed every 24 hours. Cells were lysed and analysed by immunoblotting with indicated antibodies. Prolonged knockdown of NBR1 also induces cell death by apoptosis.

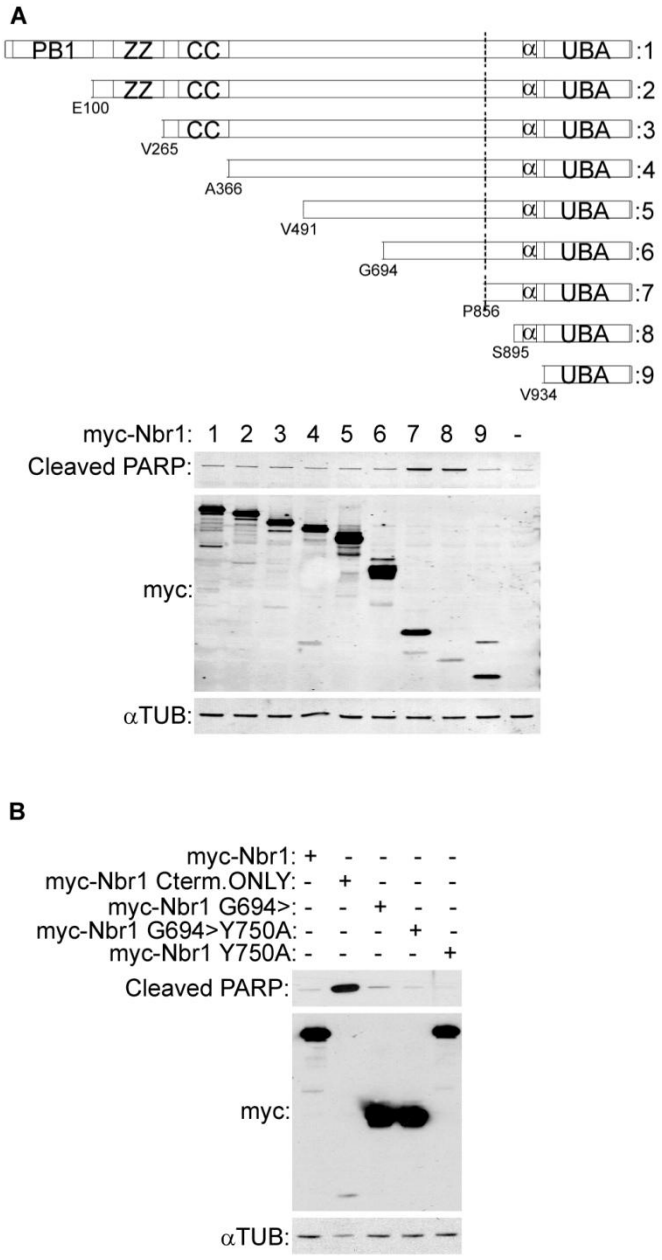

Figure 5.15. Apoptotic cell death by C-terminal-ONLY Nbr1 mutant is due to lack of G694-P856 amino acids but independent of LIRs. 293T cells were transfected with myc tagged WT or the indicated serial deletions (TOP) as well as GFP as control before being analysed by immunoblotting for indicated antibodies (BOTTOM). Loss of G694-P856 amino acids results in the C-terminal-ONLY induced cell death by apoptosis **(A)**. 293T cells were transfected with myc tagged full-length Nbr1 (myc-Nbr1), C-terminal-ONLY Nbr1 (myc-Nbr1 Cterm.ONLY), a truncated Nbr1 mutant from G694 which lacks LIR2 (myc-Nbr1 G694>), and this truncated mutant with the additional point mutation in the main LIR (myc-Nbr1 G694> Y750A), as well as a full length Nbr1 with just the point mutation in the main LIR (myc-Nbr1 Y750A). Cells were lysed and analysed by immunoblotting for indicated antibodies. Cell death by the C-terminal-ONLY Nbr1 mutant is not due lack of one or both LIRs **(B)**.

5.10 Identification of novel C-terminal specific Nbr1 binding partners by SILAC

To gain insight into Nbr1 mechanism of action on RTK trafficking, as well as to identify potential new functions for the protein, quantitative mass spectrometry by SILAC was used. Given the demonstrated importance of Nbr1 C-terminal 133 amino acids (P856-Y988) for its role in RTK trafficking as well as its dominant negative lethality, the specific binding partners of this region were determined by quantitative comparison of identified proteins in immunoprecipitates of Full-length myc-Nbr1 versus that of myc-Nbr1ΔCterm which lacks the last 133 amino acids. To do this, a large dish of heavy (K+6, R+10) or light labelled 293T cells were transfected with myc-Nbr1 or myc-Nbr1ΔCterm., respectively. After cell lysis, equal amounts of the heavy (H) and light (L) labelled lysates were mixed and subjected to immunoprecipitation by an anti-myc antibody for 1 hour. The immunoprecipitation time was kept at minimum to reduce swapping of proteins between heavy and light complexes [Wang and Huang, 2008]. The proteins were subsequently run on an SDS-gel, Trypsin digested, and analysed by FTICR-TRAP mass spectrometry. Data analysis and quantification was carried out by MaxQuant, a powerful software specifically designed for SILAC data analysis [Cox and Mann, 2008]. To insure a low false positive rate and a high degree of significance in quantifications, the results were filtered for the presence of at least 3 quantifiable peptides per protein hit. A total of 111 proteins were identified, and false positive rate of 0.9% was estimated by searching the data against a reverse database and calculating the ratio of the number of hits from the reverse search to that of the forward search. An adjusted Heavy to Light (H/L) ratio of 0.475 was determined by MaxQuant for Nbr1 itself, suggestive of a difference in the expression levels of full-length and the C-terminal deleted mutant. When the ratios were further normalised to this value, of the total 111 proteins identified 15 were found

to be at least three fold enriched in the full-length immunoprecipitate, suggesting that they could be preferentially associated with the C-terminal of Nbr1 (Table 5).

Protein Name	Protein ID	Adjusted H/L Ratio	Adjusted H/L Ratio / Nbr1 Ratio	Ratio Count
Heterogeneous nuclear ribonucleoprotein U-like protein 1	HNRNPUL1	10.697	22.520	10
Heat shock 110 kDa protein	HSP110	9.377	19.741	3
Ewing sarcoma breakpoint region 1	EWSR1	8.177	17.215	4
KH type-splicing regulatory protein	KHSRP	7.682	16.173	3
Heat shock 70 kDa protein 4	HSPA4	6.792	14.299	5
Nucampholin homolog	NCM	5.035	10.600	3
Ribosomal RNA upstream binding transcription factor	UBTF	4.283	9.017	7
Ubiquitin	UBC	4.010	8.442	10
Bromodomain-containing protein 2	BRD2	3.469	7.303	4
Pinin	PNN	3.262	6.867	12
Heat shock protein HSP 90-α	HSP90AA1	2.692	5.667	3
60S ribosomal protein L10a	RPL10A	1.652	3.478	3
Protein transport protein Sec16A	SEC16A	1.447	3.046	14
Trinucleotide repeat-containing gene 6B protein	TNRC6B	1.436	3.023	13

Table 5. List of the identified proteins with at least three fold enrichment relative to Nbr1 in full-length (H) versus ΔC-term. (L) immunoprecipitates. Quantification was performed using MaxQuant software. **Adjusted Heavy to Light (H/L) ratio** was calculated by the software. This was then divided by the calculated ratio for Nbr1 to determine the **Adjusted H/L Ratio / Nbr1 Ratio**. The **Ratio count** is the number of independent quantified peptides. [Yellow highlight: RNA binding/metabolism; Red highlight: Trafficking; Grey highlight: Ubiquitin].

Amongst the listed proteins (Table 5), a significant number have RNA binding capabilities or have been shown to be involved in RNA metabolism (Table 5-Yellow highlighted). Ubiquitin is also amongst the enriched proteins (Table 5-Grey highlighted) which is not surprising as the UBA domain is located within the C-terminal. Furthermore, a trafficking protein known as SEC16A which is part of the COPII coat protein complex is also amongst the enriched hits (Table 5-Red highlighted). A number of Heat shock proteins which are molecular chaperones were also found amongst the enriched hits (Table 5), which might be suggestive of folding complications for the C-terminal of Nbr1. Amongst the known binding partners of Nbr1, P62 was identified. However, as expected form the fact that it binds to the N-terminal PB1 domain, P62 to Nbr1 ratio was around 1 and was therefore not reported.

5.11 Conclusions

The evidence presented in this chapter Nbr1 as an inhibitor of ligand mediated RTK degradation. As shown in Figure 5.4, the C-terminal 133 amino acids of Nbr1 are essential for this activity (Figure 5.4A and 5.4B). Interestingly in chapter four it was demonstrated that the same region of Nbr1 also binds to Spred2, and that this binding is essential for Spred2 mediated down-regulation of ERK1/2 signalling by targeting the activated receptors to the lysosomal degradation pathway. As Nbr1 inhibits receptor degradation and consequently leads to enhancement of downstream ERK1/2 signalling (Figure 5.1A and 5.1B), it is possible that Spred2 binding to the critical C-terminal of Nbr1 could be interfering with its activity. Alternatively, Spred2 binding could be altering Nbr1 function from an inhibitor to an enhancer of RTK degradation. This is supported by the fact that while NBR1 does not have a negative impact on ERK1/2 signalling on its own, its co-expression with Spred2 results in a

synergistic inhibition of ERK1/2 (Figure 4.10B), suggestive of a cooperative rather than an antagonistic mechanism of functional interaction. Figure 5.4 results also suggest that within Nbr1 further regions of functional significance other than the C-terminal must exist as a C-terminal-ONLY mutant on its own is not sufficient to block RTK degradation (Figure 5.4C and 5.4D). The identity of such regions remains to be determined.

The results presented in this chapter also show correlation between the late endocytic localisation of Nbr1 and its function in the context of RTK degradation, suggesting that this localisation must be important for the protein function (Figures 5.4 and 5.5). The N-terminal PB1, and ZZ domains (Figure 5.5B) as well as the two LIR regions (Figure 5.10) of Nbr1 are dispensable for the late endocytic localisation of the protein. Moreover, the autophagosomal localisation of Nbr1 does not require the C-terminal of the protein and seems to be solely dependent on the presence of LIRs (Figure 5.11). The fact that late endocytic and autophagic localisations of Nbr1 are independent of each other suggests that the function of the protein in each context might be independent of the other, too. This is not surprising as association of Nbr1 with LC3 seems to primary result in its removal from the cytoplasm and degradation via the autophagosomal pathway [Kirkin et al., 2009]. It is proposed that along with its own degradation by autophagy, Nbr1 could bring other cargos - mainly ubiquitinated proteins - to autophagosomes for degradation [Kirkin et al., 2009]. In line with the above hypothesis, knockdown or over-expression of Nbr1 does not affect the autophagy machinery (Figure 5.13), ruling out a mechanistic involvement at the level induction or maturation of autophagosomes.

In chapter four it was shown that NBR1 specifically localises to the endosomal limiting membranes (Figure 4.3C). However, the mechanism of NBR1 membrane association was unknown. Here it was shown that the C-terminal of Nbr1 contains a well conserved

membrane interacting amphipathic α-helix named JUBA (Figure 5.7). JUBA is crucial for Nbr1 association to endosomal limiting membranes (Figure 5.8), and both UBA and JUBA are essential for the late endocytic localisation of Nbr1 (Figure 5.9). Since such amphipathic α-helices get inserted into the lipid bilayer, they have been proposed to act as curvature inducing modules, bending the target membranes that they interact with [McMahon and Gallop, 2005]. Whether such function is part of Nbr1 role in the context of RTK trafficking is an intriguing possibility. It has also been suggested that amphipathic α-helices could act as curvature sensors, as thermodynamically they might be only capable of inserting themselves into membranes with the right degree of curvature [McMahon and Gallop, 2005]. In this scenario, JUBA could simply be acting as a curvature sensor, thereby providing further specificity with regard to the targeting of Nbr1. Interestingly, despite numerous similarities at the level of domain architecture between Nbr1 and P62, JUBA seems to be a unique feature of Nbr1 and a similar region cannot be found in P62.

The mechanism by which Nbr1 abrogates ligand mediated RTK degradation is not clear at the moment. However, as mentioned in the introduction to this chapter, a number of other proteins which have roles in vesicular trafficking have been reported to interact with Nbr1. It would be interesting to see if Nbr1 abrogation of RTK degradation depends on any of these interactions. In particular, USP8 is interesting as the phenotype of Nbr1 expression (Figure 5.1A and 5.1B) seems to mimic that of USP8 loss [Row et al., 2006; Alwan and van Leeuwen, 2006], which could be suggestive of a functional relationship. It remains to be determined if this or any of the other known interacting partners of Nbr1 are involved in its effect on RTK trafficking.

Finally, the results of this chapter suggest that NBR1 must have a vital function the loss of which results in cell death by apoptosis (Figure 5.14C). Intriguingly, expression of a C-terminal-ONLY Nbr1 mutant can mimic this lethality (Figure 5.14A), suggestive of a dominant negative mode of action. Results of Figure 5.15 point to the loss of a region within G694-P856 amino acids as key for this dominant negative activity (Figure 5.15A). However, the responsible region appears to be unrelated to the main LIR which is also located within G694-P856 amino acids. In fact, loss of one or both LIRs does not induce any detectable apoptosis (Figure 5.15B), suggesting against an autophagy related role as the vital function of Nbr1.

Whether regulation of RTK trafficking by Nbr1 is a vital function is an interesting possibility. However, it is also possible that other unknown Nbr1 dependent cellular activities exist the loss of which can cause lethality by apoptosis. The here reported proteins identified by SILAC mass spectrometry analysis of Nbr1 C-terminal specific binding partners could be potentially revealing such novel functions (Table 5). SEC16A is one of these proteins with a role in ER to Golgi trafficking [Watson et al., 2006; Bhattacharyya and Glick, 2007]. Interestingly, as mentioned in the introduction to this chapter, another protein reported to interact with Nbr1 is also involved in ER/Golgi trafficking (Tmp21) [Jenne et al., 2002; Wang et al., 2010]. This implies a potential role in the early secretory pathway for Nbr1. Furthermore, presence of a number of RNA binding proteins as well as proteins involved in different RNA related processes suggests a potential role for Nbr1 in RNA metabolism. However, it is also possible that these proteins simply associate with the mRNA translation machinery, and since the full-length Nbr1 is longer than the C-terminal deleted mutant, more of them tend to be associated with the full-length protein during the process of protein synthesis. Future studies should reveal if there really is a role in the early secretory pathway

or RNA metabolism for Nbr1, and whether such roles are vital for cell survival. It also needs to be established if the lethality due to the loss of NBR1 is cell-type specific or a general phenomenon that applies to all cell-types.

CHAPTER 6

Discussion

Signalling from RTKs is tightly regulated by extrinsic and intrinsic control mechanisms deregulation of which is a major contributor to most cancers [Vogelstein et al., 2004]. However, the majority of these control mechanisms have remained poorly defined. Sprouty and their related Spred family of proteins are two such groups of intrinsic signalling regulators, which inhibit signalling downstream of various RTKs such as FGFRs through a negative feed-back mode of action [Wakioka et al., 2001; Kato et al., 2003; Nonami et al., 2004; King et al., 2005; Bundschu et al., 2005; Sivak et al., 2005; Hacohen et al., 1998; Casci et al., 1999; Kramer et al., 1999; Reich et al., 1999]. Down-regulation of Sprouty and Spred expression has been implicated in a number of cancers [Lo et al., 2004; Kwabi-Addo et al., 2004; Wang et al., 2006; Fong et al., 2006; Yoshida et al., 2006]. However, despite several years of research, the molecular mechanisms of signal attenuation by these proteins have remained unclear and subject to controversies. Employing a variety of techniques from mass-spectrometry and biochemical analysis to cell-imaging by confocal microscopy, signal attenuation downstream of FGFRs by Sprouty and Spred was studied in this thesis. Novel interacting partners as well as phosphorylation sites of SPRY2 were unravelled using a mass-spectrometry approach. Spred2 inhibition of FGFR signalling was investigated and demonstrated to be dependent on its interaction with the multi-domain scaffold protein NBR1. Finally, NBR1 was characterised as a novel late endosomal regulator of RTK trafficking and signalling, and the interplay between its various regions for protein localisation and function was studied.

In the third chapter, immunoprecipitation coupled with mass-spectrometry was used to identify novel SPRY2 interacting partners and phosphorylation sites. SPRY2 was chosen as it is the most conserved and the most potent ERK1/2 inhibitor of all mammalian Sproutys [Mason et al., 2006]. The LC-MS/MS analysis of SPRY2 immunoprecipitates revealed a

significant number of proteins involved in Clathrin mediated endocytosis (Table 3.1), suggesting that SPRY2 might have a role in regulation of receptor internalisation/trafficking. Analysis of protein interaction networks by STRING showed a network of a number of these endocytosis related interacting partners existed (Figure 3.2), indicating that they might be interacting with SPRY2 as pre-existing multi-protein complex. Mass-spectrometry analysis also revealed Casein Kinases I and II (CKI & CKII) as well as the Protein Phosphatase 1 (PP1) as SPRY2 interacting partners (Table 3.1). It is therefore possible that SPRY2 could be a substrate for these proteins. Finally, a large number of identified SPRY2 interacting partners were ribosomal subunits and molecular chaperones (Table 3.1). This is probably an artefact of over-expression and highlights the fact that a significant fraction of ectopic SPRY2 was in association with the translation and folding machineries during its synthesis.

An endocytic role for Sprouty could potentially address some of the controversies surrounding its function. Receptor signalling and endocytosis are intimately related [Sorkin and von Zastrow, 2009]. However, the effect of endocytosis on signalling can be variable depending on the exact endocytic route as well as the trafficking dynamics, which are determined by multiple factors such as the type of receptor, the amount of ligand, and the availability of trafficking molecules [Sorkin and von Zastrow, 2009]. A number of previous studies on SPRY2 also argued for an endocytosis related role. For instance, SPRY2 was shown to inhibit EGFR internalisation and consequently enhance ERK1/2 signalling by binding to and sequestering c-CBL [Wong et al., 2002a; Rubin et al., 2003]. Down-regulation of FGF signalling by SPRY2, however, was not dependent on the interaction with CBL [Mason et al., 2004], suggesting that other interactions must be mediating this function. It, therefore, remains to be determined if any of the here identified endocytic related interacting partners of SPRY2 are required for the protein function in the context of FGF signalling.

In chapter three, the results of mass-spectrometry analysis of SPRY2 phosphorylations were also described. A novel strategy developed by a post-doc in our lab, Steve Sweet, which makes use of both CID and ECD fragmentations, was employed to identify and correctly localise SPRY2 sites of phosphorylations [Sweet et al., 2008]. A total of 16 SPRY2 phosphorylation sites were identified, 11 of which were novel (Table 3.3). A recently published mass-spectrometry study of SPRY2 phosphorylation sites confirmed 3 of these 11 sites [Brady et al., 2009]. Quantitative proteomics by SILAC was also used to study the dynamics of SPRY2 phosphorylations. It was shown that while the majority of SPRY2 phosphorylations did not change in response to FGF stimulation, Y55 phosphorylation was increased and T56 phosphorylation was decreased (Table 3.4). Considering this reciprocal regulation, as well as the proximity of T56 to the pivotal Y55, it will be interesting to see if T56 phosphorylation has any effect on SPRY2 function.

In the fourth chapter, Spred2 mechanism of signal attenuation was investigated. Spred2 was chosen as a mouse knockout study had revealed a physiological link between it and FGF signalling in the context of bone morphogenesis [Bundschu et al., 2005]. The EVH1 domain of Spreds is crucial for their inhibition signalling but the molecular mechanism of this inhibition was not clear [Wakioka et al., 2001; King et al., 2005]. As EVH1 domains are protein-protein interaction domains, it was hypothesized that a functionally significant binding partner of Spred must be interacting with its EVH1 domain. In a Yeast Two-Hybrid screen carried out by Mona Yekezare in Laura Machesky's lab, NBR1 was identified as potential EVH1 domain specific binding partner of Spred2. The work presented in chapter four confirmed NBR1 as a novel direct binding partner of Spred2 EVH1 domain. Spred2 interacted with NBR1 in an EVH1 domain dependent manner *in vitro* (Figure 4.1) and *in vivo*

(Figure 4.2, 4.4, and 4.5), and this was necessary for Spred2 mediated inhibition of ERK1/2 (Figure 4.10). It was also shown that NBR1 was a specific late endosomal protein, and Spred2 interaction with NBR1 targeted FGFR to the lysosomal degradation pathway, thereby providing a mechanism for inhibition of downstream signalling by Spred.

These results concur with a large body of evidence that puts receptor trafficking at the centre of signal propagation [Sorkin and von Zastrow, 2009; Scita and Di Fiore, 2010]. Interestingly, Spred2 activity seems to be limited to the ERK1/2 pathway [Wakioka et al., 2001; Nonami et al., 2004; King et al., 2005]. As mentioned in the first chapter, apart from a general signal termination by receptor degradation, endocytosis can result in pathway specific signal regulation by compartmentalisation [Miaczynska et al., 2004b]. For example, RTK mediated ERK1/2 signalling has been demonstrated to be enhanced by receptor internalisation [Vieira et al., 1996; Kranenburg et al., 1999; MacInnis and Campenot, 2002]. This has been attributed to the ERK1/2 specific signalling scaffold proteins such as the MP1-P14 complex, which are specifically endosomal [Wunderlich et al., 2001; Teis et al., 2002]. In contrast, removal of activated receptors from the plasma membrane has been shown to result in termination of those downstream signalling pathways which require plasma-membrane associated molecules. These include the PLC/PKC and the PI3K/AKT pathways, both of which require the plasma-membrane specific lipid Phosphatidylinositol-4,5 phosphate as substrate [Haugh and Meyer, 2002]. Such data suggest that, at least in a short timescale, diversion of receptor trafficking by Spred2 could be impacting certain downstream signalling pathways more than others. In particular, a change in the endocytic trafficking route would mean that pathways such as ERK1/2 which require specific endosomal signalling platforms could be preferentially affected, in line with the reported ERK1/2 specific effect of Spred2 [Wakioka et al., 2001; Nonami et al., 2004; King et al., 2005].

The results of chapter four were indicative of novel endocytic related role for NBR1. In chapter five, the exact function of NBR1 on its own in the context of RTK trafficking was investigated. It was demonstrated that ectopic expression of Nbr1 could abrogate ligand induced lysosomal degradation of RTKs and consequently enhance downstream ERK1/2 signalling (Figure 5.1). In theory, such inhibition of degradation could be achieved at various steps of RTK trafficking. These include receptor internalisation, recycling, early to late endosomal transition, late endocytic MVB maturation, or lysosomal fusion of mature MVBs. In mature MVBs, signalling receptors are trapped within intra-luminal vesicles and away from cytosolic signalling components. Thus, as Nbr1 enhances downstream signalling, it is unlikely to be functioning at the MVB–lysosome fusion step. It was also demonstrated that Nbr1 over-expression did not affect early to late endosomal transition (Figure 5.3). As a result, Nbr1 must be functioning at internalisation, recycling, or MVB maturation stages.

The molecular interactions involved in Nbr1 mediated abrogation of RTK degradation are not known at the moment. A number of known Nbr1 interacting proteins, however, have links with vesicular trafficking. It remains to be determined if any of these proteins are part of the molecular mechanism involved in Nbr1 inhibition of RTK degradation. USP8, an Nbr1 interacting de-ubiquitinating enzyme, is particularly interesting with this regard as its loss blocks RTK degradation [Row et al., 2006; Alwan and van Leeuwen, 2006], thus mimicking the phenotype of Nbr1 ectopic expression (Figure 5.1A and 5.1B). Future studies should reveal whether a functional epistasis exists between Nbr1 and USP8.

In chapter four, it was demonstrated that the C-terminal of NBR1 was the binding site of Spred2. Spred2 interaction with NBR1 resulted in targeting activated receptors for degradation in lysosomes. In contrast, in chapter five it was revealed that Nbr1 on its own inhibited RTK degradation (Figure 5.1A and 5.1B), and that this inhibition was dependent on

its C-terminal (Figure 5.4A and 5.4B). This suggests that the C-terminal of Nbr1 is essential for protein function and that Spred2 binding to the critical C-terminal is probably interfering with Nbr1 activity. However, in chapter four it was shown that NBR1 could cooperate with Spred2 in inhibition of ERK1/2 signalling (Figure 4.10B). This supports a synergistic rather than an antagonistic mechanism of functional interaction: Spred2 binding to Nbr1 C-terminal switches its mode of action from an inhibitor to an enhancer of RTK degradation. A schematic representation of the proposed mechanism for Spred and Nbr1 functional interaction in regulation of RTK trafficking is depicted in (Figure 6.1).

In chapter five, it was also shown that while the C-terminus of Nbr1 was necessary for inhibition of RTK degradation, it was not sufficient for this function (Figure 5.4), indicating that other functionally significant regions of the protein must exist outside the C-terminal. The identity of such regions remains to be determined. The C-terminal of Nbr1 was also necessary but not sufficient for late endocytic localisation of the protein (Figures 5.5), revealing a link between protein localisation and function. Further analysis of Nbr1 late endocytic localisation showed that the two LIR regions of the protein were dispensable for late endocytic localisation (Figure 5.10). On the other hand, the autophagosomal localisation of Nbr1 did not rely on the C-terminal of the protein and was exclusively dependent on the presence of LIRs (Figure 5.11). Thus, late endocytic and autophagic localisations of Nbr1 must be independent, implicating that the function of the protein in each context might be independent, too. It was also revealed that neither knockdown nor over-expression of Nbr1 did affect the autophagy machinery (Figure 5.13), ruling out a mechanistic role for Nbr1 in autophagy induction or clearance. These results are in agreement with Kirkin et al. findings that Nbr1-LC3 interaction primary results in Nbr1 degradation, possibly along with any potential ubiquitinated cargos which might be interacting with the UBA domain of the protein [Kirkin et al., 2009].

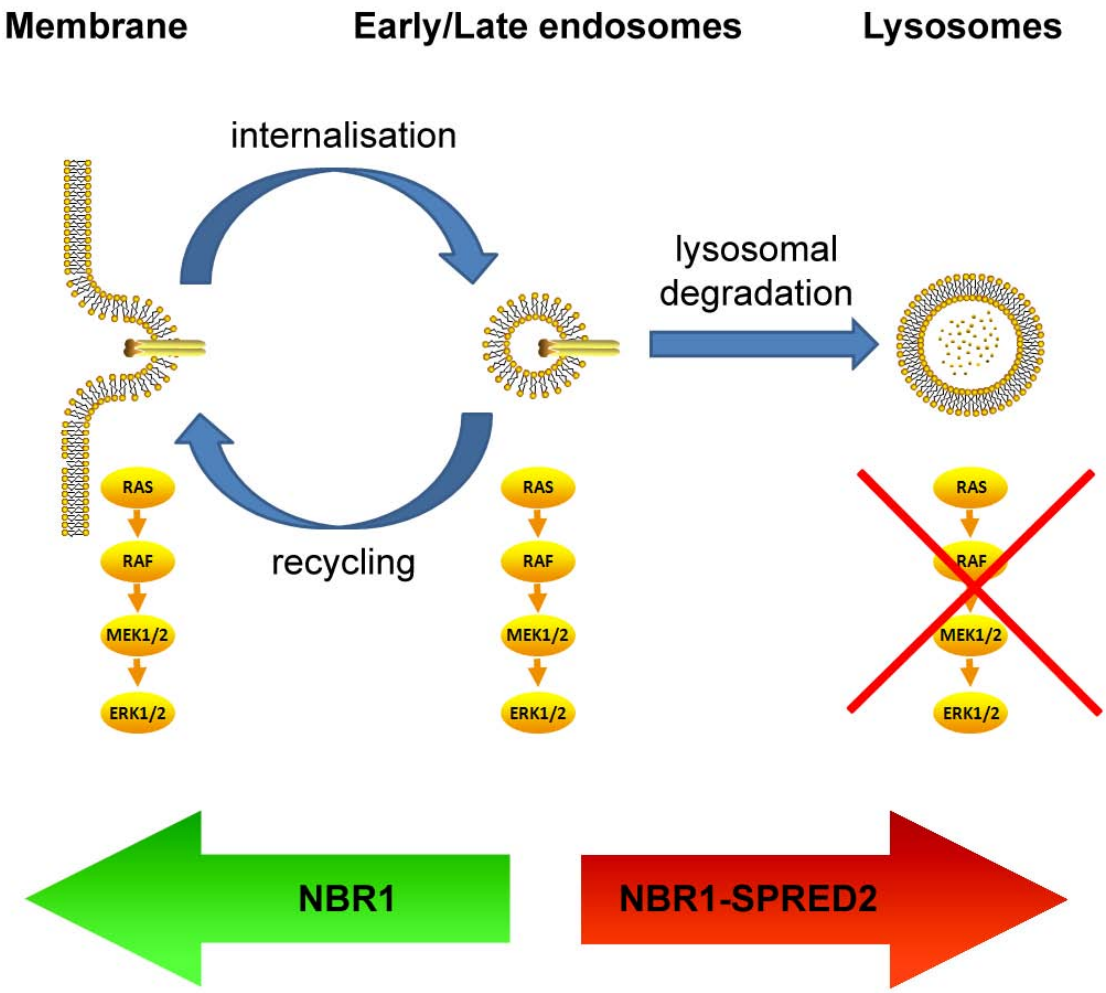

Figure 6.1. Schematic representation of the proposed mechanism of action for Nbr1 and Spred2. Nbr1 abrogates lysosomal degradation of RTKs by delaying receptor trafficking towards the degradatory pathway. Spred2 binding to Nbr1 switches is mode of action as an inhibitor to an enhancer of RTK degradation.

In chapter four, it was demonstrated that NBR1 specifically localised to endosomal limiting membranes (Figure 4.3C). However, the mechanism of this membrane association was not clear. In chapter five, it was shown that the C-terminal of Nbr1 contains a conserved amphipathic α-helix which is crucial for protein association with endosomal limiting membranes (Figure 5.7 and 5.8). Due to its proximity to the UBA domain, this α-helix was named Juxta-UBA (JUBA). JUBA and UBA were both shown to be essential for late endocytic localisation of Nbr1 (Figure 5.9). In fact, there seems to be cooperation between the two regions for correct localisation of Nbr1, as the effect of loss of both regions (Figure 5.5C) is much more dramatic than loss of each individual region (Figure 5.9).

Finally, in chapter five it was demonstrated that NBR1 depletion by siRNA results in cell death by apoptosis (Figure 5.14C). Expression of a C-terminal-ONLY Nbr1 mutant also induced cell death by apoptosis (Figure 5.14A), suggestive of a dominant negativity. These results argue for some vital NBR1 function which can be disrupted by either sufficient depletion of the protein or expression of a truncated C-terminal-ONLY mutant. It is not clear at the moment what the vital function of Nbr1 is. An autophagy related role was ruled out as the vital function of Nbr1 (Figure 5.15B). Whether regulation of RTK trafficking by Nbr1 is crucial for survival is an interesting possibility. It is also possible that some yet unknown Nbr1 cellular activity exist disruption of which can compromise viability. The specific interacting partners of Nbr1 C-terminal identified in chapter five by SILAC mass spectrometry analysis could help reveal if such novel functions exist for Nbr1 (Table 5).

BIBLIOGRAPHY

1. **Abe, M.**, and M.C. Naski. 2004. Regulation of sprouty expression by PLCgamma and calcium-dependent signals. Biochem Biophys Res Commun. 323: 1040-1047.
2. **Abraira, V.E.**, Hyun, N., Tucker, A.F., Coling, D.E., Brown, M.C., Lu, C., Hoffman, G.R., and L.V. Goodrich. 2007. Changes in Sef levels influence auditory brainstem development and function, J Neurosci 27: 4273–4282.
3. **Ahmed, Z.**, Schüller, A.C., Suhling, K., Tregidgo, C., and J.E. Ladbury. 2008. Extracellular point mutations in FGFR2 elicit unexpected changes in intracellular signaling. Biochem J. 413: 37-49.
4. **Altomare, D.A.** and J.R. Testa. 2005. Perturbations of the AKT signaling pathway in human cancer. Oncogene 24: 7455–7464.
5. **Alwan, H.A.**, and J.E. van Leeuwen. 2006. UBPY-mediated epidermal growth factor receptor (EGFR) de-ubiquitination promotes EGFR degradation. J Biol Chem. 282(3):1658-1669.
6. **Amaya, E.**, Musci, T.J., and M.W. Kirschner. 1991. Expression of a dominant negative mutant of the FGF receptor disrupts mesoderm formation in Xenopus embryos. Cell. 66: 257-270.
7. **Amit, I.**, Citri, A., Shay, T., Lu, Y., Katz, M., Zhang, F., Tarcic, G., Siwak, D., Lahad, J., Jacob-Hirsch, J., Amariglio, N., Vaisman, N., Segal, E., Rechavi, G., Alon, U., Mills, G.B., Domany, E., and Y. Yarden. 2007. A module of negative feedback regulators defines growth factor signaling. Nat Genet. 39: 503-512.
8. **Anderson, J.**, Burns, H.D., Enriquez-Harris, P., Wilkie, A.O., and J.K. Heath. 1998. Apert syndrome mutations in fibroblast growth factor receptor 2 exhibit increased affinity for FGF ligand. Hum Mol Genet. 7: 1475-1483.

9. **Arman, E.**, Haffner-Krausz, R., Chen, Y., Heath, J.K., and P. Lonai. 1998. Targeted disruption of fibroblast growth factor (FGF) receptor 2 suggests a role for FGF signaling in pregastrulation mammalian development. Proc Natl Acad Sci U S A. 95: 5082-5087.

10. **Avet-Loiseau, H.**, Li, J.Y., Facon, T., Brigaudeau, C., Morineau, N., Maloisel, F., Rapp, M.J., Talmant, P., Trimoreau, F., Jaccard, A., Harousseau, J.L., and R. Bataille. 1998. High incidence of translocations t(11;14)(q13;q32) and t(4;14)(p16;q32) in patients with plasma cell malignancies. Cancer Res. 58: 5640-5645.

11. **Ayada, T.**, Taniguchi, K., Okamoto, F., Kato, R., Komune, S., Takaesu, G., and A. Yoshimura. 2009. Sprouty4 negatively regulates protein kinase C activation by inhibiting phosphatidylinositol 4,5-biphosphate hydrolysis. Oncogene. 28: 1076-1088.

12. **Ball, L.J.**, Jarchau, T., Oschkinat, H., and U. Walter. 2002. EVH1 domains: structure, function and interactions. FEBS Lett. 513: 45-52.

13. **Basson, M.A.**, Akbulut, S., Watson-Johnson, J., Simon, R., Carroll, T.J., Shakya, R., Gross, I., Martin, G.R., Lufkin, T., McMahon, A.P., Wilson, P.D., Costantini, F.D., Mason, I.J., and J.D. Licht. 2005. Sprouty1 is a critical regulator of GDNF/RET-mediated kidney induction. Dev Cell. 8: 229-239.

14. **Basson, M.A.**, Watson-Johnson, J., Shakya, R., Akbulut, S., Hyink, D., Costantini, F.D., Wilson, P.D., Mason, I.J., and J.D. Licht. 2006. Branching morphogenesis of the ureteric epithelium during kidney development is coordinated by the opposing functions of GDNF and Sprouty1. Dev Biol. 299: 466-477.

15. **Bange, J.**, Prechtl, D., Cheburkin, Y., Specht, K., Harbeck, N., Schmitt, M., Knyazeva, T., Müller, S., Gärtner, S., Sures, I., Wang, H., Imyanitov, E., Häring, H.U., Knayzev, P., Iacobelli, S., Höfler, H., and A. Ullrich. 2002. Cancer progression and tumor cell motility are associated with the FGFR4 Arg(388) allele. Cancer Res. 62: 840-847.

16. **Beausoleil, S.A.**, Villen, J., Gerber, S.A., Rush, J., and S.P. Gygi. 2006. A probability-based approach for high-throughput protein phosphorylation analysis and site localization. Nat. Biotechnol. 24: 1285-1292.

17. **Beenken, A.** And M. Mohammadi. 2009. The FGF family: biology, pathophysiology and therapy. Nature Rev. Drug Discov. 8: 235–253.

18. **Bendall, S.C.**, Hughes, C., Stewart, M.H., Doble, B., Bhatia, M., and G.A. Lajoie. 2008. Prevention of amino acid conversion in SILAC experiments with embryonic stem cells. Mol Cell Proteomics. 7: 1587-1597.

19. **Bhattacharyya, D.**, and B.S. Glick. 2007. Two mammalian Sec16 homologues have nonredundant functions in endoplasmic reticulum (ER) export and transitional ER organization. Mol Biol Cell. 18: 839-849.

20. **Birrer, M.J.**, Johnson, M.E., Hao, K., Wong, K.K., Park, D.C., Bell, A., Welch, W.R., Berkowitz, R.S., and S.C. Mok. 2007. Whole genome oligonucleotide-based array comparative genomic hybridization analysis identified fibroblast growth factor 1 as a prognostic marker for advanced-stage serous ovarian adenocarcinomas. J Clin Oncol. 25: 2281-2287.

21. **Bjørkøy, G.**, Lamark, T., Brech, A., Outzen, H., Perander, M., Øvervatn, A., Stenmark, H., and T. Johansen. 2005. p62/SQSTM1 forms protein aggregates degraded by autophagy and has a protective effect on huntingtin-induced cell death. J. Cell Biol. 171: 603–614.

22. **Blum, R.,** Feick, P., Puype, M., Vandekerckhove, J., Klengel, R., Nastainczyk, W., and I. Schulz. 1996. Tmp21 and p24A, two type I proteins enriched in pancreatic microsomal membranes, are members of a protein family involved in vesicular trafficking. J. Biol. Chem. 271: 17183–17189.

23. **Böttcher, R.T.**, Pollet, N., Delius, H., and C. Niehrs. 2004. The transmembrane protein XFLRT3 forms a complex with FGF receptors and promotes FGF signalling. Nat Cell Biol. 6: 38-44.

24. **Brady, S.C.**, Coleman, M.L., Munro, J., Feller, S.M., Morrice, N.A., and M.F. Olson. 2009. Sprouty2 association with B-Raf is regulated by phosphorylation and kinase conformation. Cancer Res. 69: 6773-6781.

25. **Brems, H.,** Chmara, M., Sahbatou, M., Denayer, E., Taniguchi, K., Kato, R., Somers, R., Messiaen, L., De Schepper, S., Fryns, J.P., Cools, J., Marynen, P., Thomas, G., Yoshimura, A., and E. Legius. 2007. Germline loss-of-function mutations in SPRED1 cause a neurofibromatosis 1-like phenotype. Nat Genet. 39: 1120-1126.

26. **Bundschu, K.,** Gattenlöhner, S., Knobeloch, K.P., Walter, U., and K. Schuh. 2006a. Tissue-specific Spred-2 promoter activity characterized by a gene trap approach. Gene Expr. Patterns 6: 247-255.

27. **Bundschu, K.**, Knobeloch, K.P., Ullrich, M., Schinke, T., Amling, M., Engelhardt, C.M., Renné, T., Walter, U., and K. Schuh. 2005. Gene disruption of Spred-2 causes dwarfism. J Biol Chem. 280: 28572-28580.

28. **Bundschu, K.**, Walter, U., and K. Schuh. 2006b. The VASP-Spred-SPRY domain puzzle. J Biol Chem. 281: 36477-36481.

29. **Burgar, H.R.**, Burns, H.D., Elsden, J.L., Lalioti, M.D., and J.K. Heath. 2002. Association of the signaling adaptor FRS2 with fibroblast growth factor receptor 1 (Fgfr1) is mediated by alternative splicing of the juxtamembrane domain. J Biol Chem. 277: 4018-4023.

30. **Cabrita, M.A.**, Jaggi, F., Widjaja, S.P., and G. Christofori. 2006. A functional interaction between sprouty proteins and caveolin-1. J Biol Chem. 281: 29201-2912.

31. **Camacho-Carvajal, M.M.**, Wollscheid, B., Aebersold, R., Steimle, V., and W.W. Schamel. 2004. Two-dimensional Blue Native/SDS Gel Electrophoresis of Multi-Protein Complexes from Whole Cellular Lysates: a proteomics approach. Molecular & Cellular Proteomics. 3: 176-82.

32. **Campbell, I.G.**, Nicolai, H.M., Foulkes, W.D., Senger, G., Stamp, G.W., Allan, G., Boyer, C., Jones, K., Bast, R.C. Jr and E. Solomon. 1994. A novel gene encoding a B-box protein within the BRCA1 region at 17q21.1. Hum. Mol. Genet. 3: 589–594.

33. **Cappellen, D.**, De Oliveira, C., Ricol, D., de Medina, S., Bourdin, J., Sastre-Garau, X., Chopin, D., Thiery, J.P., F. Radvanyi. 1999. Frequent activating mutations of FGFR3 in human bladder and cervix carcinomas. Nat Genet. 23: 18-20.

34. **Casci, T.**, J. Vinos, and M. Freeman. 1999. Sprouty, an intracellular inhibitor of Ras signaling. Cell 96: 655-665.

35. **Cha, J.Y.**, Maddileti, S., Mitin, N., Harden, T.K., and C.J. Der. 2009. Aberrant receptor internalization and enhanced FRS2-dependent signaling contribute to the transforming activity of the fibroblast growth factor receptor 2 IIIb C3 isoform. J. Biol. Chem. 284: 6227–6240.

36. **Chambers, D.** and I. Mason. 2000a. Expression of sprouty2 during early development of the chick embryo is coincident with known sites of FGF signalling. Mech. Dev. 91: 361-364.

37. **Chambers, D.**, Medhurst, A. D., Walsh, F. S., Price, J. and I. Mason. 2000b. Differential display of genes expressed at the midbrain – hindbrain junction identifies sprouty2: an FGF8-inducible member of a family of intracellular FGF antagonists. Mol. Cell Neurosci. 15:22-35.

38. **Chan, E.Y.**, Kir, S., and S.A. Tooze. 2007. siRNA screening of the kinome identifies ULK1 as a multidomain modulator of autophagy. J Biol Chem. 282: 25464-25474.

39. **Chandramouli, S.**, Yu, C.Y., Yusoff, P., Lao, D.H., Leong, H.F., Mizuno, K., and G.R. Guy. 2008. Tesk1 interacts with Spry2 to abrogate its inhibition of ERK phosphorylation downstream of receptor tyrosine kinase signaling. J Biol Chem. 283: 1679-1691.

40. **Chen, F.**, Hasegawa, H., Schmitt-Ulms, G., Kawarai, T., Bohm, C., Katayama, T., Gu, Y., Sanjo, N., Glista, M., Rogaeva, E., Wakutani, Y., Pardossi-Piquard, R., Ruan, X., Tandon, A., Checler, F., Marambaud, P., Hansen, K., Westaway, D., St George-Hyslop, P., and P. Fraser. 2006. TMP21 is a presenilin complex component that modulates gamma-secretase but not epsilon-secretase activity. Nature 440: 1208-1212.

41. **Chen, H.**, Xu, C.F., Ma, J., Eliseenkova, A.V., Li, W., Pollock, P.M., Pitteloud, N., Miller, W.T., Neubert, T.A., M. Mohammadi. 2008. A crystallographic snapshot of tyrosine trans-phosphorylation in action. Proc Natl Acad Sci U S A. 105: 19660-19665.

42. **Chesi, M.**, Nardini, E., Brents, L.A., Schröck, E., Ried, T., Kuehl, W.M., and P.L. Bergsagel. 1997. Frequent translocation t(4;14)(p16.3;q32.3) in multiple myeloma is associated with increased expression and activating mutations of fibroblast growth factor receptor 3. Nat Genet. 16: 260-264.

43. **Cho, J.Y.**, Guo, C., Torello, M., Lunstrum, G.P., Iwata, T., Deng, C., and W.A. Horton. 2004. Defective lysosomal targeting of activated fibroblast growth factor receptor 3 in achondroplasia. Proc Natl Acad Sci U S A. 101: 609-614.

44. **Chow, S.Y.**, Yu, C.Y., and G.R. Guy. 2009. Sprouty2 interacts with protein kinase C delta and disrupts phosphorylation of protein kinase D1. J Biol Chem. 284: 19623-19636.

45. **Christofori, G.** 2003. Split personalities: the agonistic antagonist Sprouty. Nat Cell Biol. 5: 377-379.

46. **Cohn, M.J.**, Izpisúa-Belmonte, J.C., Abud, H., Heath, J.K., and C. Tickle. 1995. Fibroblast growth factors induce additional limb development from the flank of chick embryos. Cell. 80: 739-46.

47. **Cole, C.**, Barber, J.D., and G.J. Barton. 2008. The Jpred 3 secondary structure prediction server. Nucleic Acids Res. 36: 197-201.

48. **Colvin, J.S.**, Bohne, B.A., Harding, G.W., McEwen D.G., and D.M. Ornitz. 1996. Skeletal overgrowth and deafness in mice lacking fibroblast growth factor receptor 3. Nat Genet. 12: 390–397.

49. **Colvin, J.S.**, White, A.C., Pratt, S.J. and D.M. Ornitz. 2001. Lung hypoplasia and neonatal death in Fgf9-null mice identify this gene as an essential regulator of lung mesenchyme Development 128: 2095–2106.

50. **Conner, M.**, Hicks, M.R., Dafforn, T., Knowles, T.J., Ludwig, C., Staddon, S., Overduin, M., Günther, U.L., Thome, J., Wheatley, M., Poyner, D.R., and A.C. Conner. 2008. Functional and biophysical analysis of the C-terminus of the CGRP-receptor; a family B GPCR. Biochemistry 47(32):8434-8444.

51. **Cooper, H.J.**, Håkansson, K., and A.G. Marshall. 2005. The role of electron capture dissociation in biomolecular analysis. Mass Spectrom Rev. 24: 201-222.

52. **Corson, L.B.**, Yamanaka, Y., Lai, K. M. And J. Rossant. 2003. Spatial and temporal patterns of ERK signaling during mouse embryogenesis. Development 130: 4527–4537.

53. **Courjal, F.**, Cuny, M., Simony-Lafontaine, J., Louason, G., Speiser, P., Zeillinger, R., Rodriguez, C., and C. Theillet. 1997. Mapping of DNA amplifications at 15 chromosomal localizations in 1875 breast tumors: definition of phenotypic groups. Cancer Res. 57: 4360-4367.

54. **Courtois-Cox, S.**, Genther Williams, S.M., Reczek, E.E., Johnson, B.W., McGillicuddy, L.T., Johannessen, C.M., Hollstein, P.E., MacCollin, M., and K. Cichowski. 2006. A negative feedback signaling network underlies oncogene-induced senescence. Cancer Cell. 10: 459-472.

55. **Cox, J.**, and M. Mann. 2008. MaxQuant enables high peptide identification rates, individualized p.p.b.-range mass accuracies and proteome-wide protein quantification. Nat Biotechnol. 26: 1367-1372.

56. **DaSilva, J.**, Xu, L., Kim, H. J., Miller, W. T., D. Bar-Sagi. 2006. Regulation of sprouty stability by Mnk1-dependent phosphorylation. Mol Cell Biol. 26: 1898-907.

57. **De Moerlooze, L.**, Spencer-Dene, B., Revest, J., Hajihosseini, M., Rosewell, I, and C. Dickson. 2000. An important role for the IIIb isoform of fibroblast growth factor receptor 2 (FGFR2) in mesenchymal–epithelial signalling during mouse organogenesis. Development 127: 483–492.

58. **Denayer, E.**, Ahmed, T., Brems, H., Van Woerden, G., Borgesius, N.Z., Callaerts-Vegh, Z., Yoshimura, A., Hartmann, D., Elgersma, Y., D'Hooge, R., Legius, E., and D. Balschun. 2008. Spred1 is required for synaptic plasticity and hippocampus-dependent learning. J Neurosci. 28: 14443-14449.

59. **Deng, C.X.**, Wynshaw-Boris, A., Shen, M.M., Daugherty, C., Ornitz, D.M., and P. Leder. 1994. Murine FGFR-1 is required for early postimplantation growth and axial organization. Genes Dev 8: 3045–3057.

60. **Dengjel, J.**, Kratchmarova, I., and B. Blagoev. 2009. Receptor tyrosine kinase signaling: a view from quantitative proteomics. Mol Biosyst 5: 1112-1121.

61. **Dhillon, A.S.**, Hagan, S., Rath, O., and W. Kolch. 2007. MAP kinase signalling pathways in cancer. Oncogene. 26: 3279-3290.

62. **Di Guglielmo**, G.M., Baass, P.C., Ou, W.J., Posner, B.I., and J.J. Bergeron. 1994. Compartmentalization of SHC, GRB2 and mSOS, and hyperphosphorylation of Raf-1 by EGF but not insulin in liver parenchyma. EMBO J 13: 4269–4277.

63. **Ding, W.**, Shi, W., Bellusci, S., Groffen, J., Heisterkamp, N., Minoo, P., and D. Warburton. 2007. Sprouty2 downregulation plays a pivotal role in mediating crosstalk between TGF-beta1 signaling and EGF as well as FGF receptor tyrosine kinase-ERK pathways in mesenchymal cells. J Cell Physiol. 212: 796-806.

64. **Dode, C.**, and J.P. Hardelin. 2004. Kallmann syndrome: fibroblast growth factor signaling insufficiency?. J Mol Med 82: 725–734.

65. **Doherty, G.J.**, and H.T. McMahon. 2009. Mechanisms of endocytosis. Annu Rev Biochem. 78: 857-902.

66. **Dono, R.**, Texido, G., Dussel, R., Ehmke, H., and R. Zeller. 1998. Impaired cerebral cortex development and blood pressure regulation in FGF-2-deficient mice. EMBO J. 17: 4213–4225.

67. **Dudka, A.A.**, Sweet, S.M., and J.K. Heath. 2010. Signal transducers and activators of transcription-3 binding to the fibroblast growth factor receptor is activated by receptor amplification. Cancer Res. 70: 3391-3401.

68. **Dutt, A.,** Salvesen, H.B., Chen, T.H., Ramos, A.H., Onofrio, R.C., Hatton, C., Nicoletti, R., Winckler, W., Grewal, R., Hanna, M., Wyhs, N., Ziaugra, L., Richter, D.J., Trovik, J., Engelsen, I.B., Stefansson, I.M., Fennell, T., Cibulskis, K., Zody, M.C., Akslen, L.A., Gabriel, S., Wong, K.K., Sellers, W.R., Meyerson, M., and H. Greulich. 2008. Drug-sensitive FGFR2 mutations in endometrial carcinoma. Proc Natl Acad Sci U S A. 105: 8713-8717.

69. **Easton, D.F.**, Pooley, K.A., Dunning, A.M., Pharoah, P.D., Thompson, D., Ballinger, D.G., Struewing, J.P., Morrison, J., Field, H., Luben, R., et al. 2007. Genome-wide association study identifies novel breast cancer susceptibility loci. Nature. 447: 1087-1093.

70. **Ebner, R.**, and R. Derynck. 1991. Epidermal growth factor and transforming growth factor-alpha: differential intracellular routing and processing of ligand-receptor complexes. Cell Regul. 2: 599-612.

71. **Edelson-Averbukh, M.**, Pipkorn, R., and W.D. Lehmann. 2007. Analysis of protein phosphorylation in the regions of consecutive serine/threonine residues by negative ion electrospray collision-induced dissociation. Approach to pinpointing of phosphorylation sites. Anal Chem. 79: 3476-3486.

72. **Edwin, F.**, Anderson, K., T.B. Patel. 2010. HECT domain-containing E3 ubiquitin ligase Nedd4 interacts with and ubiquitinates Sprouty2. J Biol Chem. 285: 255-264.

73. **Edwin, F.**, Singh, R., Endersby, R., Baker, S. J., and T.B. Patel. 2006. The tumor suppressor PTEN is necessary for human Sprouty 2-mediated inhibition of cell proliferation. J. Biol Chem. 281: 4816-22.

74. **Egan, J. E.**, Hall, A. B., Yatsula, B. A. and D. Bar-Sagi. 2002. The bimodal regulation of epidermal growth factor signaling by human Sprouty proteins. Proc. Natl. Acad. Sci. USA 99: 6041-46.

75. **Engelhardt, C.M.**, Bundschu, K., Messerschmitt, M., Renné, T., Walter, U., Reinhard, M., and K. Schuh. 2004. Expression and subcellular localization of Spred proteins in mouse and human tissues. Histochem Cell Biol. 122: 527-538.

76. **Eswarakumar, V.P.**, Lax, I., and J. Schlessinger. 2005. Cellular signaling by fibroblast growth factor receptors. Cytokine Growth Factor Rev. 16: 139-149.

77. **Eswarakumar, V.P.**, Monsonego-Ornan, E., Pines, M., Antonopoulou, I., Morriss-Kay, G.M., and P. Lonai. 2002. The IIIc alternative of Fgfr2 is a positive regulator of bone formation. Development 129: 3783–3793.

78. **Faham, S.**, Hileman, R.E., Fromm, J.R., Linhardt, R.J., and D.C. Rees. 1996. Heparin structure and interactions with basic fibroblast growth factor. Science. 271: 1116-1120.

79. **Falasca, M.**, Logan, S.K., Lehto, V.P., Baccante, G., Lemmon, M.A., and J. Schlessinger. 1998. Activation of phospholipase C gamma by PI 3-kinase-induced PH domain-mediated membrane targeting. EMBO J 17: 414–422.

80. **Feldman, B.**, Poueymirou, W., Papaioannou, V.E., DeChiara, T.M., and M. Goldfarb. 1995. Requirement of FGF-4 for postimplantation mouse development. Science. 267: 246-249.

81. **Floss, T.**, Arnold, H.H., and T. Braun. 1997. A role for FGF-6 in skeletal muscle regeneration. Genes Dev. 11: 2040–2051.

82. **Fong, C.W.**, Chua, M.S., McKie, A.B., Ling, S.H., Mason, V., Li, R., Yusoff, P., Lo, T.L., Leung, H.Y., So, S.K., and G.R. Guy. 2006. Sprouty 2, an inhibitor of mitogen-activated protein kinase signaling, is down-regulated in hepatocellular carcinoma. Cancer Res. 66: 2048-2058.

83. **Fong, C.W.**, Leong, H. F., Wong, E. S., Lim, J., Yusoff, P., and G.R. Guy. 2003. Tyrosine phosphorylation of Sprouty2 enhances its interaction with c-Cbl and is crucial for its function. J Biol Chem. 278: 33456-64.

84. **Franco B.**, Guioli S, Pragliola A, Incerti B, Bardoni B, Tonlorenzi R, Carrozzo R, Maestrini E, Pieretti M, Taillon-Miller P, et al. 1991. A gene deleted in Kallmann's syndrome shares homology with neural cell adhesion and axonal path-finding molecules. Nature. 353: 529-36.

85. **Freier, K.,** Schwaenen, C., Sticht, C., Flechtenmacher, C., Mühling, J., Hofele, C., Radlwimmer, B., Lichter, P., and S. Joos. 2007. Recurrent FGFR1 amplification and high FGFR1 protein expression in oral squamous cell carcinoma (OSCC). Oral Oncol. 43: 60-66.

86. **Fritzsche, S.**, Kenzelmann, M., Hoffmann, M.J., Muller, M., Engers, R., Grone, H.J., and W.A. Schulz. 2006. Concomitant down-regulation of SPRY1 and SPRY2 in prostate carcinoma. Endocr Relat Cancer. 13: 839-849.

87. **Furdui, C.M.**, Lew, E.D., Schlessinger, J., and K.S. Anderson. 2006. Autophosphorylation of FGFR1 kinase is mediated by a sequential and precisely ordered reaction. Mol Cell. 21: 711-717.

88. **Furthauer, M.**, Lin, W., Ang, S.L., Thisse, B., and C. Thisse. 2002. Sef is a feedback-induced antagonist of Ras/MAPK-mediated FGF signalling. Nat Cell Biol 4: 170–174.

89. **Fürthauer, M.**, Reifers, F., Brand, M., Thisse, B., and C. Thisse. 2001. Sprouty4 acts in vivo as a feedback-induced antagonist of FGF signaling in zebrafish. Development. 128: 2175-2186.

90. **Galabova-Kovacs, G.**, Kolbus, A., Matzen, D., Meissl, K., Piazzolla, D., Rubiolo, C., Steinitz, K., and M. Baccarini. 2006. ERK and beyond: insights from B-Raf and Raf-1 conditional knockouts. Cell Cycle. 5: 1514-1518.

91. **Geetha, T.**, Jiang J., and M.W Wooten. 2005. Lysine 63 polyubiquitination of the nerve growth factor receptor TrkA directs internalization and signaling. Mol Cell. 20: 301-312.

92. **Ghosh, P.**, Dahms, N.M., S. Kornfeld. 2003. Mannose 6-phosphate receptors: new twists in the tale. Nat Rev Mol Cell Biol. 4: 202-212.

93. **González-Martínez, D.**, Kim, S.H., Hu, Y., Guimond, S., Schofield, J., Winyard, P., Vannelli, G.B., Turnbull, J., and P.M. Bouloux. 2004. Anosmin-1 modulates fibroblast

growth factor receptor 1 signaling in human gonadotropin-releasing hormone olfactory neuroblasts through a heparan sulfate-dependent mechanism. J Neurosci. 24: 10384-10392.

94. **Goriely, A.**, Hansen, R.M., Taylor, I.B., Olesen, I.A., Jacobsen, G.K., McGowan, S.J., Pfeifer, S.P., McVean, G.A., Meyts, E.R., and A.O. Wilkie. 2009. Activating mutations in FGFR3 and HRAS reveal a shared genetic origin for congenital disorders and testicular tumors. Nat Genet. 41: 1247-1252.

95. **Gorringe, K.L.**, Jacobs, S., Thompson, E.R., Sridhar, A., Qiu, W., Choong, D.Y., and I.G. Campbell. 2007. High-resolution single nucleotide polymorphism array analysis of epithelial ovarian cancer reveals numerous microdeletions and amplifications. Clin Cancer Res. 13: 4731-4739.

96. **Gotoh, N.** 2008. Regulation of growth factor signaling by FRS2 family docking/scaffold adaptor proteins. Cancer Sci. 99: 1319-1325.

97. **Gotoh, N.,** Laks, S., Nakashima, M., Lax, I., and J. Schlessinger. 2004. FRS2 family docking proteins with overlapping roles in activation of MAP kinase have distinct spatial-temporal patterns of expression of their transcripts. FEBS Lett. 564: 14–18.

98. **Gotoh, N.**, Manova, K., Tanaka, S., Murohashi, M., Hadari, Y., Lee, A., Hamada, Y., Hiroe, T., Ito, M., Kurihara, T., Nakazato, H., Shibuya, M., Lax, I., Lacy, E., and J. Schlessinger. 2005. The docking protein FRS2{alpha} is an essential component of multiple fibroblast growth factor responses during early mouse development. Mol Cell Biol. 25: 4105–4116.

99. **Greenman, C.,** Stephens, P., Smith, R., Dalgliesh, G.L., Hunter, C., Bignell, G., Davies, H., Teague, J., Butler, A., Stevens, C., Edkins, S., O'Meara, S., et al. 2007. Patterns of somatic mutation in human cancer genomes. Nature. 446: 153-158.

100. **Griner, E.M.**, and M.G. Kazanietz. 2007. Protein kinase C and other diacylglycerol effectors in cancer. Nat Rev Cancer. 7: 281-294.

101. **Gross, I.**, Bassit, B., Benezra, M., and J.D. Licht. 2001. Mammalian sprouty proteins inhibit cell growth and differentiation by preventing ras activation, J. Biol. Chem. 276 : 46460–46468.

102. **Gross, I.**, Morrison, D. J., Hyink, D. P., Georgas, K., English, M.A., Mericskay, M., Hosono, S., Sassoon, D., Wilson, P. D., Little, M., and J.D. Licht. 2003. The receptor tyrosine kinase regulator Sprouty1 is a target of the tumor suppressor WT1 and important for kidney development, J. Biol. Chem. 278: 41420–41430.

103. **Grosshans, B.L.**, Ortiz, D., and P. Novick. 2006. Rabs and their effectors: achieving specificity in membrane traffic. Proc Natl Acad Sci U S A. 103: 11821-11827.

104. **Guo, L.,** Degenstein, L., and E. Fuchs. 1996. Keratinocyte growth factor is required for hair development but not for wound healing, Genes Dev. 10: 165–175.

105. **Guy, G.R.,** Wong, E.S., Yusoff, P., Chandramouli, S., Lo, T.L., Lim, J., and C.W. Fong. 2003. Sprouty: how does the branch manager work? J Cell Sci. 116: 3061-3068.

106. **Hacohen, N.**, S. Kramer, D. Sutherland, Y. Hiromi, and M.A Krasnow. 1998. Sprouty encodes a novel antagonist of FGF signaling that patterns apical branching of the Drosophila airways. Cell 92: 253-263.

107. **Hadari, Y.R.,** Gotoh, N., Kouhara, H., Lax, I., and J. Schlessinger. 2001. Critical role for the docking-protein FRS2 alpha in FGF receptor-mediated signal transduction pathways. Proc Natl Acad Sci U S A. 98: 8578-8583.

108. **Hadari, Y.R.,** Kouhara, H., Lax, I., and J. Schlessinger. 1998. Binding of Shp2 tyrosine phosphatase to FRS2 is essential for fibroblast growth factor-induced PC12 cell differentiation. Mol Cell Biol. 18: 3966–3973.

109. **Haglund, K.**, Schmidt, M.H., Wong, E.S., Guy, G.R., and I. Dikic. 2005. Sprouty2 acts at the Cbl/CIN85 interface to inhibit epidermal growth factor receptor downregulation. EMBO Rep. 6: 635-41.

110. **Haines, B.P.**, Wheldon, L.M., Summerbell, D., Heath, J.K., and P.W. Rigby. 2006. Regulated expression of FLRT genes implies a functional role in the regulation of FGF signalling during mouse development. Dev Biol. 297: 14-25.

111. **Hall, A.B.,** Jura, N., DaSilva, J., Jang, Y. J., Gong, D., and D. Bar-Sagi. 2003. hSpry2 is targeted to the ubiquitin-dependent proteasome pathway by c-Cbl, Curr. Biol. 13: 308–314.

112. **Hanafusa, H.**, Torii, S., Yasunaga, T. and E. Nishida. 2002. Sprouty1 and Sprouty2 provide a control mechanism for the Ras/MAPK signalling pathway. Nature Cell Biol. 4: 850−858.

113. **Hanafusa, H.**, Torii, S., Yasunaga, T., Matsumoto, K., and E. Nishida. 2004. Shp2, an SH2-containing protein-tyrosine phosphatase, positively regulates receptor tyrosine kinase signaling by dephosphorylating and inactivating the inhibitor Sprouty. J Biol Chem. 279: 22992-5.

114. **Harduf, H.,** Halperin, E., Reshef, R., and D. Ron. 2005. Sef is synexpressed with FGFs during chick embryogenesis and its expression is differentially regulated by FGFs in the developing limb. Dev Dyn 233: 301–312.

115. **Harmer, N.J.**, Sivak, J.M., Amaya, E., and T.L. Blundell. 2005. 1.15 A crystal structure of the X. tropicalis Spred1 EVH1 domain suggests a fourth distinct peptide-binding mechanism within the EVH1 family. FEBS Lett. 579: 1161-1166.

116. **Hart, K.C.**, Robertson, S.C., Kanemitsu, M.Y., Meyer, A.N., Tynan, J.A., and D.J. Donoghue. 2000. Transformation and Stat activation by derivatives of FGFR1, FGFR3, and FGFR4. Oncogene. 19: 3309-3320.

117. **Haucke V.** 2005. Phosphoinositide regulation of clathrin-mediated endocytosis. Biochem Soc Trans. 33: 1285-1289.

118. **Haugh, J.M.,** and Meyer, T. 2002. Active EGF receptors have limited access to PtdIns(4, 5)P(2) in endosomes: implications for phospholipase C and PI 3-kinase signaling. J. Cell Sci. 115(2):303–310.

119. **Haugsten, E.M.**, Sørensen, V., Brech, A., Olsnes, S., and J. Wesche. 2005. Different intracellular trafficking of FGF1 endocytosed by the four homologous FGF receptors. J Cell Sci. 118: 3869-3881.

120. **Hebert, J.M.**, Rosenquist, T., Gotz, J., and G.R. Martin. 1994. FGF5 as a regulator of the hair growth cycle: evidence from targeted and spontaneous mutations. Cell 78: 1017–1025.

121. **Hernández, S.**, de Muga, S., Agell, L., Juanpere, N., Esgueva, R., Lorente, J.A., Mojal, S., Serrano, S., and J. Lloreta. 2009. FGFR3 mutations in prostate cancer: association with low-grade tumors. Mod Pathol. 22: 848-856.

122. **Hu, Y.**, Guimond, S.E., Travers, P., Cadman, S., Hohenester, E., Turnbull, J.E., Kim, S.H., and P.M. Bouloux. 2009. Novel mechanisms of fibroblast growth factor receptor 1 regulation by extracellular matrix protein anosmin-1. J Biol Chem. 284: 29905-29920.

123. **Hunter, D.J.**, Kraft, P., Jacobs, K.B., Cox, D.G., Yeager, M., Hankinson, S.E., Wacholder, S., Wang, Z., Welch, R., Hutchinson, A., Wang, J., Yu, K., Chatterjee, N., Orr, N., Willett, W.C., Colditz, G.A., Ziegler, R.G., Berg, C.D., Buys, S.S., McCarty, C.A., Feigelson, H.S., Calle, E.E., Thun, M.J., Hayes, R.B., Tucker, M., Gerhard, D.S.,

Fraumeni, J.F. Jr, Hoover, R.N., Thomas, G., and S.J. Chanock. 2007. A genome-wide association study identifies alleles in FGFR2 associated with risk of sporadic postmenopausal breast cancer. Nat Genet. 39: 870-874.

124. **Ibrahimi, O.A.**, Eliseenkova, A.V., Plotnikov, A.N., Yu, K., Ornitz, D.M., and M. Mohammadi. 2001. Structural basis for fibroblast growth factor receptor 2 activation in Apert syndrome. Proc Natl Acad Sci USA 98: 7182–7187.
125. **Iliuk, A.**, Galan, J., and W.A. Tao. 2009. Playing tag with quantitative proteomics. Analytical and Bioanalytical Chemistry 393: 503-513.
126. **Impagnatiello, M.A.**, Weitzer, S., Gannon, G., Compagni, A., Cotton, M. and G. Christofori. 2001. Mammalian sprouty-1 and -2 are membrane-anchored phosphoprotein inhibitors of growth factor signaling in endothelial cells. J. Cell Biol. 152: 1087-98.
127. **Inoue, H.**, Kato, R., Fukuyama, S., Nonami, A., Taniguchi, K., Matsumoto, K., Nakano, T., Tsuda, M., Matsumura, M., Kubo, M., Ishikawa, F., Moon, B.G., Takatsu, K., Nakanishi, Y., and A. Yoshimura. 2005. Spred-1 negatively regulates allergen-induced airway eosinophilia and hyperresponsiveness. J Exp Med. 201: 73–82.
128. **Jarvis, L.A.**, Toering, S. J., Simon, M. A., Krasnow, M.A., and R.K. Smith-Bolton. 2006. Sprouty proteins are in vivo targets of Corkscrew/SHP-2 tyrosine phosphatases. Development. 133: 133-142
129. **Jenne, N.**, Frey, K., Brugger, B. and F.T. Wieland. 2002. Oligomeric state and stoichiometry of p24 proteins in the early secretory pathway. J. Biol. Chem. 277: 46504–46511.
130. **Jensen, L.J.**, Kuhn, M., Stark, M., Chaffron, S., Creevey, C., Muller, J., Doerks, T., Julien, P., Roth, A., Simonovic, M., Bork, P., and C. von Mering. 2009. STRING 8--a

global view on proteins and their functional interactions in 630 organisms. Nucleic Acids Res. 37(Database issue):D412-6.

131. **Jiang, X.**, Huang, F., Marusyk, A., and A. Sorkin. 2003. Grb2 regulates internalization of EGF receptors through clathrin-coated pits. Mol. Biol. Cell 14: 858–870.
132. **Jin, M.H.**, Sawamoto, K., Ito, M., and H. Okano. 2000. The interaction between the Drosophila secreted protein argos and the epidermal growth factor receptor inhibits dimerization of the receptor and binding of secreted spitz to the receptor. Mol Cell Biol. 20: 2098-2107.
133. **Johne, C.**, Matenia, D., Li, X.Y., Timm, T., Balusamy, K., and E.M. Mandelkow. 2008. Spred1 and TESK1--two new interaction partners of the kinase MARKK/TAO1 that link the microtubule and actin cytoskeleton. Mol Biol Cell. 19: 1391-1403.
134. **Kanazawa, C.**, Morita, E., Yamada, M., Ishii, N., Miura, S., Asao, H., Yoshimori, T., and K. Sugamura. 2003. Effects of deficiencies of STAMs and Hrs, mammalian class E Vps proteins, on receptor downregulation. Biochem Biophys Res Commun. 309: 848-856.
135. **Katoh, Y.**, and M. Katoh. 2006. FGF signaling inhibitor, SPRY4, is evolutionarily conserved target of WNT signaling pathway in progenitor cells. Int J Mol Med. 17: 529-532.
136. **Kato, R.**, A. Nonami, T. Taketomi, T. Wakioka, A. Kuroiwa, Y. Matsuda, and A. Yoshimura. 2003. Molecular cloning of mammalian Spred-3 which suppresses tyrosine kinase-mediated Erk activation. Biochem Biophys Res Commun. 302: 767-772.
137. **Kim, H.J.**, Taylor, L.J., and D. Bar-Sagi. 2007. Spatial regulation of EGFR signaling by Sprouty2. Curr Biol. 17: 455-461.

138. **King, J.A.**, Corcoran, N.M., D'Abaco, G.M., Straffon, A.F., Smith, C.T., Poon, C.L., Buchert, M., I, S., Hall, N.E., Lock, P., and C.M. Hovens. 2006. Eve-3: a liver enriched suppressor of Ras/MAPK signaling. J Hepatol. 44: 758-67.

139. **King, J.A.**, Straffon, A.F., D'Abaco, G.M., Poon, C.L., I, S.T., Smith, C.M., Buchert, M., Corcoran, N.M., Hall, N.E., Callus, B.A., Sarcevic, B., Martin, D., Lock, P., and C.M. Hovens. 2005. Distinct requirements for the Sprouty domain for functional activity of Spred proteins. Biochem J. 388: 445-454.

140. **Kirkin, V.**, Lamark, T., Sou, Y.S., Bjørkøy, G., Nunn, J.L., Bruun, J.A., Shvets, E., McEwan, D.G., Clausen, T.H., Wild, P., Bilusic, I., Theurillat, J.P., Øvervatn, A., Ishii, T., Elazar, Z., Komatsu, M., Dikic, I., and T. Johansen. 2009. A role for NBR1 in autophagosomal degradation of ubiquitinated substrates. Mol Cell. 33: 505-16.

141. **Klein, O.D.**, Minowada, G., Peterkova, R., Kangas, A., Yu, B.D., Lesot, H., Peterka, M., Jernvall, J., and G.R. Martin. 2006. Sprouty genes control diastema tooth development via bidirectional antagonism of epithelial-mesenchymal FGF signaling. Dev Cell 11: 181–190.

142. **Klionsky, D.J.**, Abeliovich, H., Agostinis, P., Agrawal, D.K. et al. 2008. Guidelines for the use and interpretation of assays for monitoring autophagy in higher eukaryotes. Autophagy 4: 151-175.

143. **Kolch, W.**, Heidecker, G., Kochs, G., Hummel, R., Vahidi, H., Mischak, H., Finkenzeller, G., Marmé, D., and U.R. Rapp. 1993. Protein kinase C alpha activates RAF-1 by direct phosphorylation. Nature. 364: 249-252.

144. **Kouhara, H.**, Hadari, Y.R., Spivak-Kroizman, T., Schilling, J., Bar-Sagi, D., Lax, I., and J. Schlessinger. 1997. A lipid-anchored Grb2-binding protein that links FGF-receptor activation to the Ras/MAPK signaling pathway. Cell. 89: 693-702.

145. **Kramer, S.**, M. Okabe, N. Hacohen, M.A. Krasnow, and Y. Hiromi. 1999. Sprouty: a common antagonist of FGF and EGF signaling pathways in Drosophila. Development 126: 2515 -2525.

146. **Kranenburg, O.**, Verlaan, I., and W.H. Moolenaar. 1999. Dynamin is required for the activation of mitogen-activated protein (MAP) kinase by MAP kinase kinase. J Biol Chem. 274: 35301–35304.

147. **Kunath, T.**, Saba-El-Leil, M.K., Almousailleakh, M., Wray, J., Meloche, S., and A. Smith. 2007. FGF stimulation of the Erk1/2 signalling cascade triggers transition of pluripotent embryonic stem cells from self-renewal to lineage commitment. Development. 134: 2895-2902.

148. **Kunii, K.**, Davis, L., Gorenstein, J., Hatch, H., Yashiro, M., Di Bacco, A., Elbi, C., and B. Lutterbach. 2008. FGFR2-amplified gastric cancer cell lines require FGFR2 and Erbb3 signaling for growth and survival. Cancer Res. 68: 2340-2348.

149. **Kurosu, H.**, and M. Kuro-o. 2008. The Klotho gene family and the endocrine fibroblast growth factors. Curr Opin Nephrol Hypertens. 17: 368-372.

150. **Kwabi-Addo, B.**, Wang, J., Erdem, H., Vaid, A., Castro, P., Ayala, G., and M. Ittmann. 2004. The expression of Sprouty1, an inhibitor of fibroblast growth factor signal transduction, is decreased in human prostate cancer. Cancer Res. 64: 4728-3475.

151. **Lampugnani, M.G.**, Orsenigo, F., Gagliani, M. C., Tacchetti, C., and E. Dejana. 2006. Vascular endothelial cadherin controls VEGFR-2 internalization and signaling from intracellular compartments. J. Cell Biol. 174: 593–604.

152. **Lange, S.**, Xiang, F., Yakovenko, A., Vihola, A., Hackman, P., Rostkova, E., Kristensen, J., Brandmeier, B., Franzen, G., Hedberg, B., Gunnarsson, L.G., Hughes, S.M., Marchand, S., Sejersen, T., Richard, I., Edström, L., Ehler, E., Udd, B., and M. Gautel.

2005. The kinase domain of titin controls muscle gene expression and protein turnover. Science 308: 1599-1603.

153. **Lao, D.H.**, Chandramouli, S., Yusoff, P., Fong, C.W., Saw, T.Y., Tai, L.P., Yu, C.Y., Leong, H.F., and G.R. Guy. 2006. A Src homology 3-binding sequence on the C terminus of Sprouty2 is necessary for inhibition of the Ras/ERK pathway downstream of fibroblast growth factor receptor stimulation. J Biol Chem. 281: 29993-30000.

154. **Lao, D.H.**, Yusoff, P., Chandramouli, S., Philp, R.J., Fong, C.W., Jackson, R.A., Saw, T.Y., Yu, C.Y., and G.R. Guy. 2007. Direct binding of PP2A to Sprouty2 and phosphorylation changes are a prerequisite for ERK inhibition downstream of fibroblast growth factor receptor stimulation. J Biol Chem. 282: 9117-26..

155. **Larsson, H.**, Klint, P., Landgren, E., and L. Claesson-Welsh. 1999. Fibroblast growth factor receptor-1-mediated endothelial cell proliferation is dependent on the Src homology (SH) 2/SH3 domain-containing adaptor protein Crk. J Biol Chem. 1999 274: 25726-25734.

156. **Lee, S.A.**, Ho, C., Roy, R., Kosinski, C., Patil, M.A., Tward, A.D., Fridlyand, J., and X. Chen. 2008. Integration of genomic analysis and in vivo transfection to identify sprouty 2 as a candidate tumor suppressor in liver cancer. Hepatology. 47: 1200-1210.

157. **Lee, S.H.**, Schloss, D. J., Jarvis, L., Krasnow, M. A. and J.L. Swain. 2001. Inhibition of angiogenesis by a mouse sprouty protein. J. Biol. Chem. 276: 4128 -33.

158. **Leeksma, O.C.**, van Achterberg, T. A., Tsumura, Y., Toshima, J., Eldering, E., Kroes, W. G., Mellink, C., Spaargaren, M., Mizuno, K., Pannekoek, H. and C.J. de Vries. 2002. Human sprouty 4, a new ras antagonist on 5q31, interacts with the dual specificity kinase TESK1. Eur. J. Biochem. 269: 2546 -56.

159. **Legouis, R.**, Hardelin, J.P., Levilliers, J., Claverie, J.M., Compain, S., Wunderle, V., Millasseau, P., Le Paslier, D., Cohen, D., Caterina, D., et al. 1991. The candidate gene for the X-linked Kallmann syndrome encodes a protein related to adhesion molecules. Cell. 67: 423-435.

160. **Lew, E.D.**, Furdui, C.M., Anderson, K.S., and J. Schlessinger. 2009. The precise sequence of FGF receptor autophosphorylation is kinetically driven and is disrupted by oncogenic mutations. Sci Signal. 2: ra6.

161. **Li, X.**, Brunton, V. G., Burgar, H. R., Wheldon, L. M. and J.K. Heath. 2004. FRS2-dependent SRC activation is required for fibroblast growth factor receptor-induced phosphorylation of Sprouty and suppression of ERK activity. J. Cell Sci. 117: 6007 -17.

162. **Li, C.**, Scott, D.A., Hatch, E., Tian, X., and S.L. Mansour. 2007. Dusp6 (Mkp3) is a negative feedback regulator of FGF-stimulated ERK signaling during mouse development. Development 134: 167–176.

163. **Lim, C.P.,** and X. Cao. Structure, function, and regulation of STAT proteins. Mol Biosyst 2:536–550.

164. **Lim, J.**, Wong, E. S., Ong, S. H., Yusoff, P., Low, B. C. and G.R. Guy. 2000. Sprouty proteins are targeted to membrane ruffles upon growth factor receptor tyrosine kinase activation. Identification of a novel translocation domain. J. Biol. Chem. 275: 32837-45.

165. **Lim, J.**, Yusoff, P., Wong, E.S., Chandramouli, S., Lao, D.H., Fong, C.W. and G.R. Guy. 2002. The cysteine-rich sprouty translocation domain targets mitogen-activated protein kinase inhibitory proteins to phosphatidylinositol 4,5-bisphosphate in plasma membranes. Mol. Cell. Biol. 22: 7953 -7966.

166. **Lin, W.**, Furthauer, M., Thisse, B., Thisse, C., Jing, N., and S.L. Ang. 2002. Cloning of the mouse Sef gene and comparative analysis of its expression with Fgf8 and Spry2 during embryogenesis. Mech Dev. 113: 163–168.

167. **Lin, W.,** Jing, N., Basson, M.A., Dierich, A., Licht, J., and S.L. Ang. 2005. Synergistic activity of Sef and Sprouty proteins in regulating the expression of Gbx2 in the mid-hindbrain region. Genesis 41: 110–115.

168. **Liu, Z.**, Xu, J., Colvin J.S., and D.M. Ornitz. 2002. Coordination of chondrogenesis and osteogenesis by fibroblast growth factor 18. Genes Dev. 16: 859–869.

169. **Lo, T.L.**, Yusoff, P., Fong, C.W., Guo, K., McCaw, B.J., Phillips, W.A., Yang, H., Wong, E.S., Leong, H.F., Zeng, Q., Putti, T.C., and G.R. Guy. 2004. The ras/mitogen-activated protein kinase pathway inhibitor and likely tumor suppressor proteins, sprouty 1 and sprouty 2 are deregulated in breast cancer. Cancer Res. 64: 6127-6136.

170. **Lock, P.**, I, S.T., Straffon, A.F., Schieb, H., Hovens, C.M., and S.S. Stylli. 2006. Spred-2 steady-state levels are regulated by phosphorylation and Cbl-mediated ubiquitination. Biochem Biophys Res Commun. 351: 1018-1023.

171. **Lodish, H.**, Berk, A., Zipursky, S.L., Matsudaira, P., Baltimore, D., Darnell, J.E. Molecular Cell Biology-fifth edition. New York: W. H. Freeman & Co.; 2003.

172. **Longatti, A.**, and S.A. Tooze. 2009. Vesicular trafficking and autophagosome formation. Cell Death Differ. 16: 956-965.

173. **Lowenstein, E.J.**, Daly, R.J., Batzer, A.G., Li, W., Margolis, B., Lammers, R., Ullrich, A., Skolnik, E.Y., Bar-Sagi, D., and J. Schlessinger. 1992. The SH2 and SH3 domain-containing protein GRB2 links receptor tyrosine kinases to ras signaling. Cell. 70: 431-442.

174. **Lu, Q.**, Hope, L.W., Brasch, M., Reinhard, C., and S.N. Cohen. 2003. TSG101 interaction with HRS mediates endosomal trafficking and receptor down-regulation. Proc Natl Acad Sci U S A. 100: 7626-7631.

175. **Lu, S.Y.**, Sheikh, F., Sheppard, P.C., Fresnoza, A., Duckworth, M.L., Detillieux, K.A., and P.A. Cattini. 2008. FGF-16 is required for embryonic heart development. Biochem Biophys Res Commun. 373: 270-274.

176. **Lu, A.**, Tebar, F., Alvarez-Moya, B., López-Alcalá, C., Calvo, M., Enrich, C., Agell, N., Nakamura, T., Matsuda, M., and O. Bachs. 2009. A clathrin-dependent pathway leads to KRas signaling on late endosomes en route to lysosomes. J Cell Biol. 184: 863-879.

177. **MacInnis, B.L.**, and R.B. Campenot. 2002. Retrograde support of neuronal survival without retrograde transport of nerve growth factor. Science 295: 1536-1539.

178. **Marais, R.,** Light, Y., Mason, C., Paterson, H., Olson, M.F., and C.J. Marshall. 1998. Requirement of Ras-GTP-Raf complexes for activation of Raf-1 by protein kinase C. Science. 280: 109-112.

179. **Marais, R.**, Light, Y., Paterson, H.F., Mason, C.S., and C.J. Marshall. 1997. Differential regulation of Raf-1, A-Raf, and B-Raf by oncogenic ras and tyrosine kinases. J Biol Chem 272: 4378–4383.

180. **Mardakheh, F.K.**, Yekezare, M., Machesky, L.M., Heath, J.K. 2009. Spred2 interaction with the late endosomal protein NBR1 down-regulates fibroblast growth factor receptor signaling. J Cell Biol. 187: 265-277.

181. **Marek, L.**, Ware, K.E., Fritzsche, A., Hercule, P., Helton, W.R., Smith, J.E., McDermott, L.A., Coldren, C.D., Nemenoff, R.A., Merrick, D.T., Helfrich, B.A., Bunn, P.A. Jr, and L.E. Heasley. 2009. Fibroblast growth factor (FGF) and FGF receptor-

mediated autocrine signaling in non-small-cell lung cancer cells. Mol Pharmacol. 75: 196-207.

182. **Marshall, C.J.** 1996. Ras effectors. Curr Opin Cell Biol 8: 197–204.

183. **Mason, J.M.**, Morrison, D.J., Bassit, B., Dimri, M., Band, H., Licht, J. D., and I. Gross. 2004. Tyrosine phosphorylation of sprouty proteins regulates their ability to inhibit growth factor signaling-a dual feedback loop, Mol. Biol. Cell 15: 2176–2188.

184. **Mason, J.M.**, Morrison, D.J., Basson, M.A., and J.D. Licht. 2006. Sprouty proteins: multifaceted negative-feedback regulators of receptor tyrosine kinase signaling. Trends Cell Biol. 16: 45-54.

185. **Matozaki, T.**, Murata, Y., Saito, Y., Okazawa, H., and H. Ohnishi. 2009. Protein tyrosine phosphatase SHP-2: a proto-oncogene product that promotes Ras activation. Cancer Sci. 100: 1786-1793.

186. **de Maximy, A. A.**, Nakatake, Y., Moncada, S., Itoh, N., Thiery, J. P. and S. Bellusci. 1999. Cloning and expression pattern of a mouse homologue of drosophila Sprouty in the mouse embryo. Mech. Dev. 81: 213 -216.

187. **McKie, A.B.**, Douglas, D.A., Olijslagers, S., Graham, J., Omar, M.M., Heer, R., Gnanapragasam, V.J., Robson, C.N., and H.Y. Leung. 2005. Epigenetic inactivation of the human sprouty2 (hSPRY2) homologue in prostate cancer. Oncogene. 24: 2166-74.

188. **McMahon, H.T.**, and J.L. Gallop. 2005. Membrane curvature and mechanisms of dynamic cell membrane remodelling. Nature 438: 590-596.

189. **Meyers, E.N.**, Lewandoski, M., G.R. Martin. 1998. An Fgf8 mutant allelic series generated by Cre- and Flp-mediated recombination. Nat Genet. 18: 136-141.

190. **Miaczynska, M.**, Christoforidis, S., Giner, A., Shevchenko, A., Uttenweiler-Joseph, S., Habermann, B., Wilm, M., Parton, R.G., and M. Zerial. 2004a. APPL proteins link Rab5 to nuclear signal transduction via an endosomal compartment. Cell. 116: 445-456.

191. **Miaczynska, M.**, Pelkmans, L., and M. Zerial. 2004b. Not just a sink: endosomes in control of signal transduction. Curr Opin Cell Biol. 16: 400-406.

192. **Min, H.**, Danilenko, D.M., Scully, S.A., Bolon, B., Ring, B.D., Tarpley, J.E., DeRose, M., and W.S. Simonet. 1998. Fgf-10 is required for both limb and lung development and exhibits striking functional similarity to Drosophila branchless. Genes Dev. 12: 3156-61.

193. **Minowada, G.**, Jarvis, L. A., Chi, C. L., Neubuser, A., Sun, X., Hacohen, N., Krasnow, M. A. and G.R. Martin. 1999. Vertebrate Sprouty genes are induced by FGF signaling and can cause chondrodysplasia when overexpressed. Development. 126: 4465 -75.

194. **Missiaglia, E.**, Selfe, J., Hamdi, M., Williamson, D., Schaaf, G., Fang, C., Koster, J., Summersgill, B., Messahel, B., Versteeg, R., Pritchard-Jones, K., Kool, M., and J. Shipley. 2009. Genomic imbalances in rhabdomyosarcoma cell lines affect expression of genes frequently altered in primary tumors: an approach to identify candidate genes involved in tumor development. Genes Chromosomes Cancer. 48: 455-467.

195. **Miyoshi, K.**, Wakioka, T., Nishinakamura, H., Kamio, M., Yang, L., Inoue, M., Hasegawa, M., Yonemitsu, Y., Komiya, S., A. Yoshimura. 2004. The Sprouty-related protein, Spred, inhibits cell motility, metastasis, and Rho-mediated actin reorganization. Oncogene. 23: 5567-76.

196. **Mizuno, E.**, Kobayashi, K., Yamamoto, A., Kitamura, N., and M. Komada. 2006. A deubiquitinating enzyme UBPY regulates the level of protein ubiquitination on endosomes. Traffic 7: 1017-1031.

197. **Mohammadi, M.**, Dikic, I., Sorokin, A., Burgess, W.H., Jaye, M., and J. Schlessinger. 1996a. Identification of six novel autophosphorylation sites on fibroblast growth factor receptor 1 and elucidation of their importance in receptor activation and signal transduction. Mol Cell Biol. 16: 977-989.

198. **Mohammadi, M.**, Dionne, C.A., Li, W., Li, N., Spivak, T., Honegger, A.M., Jaye, M., and J. Schlessinger. 1992. Point mutation in FGF receptor eliminates phosphatidylinositol hydrolysis without affecting mitogenesis. Nature 358: 681–684.

199. **Mohammadi, M.**, Honegger, A.M., Rotin, D., Fischer, R., Bellot, F., Li, W., Dionne, C.A., Jaye, M., Rubinstein, M., and J. Schlessinger. 1991. A tyrosine-phosphorylated carboxy-terminal peptide of the fibroblast growth factor receptor (Flg) is a binding site for the SH2 domain of phospholipase C-gamma 1. Mol Cell Biol. 11: 5068-5078.

200. **Mohammadi, M.**, Olsen, S.K., and O.A. Ibrahimi. 2005. Structural basis for fibroblast growth factor receptor activation. Cytokine Growth Factor Rev. 16: 107-137.

201. **Mohammadi, M.**, Schlessinger, J., and S.R. Hubbard. 1996b. Structure of the FGF receptor tyrosine kinase domain reveals a novel autoinhibitory mechanism. Cell 86: 577–558.

202. **Moscat, J.**, and M.T. Diaz-Meco. 2009. p62 at the crossroads of autophagy, apoptosis, and cancer. Cell. 137: 1001-1004.

203. **Mosesson, Y.**, Mills, G.B., and Y. Yarden. 2008. Derailed endocytosis: an emerging feature of cancer. Nat Rev Cancer 8: 835-850.

204. **Müller, S.**, Kursula, I., Zou, P., and M. Wilmanns. 2006. Crystal structure of the PB1 domain of NBR1. FEBS Lett. 580: 341-344.

205. **Munro, N.P.** and M.A. Knowles. 2003. Fibroblast growth factors and their receptors in transitional cell carcinoma. J. Urol. 169: 675–682.

206. **Nada, S.**, Hondo, A., Kasai, A., Koike, M., Saito, K., Uchiyama, Y., and M. Okada. 2009. The novel lipid raft adaptor p18 controls endosome dynamics by anchoring the MEK-ERK pathway to late endosomes. EMBO J. 28(5):477-489.

207. **Nadeau, R.J.**, Toher, J.L., Yang, X., Kovalenko, D., and R. Friesel. 2007. Regulation of Sprouty2 stability by mammalian Seven-in-Absentia homolog 2. J Cell Biochem. 100: 151-60.

208. **Nakamura, K.**, Kimple, A.J., Siderovski, D.P., and G.L. Johnson. 2010. PB1 domain interaction of p62/sequestosome 1 and MEKK3 regulates NF-kappaB activation. J Biol Chem. 285: 2077-2089.

209. **Nakamura, N.**, Yamamoto, A., Wada, Y., and M Futai. 2000. Syntaxin 7 mediates endocytic trafficking to late endosomes. J Biol Chem. 275: 6523-6529.

210. **Narayan, K.**, and M.A. Lemmon. 2006. Determining selectivity of phosphoinositide-binding domains. Methods 39: 122-133.

211. **Ng, C.**, Jackson, R.A., Buschdorf, J.P., Sun, Q., Guy, G.R., and J. Sivaraman. 2008. Structural basis for a novel intrapeptidyl H-bond and reverse binding of c-Cbl-TKB domain substrates. EMBO J. 27: 804-816.

212. **Nobuhisa, I.**, Kato, R., Inoue, H., Takizawa, M., Okita, K., Yoshimura, A., and T. Taga. 2004. Spred-2 suppresses aorta-gonad-mesonephros hematopoiesis by inhibiting MAP kinase activation. J Exp Med. 199: 737–742.

213. **Nonami, A.**, Kato, R., Taniguchi, K., Yoshiga, D., Taketomi, T., Fukuyama, S., Harada, M., Sasaki, A., and A. Yoshimura. 2004. Spred-1 negatively regulates interleukin-3-mediated ERK/mitogen-activated protein (MAP) kinase activation in hematopoietic cells. J Biol Chem. 279: 52543-52551.

214. **Nonami, A.**, Taketomi, T., Kimura, A., Saeki, K., Takaki, H., Sanada, T., Taniguchi, K., Harada, M., Kato, R., A. Yoshimura. 2005. The Sprouty-related protein, Spred-1, localizes in a lipid raft/caveola and inhibits ERK activation in collaboration with caveolin-1. Genes Cells. 10: 887-895.

215. **Nutt, S.L.**, Dingwell, K. S., Holt, C. E. and E. Amaya. 2001. Xenopus Sprouty2 inhibits FGF-mediated gastrulation movements but does not affect mesoderm induction and patterning. Genes Dev. 15:1152 -1166.

216. **Ohbayashi, N.**, Shibayama, M., Kurotaki, Y., Imanishi, M., Fujimori, T., Itoh, N., and S. Takada. 2002. FGF18 is required for normal cell proliferation and differentiation during osteogenesis and chondrogenesis. Genes Dev. 16: 870-879.

217. **Ohba, Y.**, K. Kurokawa, and M. Matsuda. 2003. Mechanism of the spatio-temporal regulation of Ras and Rap1. EMBO J. 22: 859-869.

218. **Olsen J.V.**, Blagoev, B., Gnad, F., Macek, B., Kumar, C., Mortensen, P., M. Mann. 2006. Global, in vivo, and site-specific phosphorylation dynamics in signaling networks. Cell. 127: 635-648.

219. **Olsen, S.K.**, Ibrahimi, O.A., Raucci, A., Zhang, F., Eliseenkova, A.V., Yayon, A., Basilico, C., Linhardt, R.J., Schlessinger, J., and M. Mohammadi. 2004. Insights into the molecular basis for fibroblast growth factor receptor autoinhibition and ligand-binding promiscuity. Proc Natl Acad Sci U S A. 101: 935-940.

220. **Ong, S.E.**, Foster, L.J., and M. Mann. 2003. Mass spectrometric-based approaches in quantitative proteomics. Methods. 29: 124-130.

221. **Ong, S.H.**, Guy, G.R., Hadari, Y.R., Laks, S., Gotoh, N., Schlessinger, J., and I. Lax. 2000. FRS2 proteins recruit intracellular signaling pathways by binding to diverse targets

on fibroblast growth factor and nerve growth factor receptors. Mol Cell Biol. 20: 979-989.

222. **Ong, S.H.**, Hadari, Y.R., Gotoh, N., Guy, G.R., Schlessinger, J., and I. Lax. 2001. Stimulation of phosphatidylinositol 3-kinase by fibroblast growth factor receptors is mediated by coordinated recruitment of multiple docking proteins. Proc Natl Acad Sci U S A. 98: 6074-6079.
223. **Orr-Urtreger, A.**, Bedford, M.T., Burakova, T., Arman, E., Zimmer, Y., Yayon, A., Givol, D., and P. Lonai. Developmental localization of the splicing alternatives of fibroblast growth factor receptor-2 (FGFR2). Dev Biol. 158: 475-486.
224. **Ostman, A.**, Hellberg, C., and F.D. Böhmer. 2006. Protein-tyrosine phosphatases and cancer. Nat Rev Cancer. 6: 307-320.
225. **Ostman, A.**, and F.D. Böhmer. 2001. Regulation of receptor tyrosine kinase signaling by protein tyrosine phosphatases. Trends Cell Biol. 11: 258-266.
226. **Owens, D.M.**, and S.M. Keyse. 2007. Differential regulation of MAP kinase signalling by dual-specificity protein phosphatases. Oncogene. 26: 3203-3213.
227. **Ozaki, K.**, Kadomoto, R., Asato, K., Tanimura, S., Itoh, N., and M. Kohno. 2001. ERK pathway positively regulates the expression of Sprouty genes, Biochem. Biophys. Res. Commun. 285:1084–1088.
228. **Ozaki, K.**, Miyazaki, S., Tanimura, S., and M. Kohno. 2005. Efficient suppression of FGF-2-induced ERK activation by the cooperative interaction among mammalian Sprouty isoforms. J Cell Sci. 118: 5861-71.
229. **Paik, J.H.**, Kollipara, R., Chu, G., Ji, H., Xiao, Y., Ding, Z., Miao, L., Tothova, Z., Horner, J.W., Carrasco, D.R., Jiang, S., Gilliland, D.G., Chin, L., Wong, W.H.,

Castrillon, D.H., and R.A. DePinho. 2007. FoxOs are lineage-restricted redundant tumor suppressors and regulate endothelial cell homeostasis. Cell. 128: 309-23.

230. **Pankiv, S.**, Clausen, T.H., Lamark, T., Brech, A., Bruun, J.A., Outzen, H., Øvervatn, A., Bjørkøy, G., and T. Johansen. 2007. p62/SQSTM1 binds directly to Atg8/LC3 to facilitate degradation of ubiquitinated protein aggregates by autophagy. J Biol Chem. 282: 24131-24145.

231. **Partanen, J.**, Schwartz, L., and J. Rossant. 1998. Opposite phenotypes of hypomorphic and Y766 phosphorylation site mutations reveal a function for Fgfr1 in anteroposterior patterning of mouse embryos. Genes Dev. 12: 2332–2344.

232. **Phoenix, T.N.**, and S. Temple. 2010. Spred1, a negative regulator of Ras-MAPK-ERK, is enriched in CNS germinal zones, dampens NSC proliferation, and maintains ventricular zone structure. Genes Dev. 24: 45-56.

233. **Piper, R.C.**, and D.J. Katzmann. 2007. Biogenesis and function of multivesicular bodies. Annu Rev Cell Dev Biol. 23:519-547.

234. **Plotnikov, A.N.**, Schlessinger, J., Hubbard, S.R., and M. Mohammadi. 1999. Structural basis for FGF receptor dimerization and activation. Cell 98: 641–650.

235. **Qi, J.**, Nakayama, K., Gaitonde, S., Goydos, J.S., Krajewski, S., Eroshkin, A., Bar-Sagi, D., Bowtell, D., and Z. Ronai. 2008. The ubiquitin ligase Siah2 regulates tumorigenesis and metastasis by HIF-dependent and -independent pathways. Proc Natl Acad Sci U S A. 105: 16713-16718.

236. **Reich, A.**, A. Sapir, and B. Shilo. 1999. Sprouty is a general inhibitor of receptor tyrosine kinase signaling. Development 126: 4139-4147.

237. **Rodriguez-Viciana, P.**, Warne, P.H., Dhand, R., Vanhaesebroeck, B., Gout, I., Fry, M.J., Waterfield, M.D., and J. Downward. 1994. Phosphatidylinositol-3-OH kinase as a direct target of Ras. Nature. 370: 527-532.

238. **Ron, D.**, Fuchs, Y., and D.S. Chorev. 2008. Know thy Sef: a novel class of feedback antagonists of receptor tyrosine kinase signaling. Int J Biochem Cell Biol. 40: 2040-2052.

239. **Rosty, C.**, Aubriot, M.H., Cappellen, D., Bourdin, J., Cartier, I., Thiery, J.P., Sastre-Garau, X., and F. Radvanyi. 2005. Clinical and biological characteristics of cervical neoplasias with FGFR3 mutation. Mol Cancer. 4: 15.

240. **Roumiantsev, S.**, Krause, D.S., Neumann, C.A., Dimitri, C,A,, Asiedu, F., Cross, N.C., and R.A. Van Etten. 2004. Distinct stem cell myeloproliferative/T lymphoma syndromes induced by ZNF198-FGFR1 and BCR-FGFR1 fusion genes from 8p11 translocations. Cancer Cell. 5: 287-298.

241. **Row, P.E.**, Prior, I.A., McCullough, J., Clague, M.J., and S. Urbé. 2006. The ubiquitin isopeptidase UBPY regulates endosomal ubiquitin dynamics and is essential for receptor down-regulation. J Biol Chem. 281: 12618-12624.

242. **Rubin, C.**, Litvak, V., Medvedovsky, H., Zwang, Y., Lev, S., and Y. Yarden. 2003. Sprouty fine-tunes EGF signaling through interlinked positive and negative feedback loops. Curr. Biol. 13: 297–307.

243. **Rubin, C.**, Zwang, Y., Vaisman, N., Ron, D., and Y. Yarden. 2005. Phosphorylation of carboxyl-terminal tyrosines modulates the specificity of Sprouty-2 inhibition of different signaling pathways. J Biol Chem. 280: 9735-44.

244. **Sanchez, P.**, De Carcer, G., Sandoval, I.V., Moscat, J., and M.T. Diaz-Meco. 1998. Localization of atypical protein kinase C isoforms into lysosome-targeted endosomes through interaction with p62. Mol Cell Biol. 18: 3069-3080.

245. **Sandilands, E.**, Akbarzadeh, S., Vecchione, A., McEwan, D.G., Frame, M.C., and J.K. Heath. 2007. Src kinase modulates the activation, transport and signaling dynamics of fibroblast growth factor receptors. EMBO Rep. 8: 1162-1169.

246. **Sasaki, A.**, Taketomi, T., Kato, R., Saeki, K., Nonami, A., Sasaki, M., Kuriyama, M., Saito, N., Shibuya, M., and A. Yoshimura. 2003. Mammalian Sprouty4 suppresses Ras-independent ERK activation by binding to Raf1, Nat. Cell Biol. 5: 427–32.

247. **Sasaki, A.**, Taketomi, T., Wakioka, T., Kato, R. and A. Yoshimura. 2001. Identification of a dominant negative mutant of Sprouty that potentiates fibroblast growth factor- but not epidermal growth factor-induced ERK activation. J. Biol. Chem. 276: 36804 -36808.

248. **Satoh, T.**, Torii, S., Nakayama, K., and E. Nishida. 2010. CrkL is a novel target of Sprouty2 in fibroblast growth factor signaling. Genes Cells. [Epub ahead of print].

249. **Schaaf, G.**, Hamdi, M., Zwijnenburg, D., Lakeman, A., Geerts, D., Versteeg, R., and M. Kool. 2010. Silencing of SPRY1 triggers complete regression of rhabdomyosarcoma tumors carrying a mutated RAS gene. Cancer Res. 70: 762-771.

250. **Schaeffer, H.J.**, Catling, A.D., Eblen, S.T., Collier, L.S., Krauss, A., and M.J. Weber. 1998. MP1: a MEK binding partner that enhances enzymatic activation of the MAP kinase cascade. Science. 281: 1668-1671.

251. **Schenck, A.**, Goto-Silva, L., Collinet, C., Rhinn, M., Giner, A., Habermann, B., Brand, M., and M. Zerial. 2008. The endosomal protein Appl1 mediates Akt substrate specificity and cell survival in vertebrate development. Cell 133: 486-497.

252. **Schlessinger J.** 2000. Cell signaling by receptor tyrosine kinases. Cell 103: 211-225.

253. **Schlessinger J.** 2002. Ligand-induced, receptor-mediated dimerization and activation of EGF receptor. Cell 110: 669-672.

254. **Schlessinger J.** 2003. Signal transduction. Autoinhibition control. Science. 300: 750-752.

255. **Schlessinger, J.,** Plotnikov, A.N., Ibrahimi, O.A., Eliseenkova, A.V., Yeh, B.K., Yayon, A., Linhardt, R.J., and M. Mohammadi. 2000. Crystal structure of a ternary FGF-FGFR-heparin complex reveals a dual role for heparin in FGFR binding and dimerization. Mol Cell. 6: 743-750.

256. **Scita, G.**, and P.P. Di Fiore. 2010. The endocytic matrix. Nature 463: 464-473.

257. **Shim, K.**, Minowada, G., Coling, D.E., and G.R. Martin. 2005. Sprouty2, a mouse deafness gene, regulates cell fate decisions in the auditory sensory epithelium by antagonizing FGF signaling. Dev Cell. 8: 553-564.

258. **Sigismund, S.**, Argenzio, E., Tosoni, D., Cavallaro, E., Polo, S., and P.P. Di Fiore PP. 2008. Clathrin-mediated internalization is essential for sustained EGFR signaling but dispensable for degradation. Dev Cell. 15:209-219.

259. **Simon, R.**, Richter, J., Wagner, U., Fijan, A., Bruderer, J., Schmid, U., Ackermann, D., Maurer, R., Alund, G., Knönagel, H., Rist, M., Wilber, K., Anabitarte, M., Hering, F., Hardmeier, T., Schönenberger, A., Flury, R., Jäger, P., Fehr, J.L., Schraml, P., Moch, H., Mihatsch, M.J., Gasser, T., and G. Sauter. 2001. High-throughput tissue microarray analysis of 3p25 (RAF1) and 8p12 (FGFR1) copy number alterations in urinary bladder cancer. Cancer Res. 61: 4514-4519.

260. **Simonsen, A.**, and S.A. Tooze. 2009. Coordination of membrane events during autophagy by multiple class III PI3-kinase complexes. J Cell Biol. 186: 773-782.

261. **Sivak, J.M.**, L.F. Petersen, and E. Amaya. 2005. FGF signal interpretation is directed by Sprouty and Spred proteins during mesoderm formation. Dev Cell. 8: 689-701.

262. **Snel, B.**, Lehmann, G., Bork, P., and M.A. Huynen. 2000. STRING: a web-server to retrieve and display the repeatedly occurring neighbourhood of a gene. Nucleic Acids Res. 28: 3442-3444.

263. **Sorkin, A.**, McClure, M., Huang, F., and R. Carter. 2000. Interaction of EGF receptor and grb2 in living cells visualized by fluorescence resonance energy transfer (FRET) microscopy. Curr Biol 10: 1395–1398.

264. **Sorkin, A.**, and M. von Zastrow. 2009. Endocytosis and signalling: intertwining molecular networks. Nat Rev Mol Cell Biol. 10: 609-622.

265. **Spinola, M.**, Leoni, V.P., Tanuma, J., Pettinicchio, A., Frattini, M., Signoroni, S., Agresti, R., Giovanazzi, R., Pilotti, S., Bertario, L., Ravagnani, F., and T.A. Dragani. 2005. FGFR4 Gly388Arg polymorphism and prognosis of breast and colorectal cancer. Oncol Rep. 14: 415-419.

266. **Stork, P.J.**, and T.J. Dillon. 2005. Multiple roles of Rap1 in hematopoietic cells: complementary versus antagonistic functions. Blood. 106: 2952-2961.

267. **Sun, X.**, Meyers, E.N., Lewandoski, M., G.R. Martin. 1999. Targeted disruption of Fgf8 causes failure of cell migration in the gastrulating mouse embryo. Genes Dev. 13: 1834-1846.

268. **Sutterlüty, H.**, Mayer, C.E., Setinek, U., Attems, J., Ovtcharov, S., Mikula, M., Mikulits, W., Micksche, M., W. Berger. 2007. Down-regulation of Sprouty2 in non-small cell lung cancer contributes to tumor malignancy via extracellular signal-regulated kinase pathway-dependent and -independent mechanisms. Mol Cancer Res. 5: 509-520.

269. **Sweet, S.M.**, and H.J. Cooper. 2007. Electron capture dissociation in the analysis of protein phosphorylation. Expert Rev Proteomics. 4: 149-159.

270. **Sweet, S.M.**, Mardakheh, F.K., Ryan, K.J., Langton, A.J., Heath, J.K., and H.J. Cooper. Targeted online liquid chromatography electron capture dissociation mass spectrometry for the localization of sites of in vivo phosphorylation in human Sprouty2. Anal Chem. 80: 6650-6657.

271. **Takeda, M.**, Arao, T., Yokote, H., Komatsu, T., Yanagihara, K., Sasaki, H., Yamada, Y., Tamura, T., Fukuoka, K., Kimura, H., Saijo, N., and K. Nishio. 2007. AZD2171 shows potent antitumor activity against gastric cancer over-expressing fibroblast growth factor receptor 2/keratinocyte growth factor receptor. Clin Cancer Res. 13: 3051-3057.

272. **Taketomi, T.**, Yoshiga, D., Taniguchi, K., Kobayashi, T., Nonami, A., Kato, R., Sasaki, M., Sasaki, A., Ishibashi, H., Moriyama, M., Nakamura, K., Nishimura, J., and A. Yoshimura. 2005. Loss of mammalian Sprouty2 leads to enteric neuronal hyperplasia and esophageal achalasia. Nat Neurosci. 8: 855–857.

273. **Tanaka, S.**, Kunath, T., Hadjantonakis, A.K., Nagy, A., and J. Rossant. 1998. Promotion of trophoblast stem cell proliferation by FGF4. Science. 282: 2072-2075.

274. **Taniguchi, K.**, Ishizaki, T., Ayada, T., Sugiyama, Y., Wakabayashi, Y., Sekiya, T., Nakagawa, R., and A. Yoshimura. 2009. Sprouty4 deficiency potentiates Ras-independent angiogenic signals and tumor growth. Cancer Sci. 100: 1648-1654.

275. **Taniguchi, K.**, Ayada, T., Ichiyama, K. Kohno, R., Yonemitsu, Y., Minami, Y., Kikuchi, A., Maehara, Y., and A. Yoshimura. 2007a. Sprouty2 and Sprouty4 are essential for embryonic morphogenesis and regulation of FGF signaling. Biochem Biophys Res Commun. 352: 896–902

276. **Taniguchi, K.**, Kohno, R., Ayada, T., Kato, R., Ichiyama, K., Morisada, T., Oike, Y., Yonemitsu, Y., Maehara, Y., and A. Yoshimura. 2007b. Spreds are essential for embryonic lymphangiogenesis by regulating vascular endothelial growth factor receptor 3 signaling. Mol Cell Biol. 27: 4541-4550.

277.

278. **Tefft, D.**, Lee, M., Smith, S., Crowe, D. L., Bellusci, S. and D. Warburton. 2002. mSprouty2 inhibits FGF10-activated MAP kinase by differentially binding to upstream target proteins. Am. J. Physiol. Lung Cell Mol. Physiol. 283:700 -706.

279. **Tefft, D.**, Lee, M., Smith, S., Leinwand, M., Zhao, J., Bringas, P. Jr, Crowe, D. L., and D. Warburton. 1999. Conserved function of mSpry-2, a murine homolog of Drosophila sprouty, which negatively modulates respiratory organogenesis. Curr. Biol. 9: 219–222.

280. **Teis, D.**, Wunderlich, W., and L.A. Huber. 2002. Localization of the MP1-MAPK scaffold complex to endosomes is mediated by p14 and required for signal transduction. Dev Cell. 3: 803-814.

281. **Teis, D.**, Taub, N., Kurzbauer, R., Hilber, D., de Araujo, M.E., Erlacher, M., Offterdinger, M., Villunger, A., Geley, S., Bohn, G., Klein, C., Hess, M.W., and L.A. Huber. 2006. p14-MP1-MEK1 signaling regulates endosomal traffic and cellular proliferation during tissue homeostasis. . J Cell Biol. 175: 861-868.

282. **Thien, C.B.**, and W.Y. Langdon. 2001. Cbl: many adaptations to regulate protein tyrosine kinases. Nat Rev Mol Cell Biol. 2: 294-307.

283. **Thussbas, C.**, Nahrig, J., Streit, S., Bange, J., Kriner, M., Kates, R., Ulm, K., Kiechle, M., Hoefler, H., Ullrich, A., and N. Harbeck. 2006. FGFR4 Arg388 allele is associated with resistance to adjuvant therapy in primary breast cancer. J Clin Oncol. 24: 3747-3755.

284. **Torii, S.**, Kusakabe, M., Yamamoto, T., Maekawa, M., and E. Nishida. 2004. Sef is a spatial regulator for Ras/MAP kinase signaling. Dev Cell. 7(1):33-44.

285. **Tsang, M.**, Friesel, R., Kudoh, T., and I.B. Dawid. 2002. Identification of Sef, a novel modulator of FGF signalling. Nat Cell Biol 4: 165–169.

286. **Tsavachidou, D.**, Coleman, M.L., Athanasiadis, G., Li, S., Licht, J.D., Olson, M.F., and B.L. Weber. 2004. SPRY2 is an inhibitor of the ras/extracellular signal-regulated kinase pathway in melanocytes and melanoma cells with wild-type BRAF but not with the V599E mutant. Cancer Res. 64: 5556-9.

287. **Tsumura, Y.**, Toshima, J., Leeksma, O. C., Ohashi, K., and K. Mizuno. 2005. Sprouty-4 negatively regulates cell spreading by inhibiting the kinase activity of testicular protein kinase. Biochem J. 387: 627-37

288. **Turner, N.**, and R. Grose. 2010. Fibroblast growth factor signalling: from development to cancer. Nat Rev Cancer. 10: 116-129.

289. **Ueda, Y.**, Hirai, S., Osada, S., Suzuki, A., Mizuno, K., and S. Ohno. 1996. Protein kinase C activates the MEK-ERK pathway in a manner independent of Ras and dependent on Raf. J Biol Chem. 271: 23512-23519.

290. **Ueda, T.**, Sasaki, H., Kuwahara, Y., Nezu, M., Shibuya, T., Sakamoto, H., Ishii, H., Yanagihara, K., Mafune, K., Makuuchi, M., and M. Terada. 1999. Deletion of the carboxyl-terminal exons of K-sam/FGFR2 by short homology-mediated recombination, generating preferential expression of specific messenger RNAs. Cancer Res. 59: 6080-6086.

291. **Van Obberghen**, E. 1994. Signaling through the insulin receptor and the insulin-like growth factor-1 receptor. Diabetologia 27: S125–134.

292. **Van Rhijn, B.W.**, van Tilborg, A.A., Lurkin, I., Bonaventure, J., de Vries, A., Thiery, J.P., van der Kwast, T.H., Zwarthoff, E.C., and F. Radvanyi. 2002. Novel fibroblast growth factor receptor 3 (FGFR3) mutations in bladder cancer previously identified in non-lethal skeletal disorders. Eur J Hum Genet. 10: 819-824.

293. **Vecchione, A.**, Cooper, H.J., Trim, K.J., Akbarzadeh, S., Heath, J.K., and L.M. Wheldon. 2007. Protein partners in the life history of activated fibroblast growth factor receptors. Proteomics. 7: 4565-78.

294. **Vieira, A.V.**, Lamaze, C., and S.L. Schmid. 1996. Control of EGF receptor signaling by clathrin-mediated endocytosis. Science 274: 2086–2089. J Cell Biol. 175: 861-868.

295. **Vogelstein, B.**, and K.W. Kinzler. 2004. Cancer genes and the pathways they control. Nat Med. 10: 789-799.

296. **Wakioka, T.**, Sasaki, A., Kato, R., Shouda, T., Matsumoto, A., Miyoshi, K., Tsuneoka, M., Komiya, S., Baron, R., and A. Yoshimura. 2001. Spred is a Sprouty-related suppressor of Ras signaling. Nature 412: 647-651.

297. **Wang, Y.**, D. Becker. 1997. Antisense targeting of basic fibroblast growth factor and fibroblast growth factor receptor-1 in human melanomas blocks intratumoral angiogenesis and tumor growth. Nat Med. 3: 887-893.

298. **Wang, F.**, Kan, M., Yan, G., Xu, J., and W.L. McKeehan. 1995. Alternately spliced NH2-terminal immunoglobulin-like Loop I in the ectodomain of the fibroblast growth factor (FGF) receptor 1 lowers affinity for both heparin and FGF-1. J Biol Chem. 270: 10231–10235.

299. **Wang, H.**, and M.G. Kazanietz. 2010. p23/Tmp21 Differentially Targets the Rac-GAP {beta} 2-Chimaerin and Protein Kinase C via their C1 Domains. Mol Biol Cell. 21: 1398-1408.

300. **Wang, J.**, Thompson, B., Ren, C., Ittmann, M., and B. Kwabi-Addo. 2006. Sprouty4, a suppressor of tumor cell motility, is down regulated by DNA methylation in human prostate cancer. Prostate. 66: 613-624.

301. **Wang, X.**, and L. Huang. 2008. Identifying dynamic interactors of protein complexes by quantitative mass spectrometry. Mol Cell Proteomics. 7: 46-57.

302. **Wang, X.**, Weng, L.P., and Q.Yu. 2000. Specific inhibition of FGF-induced MAPK activation by the receptor-like protein tyrosine phosphatase LAR. Oncogene. 19: 2346-2353.

303. **Waters, S.**, Marchbank, K., Solomon, E., Whitehouse, C., and M. Gautel. 2009. Interactions with LC3 and polyubiquitin chains link nbr1 to autophagic protein turnover. FEBS Lett. 583: 1846-1852.

304. **Watson, P.**, Townley, A.K., Koka, P., Palmer, K.J., D.J. Stephens. 2006. Sec16 defines endoplasmic reticulum exit sites and is required for secretory cargo export in mammalian cells. Traffic. 7: 1678-1687.

305. **Webster, M.K.**, and D.J. Donoghue. 1997. FGFR activation in skeletal disorders: too much of a good thing. Trends Genet 13: 178–182.

306. **Wellbrock, C.**, Karasarides, M., and R. Marais. 2004. The RAF proteins take centre stage. Nat Rev Mol Cell Biol 5: 875– 885.

307. **Wheldon, L.M.**, Haines, B.P., Rajappa, R., Mason, I., Rigby, P.W., and J.K. Heath. 2010. Critical role of FLRT1 phosphorylation in the interdependent regulation of FLRT1 function and FGF receptor signalling. PLoS One. 5: e10264.

308. **Wiedemann, M.** And B. Trueb. 2000. Characterization of a novel protein (FGFRL1) from human cartilage related to FGF receptors. Genomics 69: 275–279.

309. **Wilkie, A.O.** 1997. Craniosynostosis: genes and mechanisms. Hum Mol Genet 6: 1647–1656.

310. **Winn, R.A.**, Marek, L., Han, S.Y., Rodriguez, K., Rodriguez, N., Hammond, M., Van Scoyk, M., Acosta, H., Mirus, J., Barry, N., Bren-Mattison, Y., Van Raay, T.J.,

Nemenoff, R.A., and L.E. Heasley. 2005. Restoration of Wnt-7a expression reverses non-small cell lung cancer cellular transformation through frizzled-9-mediated growth inhibition and promotion of cell differentiation. J Biol Chem. 280: 19625-34.

311. **Witze, E.S.**, Old, W.M., Resing, K.A., and N.G. Ahn. 2007. Mapping protein post-translational modifications with mass spectrometry. Nat Methods. 4: 798-806.

312. **Wong, E.S.**, Fong, C.W., Lim, J., Yusoff, P., Low, B.C., Langdon, W.Y., and G.R. Guy. 2002a. Sprouty2 attenuates epidermal growth factor receptor ubiquitylation and endocytosis, and consequently enhances Ras/ERK signaling. EMBO J. 21: 4796-4808.

313. **Wong, A.**, Lamothe, B., Lee, A., Schlessinger, J., and I. Lax. 2002b. FRS2 alpha attenuates FGF receptor signaling by Grb2-mediated recruitment of the ubiquitin ligase Cbl. Proc Natl Acad Sci U S A. 99: 6684-6689.

314. **Wong, E.S.**, Lim, J., Low, B. C., Chen, Q., Guy, G. R. (2000). Evidence for direct interaction between Sprouty and Cbl. J Biol Chem. 276:5866-75.

315. **Woodgett, J.R.** 2005. Recent advances in the protein kinase B signaling pathway. Curr Opin Cell Biol. 17: 150-157.

316. **Wu, X.**, Alexander, P.B., He, Y., Kikkawa, M., Vogel, P. D., and S.L. McKnight. 2005. Mammalian sprouty proteins assemble into large monodisperse particles having the properties of intracellular nanobatteries. Proc Natl Acad Sci U S A. 102: 14058-62.

317. **Wunderlich, W.**, Fialka, I., Teis, D., Alpi, A., Pfeifer, A., Parton, R.G., Lottspeich, F., and L.A. Huber. 2001. A novel 14-kilodalton protein interacts with the mitogen-activated protein kinase scaffold mp1 on a late endosomal/lysosomal compartment. J Cell Biol. 152: 765-776.

318. **Xiao, S.**, Nalabolu, S.R., Aster, J.C., Ma, J., Abruzzo, L., Jaffe, E.S., Stone, R., Weissman, S.M., Hudson, T.J., and J.A. Fletcher. 1998. FGFR1 is fused with a novel

zinc-finger gene, ZNF198, in the t(8;13) leukaemia/lymphoma syndrome. Nat Genet. 18: 84-87.

319. **Xu, X.**, Weinstein, M., Li, C., Naski, M., Cohen, R.I., Ornitz, D.M., Leder, P., and C. Deng. 1998. Fibroblast growth factor receptor 2 (FGFR2)-mediated reciprocal regulation loop between FGF8 and FGF10 is essential for limb induction. Development. 125: 753-765.

320. **Xu, J.**, Liu, Z., and D.M. Ornitz. 2000. Temporal and spatial gradients of Fgf8 and Fgf17 regulate proliferation and differentiation of midline cerebellar structures. Development 127: 1833–1843.

321. **Yagasaki, F.**, Wakao, D., Yokoyama, Y., Uchida, Y., Murohashi, I., Kayano, H., Taniwaki, M., Matsuda, A., and M. Bessho. 2001. Fusion of ETV6 to fibroblast growth factor receptor 3 in peripheral T-cell lymphoma with a t(4;12)(p16;p13) chromosomal translocation. Cancer Res. 61: 8371-8374.

322. **Yan, J.**, Li, F., Ingram, D.A., and L.A. Quilliam. 2008. Rap1a is a key regulator of fibroblast growth factor 2-induced angiogenesis and together with Rap1b controls human endothelial cell functions. Mol Cell Biol. 28: 5803-5810.

323. **Yamaguchi, T.P.**, Harpal, K., Henkemeyer, M., and J. Rossant. 1994. Fgfr-1 is required for embryonic growth and mesodermal patterning during mouse gastrulation. Genes Dev. 8: 3032–3044.

324. **Yin, B.W**. and K.O. Lloyd. 2001. Molecular cloning of the ca125 ovarian cancer antigen. Identification as a new mucin, muc16. J. Biol. Chem. 276: 27371–27375.

325. **Yigzaw, Y.**, Cartin, L., Pierre, S., Scholich, K. and T.B. Patel. 2001. The C terminus of sprouty is important for modulation of cellular migration and proliferation. J. Biol. Chem. 276: 22742−47.

326. **Yigzaw, Y.**, Poppleton, H. M., Sreejayan, N., Hassid, A., and T.B. Patel. 2003. Protein-tyrosine phosphatase-1B (PTP1B) mediates the anti-migratory actions of Sprouty. J Biol Chem. 278: 284-88.

327. **Yoon, S.**, and R. Seger. 2006. The extracellular signal-regulated kinase: multiple substrates regulate diverse cellular functions. Growth Factors. 24: 21-44.

328. **Yoshida, T.**, T. Hisamoto, J. Akiba, H. Koga, K. Nakamura, Y. Tokunaga, S. Hanada, H. Kumemura, M. Maeyama, M. Harada, H. Ogata, H. Yano, M. Kojiro, T. Ueno, A. Yoshimura, and M. Sata. 2006. Spreds, inhibitors of the Ras/ERK signal transduction, are dysregulated in human hepatocellular carcinoma and linked to the malignant phenotype of tumors. Oncogene 25: 6056-6066.

329. **Yu, K.**, Herr, A.B., Waksman, G., and D.M. Ornitz. 2000. Loss of fibroblast growth factor receptor 2 ligand-binding specificity in Apert syndrome. Proc Natl Acad Sci USA 97: 14536–14541.

330. **Yusoff, P**., Lao, D. H., Ong, S. H., Wong, E. S., Lim, J., Lo, T. L., Leong, H. F., Fong, C. W. and G.R. Guy. 2002. Sprouty2 inhibits the Ras/MAP kinase pathway by inhibiting the activation of Raf. J. Biol. Chem. 277: 3195 -201.

331. **Zhang, S.**, Lin, Y., Itaranta, P., Yagi, A., and S. Vainio. 2001. Expression of Sprouty genes 1, 2 and 4 during mouse organogenesis. Mech Dev. 109: 367-70.

332. **Zhou, Y.X.**, Xu, X., Chen, L., Li, C., Brodie, S.G., and C.X. Deng. 2000. A Pro250Arg substitution in mouse Fgfr1 causes increased expression of Cbfa1 and premature fusion of calvarial sutures. Hum Mol Genet 9: 2001–2008.

333. **Zoncu, R.**, Perera, R.M., Balkin, D.M., Pirruccello, M., Toomre, D., and P. De Camilli. 2009. A phosphoinositide switch controls the maturation and signaling properties of APPL endosomes. Cell. 136: 1110-1121.